

Evaluation of Recycled Base Aggregates

Hani H. Titi, Ph.D., P.E., M. ASCE
Habib Tabatabai, Ph.D., P.E., S.E.
Jessie Ramirez
Mohammad Sooman

Department of Civil and Environmental Engineering
University of Wisconsin-Milwaukee

WisDOT ID 0092-17-01

July 2019



RESEARCH & LIBRARY UNIT



WISCONSIN HIGHWAY RESEARCH PROGRAM

WISCONSIN DOT
PUTTING RESEARCH TO WORK

Technical Report Documentation Page

1. Report No. WHRP 0092-17-01	2. Government Accession No.	3. Recipient's Catalog No.	
4. Title and Subtitle Evaluation of Recycled Base Aggregates		5. Report Date July 2019	
		6. Performing Organization Code	
7. Authors Hani H. Titi, Habib Tabatabai, Jessie Ramirez, and Mohammad Sooman		8. Performing Organization Report No.	
9. Performing Organization Name and Address Department of Civil and Environmental Engineering University of Wisconsin-Milwaukee 3200 N. Cramer St. Milwaukee, WI 53211		10. Work Unit No. (TRAIS)	
		11. Contract or Grant No. WHRP 0092-17-01	
12. Sponsoring Agency Name and Address Wisconsin Highway Research Program Wisconsin Department of Transportation Research & Library Unit 4822 Madison Yards Way Madison, WI 53705		13. Type of Report and Period Covered Final Report October 2016 - July 2019	
		14. Sponsoring Agency Code	
15. Supplementary Note			
16. Abstract <p>This study intended to provide quantitative evaluation of the use of RAP and RCA as base layers in HMA pavements. The study used field and laboratory testing programs and data from WisDOT PIF database quantify the performance of base materials and test sections on pavements with CA, RCA, and RAP base layers. Analysis of the particle size distributions for the investigated CA, RCA, and RAP base materials indicated high sand size fractions in both RCA and RAP base materials compared with CA base materials. The RCA base materials exhibited the highest absorption and high percentages of mass loss in Micro-Deval test. The predicted CBR and resilient modulus values for all investigated base layer types are comparable. Difficulties were noted in retrieving RCA base materials from STH 78, STH 32, and STH 50 leading the research team to believe this is due self-cementing effects. The results of the FWD analyses pertaining to D0 and SNeff demonstrate that, in general, the investigated HMA pavement sections with RCA base layers exhibited the lowest deflections and the highest structural capacity (SNeff) compared with those pavement sections with CA and RAP base layers. The pavement sections with CA base layers exhibited the highest deflection and the lowest structural capacity. In general, the back-calculated base layer moduli (EBase) for all investigated pavement tests indicate the highest average values for RCA base layers followed by the RAP base layers, while the CA base layers possessed the lowest average values. The most commonly observed pavement surface distress in the investigated pavement test sections included: transverse cracking, longitudinal cracking, alligator (fatigue) cracking, rutting, bleeding, edge cracking, pavement edge heave, and block cracking. Based on the visual distress survey of the investigated pavement sections, fatigue cracking is the most commonly observed surface distress associated with CA and RAP base layers. Transverse and longitudinal cracks were commonly observed on pavement sections with RCA base layers. The general ranking of the investigated pavements was based on the overall average and does not account for the pavement age. An attempt to correlate the calculated PCI average values with pavement age did not lead to a reliable trend. The pavement surface profile measurements results indicated relatively high IRI values and high variability exhibited by the pavement sections on RCA base layer materials. The average IRI value for all pavement sections indicates the pavement test sections with RAP base layers exhibited the smoothest ride quality.</p> <p>Based on the results of this study, the research team believes that the performance of the HMA pavements with RCA (with the exception of STH 78) and RAP is satisfactory/adequate and comparable with the performance of the HMA pavements with CA base course layers. The research team recommends that WisDOT continues the practice of using the RCA and RAP in base course layers of HMA pavements with implementing control measures listed in Chapter 7 of this report.</p>			
17. Key Words Base Layer Aggregate, Base Layer Modulus, Aggregate Degradation, FWD, Aggregate Resilient Modulus, AASHTOWare Pavement ME Design, Micro-Deval, Sodium Sulfate Soundness, DCP, GPR, PCI.		18. Distribution Statement No restriction. This document is available to the public through the National Technical Information Service 5285 Port Royal Road Springfield VA 22161	
19. Security Classif. (of this report) Unclassified	20. Security Classif. (of this page) Unclassified	21. No. of Pages 257	22. Price

DISCLAIMER

This research was funded through the Wisconsin Highway Research Program by the Wisconsin Department of Transportation and the Federal Highway Administration under Project 0092-17-01. The contents of this report reflect the views of the authors, who are responsible for the facts and accuracy of the data presented herein. The contents do not necessarily reflect the official views of the Wisconsin Department of Transportation or the Federal Highway Administration at the time of publication.

This document is disseminated under the sponsorship of the Department of Transportation in the interest of information exchange. The United States Government assumes no liability for its contents or use thereof. This report does not constitute a standard, specification, or regulation.

The United States Government does not endorse products or manufacturers. Trade and manufacturers' names appear in this report only because they are considered essential to the object of the document.

Acknowledgements

This research project is financially supported by Wisconsin Highway Research Program (WHRP) and Wisconsin Department of Transportation (WisDOT).

The research team would like to acknowledge and thank Mr. Daniel Reid and Ms. Tracy Petersen of WisDOT for their help, support, and effort during field testing.

The input and guidance of WHRP Geotechnical Oversight Committee members and WisDOT engineers Mr. Andrew Zimmer, Mr. Robert Arndorfer, and Mr. Jeffrey Horsfall, is greatly appreciated.

The research team would like to thank Mr. Joseph Allaby and Mr. Michael Wolf of WisDOT Pavement Data Unit.

The research team would like to thank Dr. Dante Fratta, for his great help in the GPR data analysis.

The research team also acknowledges the help and support of UW-Milwaukee students for their help and support in various capacities for this project: Mr. Victor Ramirez, Mr. Omar Saleh, Ms. Alise Fitzsimmons, Ms. Kelli Swenson.

The help and support of Mr. Dennis Scott of SSI in providing the walking profiler is greatly appreciated.

Table of Contents

Chapter 1: Introduction	1
1.1 Problem Statement.....	1
1.2 Research Objectives.....	1
1.3 Background.....	2
1.4 Organization of the Report.....	4
Chapter 2: Background	5
2.1 Introduction.....	5
2.2 Characterization of Recycled Aggregates Properties.....	6
2.2.1 Variability in Materials Source.....	6
2.2.2 Physical Properties.....	6
2.2.3 Strength, Resilient Modulus and Deformation Properties.....	12
2.2.4 Durability and Self-Cementing.....	16
2.2.5 Permeability, Density and Bearing Capacity.....	17
2.3 State Transportation Agencies Specifications.....	18
2.4 Recycled Aggregate Base Materials Survey.....	28
Chapter 3: Research Methodology	47
3.1 Selection of Pavement Test Sites.....	47
3.2 Non-Destructive Field Testing at Selected Pavement Sites.....	47
3.2.1 Falling Weight Deflectometer Tests.....	47
3.2.2 Ground Penetrating Radar.....	50
3.2.3 Visual and Automated Pavement Surface Distress Surveys.....	50
3.2.4 Pavement Surface Profile Measurements.....	51
3.3 Sampling of Base Layer Aggregates and Field Testing.....	51
3.3.1 Pavement Surface Coring.....	51
3.3.2 Drainability Testing of Base Aggregates.....	52
3.3.3 Dynamic Cone Penetration Test.....	53
3.3.4 Sampling of Base Aggregates.....	53
3.4 Laboratory Testing of Base Aggregate.....	54
3.4.1 Particle Size Analysis.....	54
3.4.2 Specific Gravity and Absorption.....	55
3.4.3 Micro-Deval Abrasion Test.....	56
Chapter 4: Laboratory Tests on Base Aggregate Materials – Analysis of Results	57
4.1 Particle Size Distribution.....	57
4.2 Specific Gravity and Absorption.....	66
4.3 Micro-Deval Abrasion.....	74
4.4 Case Study – RCA Base Layer Material at STH 78.....	79
Chapter 5: Field Tests on Aggregate Base Layers – Analysis of Results	86
5.1 Dynamic Cone Penetration Test Results.....	86
5.2 Falling Weight Deflectometer Test Results.....	98
5.3 Ground Penetrating Radar.....	119
5.4 Base Layers Drainability Test Results.....	121
5.5 Pavement Surface Visual Distress Surveys and Profile Measurements.....	125

Chapter 6:	Long Term Performance of HMA Pavements Constructed on Recycled Base Layers.....	136
	6.1 Case Studies – CA versus RAP Base Layer.....	136
	6.1.1 STH 59 West of Edgerton, Rock County.....	136
	6.1.2 STH 25 near Maxville, Buffalo County.....	146
	6.1.3 STH 77 near Webb Lake, Burnett County.....	152
	6.2 Case Studies – HMA Pavement with RCA Base Layer.....	156
	6.2.1 STH 78 from Prairie du Sac to Merrimac.....	156
	6.3 Comparisons of All Investigated Pavement Sections.....	156
Chapter 7:	Summary, Conclusions, and Recommendations.....	168
References	172
Appendices	178
	Appendix A: Survey of State DOTs on: Performance of RCA and RAP as Base Layers in HMA Pavements	
	Appendix B: Particle Size Distribution of the Investigated Base Aggregates	
	Appendix C: Dynamic Cone Penetrometer Test Results	
	Appendix D: Typical Sections of the Investigate HMA Pavements and Measured Dimensions and Unit Weight of HMA Cores	
	Appendix E: Results of the FWD Tests	
	Appendix F: Pavement Condition Index for all Pavement Test Sections	
	Appendix G: IRI Results from Pavement Surface Profiles Measurements	

List of Figures

Figure 2.1:	Absorption values for RCA and RAP materials from different resources (data obtained from Edil et al., 2012).....	10
Figure 2.2:	Gradation of RCA and RAP materials from different resources compared with MnDOT class 5 and blend aggregate (data obtained from Edil et al., 2012).....	11
Figure 2.3:	Midwest State DOTs maximum and minimum values for gravel, sand, and fines.....	23
Figure 2.4a:	Midwest State DOTs maximum and minimum values for gravel, sand, and fines.....	24
Figure 2.4b:	Midwest State DOTs RCA grain size distributions.....	25
Figure 2.5:	State DOTs surveyed in this study.....	27
Figure 2.6:	Most commonly used materials in base course layers.....	29
Figure 2.7:	Allowing the use of RCA as regular, drainable, base and subbase layers...	30
Figure 2.8:	Allowing the use of RAP as regular, drainable, base and subbase layers...	31
Figure 2.9:	Specifications for RCA materials.....	34
Figure 2.10:	Specifications for RAP materials.....	35
Figure 2.11:	Issues or problems with RCA performance as base layers.....	36
Figure 2.12:	Issues or problems with RAP performance as base layers.....	37
Figure 2.13:	Case history on performance issues.....	38
Figure 2.14:	HMA pavement performance issues when using RCA base layers.....	38
Figure 2.15:	HMA pavement performance issues when using RAP base layers.....	39
Figure 2.16:	Construction control methods for RCA and RAP.....	40
Figure 2.17:	Blends of RCA, RAP, and CA.....	41
Figure 2.18:	Importance scale for RCA material (where rating of zero is very low importance and rating of 5 is very high importance).....	42
Figure 2.19:	Importance scale for RAP material (where rating of zero is very low importance and rating of 5 is very high importance).....	43
Figure 2.20:	Comparison of RCA/RAP vs. virgin aggregate.....	44
Figure 3.1:	Wisconsin counties in which the investigated HMA pavements were selected for this study.....	48
Figure 3.2:	WisDOT KUAB FWD test system with GPR units used in this study.....	50
Figure 3.3:	The CS8800 Walking Profiler System provided by Surface Systems & Instruments, Inc. used to measure pavement surface profiles.....	51
Figure 3.4:	Coring of HMA surface at STH 22 in Waupaca and trench cutting at STH 78 in Sauk County.....	52
Figure 3.5:	Field drainability test conducted on the investigated aggregate base layers..	53
Figure 3.6:	DCP field testing on Calhoun Road RCA base layer, aggregate sampling from STH 25 base layer, and holes filled with cold asphalt mix at STH 25 in Maxville.....	54
Figure 4.1:	Particle size distribution of the investigated CA, RCA, and RAP base course materials and the current WisDOT gradation specification limits for the 1¼" dense graded base course materials.	58

Figure 4.2:	Particle size characteristics of the investigated CA, RCA, and RAP base materials.....	63
Figure 4.3:	Lognormal distribution representing the amount of gravel, sand, and fines materials in the investigated CA, RCA, and RAP base materials.....	65
Figure 4.4:	Particle size characteristics of the investigated aggregates.....	67
Figure 4.5:	Coefficients of uniformity and gradation for the investigated base layer materials.....	70
Figure 4.6:	Specific gravity and absorption test results for investigated CA, RCA, and RAP base materials.....	72
Figure 4.7:	Variability of specific gravity and absorption test results for investigated CA, RCA, and RAP base materials.....	63
Figure 4.8:	Mass loss of coarse aggregates fraction for CA and RCA base materials due to the Micro-Deval test.....	75
Figure 4.9:	Comparison of mass loss of coarse aggregates from Micro-Deval abrasion versus absorption for various Wisconsin virgin aggregates.....	78
Figure 4.10:	Particle size distribution of the investigated RCA base course material at STH 78 with data from 2009 and 2018.....	79
Figure 4.11:	Particle size characteristics of the investigated RCA base material for STH 78.....	81
Figure 4.12:	Mass loss of the RCA base material at STH 78.....	82
Figure 4.13:	Pictures of the RCA base material from STH 78 before and after Micro-Deval abrasion test.....	83
Figure 4.14:	Moisture content of the investigated RCA base course layer of STH 78 at several locations.....	85
Figure 5.1:	Penetration resistance with depth from DCP test and distribution with depth of the corresponding estimated CBR and base layer modulus for the RCA base at STH 50, Kenosha.....	88
Figure 5.2:	Penetration resistance with depth from DCP test and distribution with depth of the corresponding estimated CBR and base layer modulus for the CA base at STH 25, Maxville.....	89
Figure 5.3:	Penetration resistance with depth from DCP test and distribution with depth of the corresponding estimated CBR and base layer modulus for the RAP base at STH 25, Maxville.....	90
Figure 5.4:	Box-Whisker comparison of the average predicted CBR values from DCP tests for RCA, CA, and RAP base layers for the investigated pavement.....	95
Figure 5.5:	Box-Whisker comparison of the average predicted layer modulus values from DCP tests for RCA, CA, and RAP base layers for the investigated pavement.....	95
Figure 5.6:	Comparison of the average predicted CBR from DCP for the RCA, CA, and RAP base layers of the investigated pavements.....	97
Figure 5.7:	Comparison of the average predicted layer modulus from DCP for the RCA, CA, and RAP base layers of the investigated pavements.....	97
Figure 5.8:	Box-Whisker plot of the measured adjusted deflection under loading plate (D ₀) normalized to 9,000 lb load for the investigated pavement test sections with crushed aggregate, recycled concrete aggregate, and reclaimed asphalt pavement base layers.....	103

Figure 5.9:	Average adjusted deflection under loading plate (D ₀) normalized to 9,000 lb load for the investigated HMA pavement test sections with crushed aggregate, recycled concrete aggregate, and reclaimed asphalt pavement base layers.....	104
Figure 5.10:	Coefficient of variation of back-calculated HMA layer modulus for the investigated pavement test sections with crushed aggregate, recycled concrete aggregate, and reclaimed asphalt pavement base layers.....	105
Figure 5.11:	Box-Whisker plot of the effective structural number for the investigated pavement test sections with crushed aggregate, recycled concrete aggregate, and reclaimed asphalt pavement base layers.....	106
Figure 5.12:	Average effective structural number for the investigated HMA pavement test sections with crushed aggregate, recycled concrete aggregate, and reclaimed asphalt pavement base layers.....	107
Figure 5.13:	Coefficient of variation of effective structural number for the investigated pavement test sections with crushed aggregate, recycled concrete aggregate, and reclaimed asphalt pavement base layers.....	108
Figure 5.14:	Box-Whisker plot of the back-calculated HMA layer modulus for the investigated pavement test sections with crushed aggregate, recycled concrete aggregate, and reclaimed asphalt pavement base layers.....	109
Figure 5.15:	Average back-calculated HMA layer modulus for the investigated pavement test sections with crushed aggregate, recycled concrete aggregate, and reclaimed asphalt pavement base layers.....	110
Figure 5.16:	Coefficient of variation of back-calculated HMA layer modulus for the investigated pavement test sections with crushed aggregate, recycled concrete aggregate, and reclaimed asphalt pavement base layers.....	111
Figure 5.17:	Box-Whisker plot of the back-calculated base layer modulus for the investigated pavement test sections with crushed aggregate, recycled concrete aggregate, and reclaimed asphalt pavement base layers.....	112
Figure 5.18:	Average back-calculated base layer modulus for the investigated pavement test sections with crushed aggregate, recycled concrete aggregate, and reclaimed asphalt pavement base layers.....	113
Figure 5.19:	Coefficient of variation of back-calculated base layer modulus for the investigated pavement test sections with crushed aggregate, recycled concrete aggregate, and reclaimed asphalt pavement base layers.....	114
Figure 5.20:	Box-Whisker plot of the back-calculated subgrade modulus for the investigated pavement test sections with crushed aggregate, recycled concrete aggregate, and reclaimed asphalt pavement base layers.....	115
Figure 5.21:	Average back-calculated subgrade modulus for the investigated pavement test sections with crushed aggregate, recycled concrete aggregate, and reclaimed asphalt pavement base layers.....	116
Figure 5.22:	Coefficient of variation of back-calculated subgrade modulus for the investigated pavement test sections with crushed aggregate, recycled concrete aggregate, and reclaimed asphalt pavement base layers.....	117
Figure 5.23:	Location and pavement layer profiles for STH 59 with CA and RAP base layers obtained from analysis.....	120

Figure 5.24:	Field drainability of the investigated RCA, CA, and RAP base course layers.....	121
Figure 5.25:	Field drainability and laboratory hydraulic conductivity of the investigated RCA, and CA base course materials.....	122
Figure 5.26:	Pavement surface distress observed on pavements with CA base layers.....	126
Figure 5.27:	Pavement surface distress observed on pavements with RCA base layers....	127
Figure 5.28:	Pavement surface distress observed on pavements with RAP base layers....	128
Figure 5.29:	PCI calculated from the visual distress survey data along the 528 ft pavement test sections.....	129
Figure 5.30:	Variation of PCI along the 528 ft surveyed test sections.....	130
Figure 5.31:	Analysis of PCI values for the investigated pavement test sections.....	131
Figure 5.32:	Pavement surface ride quality expressed as IRI and calculated based on the walking profiler measurements.....	133
Figure 5.33:	Variation of IRI along the 600-ft test sections.....	134
Figure 5.34:	Histogram and the corresponding lognormal distribution representation of the IRI values based on the 25 ft subsection for the investigated pavement test sections with CA, RCA, and RAP base layers.....	135
Figure 6.1:	STH 59 pavement sections with RAP and CA base layers in 2009 before reconstruction and in 2011 and 2018 after reconstruction.....	138
Figure 6.2:	Results of FWD test conducted in 2009 on STH 59 pavement section I (pictured in Figure 6.1 a) with crushed aggregate base just before milling and relay of the 5-inch-thick HMA layer.....	139
Figure 6.3:	Comparison of structural capacity of pavement section I on STH 59 before reconstruction (pavement had CA base layer in 2009) and one year after reconstruction (RAP base layer – mill and relay 2009).....	141
Figure 6.4:	Pavement structural capacity and surface deflection for STH 59 with a CA base layer before re-construction to a RAP base layer.	141
Figure 6.5:	Comparison of rutting, ride quality and cracking performance for STH 59 segments with CA and RAP base layers.....	143
Figure 6.6:	Comparison of average PCI variation with time for the HMA pavement segments of STH 59 constructed on CA and RAP base layers.....	144
Figure 6.7:	Comparison of average IRI and rutting for the STH 59 segments with CA and RAP base layers.....	145
Figure 6.8:	Pavement test sections at STH 25 near Maxville.....	148
Figure 6.9:	Comparison of ride quality and cracking performance for STH 25 segments with CA and RAP base layers.....	149
Figure 6.10:	Comparison of average PCI for the STH 25 segments with CA and RAP base layers.....	150
Figure 6.11:	Comparison of average IRI and rutting for the STH 25 segments with CA and RAP base layers.....	151
Figure 6.12:	Comparison of ride quality and cracking performance for STH 77 segments with CA and RAP base layers (segments constructed on CA and RAP base layers in the years 2011 and 2012, respectively).....	153
Figure 6.13:	Comparison of average PCI variation with time for the HMA pavement segments of STH 77 constructed on CA and RAP base layers in the years 2011 and 2012.....	154

Figure 6.14:	Comparison of average IRI and rutting for the STH 77 segments with CA and RAP base layers.....	155
Figure 6.15:	Comparison of rutting, ride quality and cracking performance for STH 78 segments with RCA base layer.....	157
Figure 6.16:	Comparison of average PCI variation with time for the HMA pavement segments of STH 78 constructed on RCA base layer.....	158
Figure 6.17:	Comparison of average IRI and rutting for the STH 78 segments with RCA base layers.....	159
Figure 6.18:	Long-term pavement performance indicators for HMA pavements with RCA base layers.....	160
Figure 6.19:	Comparison of the investigated pavement performance based on the type of base layer (average PCI for the total length of the project versus pavement age).....	163
Figure 6.20:	Comparison of the investigated pavement performance based on the type of base layer (average IRI for the total length of the project versus pavement age).....	163
Figure 6.21:	Comparison of the investigated pavement performance based on the type of base layer (average rut depth for the total length of the project versus pavement age).....	164
Figure 6.22:	Comparison of the investigated pavement performance based on the type of base layer (average fatigue cracking for the total length of the project versus pavement age).....	164
Figure 6.23:	Comparison of the investigated pavement performance based on the type of base layer (average transverse cracking for the total length of the project versus pavement age).....	165
Figure 6.24:	Comparison of the investigated pavement performance based on the type of base layer (average longitudinal cracking for the total length of the project versus pavement age).....	165
Figure 6.25:	Comparison of the investigated pavement performance based on the type of base layer (average PCI for all pavement sections vs. pavement age).....	166
Figure 6.26:	Comparison of the investigated pavement performance based on the type of base layer (average IRI for all pavement sections vs. pavement age).....	166
Figure 6.27:	Comparison of the investigated pavement performance based on the type of base layer (average rutting for all pavement sections vs. pavement age)..	167
Figure 6.28:	Comparison of the investigated pavement performance based on the type of base layer (average cracking for all pavement sections vs. pavement age).....	167

List of Tables

Table 2.1:	Flexible pavement performance parameters and contributing factors (Saeed, 2008).....	7
Table 2.2:	Recycled aggregate particle properties that influence pavement performance (Saeed, 2008).....	8
Table 2.3:	Relevance of recycled material mass properties for various applications (Saeed, 2008).....	8
Table 2.4:	Links between aggregate properties and performance of flexible pavements (modified from Saeed, 2008).....	8
Table 2.5:	Typical physical properties of RAP and RCA by FHWA (2008) (Edil et al., 2012).....	9
Table 2.6:	Properties of typical RCA materials (Blankenagel, 2005).....	10
Table 2.7:	State DOTs allowing RCA material for base and subbase layers and the maximum and minimum percent passing by mass for gravel, sand, and fines.....	20
Table 2.8:	Midwest State DOTs allowing RCA material for base and subbase.....	27
Table 3.1:	Field and laboratory tests conducted on pavement test sections.....	49
Table 3.2:	ASTM and AASHTO standard test methods employed.....	55
Table 4.1:	Particle size characteristics of the investigated base RCA, CA, and RAP base course.....	62
Table 4.2:	Classification of the investigated base layer materials according to the USCS.....	69
Table 4.3:	Results of specific gravity and absorption tests on the investigated RCA, CA, and RAP base materials (coarse fraction).....	71
Table 4.4:	Mass loss of coarse aggregates by Micro-Deval abrasion test for the investigated CA, RCA, and RAP base materials.....	74
Table 4.5:	Particle size characteristics of the investigated RCA base course of STH 78.....	80
Table 5.1:	Summary of CA base layer thicknesses and the corresponding estimated CBR and layer modulus for the investigated pavements.....	92
Table 5.2:	Summary of RCA base layer thicknesses and the corresponding estimated CBR and layer modulus for the investigated pavements.....	93
Table 5.3:	Summary of RAP base layer thicknesses and the corresponding estimated CBR and layer modulus for the investigated pavements.....	94
Table 5.4:	Statistical summary of predicted CBR and layer modulus of the RCA and CA base layer materials.....	96
Table 5.5:	Statistical summary of adjusted deflection under loading plate (D_0) normalized to 9,000 lb load for investigated HMA pavement test sections with CA, RCA, and RAP base layers.....	99
Table 5.6:	Statistical summary of back-calculated layer moduli for the investigated HMA pavement test sections with CA, RCA, and RAP base layers.....	101

Table 5.7:	Field drainability test results on CA and RCA base layers and laboratory permeability tests on CA and RCA base materials.....	123
Table 5.8:	Field drainability test results on RAP base layers.....	124

Chapter 1

Introduction

1.1 Problem Statement

There has been great interest in recent years in using Recycled Asphalt Pavement (RAP) and Recycled Concrete Aggregate (RCA) as a base course in Wisconsin and elsewhere for the economic and environmental benefits offered by such a practice. Recent examples include the I-94 corridor reconstruction in Kenosha, Racine and Milwaukee Counties, and the Beltline reconstruction in Dane County.

Laboratory studies showed that RAP and RCA have resilient modulus values equal to or higher than typical natural aggregates and also generally have higher durability, especially to freeze-thaw cycles. However, it is also recognized that RAP exhibits temperature sensitivity and larger permanent deformations than natural aggregates and RCA exhibits tufa formation and potentially lower drainability than natural aggregates.

How these characteristics manifest themselves in the field, especially in northern climates, can only be assessed by long-term observation of field performance. For this purpose, Minnesota Department of Transportation (MnDOT) constructed and monitored test sections at the MnROAD facility through a pooled fund, in which Wisconsin Department of Transportation (WisDOT) was a member. These test sections showed comparable performance to the control section of natural aggregate 2009-2013. However, there are reports now that rutting and cracking are being observed.

Wisconsin Department of Transportation (WisDOT) has been using RAP and RCA as a base course for over thirty years. The qualitative assessment of WisDOT roads constructed with RAP and RCA is that they are performing adequately. This anecdotal impression needs to be verified quantitatively if the use of RAP and RCA in base aggregates is to continue. A quantitative review is needed of WisDOT experience through collection and comparison of pavement distress surveys of roadways using RAP and RCA as a base course compared with those using natural mineral aggregates.

1.2 Research Objectives

The intended outcome of this study is to meet the following objectives:

1. Conduct new surveys to collect and analyze pavement distress for Hot Mix Asphalt (HMA) roadways constructed in Wisconsin using RAP and RCA as a base course aggregate and compare with similar roadways constructed with natural aggregates to verify the performance of roadways constructed with recycled base aggregates.

2. If any negative attributes exist regarding the use of RAP and RCA, the results of the research will help to determine if there are any techniques that can be used, such as blending of recycled aggregates with natural aggregates, which would produce satisfactory results using recycled aggregates.
3. Depending on the outcome of the research, develop specification language and construction guidance regarding the use of recycled aggregates as a base course.

1.3 Background

In flexible pavement systems, the base course layer acts to distribute traffic loads to the underlying sub-base and subgrade layers, as well as to facilitate drainage. The base course must also provide support to the wearing surface to prevent tensile fatigue cracking. Base course aggregate must have adequate permeability, durability, and angularity. Pertinent properties of unbound aggregate are characterized by parameters such as resilient modulus (M_R), saturated hydraulic conductivity (k_{sat}), strength (CBR), maximum dry density ($\gamma_{d,max}$), optimum water content (w_{opt}), etc.; these parameters are critical for a mechanistic-empirical based pavement design method.

Around two billion tons of aggregate are produced in the United States annually, and aggregate production is projected to exceed 2.5 billion tons by the year 2020 (Ceylan, 2014). These figures raise issues related to sustainability, as quarries gradually become depleted and environmental regulations become more stringent. With high demand for construction aggregate and an increasing public desire to manage waste materials in a responsible manner, there has been increasing interest in the prospect of utilizing by-products and reclaimed material for pavement construction purposes. For base courses in flexible pavement systems, the use of RAP and RCA has been the subject of increased research in recent years (Gabr and Cameron, 2012).

Tremendous amounts of recycled asphalt pavement are generated from road resurfacing projects; over 100 million tons of reclaimed asphalt pavements are milled annually in the United States (Dong and Huang, 2014). The amount of recycled asphalt concrete produced often exceeds the amount that can feasibly be reused for HMA mixing (Thakur et al., 2010). Excess RAP generated on site can be utilized near the site as a base course, reducing material transportation costs. RAP is pulverized and processed on-site to reach the desired gradation.

RAP possesses a number of characteristics that make it an attractive choice for use in unbound base course material. Several studies have shown that the M_R of RAP is higher than that of virgin aggregate (Bennert et al., 2000; Bejarano et al., 2003). Kim et al. (2007) found that pavements with various percentages of RAP in the base course performed similarly with respect to strength and stiffness compared with pavements with 100% virgin aggregate base courses.

RAP tends to have a high fine content due to the crushing and milling process. Fine RAP particles tend to be coated with hydrophobic asphalt, which reduces the ability to hold excess

moisture (Attia and Abdelrahman, 2010; Edil et al., 2012). Nokkaew et al. (2012) found k_{sat} values between 3.7×10^{-5} m/s and 3.7×10^{-4} m/s for RAPs compacted to 95% of maximum dry density. As asphalt is a viscoelastic binding agent, RAP tends to show deformation over time under sustained stresses (creep), and numerous studies have shown that pavements with RAP base courses are susceptible to rutting (Bleakley and Cosentino, 2013; Dong and Huang, 2014). Dong and Huang (2014) found that RAP showed larger permanent deformation than limestone aggregate and gravel following repeated triaxial load testing. Researchers have also noted the relative weakness of RAP. Bennert et al. (2000) found that natural aggregate had higher shear strength than pure RAP. Thakur et al. (2010) found a decrease in CBR values in RAP with increasing binder content and decreasing fines content. Bleakly and Cosentino (2003) found that the limerock bearing ratio (LBR, a variation of the CBR test) values for RAP fell short of acceptable limits; the researchers found that strength issues can be mitigated by using RAP blended with natural aggregate or by chemical stabilization.

Documented freeze-thaw behavior of RAP is inconsistent in the literature. Bozyurt (2011) found the summary resilient modulus (SRM) of RAP decreased at a relatively rapid rate after five freeze-thaw cycles, with a decreasing rate after subsequent cycles. Attia and Abdelrahman (2010), however, reported an increase in SRM after freeze-thaw cycling.

RCA is produced by crushing concrete demolition waste from existing concrete structures, ensuring the removal of any reinforcing steel. RCA contains residual cement paste and mortar, which results in higher water absorption capacity as well as lower density compared with natural aggregate, as well as lowering abrasion resistance (e.g., LA abrasion test). Due to the crushing processing method, RCA tends to show more angularity than virgin aggregate (Butler et al., 2013). Ceylan (2014) reports that pavement sections with RCA base courses showed pavement condition index (PCI) values and international roughness index (IRI) values that were slightly higher than sections with natural aggregate base courses; however, these differences were not found to be significant at the 95% confidence level. Edil et al. (2012) reported a 30% LA abrasion loss for RCA material, compared with a loss of 23% for class 5 natural aggregate. Edil et al. (2012) conducted Micro-Deval trials on RCA samples sourced from Texas and California with varying (5, 10, and 30) wet/dry cycles. California RCA showed losses of 16% over all cycles, Texas RCA showed 17%, 19% and 21% losses at 5, 10, and 30 wet/dry cycles respectively, and class 5 aggregate showed losses of 12% for 5 and 10 wet dry cycles, and 11% after 30 cycles. No clear trends in Micro-Deval losses were observed with respect to varying wet/dry cycles.

RCA shows unique behavior due to the presence of cement paste. The RCA base course may show an increase in strength due to hydration and pozzolanic reactions that produce Calcium Silica Hydrate (C-S-H) (Jayakody, 2014). In addition, complications related to drainage may occur due to the cement paste. Tufa is the formation of precipitates from water supersaturated with calcite. Tufa acts to block drainage paths, resulting in an accumulation of moisture in base layers. Ceylan (2014) found that tufa formation appears to be directly related to

the proportion of fines (smaller than #4 sieve). Reducing the amount of fines in the RCA reduced tufa formation, but the potential for tufa formation could not be completely eliminated. Ceylan (2014) points out the need for additional research in the area of tufa formation.

Many states limit the proportion of reclaimed material that can be used in pavement base courses. In Wisconsin, Section 301 of WisDOT Standard Specifications for Highway and Structure Construction provides specifications for base course aggregate.

Extensive testing of pavement with a reclaimed base course has been conducted at the MnROAD facility. MnDOT boasts over 30 years' experience in flexible pavement construction using RAP and suggests that adherence to best practices will produce a pavement that can outperform pavements with natural aggregate base courses (Johnson and Clyne, 2012).

Hydraulic conductivity is a key parameter for drainage considerations in a base course. A number of laboratory and field procedures exist to determine soil permeability. Laboratory procedures include constant and falling-head permeameters, conductivity tests with pressure chambers or consolidometers. Values can also be determined empirically through grain size distribution correlations. In the field, hydraulic conductivity can be measured by a number of means. Selection of an appropriate field test depends on the position of the water table and the level of soil saturation. Ring infiltrometers are commonly used, as well as air entry permeameters. The Guelph permeameter (Humboldt Manufacturing Company) can measure in-situ hydraulic conductivity within a two-hour timeframe and can take readings from 15-75 cm below the ground surface.

1.4 Organization of the Report

This report is organized in seven chapters. Chapter One introduces the problem statement and objective of the research. The literature review and synthesis is presented in Chapter Two, and the research methodology is discussed in Chapter Three. Chapters Four and Five present a detailed analysis of laboratory and field testing programs, respectively, with critical analysis of the outcome. Long-term pavement performance evaluation of Wisconsin pavements on CA, RCA, and RAP base layers is presented in Chapter Six. Critical evaluation of the research outcome, followed by conclusions and recommendations, is provided in Chapter Seven.

Chapter 2

Background

This chapter presents background information on the use of the recycled aggregate materials as unbound base course layers in HMA pavements. The objective of this literature review is to present the current mechanical, physical, strength, and durability parameters of RAP and RCA in terms their adequacy for use as base course layers in HMA pavement construction. The Midwest state highway agencies specifications for recycled aggregates are summarized also in this chapter. In addition, this chapter includes the results of a comprehensive survey conducted to obtain information from state highway agencies on the use of recycled aggregates in HMA pavement base layers as well as the performance of these pavements.

2.1 Introduction

Around two billion tons of aggregate are produced in the United States annually, and aggregate production is projected to exceed 2.5 billion tons by the year 2020 (Ceylan, 2014). These figures raise issues related to sustainability, as quarries gradually become depleted and environmental regulations become more stringent. With high demand for construction aggregate and an increasing public desire to manage waste materials in a responsible manner, there has been increasing interest in the prospect of utilizing by-products and reclaimed material for pavement construction purposes. For base courses in flexible pavement systems, the use of Recycled Asphalt Pavement and Recycled Concrete Aggregate has been the subject of increased research in recent years (Gabr and Cameron, 2012).

Recycled Asphalt Pavement or Reclaimed Asphalt Pavement (RAP) refers to the removal of existing HMA pavement layers (e.g., by milling) and reprocessing (e.g., crushing) for reuse as base course materials. The process of producing the RAP whether milling or crushing leads to higher fractions of finer particles. (Guthrie et al., 2007; FHWA, 2008; Edil et al., 2012). Recycled Concrete Aggregate (RCA) refers to the removal and crushing Portland Cement Concrete (PCC) waste such as PCC pavements and buildings, ensuring the removal of any reinforcing steel, tie bars, and dowel bars. PCC waste is usually crushed to produce particle size distributions conforming with typical aggregate gradation. One major difference between RAP and RCA is the absorption where RAP materials have low absorption resulting from the asphalt cement coating around aggregate particles, which minimizes water intrusion. On the other hand, RCA materials have high water absorption due to the presence of the cement paste (Edil et al., 2012; FHWA, 2008; Poon et al., 2006; Kuo et al., 2002).

2.2 Characterization of Recycled Aggregates Properties

There have been significant number of studies on the properties of RAP and RCA including strength, permanent deformation and modulus evaluations, durability characterization, drainability, and self-cementing behavior. Recycled aggregate properties and characteristics that are of importance to the base layer performance are the same one for natural/virgin aggregate. These properties are discussed and presented in detail in WHRP aggregate base durability study by Titi et al. (2018). In addition, Saeed (2008) presented updated tables (Tables 2.1-2.4) on the important recycled aggregate properties and their relation to pavement base layer pavement characterization/performance in his NCHRP report 598. In NCHRP synthesis 524, Tutumluer et al. (2018) presented summaries of aggregate quality requirements for pavements including the properties of recycled aggregates for base layers.

The relevant studies investigating the properties and characteristics of the recycled aggregates with focus on RAP and RCA for use in pavement base course layers are discussed below.

2.2.1 Variability in Materials Source

Variability is a material inability to contain the same physical and mechanical properties for every sample taken. For example, variability in RCA material includes original concrete mixture ingredients, construction practices, consolidation and curing, and particle size distribution. The original ingredients used to mix, and cure concrete can vary from ready mix companies. Not every batch of concrete will be the same. Drive time to job site, gradation of material, amounts and proportioning of material can all influence the properties of concrete. Construction practices affect the outcome of concrete for example, the amount of time and effort vibrating air out of the mixture or even the operator that crushes concrete. Poorly consolidated concrete material will create a variance in the concrete mixture, physical properties will change if the concrete is not consolidated correctly. Excessive amounts of entrapped air create more pores in the concrete resulting in more permeable pores which will affect its resistance to frost damage, increase absorption which will affect the optimum moisture content. Entrapped air will also reduce its strength effecting its resistance to abrasion and impact, and insufficient soundness will accelerate freeze thaw cycling. Variability in particle size distribution will directly impact the self-cementing, density, permeability, and durability of RCA material.

2.2.2 Physical Properties

Typical physical properties and other mechanical and durability related properties of RCA and RAP are summarized in Tables 2.5 and 2.6. Blankenagel (2005) reports on tests performed by others on specific gravity, absorption and LA Abrasion tests on RCA materials. As presented in Table 2.5, the RCA data have lower specific gravity and higher absorption than

virgin aggregates with absorption increasing as particle size decreases. LA Abrasion loss depends on the original strength of concrete.

Table 2.1: Flexible pavement performance parameters and contributing factors (Saeed, 2008).

Distress	Description of distress	Unbound layer failure mechanism	Contributing factors
Fatigue Cracking	Fatigue cracking first appears as fine, longitudinal hairline cracks running parallel to one another in the wheel path and in the direction of traffic; as the distress progresses the cracks interconnect, forming many-sided, sharp angled pieces; eventually cracks become wider and, in later stages, some spalling occurs with loose pieces prevalent. Fatigue cracking occurs only in areas subjected to repeated loadings.	Lack of base stiffness causes high deflection/strain in the HMA surface under repeated wheel loads, resulting in fatigue cracking of the HMA surface. High flexibility in the base allows excessive bending strains in the HMA surface. The same result can also be due to inadequate base thickness. Changes in base properties (e.g., moisture induced) with time can render the base inadequate to support loads.	Low modulus of the base layer Low density of the base layer Improper gradation High fines content High moisture level Lack of adequate particle angularity and surface texture Degradation under repeated loads and freeze-thaw cycling
Rutting/Corrugation	Rutting appears as a longitudinal surface depression in the wheel path and may not be noticeable except during and following rains. Pavement uplift may occur along the sides of the rut. Rutting results from a permanent deformation in one or more pavement layers or subgrade, usually caused by consolidation and/or lateral movement of the materials due to load.	Inadequate shear strength in the base allows lateral displacement of particles with applications of wheel loads and results in a decrease in the base layer thickness in the wheel path. Rutting may also result from densification of the base due to inadequate initial density. Changes in base (mainly degradation producing fines) can result in rutting. The base can also lose shear strength from moisture-induced damage, which will cause rutting.	Low shear strength Low base material density Improper gradation High fines content High moisture level Lack of particle angularity and surface texture Degradation under repeated loads and freeze-thaw cycling High moisture content coupled with traffic can contribute to stripping
Depressions	Depressions are localized low areas in the pavement surface caused by settlement of the foundation soil or consolidation in the subgrade or base/subbase layers due to improper compaction. Depressions contribute to roughness and cause hydroplaning when filled with water.	Inadequate initial compaction or nonuniform material conditions result in additional reduction in volume with load applications. Changes in material conditions due to poor durability or frost effects may also result in localized densification with eventual fatigue failure.	Low density of base material Low shear strength of the base material combined with inadequate surface thickness
Frost Heave	Frost heave appears as an upward bulge in the pavement surface and may be accompanied by surface cracking, including alligator cracking with resulting potholes. Freezing of underlying layers resulting in an increased volume of material cause the upheaval. An advanced stage of the distortion mode of distress resulting from differential heave is surface cracking with random orientation and spacing.	Ice lenses are created within the base/subbase during freezing temperatures, particularly when freezing occurs slowly, as moisture is pulled from below by capillary action. During spring thaw large quantities of water are released from the frozen zone, which can include all unbound materials.	Freezing temperatures Source of water Permeability of material high enough to allow free moisture movement to the freezing zone, but low enough to also allow suction or capillary action to occur

Table 2.2: Recycled aggregate particle properties that influence pavement performance (Saeed, 2008).

Physical properties	Chemical properties	Mechanical properties
Particle gradation and shape (max/min sizes) Particle surface texture Pore structure, absorption, porosity Permeability (hydraulic properties) Specific gravity Thermal properties Volume change (in wetting & drying) Freezing/thawing resistance Deleterious substances	Solubility Base exchange Surface charge Chemical reactivity (resistance to attack by chemicals, chemical compound reactivity, oxidation and hydration reactivity, organic material reactivity) Chloride content pH-level	Particles strength Particle stiffness Wear resistance Resistance to degradation Particle shape of abraded fragments

Table 2.3: Relevance of recycled material mass properties for various applications (Saeed, 2008).

Mass Property of Material	Relevance of Mass Property to the Use of Recycled Material as					
	Structural Layer	Construction Platform	Drainage Layer	Frost Blanke	Control Pumping	Select Fill
Shear Strength	Y	Y	N	N	N	N
California Bearing Ratio (CBR)	Y	Y	N	N	N	Y
Cohesion & Angle of Internal Friction	Y	N	N	N	N	N
Resilient or Compressive Modulus	Y	Y	Y	Y	Y	Y
Density	Y	Y	N	Y	Y	Y
Permeability	N	N	Y	Y	Y	N
Frost Resistance	Y	N	Y	Y	N	Y
Durability Index	Y	N	Y	Y	Y	N
Resistance to moisture damage	Y	N	N	N	N	N

Y: Relevant; N: Not relevant

Table 2.4: Links between aggregate properties and performance of flexible pavements (modified from Saeed, 2008).

Performance parameter	Related aggregate property	Test measures
Fatigue Cracking	Stiffness	Resilient modulus, Poisson's ratio, gradation, fines content, particle angularity and surface texture, frost susceptibility degradation of particles, density
Rutting, Corrugations	Shear Strength	Failure stress, angle of internal friction, cohesion, gradation, fines content, particle geometrics (texture, shape, angularity), density, moisture effects
Fatigue Cracking, Rutting, Corrugations	Toughness	Particle strength, particle degradation, particle size, gradation, high fines
	Durability	Particle deterioration, strength loss
	Frost Susceptibility	Permeability, gradation, percent minus 0.02 mm size, density, nature of fines
	Permeability	Gradation, fines content, density

Table 2.5: Typical physical properties of RAP and RCA by FHWA (2008) (Edil et al., 2012).

RAP	Physical Properties	
	Unit Weight	1,940 – 2,300 kg/m ³ (120 - 140 pcf)
	Moisture Content	Normal: Up to 5% Maximum: 7 - 8%
	Asphalt Content	Normal: 4.5 – 6%
	Asphalt Penetration	Normal: 10 – 80% at 25°C (77°F)
	Absolute Viscosity or Recovered Asphalt Cement	Normal: 4,000 – 25,000 poises at 60°C (140°F)
	Mechanical Properties	
	Compacted Unit Weight	1600 – 2,000 kg/m ³ (100 – 125 pcf)
	California Bearing Ratio (CBR)	100% RAP: 20 – 25% 40% RAP and 60% Natural Aggregate: 150% or higher
RCA	Physical Properties	
	Specific Gravity	2.2 to 2.5 (Coarse Particles) 2.0 to 2.3 (Fine Particles)
	Absorption	2 to 6% (Coarse Particles) 4 to 8% (Fine Particles)
	Mechanical Properties	
	LA Abrasion Loss	20 – 45% (Coarse Particles)
	Magnesium Sulfate Soundness Loss	4% or Less (Coarse Particles) Less than 9 (Fine particles)
	California Bearing Ratio (CBR)	94 – 148%

Table 2.6: Properties of typical RCA materials (Blankenagel, 2005).

Author	Bulk Specific Gravity		Absorption (%)		L. A. Abrasion (%)
	Coarse*	Fine	Coarse*	Fine	
Hansen (2)	2.49	2.28	3.7	9.8	22 - 40
Fergus (2, 5)	2.52	2.23	2.54	6.5	-
Chini (4)	-	-	-	-	26 - 37
Yrjanson (5)	2.4	2.2	4.3	5.9	20 - 45
Yrjanson (5)	2.45	2.36	3.31	6.45	-

*Coarse aggregate consists of particles retained on the No. 4 standard sieve.

The absorption values for RCA, RAP, VA, and RCA-VA blend from a study by Edil et al. (2012) are depicted in Figure 2.1. The absorption of values for RCA materials ranged from 5 to 6.5% while the values for the RAP materials ranged from 0.6 to 3%.

Figure 2.2 depicts the gravel, sand, and fines size fractions of RCA and RAP materials as well as class 5 MnDOT virgin aggregate. The RAP and RCA material were obtained from different states and were subjected to various tests by Edil et al. (2012). The sand size fraction of RAP and RCA is of interest to the current WHRP study based on our analysis of the RCA and RAP gradation of various base layer samples obtained from Wisconsin HMA pavements. An examination of the figure indicated that two out of the seven RCA and five out of the seven RAP samples possessed sand size fraction of more than 50%. The class 5 MnDOT aggregate as well as the MN blend (50% RCA and 50% class 5 VA) also contained sand size fraction of more than 50%.

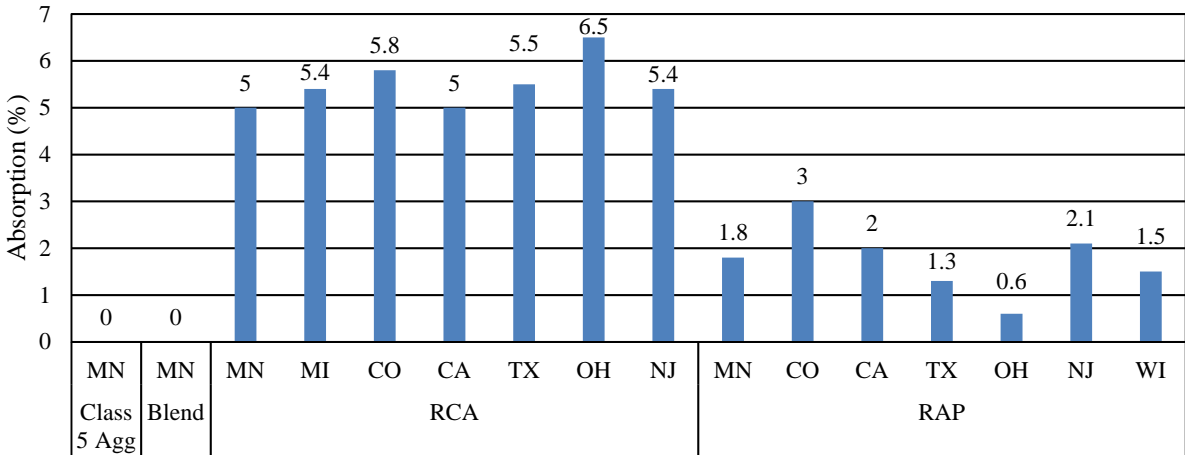


Figure 2.1: Absorption values for RCA and RAP materials from different resources (data obtained from Edil et al., 2012).

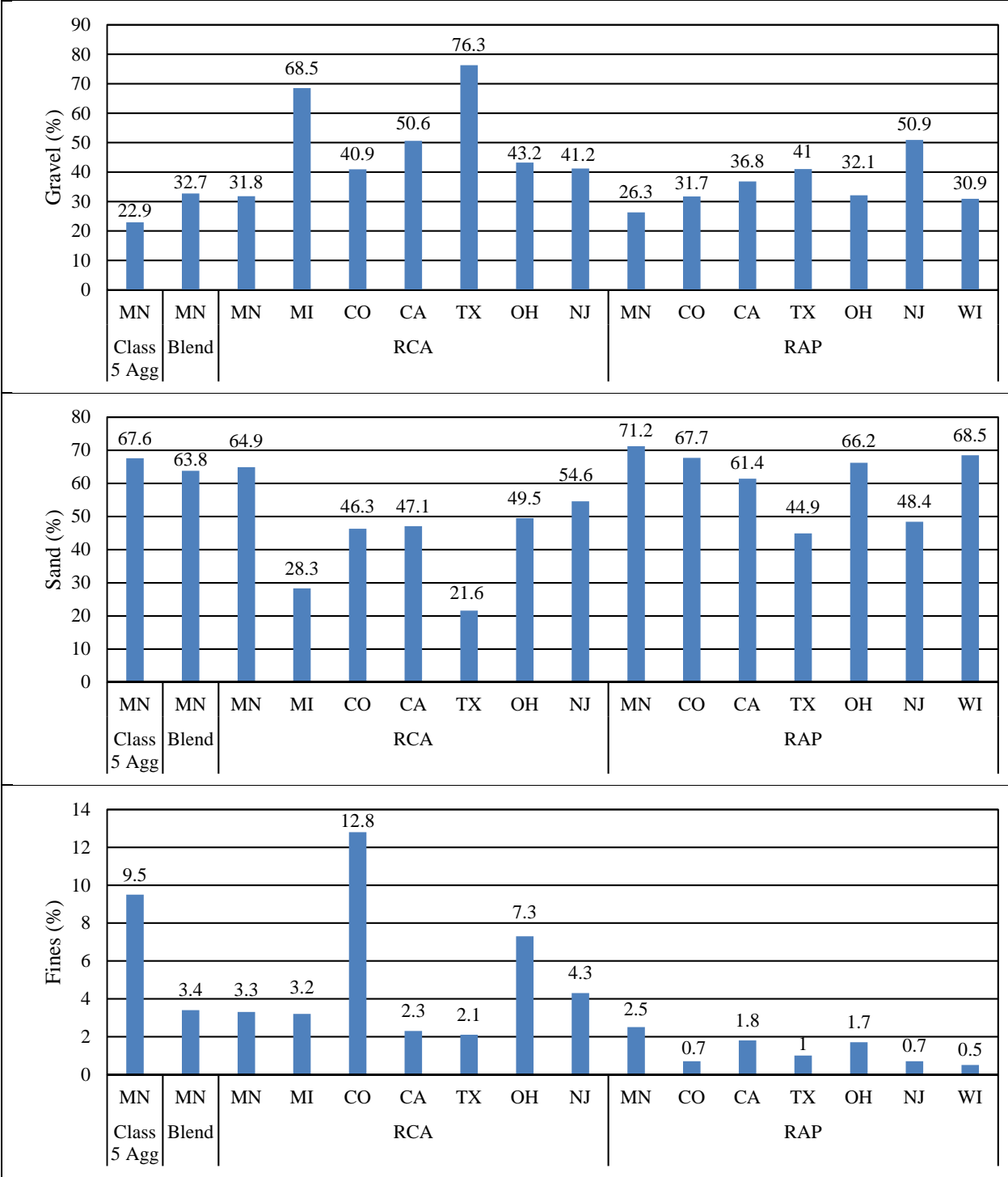


Figure 2.2: Gradation of RCA and RAP materials from different resources compared with MnDOT class 5 and blend aggregate (data obtained from Edil et al., 2012).

2.2.3 Strength, Resilient Modulus, and Deformation Properties

Gabr et al. (2013) conducted a repeated load triaxial testing (RLTT) on three base materials; two recycled concrete aggregate materials, and a virgin aggregate (VA). The RLTT specimens were tested to a target dry unit weight ratio of 98% of maximum dry unit weight using Modified Proctor compaction test at three different moisture contents of 60, 80, and 90% of optimum moisture content. Their test result concluded that the resilient modulus of the two RCA ranged between 340 and 715 MPa (49.3 and 103.7 ksi), and the moduli of VA varied in range from 270 and 450 MPa (39.2 and 65.3 ksi). Resilient modulus according to Gabr et al. (2013) was dependent on both moisture content and applied stress. Also, two specimens of VA failed the AUSTROADS test protocol for RLTT at 90% moisture content; however, none of the RCA specimens failed at these specified moisture contents.

Arshad and Ahmed (2017) performed a study to evaluate the properties of RAP blends as base/subbase layers for flexible pavements. The study focused on blends containing 50% and 75% RAP with virgin aggregates and RCA. Researchers conducted laboratory tests to measure resilient modulus (M_R) and constrained modulus (M_C) for virgin aggregates and the RAP blends. Samples containing 75% RAP/25% aggregate showed a significant increase in M_R values, especially under greater bulk stresses. M_C values, on the other hand, decreased with higher RAP proportions. The study also discovered that an increase in the percentage of RAP contents led to an increase in the accumulated strains under cyclic loading. Another finding was the relationship between M_R and bulk stress. A power law with a coefficient of correlation value between 0.96 and 0.99 can represent the relation. From 0 to 50% RAP content, there is little change in permanent strain. The same trend was noted when RAP content increased from 50 to 75%. When RAP contents increased from 50 to 75% there was marginal increase in M_R , as well. The constrained modulus test results showed greater permanent strain than the resilient modulus test results for the same RAP proportions.

A characterizing of Recycled Concrete Materials (RCM) available in Utah County was carried out by Blankenagel (2005) for two main sources of RCA. In this study, demolition and haul-back materials were investigated. The main objective of this study was to evaluate the physical properties, strength parameters, and durability characteristics. A non-destructive and laboratory testing were conducted. In the field, RCM was monitored over a year period to obtain stiffness variation in the base layer. Also, in situ testing such as Ground Penetrating Rader (GPR), heavy Clegg impact soil tester (HCIST), soil stiffness gauge (SSG), and a portable falling-weight deflectometer (PFWD) were performed. Laboratory tests included California bearing ratio (CBR), unconfined compressive strength (UCS), stiffness, freeze-thaw cycling, moisture susceptibility, LA abrasion, salinity, and alkalinity. It was found that RCM base layer was susceptible to stiffness changes due to changes in moisture content in both spring and summer testing. In the spring thaw, 60 % loss in CBR and stiffness losses compared with summer-time value. Furthermore, average CBR and UCS for both demolition and haul-back

materials are 22, 55% and 1,260, 1,820 kPa, respectively. In addition, both materials exhibited strength and stiffness losses during freeze-thaw cycling; however, the demolition material reached a residual stiffness faster than the haul-back material. It was noted an increase in UCS of 180% during 7-day curing period due to self-cementing that exhibited by both materials. Likewise, an increase of strength and stiffness for both materials after compaction in the first 2-3 days due to unhydrated cement interaction with water to form new cementitious bonds. Batch plant overruns refer to excess concrete produced at a batch plant but never delivered to a job site, and haul-back material refers to excess concrete delivered to a job site but returned to the batch plant.

Alam et al. (2010) performed a study to investigate the resilient modulus of pavement base layers with varying RAP contents. Samples with 100% RAP, RAP/Class 6 (CL 6) material at 30, 50, and 70% RAP, and RAP/taconite at 50% RAP were tested. Testing was also performed with varying moisture contents and dry densities. Moisture contents of 7 and 8%, as well as dry densities of 125, 130, and 135 pcf were used. Their findings showed that M_R increases with increased RAP content and dry density. Researchers also noted that moisture content had little to no effect on M_R . Sensitivity analysis using AASHTOWare Pavement ME Design performed on different RAP contents showed a decrease in distress level with an increase in RAP content. The researchers noted that the binder content of the original mix was 5.5%. The collected RAP had an average binder content of 3.65%. Huesemann et al. (2005) stated that the leaching of the old asphalt pavement does not exceed typical groundwater standards and is therefore not a hazardous waste. Alam et al. (2010) concluded that RAP is an acceptable alternative for pavement base layers, even at high percentages of RAP content.

A study by Song and Ooi (2010) analyzes the resilient modulus of a crushed RAP, a basaltic virgin aggregate, and a 50% RAP/50% virgin aggregate blend for use in pavement base and subbase layers. The RAP is made up of Type A basalt, while the virgin aggregate is a lower grade Type B basalt from a Hawaiian quarry. A number of laboratory tests were performed to measure the basic material properties. Before the resilient modulus test, all samples underwent 500 cycles of a 95 kPa deviator stress with a 105 kPa confining pressure. This was done to condition the samples and simulate base layer compaction. The resilient modulus test was run following AASHTO T 307 where M_R variation was investigated at different values of water content, density, stress level, and RAP content. The results show a decrease in stiffness for all samples when water content was increased. For the virgin aggregate and blended sample, the M_R increased with increased dry density. For RAP, the dry density did not have a significant effect on the M_R . Higher resilient modulus values were observed for all samples when the confining and deviator stresses were increased. M_R showed a linear relationship with deviator stress at each of the five confining stress levels. Researchers noted that the blended sample was more “sensitive” to confining stress, while the 100% virgin aggregate sample was more “sensitive” to deviator stress. Researchers also noted that higher percentages of RAP increased the stiffness of

the base course materials. A model was presented to predict the M_R with respect to the water content, density, stress level, and percent RAP.

Cerni and Colagrande (2012) executed a study to compare the resilient modulus of pavement subbases comprised of recycled aggregates with those of virgin aggregates. Two virgin aggregate samples were tested. Mixture 1 contained crushed lime rocks. Mixture 2 was the same as mixture 1, except for the substitution of silty clay in place of the fine lime material. The silty clay component allowed researchers to test the influence of fine material with plastic properties on the resilient modulus. All three samples were compacted with a Gyratory Compactor and conditioned by a series of vertical loads to stabilize plastic deformation prior to resilient modulus testing. The effects of tension state and saturation on resilient modulus were studied during the triaxial testing. The results showed that the recycled blend performed very similarly to both virgin aggregate blends. The recycled material exhibited a low susceptibility to water. The M_R of the recycled blend at optimum moisture level varied by only 7% with the M_R values at saturation. The low susceptibility proves that recycled material can provide a stable subbase when moisture conditions vary. The researchers also noted that the stiffness of the recycled blend increased with confining pressure, making it a suitable material for deep pavement layers.

Gabr et al. (2013) evaluated the use of RCA as pavement base course material. Three specimens were tested, including two RCA samples from two different sources and one virgin aggregate sample (quartzite). Researchers performed a variety of material property tests in addition to the repeated load triaxial test (RLTT). The M_R and permanent deformation were tested at 60, 80, and 90% of optimum moisture content. The resilient modulus of the RCA was greater than that of the virgin aggregate. The M_R of the RCA ranged between 490 and 1,020 MPa, while the M_R values for the virgin aggregate ranged between 480 and 685 MPa. The permanent deformation varied with moisture content for all samples. The least deformation was observed at 60% of the optimum moisture content for each sample. The RCA materials exhibited acceptable deformation rates at every moisture content, but the virgin aggregates failed to meet requirements at 80 and 90% of the optimum moisture content. Testing showed RCA shrinkage lasted 84 days with 1,600 micro-strain was the maximum dry shrinkage measured. The RCA samples had increased compressive strength over time, displaying the self-cementing abilities of recycled concrete aggregates. CBR values increased with moisture content for every sample. One RCA sample had CBR values greater than the virgin aggregate, but the other did not.

Sangiorgi et al. (2017) performed a study to compare the properties of a 100% RAP Cold Recycled Mixture (CRM) with Hot Mix Asphalt as a pavement base layer. The recycled mixture consisted of RAP, cement, and bituminous emulsion. The CRM and HMA were tested in the laboratory and field. The results of the gyratory compaction and air voids content analysis showed little difference between the CRM and HMA. The compactability and workability of the 100% RAP CRM was very similar to the HMA. However, the CRM and HMA exhibited significant differences in indirect tensile and modulus test results. The indirect tensile strength

(ITS) was 0.51 MPa for CRM and 0.90 MPa for HMA. While the ITS of CRM was much lower than that of HMA, the indirect tensile strength of CRM would still be acceptable under Italian specifications for base layers containing 30% RAP (0.35 MPa). In wet conditions, the reduction in ITS was approximately the same for the two mixtures, proving that a high RAP content does not affect water susceptibility. Like the ITS results, the indirect tensile stiffness modulus values (ITSM) of CRM were lower than those of HMA at every temperature tested. The ITSM of the CRM would still pass regulations, though. The tests performed on core samples from the field yielded results similar to the laboratory tests. However, the ITS and ITSM values for the 100% RAP CRM from the field were much higher compared with the laboratory samples. The ITS of the field CRM increased to 0.97 MPa. The researchers concluded that the properties of the Cold Recycled Mixture are highly dependent on the mix design and RAP quality.

Bradshaw et al. (2016) evaluated the resilient moduli of RAP and virgin aggregate blends. Subbase samples from Route 165 in Rhode Island were tested. When Route 165 was reconstructed during the 1980s an unbound mixture of cold recycled RAP/virgin aggregates was blended off-site and laid down as subbase. The same stretch of road was reconstructed in 2013 using full-depth reclamation (FDR). The asphalt pavement layer was pulverized and blended with the 1980s RAP mixture subbase to produce the in-situ FDR RAP blends. For the study, several stabilizers (liquid calcium chloride, asphalt emulsion, and Portland cement) were added to the FDR RAP samples. The RAP content of the FDR RAP blends was estimated to be 57 to 71%, while the RAP content of the cold recycled material was estimated to be 14 to 39%. The specimens tested included the cold recycled RAP blend, the untreated FDR RAP blend, the FDR RAP blend treated with calcium chloride, the FDR RAP blend treated with asphalt emulsion, and the FDR RAP blend treated with Portland cement. The samples were compacted at optimum moisture content and 95% max dry density for the resilient modulus test. The M_R varied from 120 to 502 MPa for the cold recycled RAP blend. Shear softening and hardening were minimal. The M_R of the untreated FDR RAP blends was higher than that of the cold recycled RAP, with values ranging from 171 to 578 MPa. This was due to the greater RAP content. Compared with the cold recycled RAP blend, these samples exhibited greater shear softening and permanent strains. Both the calcium chloride-treated and emulsion-treated FDR RAP blends had M_R values within the untreated FDR RAP range but showed increased permanent deformation. The M_R was the highest for the FDR RAP treated with Portland cement. M_R values varied from 528 to 1,898 MPa for the 7-day sample. The Portland cement-treated RAP experienced much less permanent deformation compared to the other samples.

A study by Kim and Labuz (2007) was performed to analyze the strength and deformation characteristics of blended RAP/aggregate base material. Researchers tested samples with optimum moisture contents of 65 and 100% of the optimum. Their test results showed the resilient modulus increased with increased confining pressure. Greater stiffness was noted at 65% of the optimum moisture content than that at 100%. The RAP samples were tested in cyclic triaxial tests at two deviator stresses (35 and 50% peak stress) to evaluate the permanent

deformation. When compared with 100% aggregate material, the RAP samples showed a permanent deformation at least two times greater, as reported by Kim and Labuz (2007). Permanent deformation increased with increased RAP content. However, the authors declared that base material containing different RAP proportions performed similarly to 100% aggregate in regard to resilient modulus and strength when properly compacted.

According to Stolle et al. (2014), shear strength is slightly reduced, and deformation is increased when RAP is mixed with natural aggregate, as determined by triaxial tests. Lukanen and Kruse (2000) recommend a maximum RAP content of 50% in base layers, claiming that RAP proportions greater than that lead to reduced strength and increase rutting. A study by Edil et al. (2012) compared the FWD results of RAP, RCA, a 50/50 blend of RCA/Class 5, and 100% Class 5 material (control). The test cells with 100% Class 5 material had the greatest elastic maximum deflections. The 50/50 RCA/Class 5, RAP, and RCA followed in that order. Edil et al. (2012) reported that RCA had the highest resilient moduli, while 100% Class 5 material had the lowest resilient moduli.

2.2.4 Durability and Self-Cementing

For a report for South Dakota DOT (SDDOT), Cooley et al. (2007) sampled city streets and interstate highways in South Dakota to assess RCA properties. Five of the six samples taken were non-plastic and met the South Dakota Aggregate Base Course requirements ($LL < 25$, $PI < 6$). The LA Abrasion test was performed on the coarse RCA materials. The results range from 25.8 to 40.7 percent loss, meeting SDDOT standards. The loss ranged from 15.2 to 19.4 percent for the fine RCA materials, as measured with Micro Deval testing. The sodium sulfate soundness test yielded measurements ranging from 9 to 36 percent loss. A loss of 5 to 17 percent was determined from the New York freeze-thaw test. A combination of Micro-Deval and New York freeze-thaw revealed losses from 23 to 33 percent.

The use of coarse recycled concrete aggregates (CRCA) in conjunction with fine recycled concrete aggregates (FRCA) as sub-base materials has been widely studied. It is known that the strength of the sub-base materials prepared with RCA increases over time, this mechanism, known as the self-cementing properties and is believed to be governed by the properties of the fine portion of the RCA (< 5 mm).

Poon et al. (2006) investigated the cause of the self-cementing effect and its influence on the overall sub-base materials properties by measuring X-ray diffraction patterns, pH values, compressive strength and permeability of various size fractions of the FRCA. The results of X-ray diffraction detected C_2S and $C_3H_2S_3$ (C-S-H) in the RCA samples, because C_2S is a less reactive compound compared to C_3S (Newman and Choo, 2003), it cannot be completely hydrated even after a long curing time. This is why C_2S was still detected in the RCA samples. However, the presence of C_2S gradually vanished as the size of RCA increased. The results revealed that the < 0.15 mm fraction of RCA could be a highly possible cause of the self-

cementing properties of RCA as this fraction contained the highest amount of C_2S . Although C_2S was not detected in the 0.3 to 0.6 mm fraction of RCA, the pH value of the solution prepared with this fraction of RCA was the highest compared to the pH values of the other fractions. The results implied that there were more amorphous hydration products in the fraction of 0.3 to 0.6 mm, which could provide sufficient lime (CaO) for additional reaction. The results indicate that the size fractions of <0.15 and 0.3 to 0.6 mm (active fractions) were most likely to be the principal cause of the self-cementing properties of the FRCA. However, the effects on the properties of the overall RCA sub-base materials were minimal if the total quantity of the active fractions was limited to a threshold by weight of the total fine aggregate.

Jitsangiam et al. (2015) studied the self-cementing characteristics of RCA. Researchers tested a high-grade RCA (HRCA) and a road base RCA (RBRCA). The HRCA was produced from demolition material of buildings and bridges. The RBRCA contained high-grade recycled concrete mixed with brick and clean rubble (roughly 5% by mass). The unconfined compressive strength (UCS), indirect tension dynamic modulus, and resilient modulus (M_R) were tested. X-ray diffractometry (XRD) and scanning electron microscope (SEM) analyses were included in the study, as well. Results showed that the HRCA exhibited more self-cementing properties than the RBRCA. The HRCA transformed from an unbound material to a bound material. The HRCA samples displayed bound material properties after 6 months, according to the UCS, indirect tension dynamic modulus, and M_R test results. Secondary hydration occurred in the HRCA samples, as proven by the XRD and SEM analyses. Unlike the HRCA, the RBRCA remained as an unbound material, exhibiting minimal self-cementing. The researchers suggest that the addition of bricks and clean rubble decreases self-cementing. Self-cementing can have negative effects. When the RCA self-cements and increases in modulus over time, transverse cracking and block cracking can occur in the pavement.

2.2.5 Permeability, Density, and Bearing Capacity

Kang et al. (2011) conducted a study to evaluate the performance mixtures of four recycled materials with aggregates for possible use in base and subbase layers as a replacement of 100% virgin aggregates. The investigated materials included recycled asphalt pavement and recycled concrete material (RCM), fly ash (FA), and foundry sand (FS). Water retention, hydraulic conductivity, resilient modulus, shear strength, and leaching of these mixtures were investigated. Kang et al. (2011) analyzed the hydraulic and mechanical characteristics of these mixtures and the results suggested that the drainage characteristics of these investigated recycled materials mixtures with aggregates are comparable or better than that of 100% aggregates. Kang et al. (2011) stated that blending RAP, RCM, and FA+RAP with aggregates increased resilient modulus of these mixtures reaching values that are comparable or better than that of 100% aggregates. Kang et al. (2011) concluded that FA, RAP, and RCM mixtures will be good replacement for virgin aggregates in base and subbase layers of roads.

Seferoglu et al. (2018) studied the bearing capacity and permeability of various RAP blends as base course materials. Researchers tested the following untreated aggregate samples: 100% virgin aggregate, 100% RAP, 10, 20, 30, 40, 50, and 60% RAP/virgin aggregate mixtures. Researchers also evaluated the performance of cement-treated RAP. The 100% RAP/1% cement, 100% RAP/2% cement, and 100% RAP/3% cement blends were tested. The laboratory tests included bitumen content, sieve analysis, modified Proctor, soaked CBR, and constant head permeability tests. Modified Proctor test results showed that the optimum moisture content (OMC) of RAP blends was lower than that of the virgin aggregate. Increasing the cement content in the 100% RAP blends; however, led to an increase in the OMC and max dry density (MDD). From the soaked CBR tests, researchers discovered that the CBR values decreased significantly as the RAP content increased. The CBR value of the virgin aggregate was 178%, compared to 31% for the 100% RAP sample. Increasing the cement content in the 100% RAP blends did increase the CBR values, though. Raising the cement content from 0 to 3% resulted in a CBR increase from 31 to 138%. Permeability tests indicated a reduction in permeability with increasing percentages of RAP. For the cement-treated RAP blends the permeability was almost zero. Seferoglu et al. (2018) recommend mixing RAP with virgin aggregates or cement for use in pavement base layers. The carrying capacity of RAP by itself is too low. The researchers suggest limiting cement content to 3%, otherwise the fine content would be too high.

A study by Edil et al. (2012) reported a relationship between RAP content and maximum dry density and optimum moisture content by using the Proctor compaction test. The test showed that a higher RAP content caused a decrease in maximum dry density and optimum moisture content. Another test was performed with a gyratory compaction device and showed the same decrease in optimum moisture content with higher RAP content, however, the maximum dry density did not change. For those tests, the maximum dry density for RAP varied from 1,978 to 2,332 kg/m³, while the optimum moisture content varied from 5 to 10.3%. For RCA, the values varied from 1,823 to 2,020 kg/m³ and 7.5 to 12.1%. Other tests included in the Edil et al. (2012) report present conflicting results for strength and stiffness, durability, and permanent deformation measurements, which illustrates the variation in aggregate properties, depending on the material type, source, original mix proportions, etc.

2.3 State Transportation Agencies Specifications

Today, more than ever, we are seeing much more emphasis and focus on sustainable and recycled resources. In the engineering and construction industry, many companies are seeking recycled materials to construct and complete civil/structural projects. While much research has been conducted to determine the physical/mechanical/durability properties of recycled material, there is still not enough data on long term performance presented. In the pavement and highway sector, state Department of Transportation agencies are utilizing recycled concrete aggregates for pavement base and subbase course layers. While many of the state DOTs utilize RCA materials for pavement base and subbase course layers, there are still several state DOTs who do not. The

research herein is to determine which states utilize RCA material for base and subbase course layers and analyze the grain size distribution and other physical and engineering properties found in the DOTs Standard Specifications (SS).

Determining the RCA grain size distribution and other parameters for DOTs was established by downloading and researching all 50 states SS. Reviewing the SS, a search criterion of “base course” was used to find the base course section and specifications. When reviewing the base course section, the subcategory “Materials” typically detailed the location and whereabouts to determine the materials allowed for base course. Once directed to the Materials section, specifications for materials, gradation, and other properties were found. If this section allowed the use for RCA, the information was further reviewed, and the gradation and other parameters were recorded. A list of states allowing RCA material for base and subbase layers was tabulated and the maximum and minimum percent passing by mass for gravel, sand, and fines (according to USGS standards) was recorded, see Table 2.7 for details.

To further investigate the research of RCA material used as base and subbase layers, we are interested in the RCA acceptance in the Midwest states due to harsh natural environments the pavements experience over the Spring, Summer, Fall, and Winter seasons. Two major concerns with RCA material is the freeze-thaw cycles and the amount of moisture the base and subbase layers will contain. Knowing which Midwest states allow RCA, we can find the typical range for gradation and further our understanding of RCA material in the Midwest. Table 2.8 contains the maximum and minimum percent passing by mass for gravel, sand, and fines found in the Midwest states. Some Midwest states contain multiple types of categories for gradation based on its use. Figure 2.3 shows the comparison of the maximum and minimum values and gravel, sand, and fines allowed for RCA gradation.

The purpose of knowing the maximum and minimum values for various types of RCA categories, we can determine the allowable range for grain size distribution. Figure 2.4 shows the upper and lower boundaries of gradation for all Midwest states and their appropriate gradation category. One can see that the gradation is within a respectable range and is in a tight group. With this information we can determine and verify what types of gradation for RCA can outperform the freeze-thaw cycles. Knowing the amounts of fine material and other specified parameters, shown in Table 2.8, we can also understand and make educated assumptions about drainability in the base and subbase layers. By looking at the upper and lower boundaries of the grain size distribution we can determine that the distribution curves are well graded. Knowing the gradation curve is well graded, how does that effect drainability in the layers? Does the amount of fines in the material absorb moisture allowing a secondary rehydration process in the RCA material? If so, will the rehydration form a cementitious material in the void spaces resulting in a reduction of drainability? Does the material gain stiffness over time due to the secondary rehydration process? Questions are raised based on the upper and lower boundaries of the RCA materials accepted in the Midwest States and should be investigated.

Table 2.7: State DOTs allowing RCA material for base and subbase layers and the maximum and minimum percent passing by mass for gravel, sand, and fines.

State DOT	Material Type	Gravel Fraction		Sand Fraction		Silt & Clay Fraction	
		(Max.) 3"- #4	(Min.) 3"- #4	(Max.) #4 - #200	(Min.) #4 - #200	(Max.) <#200	(Min.) <#200
California	Class 2, 1 1/2"	100	45	50	6	12	0
	Class 2, 3/4"	100	87	65	5	12	0
	Class 3, 1 1/2"	100	45	65	6	19	0
	Class 3, 3/4"	100	87	75	7	19	0
Colorado	Class 1	100	95	65	30	15	3
	Class 2	100	95			15	3
	Class 4	100	50	50	30	12	3
	Class 5	100	95	70	30	15	3
	Class 6	100	95	65	25	12	3
Connecticut	B	95	25	45	0	5	0
Delaware	RCA	100	50	50	2		
Illinois	Type A-CA6	100	60	56	30	12	4
	Type A-CA10	100	65	60	40	12	5
	Type B-CA6	100	60	56	30	12	4
	Type B-CA10	100	65	60	40	13	5
	Type B-CA12	100	75	70	35	13	5
	Type B-CA19	100	90	75	10	15	5
	Type C-CA7	100	30	10	0		
	Type C-CA11	100	30	12	0		
	Type C-CA5	100	0	6	0		
Iowa	12b	100	50	30	5	7	3
Louisiana	RPCC	100	70	65	12	8	0
Maine	Type D	80	25	30	0	7	0
Maryland	Base Coarse	100	50	55	12	8	0
Massachusetts	RCA	100	50	60	8	10	0
Michigan	21AA	100	50	45	20	8	4
	21A	100	50	45	20	8	4
	22A	100	65	50	30	8	4
Minnesota	Class 3	100		100	0	6	0
	Class 4	100		100	0	6	0
	Class 5	100	25	65	0	6	0
	Class 5Q	100	35	45	0	6	0
	Class 6	100	25	65	0	6	0

Table 2.7 (Cont.): State DOTs allowing RCA material for base and subbase layers and the maximum and minimum percent passing by mass for gravel, sand, and fines.

State DOT	Material Type	Gravel Fraction		Sand Fraction		Silt & Clay Fraction	
		(Max.) 3" - #4	(Min.) 3" - #4	(Max.) #4 - #200	(Min.) #4 - #200	(Max.) <#200	(Min.) <#200
Mississippi	3/4"	100	50	65	15	15	5
	No. 610	100	50	65	12	12	5
	No. 825B	100	60	70	9	18	4
Missouri	Type 1	100	60	60	10		
	Type 2	100	60	60	10	15	0
	Type 3	100	70	50	15	12	0
Nebraska	RCA	100	85	50	20	8	0
New Mexico	Type 1	100	80	60	20	10	3
	Type 2	100	80	70	30	15	6
North Carolina	ABC	100	45	40	0	12	0
North Dakota	Salv. B. Course	100	90	85	15	12	0
Oklahoma	A	100	30	60	8	12	4
	B	100	25	50	7	10	3
	C	100	60	60	15	5	0
	D	100	25	10	0	2	0
Pennsylvania	1	60	0				
	3	100	0				
	467	100	10	5	0		
	5	100	0				
	57	100	25	10	0		
	67	100	20	10	0		
	7	100	40	15	0		
	8	100	85	30	0		
	10	100	85	30	10		
	2A	100	36	50	10		
OGS	100	36	40	0			
Rhode Island	1B	100	50	55	8	10	2
South Carolina	RCA	100	48	60	11	12	0
South Dakota	Subbase	100	70	70	10	15	0
	Base Coarse	100	68	70	13	12	3
Tennessee	Grading A	100	35	10	0		
	Grading B	100	65	55	4		
Texas	Grade 1-2	100	35	55	10		
	Grade 3	100	90	55	15		
	Grade 5	100	35	55	10		
Vermont	RCA	100	30	40	15	6	0
Wisconsin	3-inch	100	40	40	5	12	2
	1 1/4"	100	42	63	8	12	2
	3/4"	100	50	70	10	15	5

Table 2.7 (Cont.): State DOTs allowing RCA material for base and subbase layers and the maximum and minimum percent passing by mass for gravel, sand, and fines.

Midwest State DOT	Material Type	Gravel Fraction		Sand Fraction		Silt & Clay Fraction	
		(Max.) 3"- #4	(Min.) 3"- #4	(Max.) #4 - #200	(Min.) #4 - #200	(Max.) <#200	(Min.) <#200
IL	Type A-CA6	100	60	56	30	12	4
	Type A-CA10	100	65	60	40	12	5
	Type B-CA6	100	60	56	30	12	4
	Type B-CA10	100	65	60	40	13	5
	Type B-CA12	100	75	70	35	13	5
	Type B-CA19	100	90	75	10	15	5
	Type C-CA7	100	30	10	0		
	Type C-CA11	100	30	12	0		
	Type C-CA5	100	0	6	0		
	Type C-CA7	100	30	10	0		
IA	12b	100	50	30	5	7	3
MI	21AA	100	50	45	20	8	4
	21A	100	50	45	20	8	4
	22A	100	65	50	30	8	4
MN	Class 3	100		100	0	6	0
	Class 4	100		100	0	6	0
	Class 5	100	25	65	0	6	0
	Class 5Q	100	35	45	0	6	0
	Class 6	100	25	65	0	6	0
ND	Salv. B. Course	100	90	85	15	12	0
SD	Subbase	100	70	70	10	15	0
	Base Coarse	100	68	70	13	12	3
WI	3-inch	100	40	40	5	12	2
	1 1/4"	100	42	63	8	12	2
	3/4"	100	50	70	10	15	5

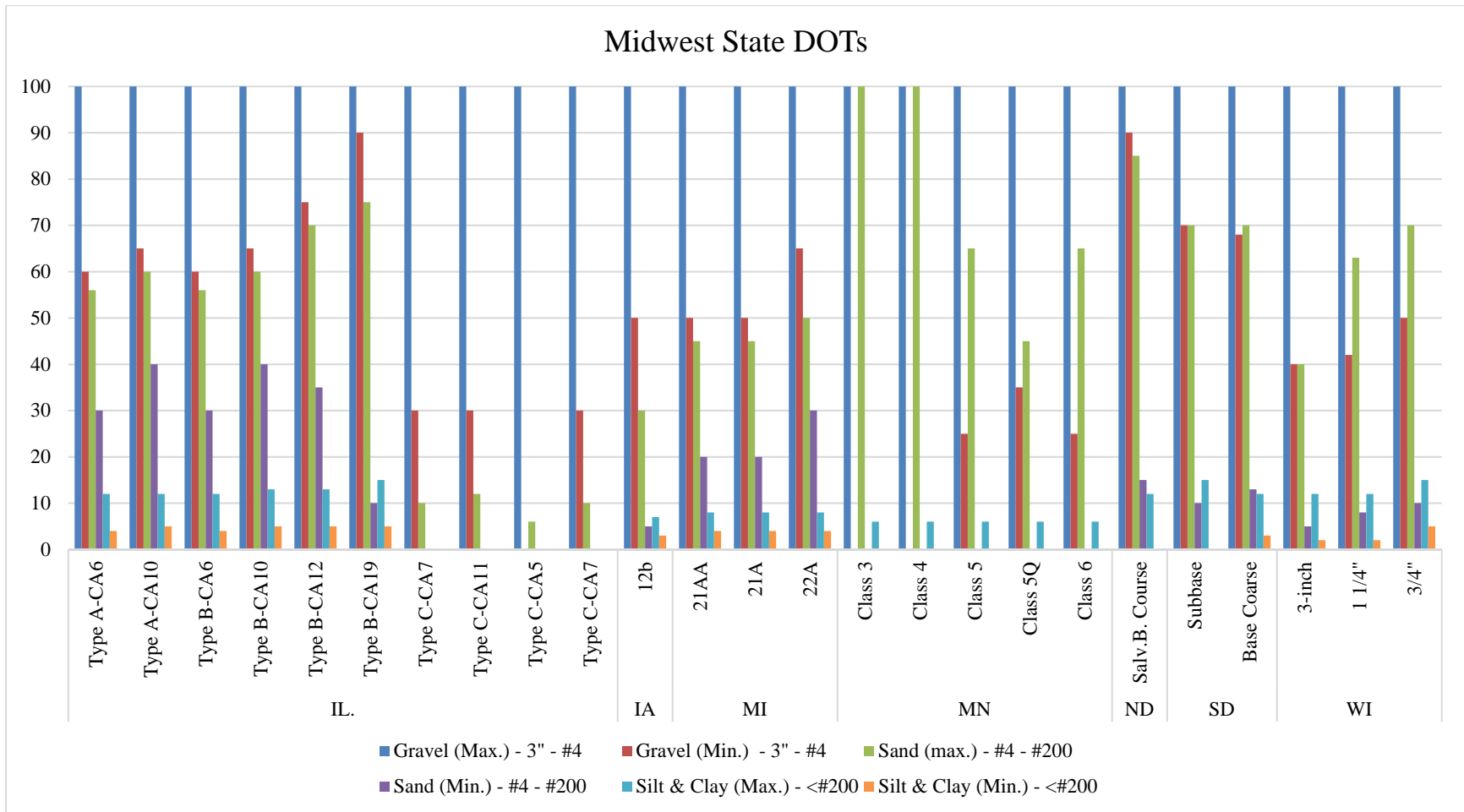


Figure 2.3: Midwest State DOTs maximum and minimum values for gravel, sand, and fines.

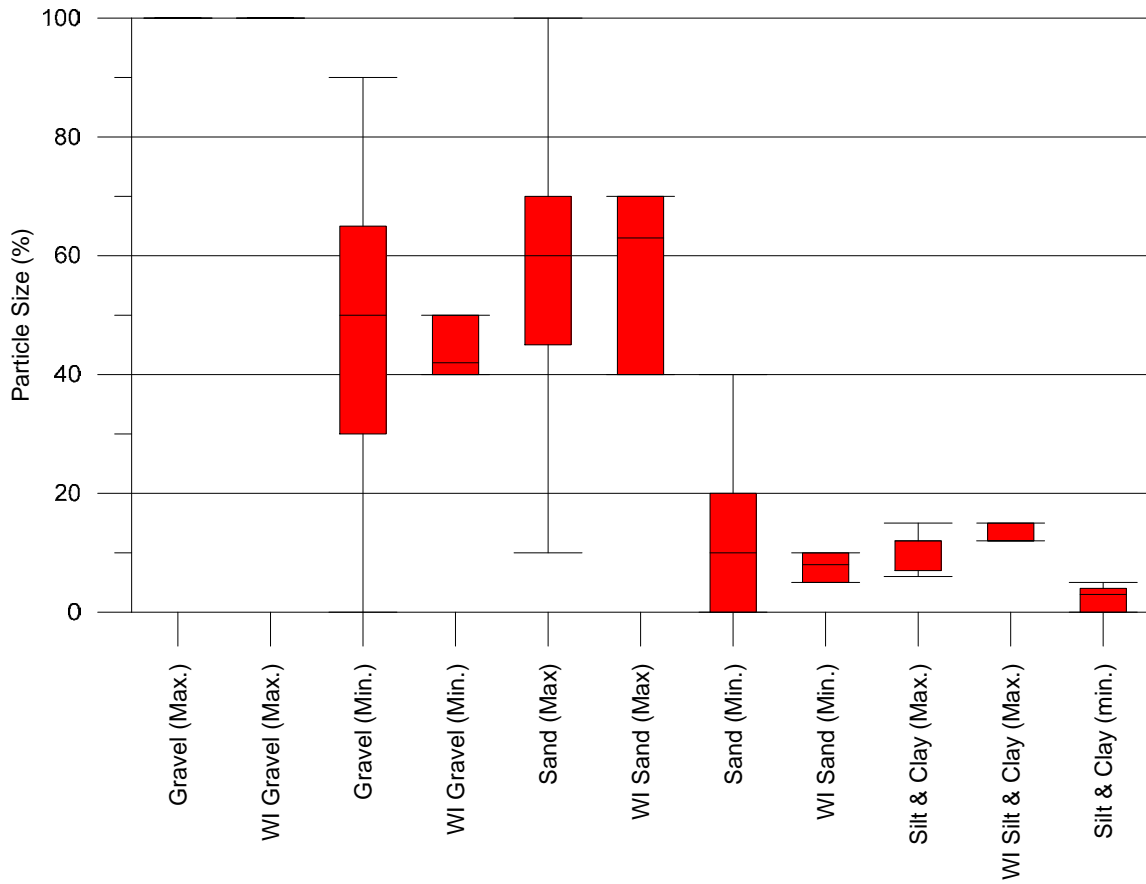


Figure 2.4a: Midwest State DOTs maximum and minimum values for gravel, sand, and fines.

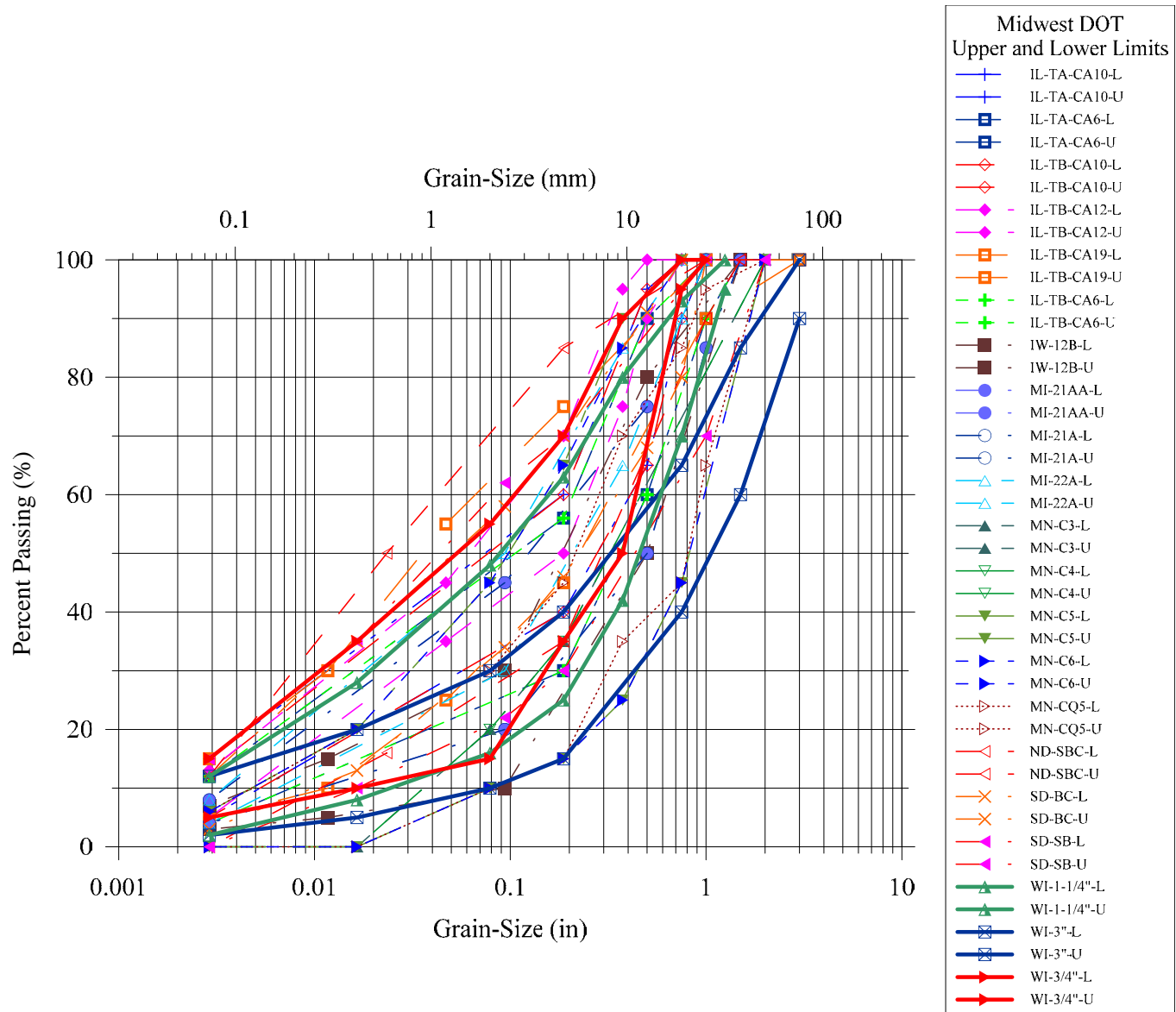


Figure 2.4b: Midwest State DOTs RCA grain size distributions.

Table 2.8: Midwest State DOTs allowing RCA material for base and subbase.

Midwest State DOT	Material Type	Parameters
IL	Type A-CA6	≤ 5% deleterious Materials
	Type A-CA10	≤ 5% deleterious Materials
	Type B-CA6	≤ 6% deleterious Materials
	Type B-CA10	≤ 6% deleterious Materials
	Type B-CA12	≤ 6% deleterious Materials
	Type B-CA19	≤ 6% deleterious Materials
	Type C-CA7	≤ 10% deleterious Materials
	Type C-CA11	≤ 10% deleterious Materials
	Type C-CA5	≤ 10% deleterious Materials
	Type C-CA7	≤ 10% deleterious Materials
MI	21AA	LA Abrasion ≤ 50%
	21A	LA Abrasion ≤ 50%
	22A	LA Abrasion ≤ 50%
ND	Salv. B. Course	≤ 3% deleterious Materials
SD	Subbase	P.I. ≤ 6, LA Abrasion ≤ 50%
	Base Coarse	LL ≤ 25, P.I. ≤ 6, LA Abrasion ≤ 40%
WI	3-inch	LL ≤ 25, PI ≤ 6
	1 1/4"	LL ≤ 25, PI ≤ 6
	3/4"	LL ≤ 25, PI ≤ 6

According to the survey and DOT specifications from various DOTs around the country, RAP material is not widely used for base and subbase purposes. Many of the responses in the survey showed that the use of RAP material is used for HMA surface and binder course. One of the 25 respondents does in fact allow the use and contains standard specifications for RAP material used as Base and Subbase purposes. Minnesota documents contain specifications for the use of RAP material as base and subbase layers.

The most commonly used material in base course layers for HMA pavements in Minnesota has been 50% recycled HMA/concrete 30% in place reclamation. Performance issues with using RAP materials in the pavement base layers identified rutting which may be a result of poor subgrade, under compacted base or lack of crushing in the base. As a result, Minnesota DOT specifications have regulated a maximum lift thickness of 6", equipment requirements for HMA base, and test roll all bases. See the survey and the summary below for some of the answers to the survey questions by MnDOT.

Compared with the most commonly used material as base course, what is the approximate percentage of RAP use?

- RAP is the most commonly used material, whether in reclamation or milling are used along with RCA to make base. So, millings/reacclimated HMA about 50% of all base and RCA about 25% of all base.

What construction control method do you use for RAP bases?

- Spot test have to meet quality compaction (the eye ball test) and either the DCP, specified density or light weight deflectometer (LWD). Then finally the base is test rolled (the final 100% coverage eyeball and depression test).

When RAP is used as base layers do you have any issues with HMA performance compared with similar pavements with virgin aggregate base layers?

- As long as material is compacted well, in lifts 6" or less with the right equipment and test rolled, then no problem.

Do you have any comment on RCA and or RAP that you believe is important to this issue?
Please specify

- Make sure high RAP is compacted well.

The survey summary is presented below:

Survey: Performance of Recycled Concrete Aggregate (RCA) and Reclaimed Asphalt Pavement (RAP) as Base Layers in HMA Pavements:

1- Question: What is the most commonly used material in base course layers for HMA pavement?

Answers:

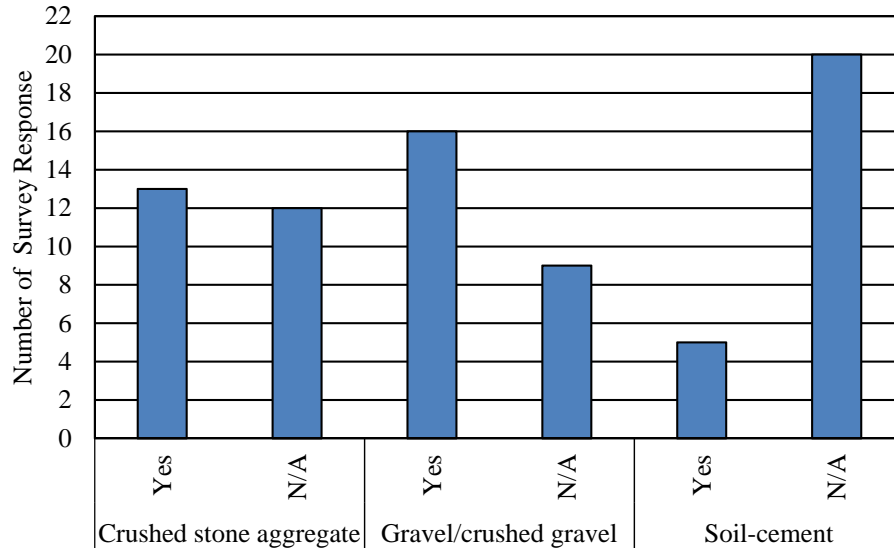


Figure 2.6: Most commonly used material in base course layers.

Comments:

- 1) Connecticut state utilizes a high percentage of reclaimed aggregates in addition to broken stone and crushed gravel products.
- 2) Crushed stone in 75% and crushed gravel in 25% of state.
- 3) Florida has a widely available source of unique unconsolidated limestone, that we refer to as limerock. We do not consider this unbound aggregate.
- 4) New HMA pavement typically isn't constructed over a base layer and is built on either chemically stabilized (lime, fly ash, or cement) soil or just prepared subgrade soils.
- 5) 50% recycled HMA/concrete (30% in place reclamation, i.e. in place recycled HMA and base, 15% gravel, and 5% crushed carbonates).

2- Question: Does your department allow the use of Recycled Concrete Aggregate (RCA) materials in HMA pavement as base, drainable base or/and subbase course layers?

Answers:

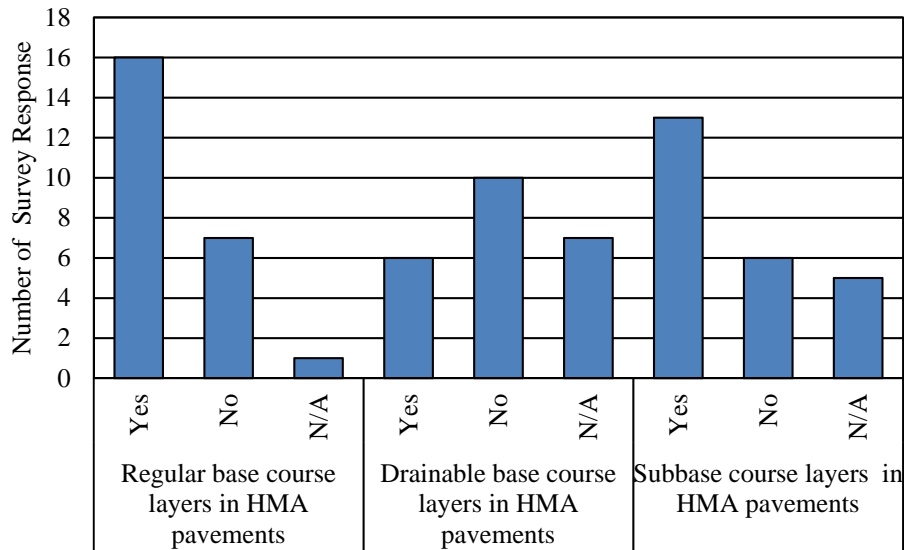


Figure 2.7: Allowing the use of RCA as regular, drainable base and subbase layers.

Comments:

- 1) Connecticut state uses subbase and processed aggregate base under HMA pavements. The materials used for this are broken stone, crushed gravel, or reclaimed aggregates.
- 2) RCA is allowed if base course properties are met for class of base specified. Gradation, R-value, and LA Abrasion.
- 3) We do use a rubblization specification for our pavement reconstruction type projects.
- 4) We use rubblization of existing concrete pavements to create subbase for new pavements/overlays where possible. We have had limited experience using RCA. We have had tufa issues with a recent project.
- 5) We allow up to 50% RCA by weight in our base courses.
- 6) WYDOT will implement a new specification for the 2020 construction season
- 7) Allowed up to 50%. Must be blended with virgin aggregate base or subbase.
- 8) Its use is not allowed in HMA.
- 9) Subbase use is generally acceptable, but not part of our standard specifications and requires a special provision or a change order. Some RCA has been blended with our untreated base course on some projects by change order or special provision, as long as the material meets the same requirements we have for an aggregate base.
- 10) The conditions when RCA is used is typically during concrete pavements reconstruction, really no experience under HMA.
- 11) As mentioned in previous question base course materials are rarely used for HMA but we do construct them occasionally. We only have one layer of base materials when used that we call "Foundation Course"
- 12) Not used for our best drainable aggregate, but we do have a moderate drainable base, where concrete is allowed.

13) SDDOT only allows RCA that is obtained from a SDDOT project/pavement. Therefore, although RCA is allowed as base for HMA, not many projects create RCA and use HMA as the new pavement.

3- Question: Does your department allow the use of Reclaimed Asphalt Pavement (RAP) materials in HMA pavement as base, drainable base or/and subbase course layers?

Answers:

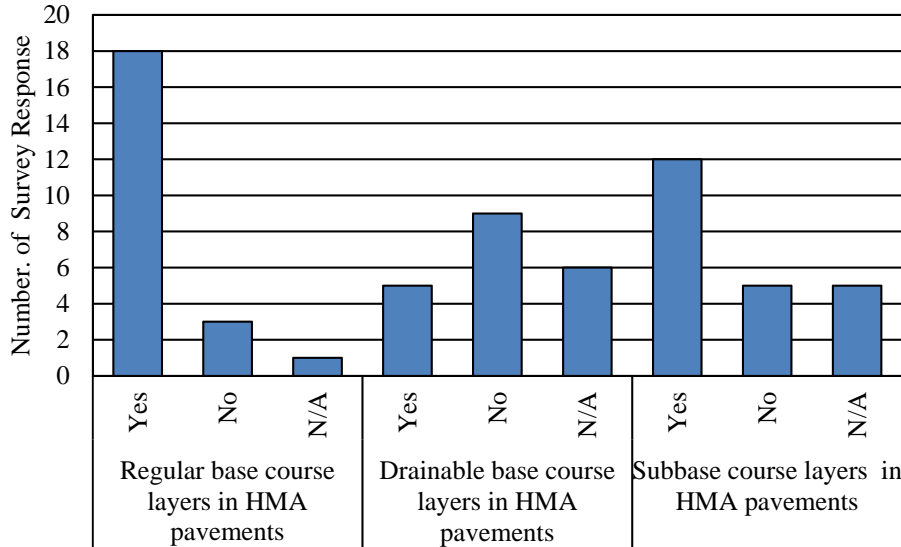


Figure 2.8: Allowing the use of RAP as regular, drainable base and subbase layers.

Comments:

- 1) Connecticut state uses subbase and processed aggregate base under HMA pavements. The materials used for this are broken stone, crushed gravel, or reclaimed aggregates.
- 2) RAP is not widely used as a base course under HMA pavements but is occasionally allowed. Allowance is based on Regional approval and satisfaction of materials properties. Most Contractors feel RAP has more value when recycled back into the asphalt.
- 3) Our use of RAP is strictly as a component of standard HMA/WMA pavement layers.
- 4) We do have a base course that allows for the use of some RAP.
- 5) Standard specifications allow RAP in HMA mix (without distinctions described above) subject to gradations permitted for HMA.
- 6) We allow up to 40% by weight of RAP in our base courses.
- 7) RAP only allowed as a top 3" surcharge on top of base course gravels
- 8) Allowed up to 50%. Must be blended with virgin aggregate base or subbase.
- 9) RAP is not allowed in HMA surface courses. It is allowed in subbase courses as FDR.
- 10) Though deviations have occurred on some projects, this is not our standard approved practice.
- 11) Its use is typically blended with the top two inches of existing base course.
- 12) Must be blended with crushed stone/gravel, maximum 25% and 30% respectively

- 13) GDOT has placed a very limited test section using 100% recycled base via cold central plant recycling.
- 14) Same comment as in question #2.
- 15) Not used for our best drainable aggregate, but we do have a moderate drainable base, where concrete is allowed.
- 16) RAP is typically blended about 50/50 with virgin granular base when used as a base course under HMA pavement.

4- Question: Compared with the most commonly used material as base course, what is the approximate percentage of RCA use?

Answers:

- 1) More than 50%. Reclaimed base material often contains RCA
- 2) 10%
- 3) Only a trace since we have only done limited projects.
- 4) We do not use RCA for base course.
- 5) RCA isn't used as a material in base course.
- 6) 1%
- 7) 0% in preservation projects and 75% for reconstruction projects
- 8) Approximately 1% or less. Not aware of any used in last 15 years.
- 9) 0.1%
- 10) Negligible.
- 11) 5%
- 12) 60%
- 13) Not exactly sure but it is very low.
- 14) 1%, recently allowed for use, but little interest as of now
- 15) 15%
- 16) 1%, most RCA is used in commercial developments and County work.
- 17) 10% for HMA pavements
- 18) RAP is the most commonly used material, whether in reclamation or milling are used along with RCA to make base. So millings/reclamated HMA about 50% of all base and RCA about 25% of all base.
- 19) Very small percent used as base under HMA

5- Question: Compared with the most commonly used material as base course, what is the approximate percentage of RAP use?

Answers:

- 1) More than 50%. Reclaimed base material often contains RAP.
- 2) 5%.
- 3) 15% for HMA base.
- 4) 0 % for base/subbase and 15% in WMA/HMA mixtures.
- 5) We do not use RAP as an aggregate base course.
- 6) No standard is specified, proportions depend on project. Use of RAP is not required but is not uncommon.
- 7) 99%.
- 8) 35%.
- 9) Not often.

- 10) 1%.
- 11) Approximately 30%.
- 12) 5% as FDR.
- 13) Negligible.
- 14) 0%.
- 15) 30%.
- 16) Less than 25 %.
- 17) 0%, RAP not used in bases, only in HMA.
- 18) RAP is the most commonly used material, whether in reclamation or milling are used along with RCA to make base. So, millings/reacclimated HMA about 50% of all base and RCA about 25% of all base.
- 19) Using a 50/50 blend of RAP with virgin granular base under HMA, most projects (guess 60%) use RAP as base.

6- Question: What are your agency's current goals regarding the use of RCA and RAP?

Answers:

- 1) No goals. Regularly utilized product.
- 2) No percentage goals specified. Allowance of RAP and RCA is based on Contractors business decision and satisfaction of required properties.
- 3) Reviewing the possibility of in line crushing for existing PCC.
- 4) To use both where appropriate.
- 5) No goals.
- 6) Regarding RAP - likely cost control and reuse of material that might otherwise be landfilled.
- 7) We have no established goals. It's allowed as a convenience to the contractor.
- 8) Increase the use of RCA and RAP in future projects.
- 9) 40% RAP Blend.
- 10) RCA for base and RAP as a % mix in asphalt pavement.
- 11) No target established.
- 12) Do not have any set goals.
- 13) The general goal is reuse in construction of reclaimed materials, but the goals are not quantified. Not much concrete is removed for recycling. There are large amounts of RAP milled, but virtually all of it goes back into the asphalt mix itself.
- 14) Use RCA as an economically driven option for subbase. Utilize, manage, encourage, and allow RAP in HMA courses. Pay attention to current research and information for adaptation.
- 15) Continue to use as is, RCA is restricted within 100 feet of a watercourse.
- 16) We continue to allow the use of recycled materials in our gravel materials and HMA mixtures. We are looking for other uses as long as the benefits outweigh the costs.
- 17) To have specifications to allow its use and let economics determine its use.
- 18) Increase use of RCA; develop specifications for RAP for base courses.
- 19) The State of Florida's goal is for 100 % use of RCA by any user.
- 20) Maintain its use specifically for PCC pavements.

- 21) I think that they close to being met. We are liberal in allowing both both HMA and RCA in base and surfacing. FYI, RCA not allowed for surfacing except for shoulders for two reasons: dust and wire mesh (tires destroying potential).
- 22) SDDOT makes effort to use all RCA and RAP generated from our pavements. SDDOT does not allow contractor furnished (tipping piles) RAP and RCA sources.

7- Question: Does your department have any of the following specifications for Recycled Concrete Aggregate (RCA) use as base layer materials?

Answers:

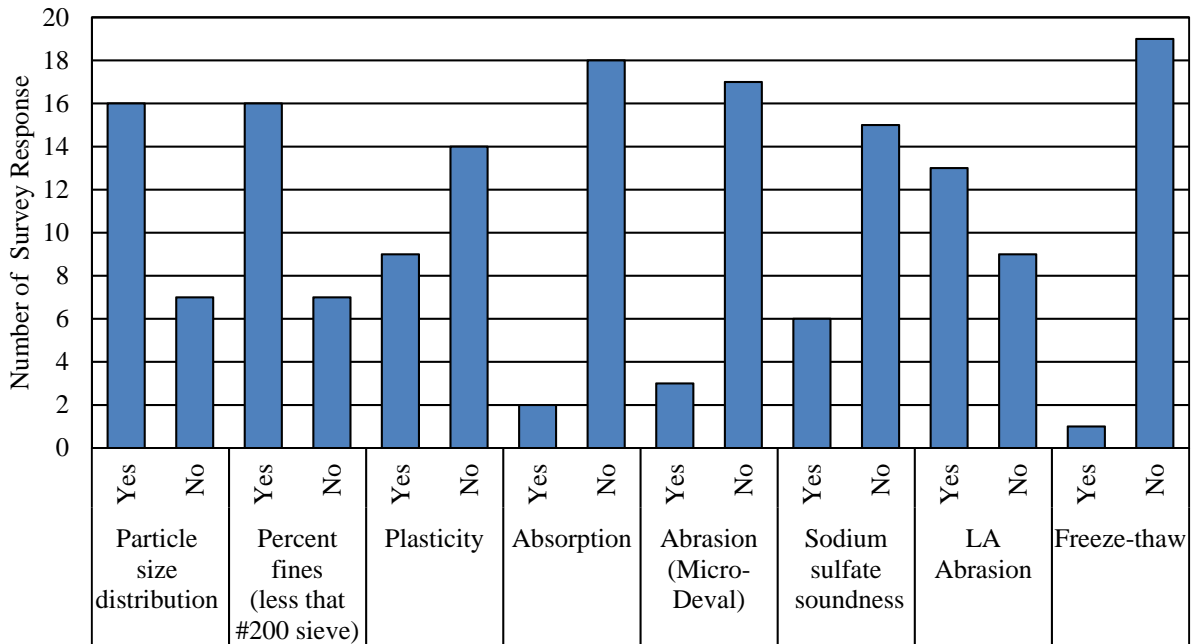


Figure 2.9: Specifications for RCA materials.

Comment:

- 1) On all reclaimed road bed materials depending on item requirements. Magnesium sulfate soundness in Connecticut.
- 2) RCA is not allowed to be used as a base layer.
- 3) When blending recycled materials into our base courses, the blend must meet the same requirements of our standard crushed aggregate base course materials.
- 4) Also include R-Value.
- 5) RCA may be used as 12" - 18" thick 'rock base', per Missouri Standard Spec Section 303. The spec has basic deleterious material, particle size distribution and shape factor requirements, and does not differentiate between RCA and crushed stone. Maximum particle size is large and may be up to 6" less than the base thickness. RCA may also be used for conventional 'aggregate base course', placed in a 4" or 6" layer, as defined in Missouri Standard Spec Section 304. The spec does not differentiate between RCA and crushed stone in material requirements.

- 6) also specify minimum percent of crushed material, 40 to 50% depending on application.
- 7) We allow RCA in our Reclaimed Pavement Borrow Material.
- 8) Percent fine on the -100 screen (5-18% passing) Spec that require it to be free of hazardous materials.
- 9) Section 815 of our Standard Specifications.
- 10) Florida has a Limerock Bearing Ratio (LBR) test modeled on the California Bearing Ratio (CBR) test. Some differences: LBR - reference pressure is 800 psi, soak time 48 hours, penetration measurement at 0.1 inch (2.54 mm) (corrected for curve inflection); CBR - reference pressure is 1,000 psi, soak time 96 hours, penetration measurement at 2.5 mm and 5 mm (corrected for curve inflection)

8- Question: Does your department have any of the following specifications for Reclaimed Asphalt Pavement (RAP) use as base layer materials?

Answers:

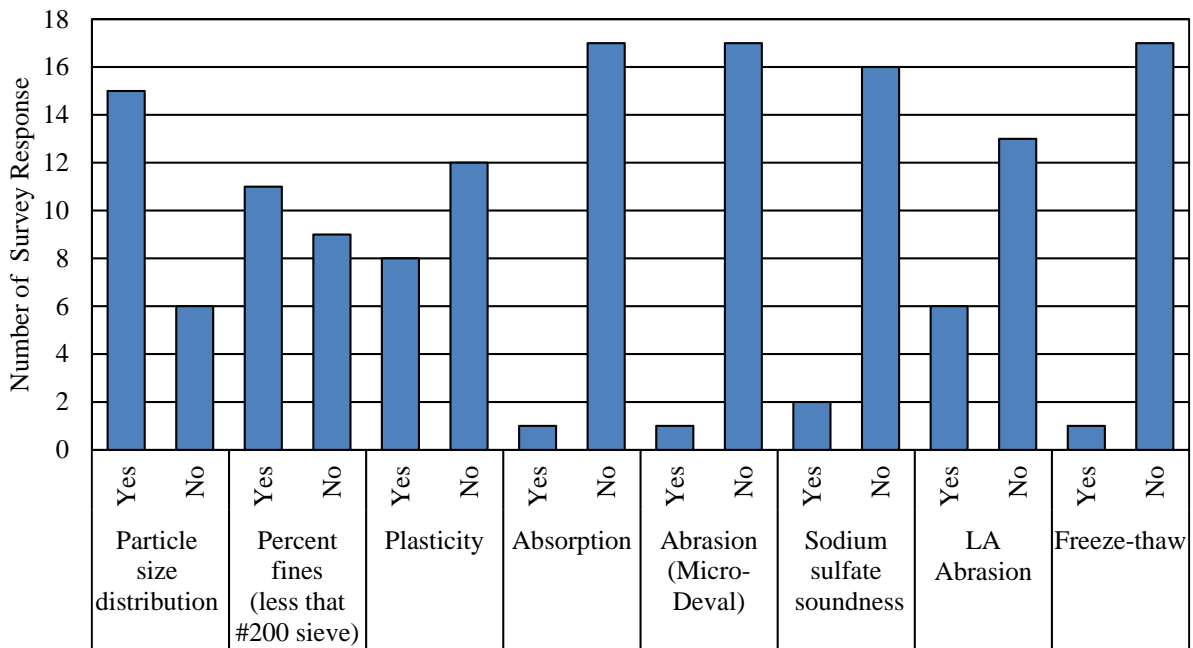


Figure 2.10: Specifications for RAP materials.

Comment:

- 1) On all reclaimed road bed materials depending on item requirements. Magnesium sulfate soundness in Connecticut.
- 2) RAP as a base is required to consist of 100% crushed recycled asphalt pavement. As such, fines contents are generally lower, and non-plastic.
- 3) 1-1/2-inch max, visual inspection when used as shoulder stone.
- 4) We do not use RAP as a base layer material.
- 5) RAP is required to processed so that 100 percent by weight passes the 2-inch sieve and 95-100 percent passes the 1-1/2-inch sieve.

- 6) Same comment as for RCA, the blended material must meet the same requirements of our crushed aggregate base courses.
- 7) RAP is only used as a base for emergency or unique cases.
- 8) RCA may be used for conventional 'aggregate base course', placed in a 4" or 6" layer, as defined in Missouri Standard Spec Section 304. The spec does not differentiate between RCA and crushed stone in material requirements.
- 9) RAP is not used exclusively for base course. The existing HMA is milled and blended with the top two inches of existing aggregate base course then graded, compacted and tested for acceptance.
- 10) We allow RCA in our reclaimed pavement borrow material.
- 11) GDOT has a draft special provision for use with 100% recycled asphalt pavement.
- 12) Since SDDOT only allows recycled pavements from our existing pavements, we assume the quality of the RCA and RAP are acceptable.

9- Question: Do you have issues/problems related to RCA performance as base layers?

Answers:

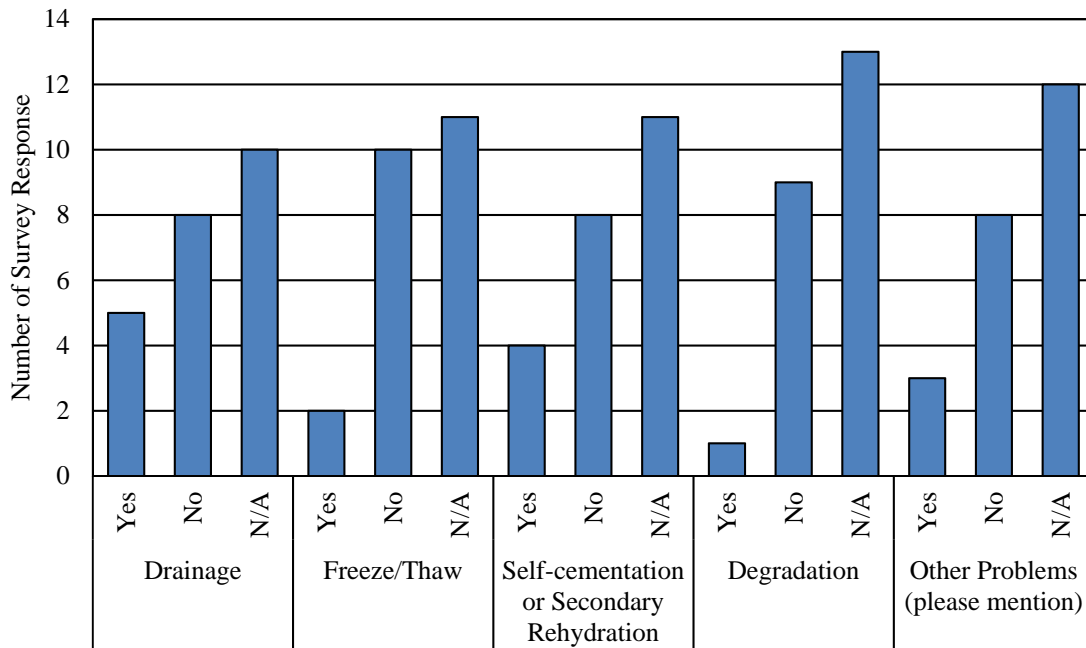


Figure 2.11: Issues or problems with RCA performance as base layers.

Comments:

- 1) Yes, typically needs more moisture to facilitate proper compaction than we typically see with crushed gravel/rock base course.
- 2) Yes, Tufa formation and PH would be of concern.
- 3) Yes, tufa clogs rodent screens and backs up water in the pavement structure.

10- Question: Do you have issues/problems related to RAP performance as base layers?

Answers:

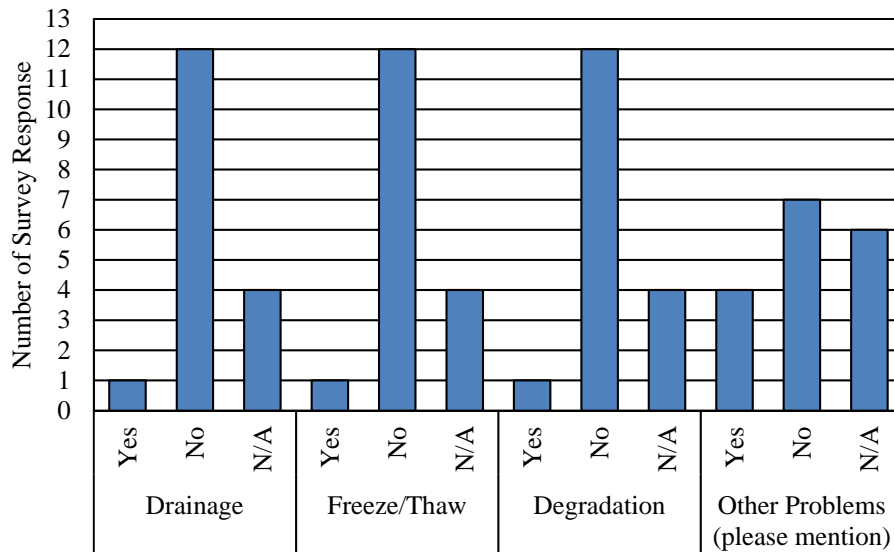


Figure 2.12: Issues or problems with RAP performance as base layers.

Comments:

- 1) Testing difficulties when measuring percent compaction due to hydrocarbons in the residual binder reading as moisture.
- 2) Our contractors have struggled with the bond between lifts of HMA, not sure if there is a correlation to RAP.
- 3) Permanent deformation is often larger than that of a granular base course layer. We recommend mixing the RAP with granular material (untreated or mixed with emulsion or foamed-asphalt).
- 4) RAP is virtually never used as a base layer, because of its greater value in asphalt mix, therefore we are not aware of problems related specifically to its use.
- 5) Environmental.

11- Question: Do you have a case history or example on performance issues of?

Answers:

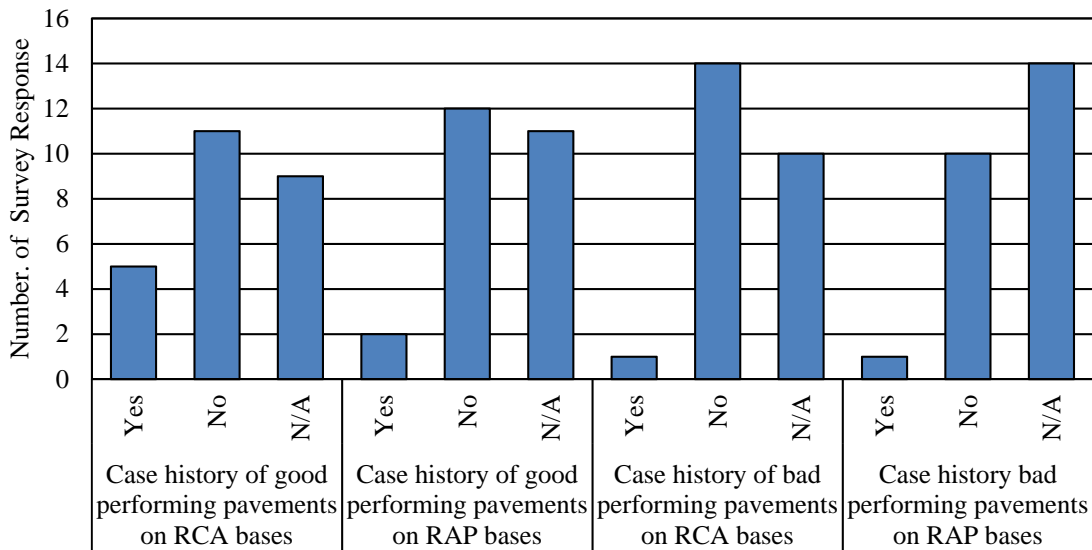


Figure 2.13: Case history on performance issues.

12- Question: Do you have any of the following HMA pavement performance issues when using RCA base layer?

Answers:

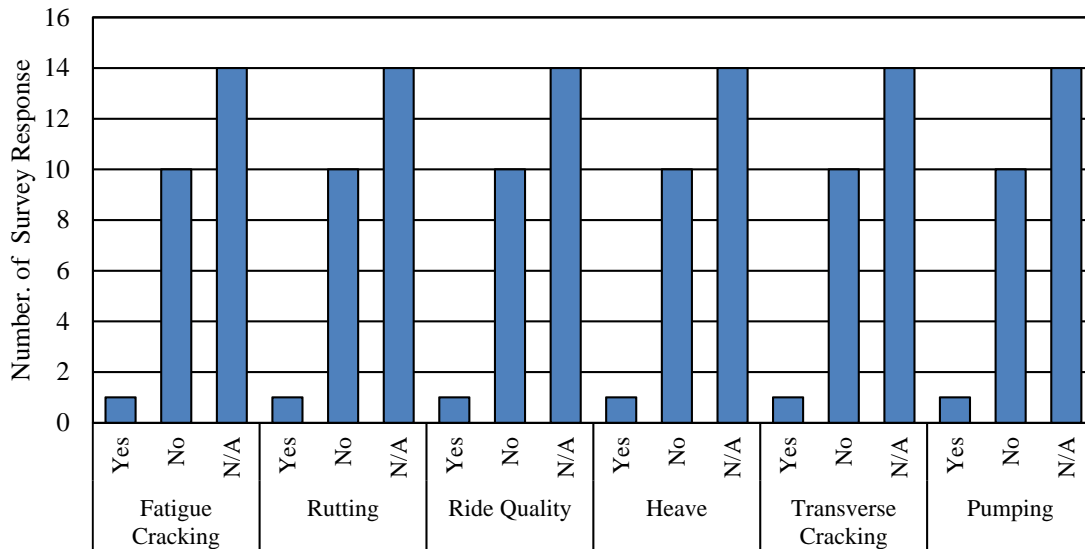


Figure 2.14: HMA pavement performance issues when using RCA base layers.

Comments:

- 1) Projects are too "young".
- 2) No history good or bad.
- 3) No problems have been identified or linked to using RCA in our base courses, but we don't see this very often, if at all.

- 4) Although allowed if blended at a ratio of 50:50 with virgin aggregate base, I am not aware of any RCA used in base layers under HMA pavements.
- 5) If we have any problems with pavements incorporating RCA in the base layer, we are not aware of it.
- 6) These pavement performance issues all occur but it may or may not be caused by the base course.
- 7) It is not used often enough to know.
- 8) As noted earlier, TDOT has just started to allow the use of RCA and we do not have any experience with performance at this time.
- 9) No history of RCA use under HMA.
- 10) Again, we rarely use a base layer for HMA so these do not apply.
- 11) We have had HMA roads experience early failure, not sure of the mechanism, but I believe that it may be from secondary cementation. This is why if RCA > 75% our gradation must be coarser.
- 12) Not many/or any HMA pavements place on RCA base.

13- Question: Do you have any of the following HMA pavement performance issues when using RAP base layer?

Answers:

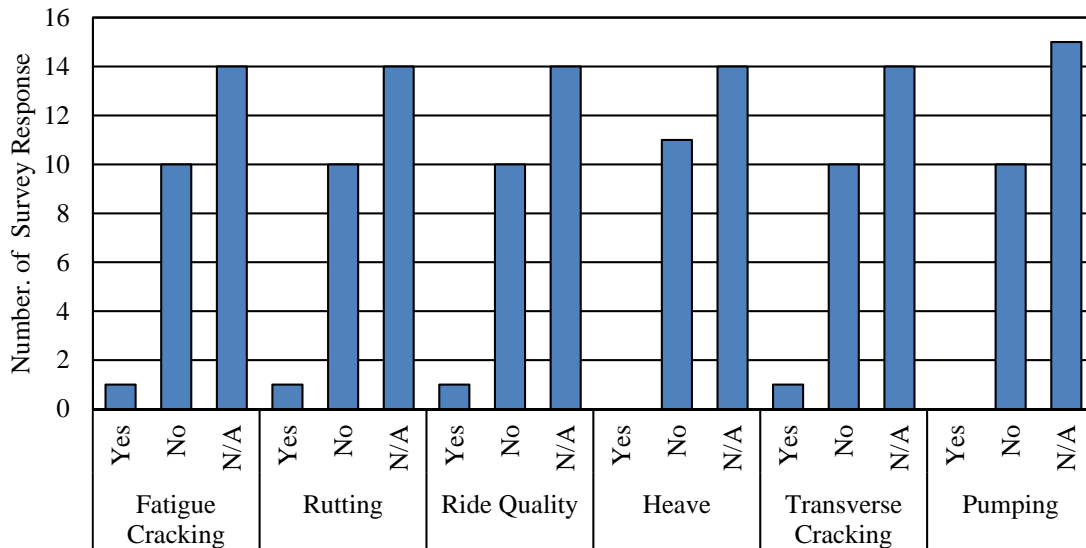


Figure 2.15: HMA pavement performance issues when using RAP base layers.

Comments:

- 1) No data/none known.
- 2) RAP as base is rarely used under HMA pavements. Concerns with long-term creep potential under flexible pavements has limited its use.
- 3) Dry mixes, we have many of these issues even in virgin mixes.
- 4) If “RAP base layer” is meant 100%RAP, then rutting/ permanent deformation (and “soft” spots) is observed especially in aviation pavements. It may be economical to have 100%RAP under the shoulder areas, but not under pavement trafficked areas. We recommend mixing the RAP with granular material (untreated or mixed with emulsion or foamed-asphalt).

- 5) No problems have been identified relating specifically to the use of RAP in base courses.
- 6) Performance studies have not been done on these issues.
- 7) When used as FDR.
- 8) If we have any problems with pavements incorporating RAP in the base layer, we are not aware of it.
- 9) As previously stated, RAP is not used exclusively for the base course.
- 10) It is not used often enough to know.
- 11) HMA base not utilized.
- 12) No history of use.
- 13) Same comment as in #12.
- 14) In the past I have heard of rutting issues with reclaimed bases, not sure whether this has been from (poor subgrade, under compacted base, or lack of crushing in the base. Have not heard of recent projects with this issue. We now regulate a maximum lift thickness of 6", have equipment requirements for HMA base, and test roll all base.

14- Question: What construction control method do you use for RCA and RAP bases?

Answers:

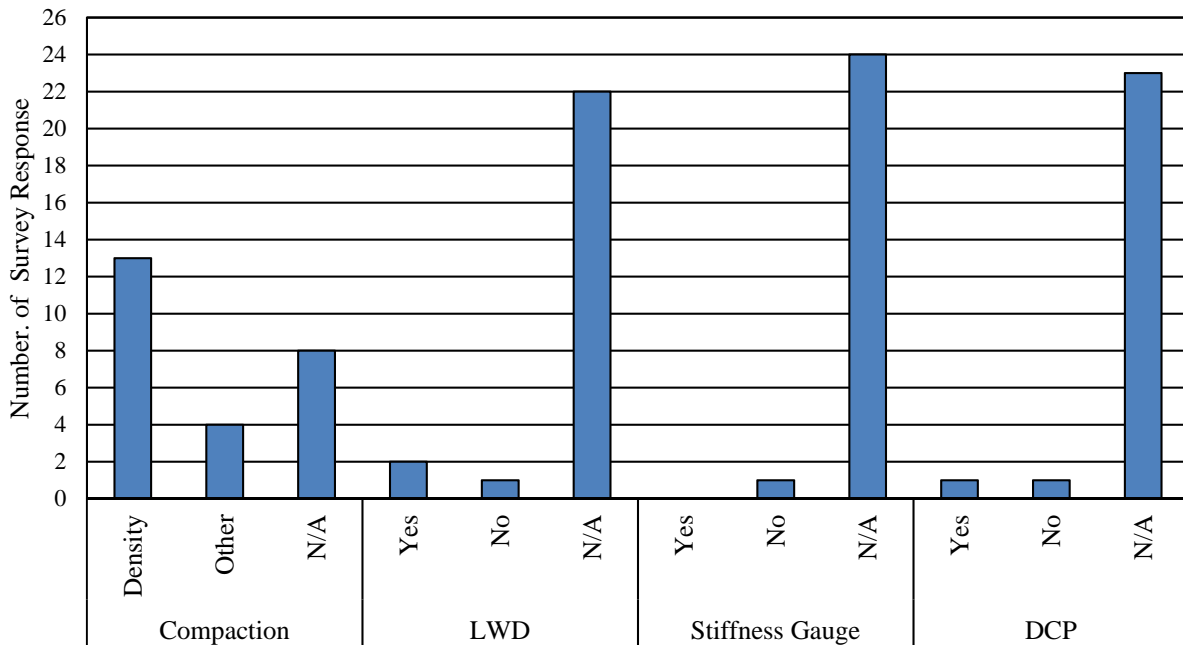


Figure 2.16: Construction control methods for RCA and RAP.

Comments:

- 1) Gradation.
- 2) Nothing specifically for these materials other than the standard specs referenced earlier.
- 3) Considering investigating the Troxler E-Gauge.

- 4) Spot test must meet quality compaction (the eye ball test) and either the DCP, specified density or LWD. Then finally the base is test rolled (the final 100% coverage eyeball and depression test)

15- Question: Do you allow the sole use of RCA or RAP? Or do you blend/mix with other materials (such as RAP + RCA mixture or RCA + Virgin Aggregate mixture)?

Answers:

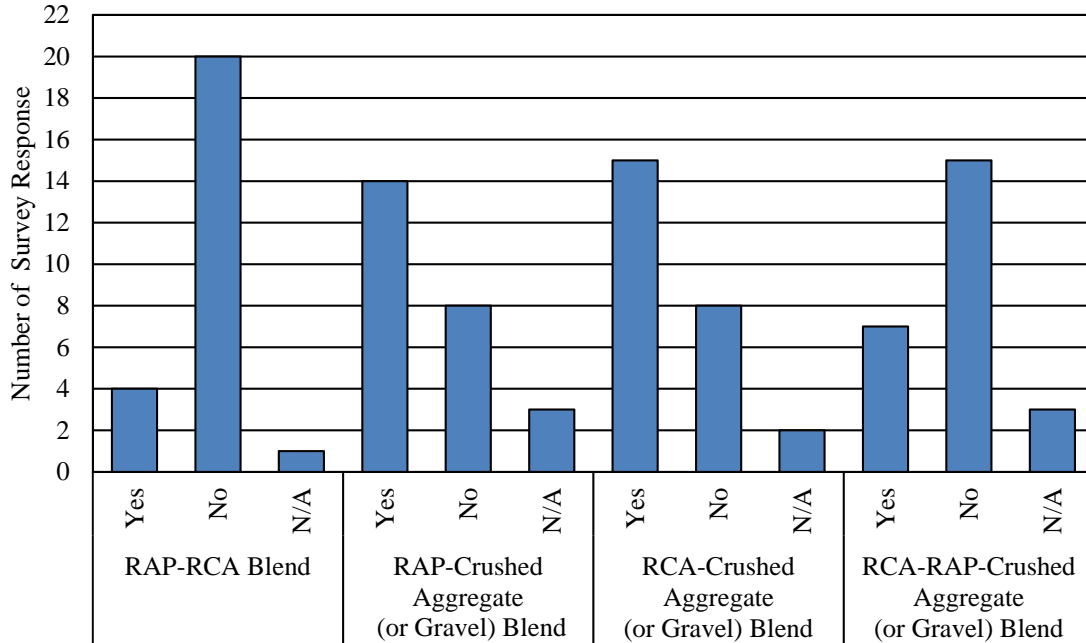


Figure 2.17: Blending of AC, RCA, and RAP.

Comments:

- 1) Not aware of blending being done but would be allowed if specifications are met.
- 2) Only in back fill or embankment applications.
- 3) No RCA is used in pavements.
- 4) 50% max (by weight).
- 5) allow 100% for subbase and between 50% and 75% for base.
- 6) It would be allowed based on the specification but not feasible.
- 7) Maximum 50% RCA blended with virgin aggregate base / subbase
- 8) Theoretically, by standard spec, this combination would be allowed for an aggregate base course.
- 9) Combination of the two is capped at 50% max (by weight)
- 10) 100% of either of these. The requirement for gradation changes as the % of RAP or RCP change.
- 11) Exception to standard but has been used.
- 12) We allow up to 20% RCA in virgin CAB.

16- Question: Rate the importance (or magnitude) of the following the potential barriers within your agency to using RCA in pavement foundations on a scale of 0-5:

Answers:

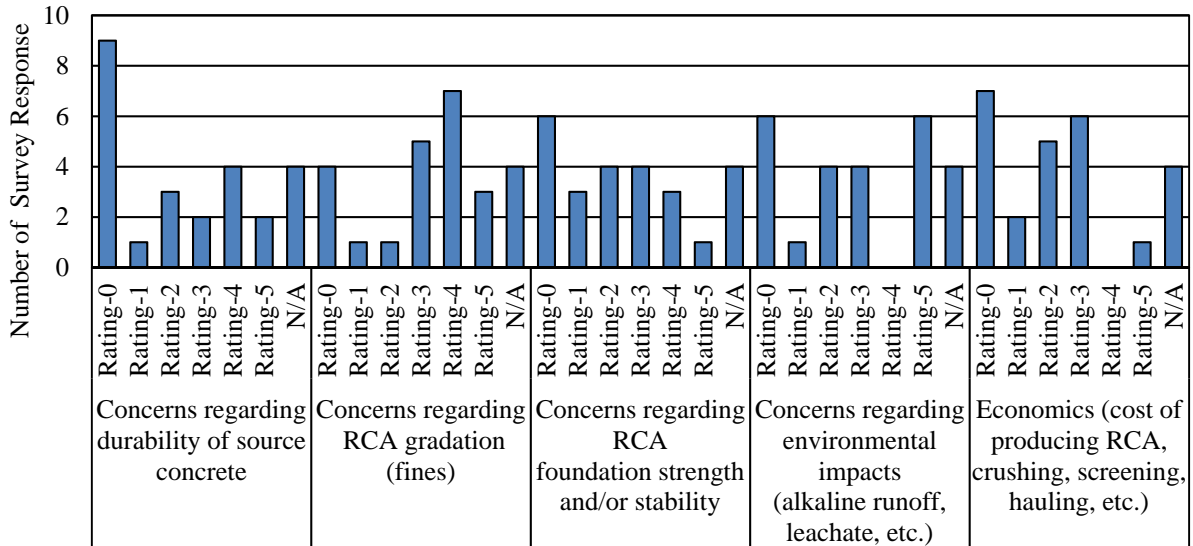


Figure 2.18: Importance scale for RCA material (where rating of zero is very low importance and rating of 5 is very high importance).

Comments:

- 1) If the material meets our specs it is ok for use. Environmental tests are also performed by suppliers.
- 2) Supply of RCA; state doesn't use rigid pavements, so RCA isn't a ready resource.
- 3) RCA is not widely used for this purpose.
- 4) No major concerns if blending at max of 50%
- 5) I don't envision ever not using RCA for aggregate base course as there is an abundant source.
- 6) Please note that it is hard to respond to this question as if these are barriers to implementation. They are more like deleterious materials in specifications. Strength - RCA has a 50% higher min. Limerock Bearing Ratio requirement. (LBR similar to CBR).
- 7) We have been using RCA for foundation course for PCC pavements more than 20 years and don't feel like we have any current barriers.

17- Question: Rate the importance (or magnitude) of the following the potential barriers within your agency to using RAP in pavement foundations on a scale of 0-5:

Answers:

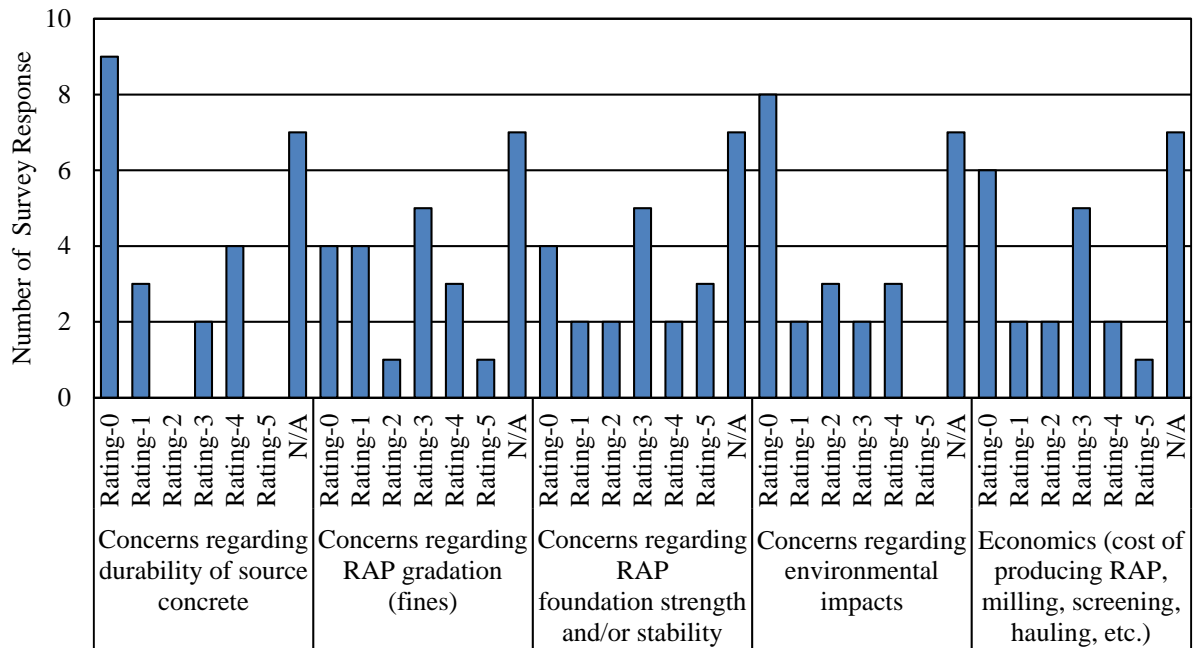


Figure 2.19: Importance scale for RAP material (where rating of zero is very low importance and rating of 5 is very high importance).

Comments:

- 1) If the material meets our specs it is ok for use. Environmental tests are also performed by suppliers.
- 2) Responses assume RAP-CA blend, not 100% RAP.
- 3) No major concerns if blending at max of 50%.
- 4) When used as FDR.
- 5) RAP is not used exclusively for base course.
- 6) We have found that the RAP used as foundation course provides better drainage than RCA and some of our natural aggregates. We have no concerns but currently the RAP is more valuable if use in the Asphalt Mix Design.

18- Question: Do you have any structural capacity issues with HMA pavements on RCA bases? RAP bases?

Answers:

- 1) Long term creep concerns with RAP as base course is a concern. This limits its use.
- 2) We have been pleased with the rubblized PCC bases and the short term performance of the pavements built on them. We don't have a comparison with RAP bases vs nonRAP bases.
- 3) No experience with RCA. No capacity issue for RAP, unless 100% RAP is used.
- 4) None that have been identified.
- 5) No solid structural coefficient at this time.

- 6) Not for RCA or RAP is not used.
- 7) RCA - Structural Layer Coefficient Design - RCA has a 50% higher minimum Limerock Bearing Ratio requirement, 150 vs. 100 for other bases, (LBR is similar to CBR) in order to have $SLC = 0.18$. This allows RCA to function as optional base to be selected by contractor based on economics. RAP - FDOT allows RAP ONLY on non-traffic shoulders and shared use paths (pedestrian and bicycles).

19- Question: How do you compare HMA pavement performance with RCA or RAP base versus the most common base (e.g., versus similar pavements with virgin aggregate base layers)?

Answers:

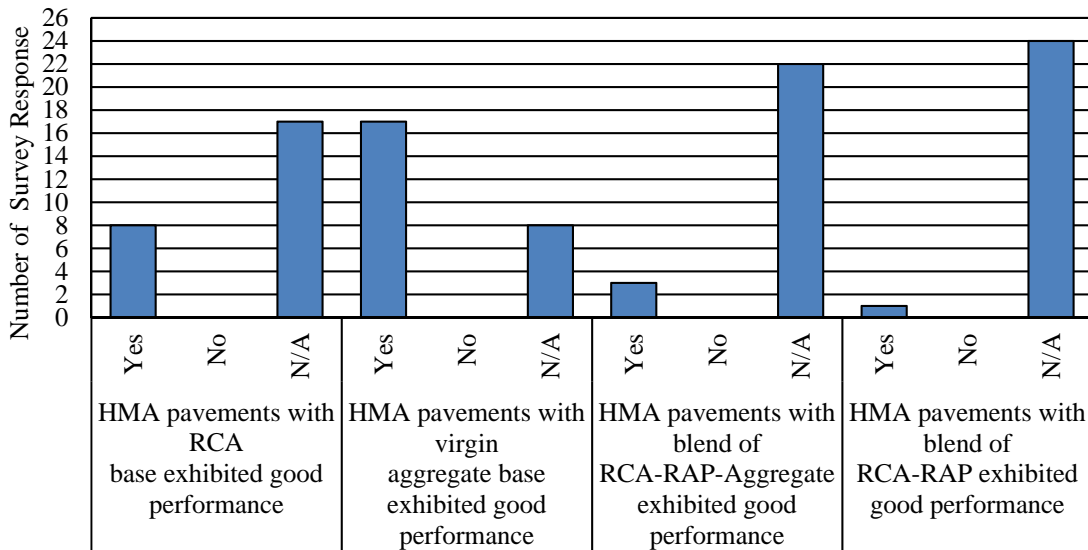


Figure 2.20: Comparison of RCA/RAP vs. virgin aggregate.

Comments:

- 1) Pavements with a blend of RAP-Aggregate (less than 100% RAP) exhibit good performance as compared with virgin aggregate base layers.
- 2) No known issues with use of reclaimed materials vs natural or crushed materials

20- Question: When RAP is used as base layers do you have any issues with HMA performance compared with similar pavements with virgin aggregate base layers?

Answers:

- 1) No known issues with use of reclaimed materials vs natural or crushed materials.
- 2) No, seems to perform as good if not better than conventional virgin aggregate base course.
- 3) RCA is not used for base layers.
- 4) Not large enough sample size, however no issues have ever been documented.
- 5) Drainage can become an issue
- 6) None we're aware of.
- 7) Insufficient experience. No problems observed.
- 8) We don't have enough information to make a judgement.

- 9) Yes, when RCA too fine. Would rather have a mixture of no more than 75% RCA. But we think that we are lessening potential of degradation by our gradation changes, making coarser with RCA > 75%.

21- Question: When RCA is used as base layers do you have any issues with HMA performance compared with similar pavements with virgin aggregate base layers?

Answers:

- 1) No known issues with use of reclaimed materials vs natural or crushed materials
- 2) Concern for long term creep under loading is there, but not documented. Use is limited as a result.
- 3) We have not made comparisons.
- 4) If "RAP base layer" is meant 100% RAP then rutting/ permanent deformation (and "soft" spots) is observed especially in aviation pavements. It may economical to have 100% RAP under the shoulder areas, but not under pavement trafficked areas. We recommend mixing the RAP with granular material (untreated or mixed with emulsion or foamed-asphalt).
- 5) No when used as FDR.
- 6) None we're aware of.
- 7) No experience.
- 8) RAP is not used exclusively.
- 9) We don't have enough information to make a judgement.
- 10) Only one very limited test section.
- 11) FDOT allows RAP ONLY on non-traffic shoulders and shared use paths (pedestrian and bicycles).
- 12) No concerns
- 13) As long as material is compacted well, in lifts 6" or less with the right equipment and test rolled, then no problem.
- 14) performs well at 50/50 blend.

22- Question: Do you have any comment on RCA and or RAP that you believe is important to this issue? Please specify?

Answers:

- 1) No known issues with use of reclaimed materials vs natural or crushed materials
- 2) The sustainability of this practice is appealing, however sacrificing durability is a high price to pay. Until we have tighter controls on the recycled materials, we are reluctant to expand their use.
- 3) Lack of material availability to be used as base layer.
- 4) FDR base has much higher modulus than gravel making it desirable.
- 5) RCA should not be used in direct contact or directly above sock wrapped underdrain as the concrete fines will plug it up.
- 6) FDOT is using more RCA for base from reconstruction of Interstates in recent years.
- 7) It is important that the processing of the RCA or RAP is done correctly, and the fines are removed from the material that is to be used for the base course. The gradation and material passing the #200 sieve are key.

- 8) Make sure high RAP is compacted well. For high RCA, make gradation coarser. Do not allow concrete brick to be use, or have an upper limit, say 10% in base (Higher cement content, finer, therefore secondary re-cementation potential).

Chapter 3

Research Methodology

This chapter describes the field and laboratory testing program conducted to investigate recycled aggregate base materials and pavement structure of selected HMA pavements. Pavement sections were subjected to nondestructive testing using the Falling Weight Deflectometer (FWD) and Ground Penetrating Radar (GPR) as well as pavement surface profile measurements, visual pavement distress surveys, drainability, and Dynamic Cone Penetrometer (DCP). Base layer materials were collected and subjected to a laboratory testing that included particle size analysis, Micro-Deval (MD) abrasion, absorption, specific gravity (G_s), and permeability.

3.1 Selection of Pavement Test Sites

The research team, in coordination with the Project Oversight Committee (POC), identified and selected various existing HMA pavement sites for field testing and base materials sampling. The criteria used for the selection of sites considered three aspects: 1) geographical variation in Wisconsin, 2) base course layers that used virgin crushed stone aggregates (CA), recycled concrete aggregates (RCA), and reclaimed asphalt pavements (RAP), and 3) HMA pavement type. The selected pavement sites are HMA pavements with aggregate base courses (CA, RCA, and RAP) that were constructed in or earlier than 2009 (with one extra project constructed in 2017). Figure 3.1 depicts Wisconsin County map in which the investigated HMA pavements were selected for this study.

3.2 Non-Destructive Field Testing at the Selected Pavement Sites

The research team in coordination with WisDOT planned the field testing program for the selected pavement sections. The testing program consisted of pavement surface layer coring, Falling Weight Deflectometer, Ground Penetrating Radar, visual distress surveys, pavement surface profile measurements, and Dynamic Cone Penetration. Table 3.1 presents a summary of the field tests conducted at the investigated pavement sections.

3.2.1 Falling Weight Deflectometer Tests

The FWD testing was conducted by WisDOT and required extensive efforts by the WisDOT team and the researchers. This included travel to various pavement sites across Wisconsin, implementing full traffic control and lane closure, selecting test sections, and executing the testing program. Once at the pavement site, the research team conducted a windshield visual distress survey/evaluation of the whole length of the site to identify representative test section(s). Figure 3.2a depicts WisDOT KUAB FWD performing FWD testing on STH 100 in Oak Creek, Milwaukee County.

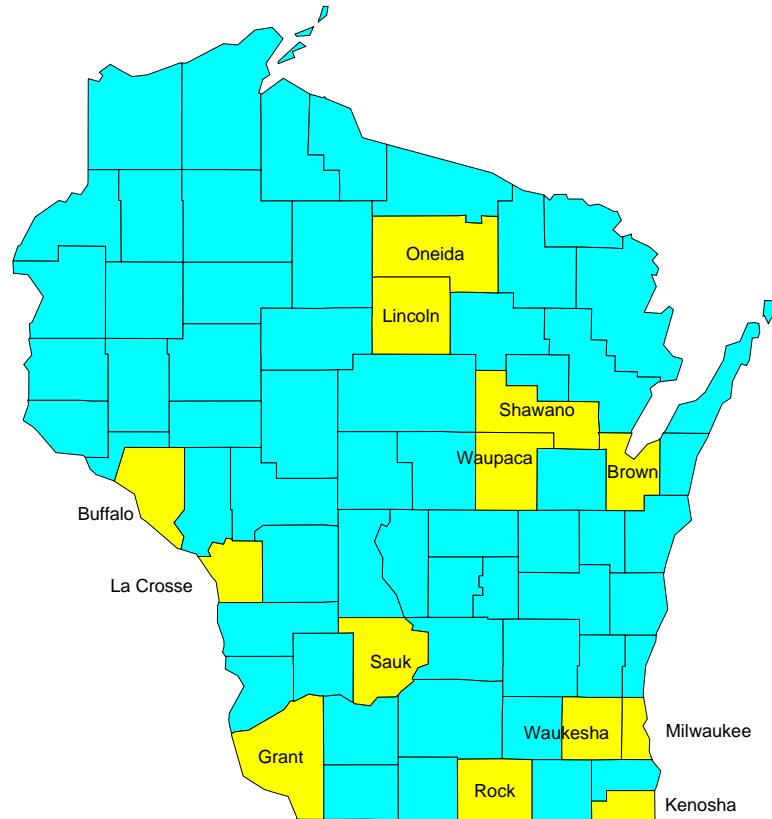


Figure 3.1: Wisconsin counties in which the investigated HMA pavements were selected for this study.

The FWD test was conducted according to ASTM D4694: Standard Test Method for Deflections with a Falling-Weight-Type Impulse Load Device. The WisDOT KUAB FWD was used with three different load drops of 5,000, 9,000, and 12,000 lb. Seven geophones were used to record pavement surface deflection located at the center of the loading plate and at 12, 24, 36, 48, 60, and 72 inches behind the loading plate. In another configuration, nine geophones were used to record pavement surface deflection with two additional geophones located at 12 inches in front of and to the left of the loading plate. Pavement surface, air temperatures and GPS coordinates were acquired at each test point.

The total length of the FWD test section for each pavement site varied between 528 ft ($\frac{1}{10}$ of a mile) and more than 5,000 ft depending on field conditions and availability of equipment. The FWD test point spacing ranged from 10 to 100 ft. The majority of the FWD tests were conducted at the outside wheel path of the outside lane of the pavement section. For a limited number of pavement test sections, FWD testing was conducted on both the outside and inside wheel paths.

Table 3.1: Field and laboratory tests conducted on pavement test sections.

Base Course Material	Project Site	HMA Coring and Base Material Sampling		Field Tests								Lab Tests					
		CL	WP	Drainability		DCP		FWD	GPR	VDS	PP	GSD	ABS	GS	MD	HC	
				CL	WP	CL	WP										
CA	STH 22/54 (Waupaca)	√**	√**	√*	√*	√**	√**	√	√	√	√	√	√	√	√	√*	
	STH 22 (Shawano)	√**	√**	√*	√*	√**	√**	√	√	√	√	√	√	√	√	√*	
	STH 33 (St. Joseph)	√***	√***	√**	√**	√***	√***	√	√	√	√	√	√	√	√	√*	
	CTH T (Blue River)	√**	√**	√*	√*	√**	√**	√	√	√	√	√	√	√	√	√*	
	STH 25 (Maxville)	√**	√**	√*	√*	√**	√**	√	√	√	√	√	√	√	√	√*	
	STH 59 (Edgerton)	-	√****	-	-	-	-	√	√	√	√	√	√	√	√	√*	
RCA	STH 100 (Oak Creek)	√**	√**	-	√*	√*	√*	√	√	√	√	√	√	√	√	√*	
	Calhoun Rd. (Brookfield)	√**	√**	√*	√*	√**	√**	√	√	√	√	√	√	√	√	√*	
	STH 86 (Tomahawk)		√**	√*		√	√	√	√	√	√	√	√	√	√	√*	
	STH 50 (Kenosha)	Site-I	√**	√***	√*	√**	√		√	√	√	√	√	√	√	√	√*
		Site-II	√**	√**	√**	√**	√**	√**	√	√	√	√	√	√	√	√	√*
	STH 32 (Kenosha)	Site-I	√**	√**	√*	√*			√	√	√	√	√	√	√	√	√*
		Site-II	√**	√**	√**	√**	√**	√**	√	√	√	√	√	√	√	√	√*
	STH 78 (Merrimac - Prairie du Sau)	Site-I	Trench	Trench	-	-	Refusal	Refusal	√	√	√	√	√	√	√	√	√*
Site-II		Trench	Trench	-	-	Refusal	Refusal	√	√	√	√	√	√	√	√	√*	
RAP	STH 22 (Shawano)	√**	√**	√*	√*		√*	√	√	√	√	√	√	√	-	-	
	STH 70 (Minocqua)	√***	√***	√*	√*	√**	√**	√	√	√	√	√	√	√	-	-	
	STH 96 (Lark-Shirley)	√**	√**	√*	√*	√**	√**	√	√	√	√	√	√	√	-	-	
	STH 59 (Edgerton)	A [§]	-	-	√*	√*	√**	√**	√	√	√	√	√	√	-	-	-
		B ^{§§}	√	√	√	√	√	√	√	√	√	√	√	√	-	-	-
	STH 25 (Maxville)	√***	√***	√*	√*	√**	√**	√	√	√	√	√	√	√	-	-	
USH 45 (Tigerton)	√ [§]	√ [§]	-	-	-		√	√	√	-	-	√	√	√	-	-	

Note: Site A[§]: By Riley Road, ABS: Absorption, Site B^{§§}: By Junk Yard, CA: Crashed Stone Aggregate, CL: Centerline, DCP: Dynamic Cone Penetration, FWD: Falling Weight Deflectometer, GPR: Ground Penetrating Radar, GSD: Grain Size Distribution, HC: Hydraulic Conductivity (Permeability), MD: Micro Deval, PP: Pavement Profiler, RAP: Recycled/ Reclaimed Asphalt Pavement, RCA: Recycled Concrete Aggregate, GS: Specific Gravity, VDS: Visual Distress Survey, WP: Wheel Path, * CL or WP I or II, ** CL or WP I and II, *** CL or WP I, II, and III, **** CL or WP I, II, III and IV (See Core Measurements), §: Base Sampling.

3.2.2 Ground Penetrating Radar

WisDOT owns and operates a GSSI SIR 3000 ground penetrating radar system (depicted in Figure 3.2b). The system consists of a high-resolution 2.0 GHz air-coupled horn antenna for primary analysis of pavement layer thicknesses. The system could also be used for assessing pavement condition/deterioration. The maximum depth of penetration is approximately 18-24 in below the pavement surface. The system also includes a 900 MHz ground-coupled antenna for primary analysis of base course and subbase layer thickness and subgrade assessment. The maximum depth of penetration is approximately 5 ft.

The GPR testing was used in conjunction with the FWD testing. Therefore, the pavement test sites and sections selected for the GPR testing are the same as for the FWD testing. The data files were compiled by WisDOT team and given to the research team for layer thickness analysis.



(a) FWD testing on STH 100 in Oak Creek



(b) GPR testing on STH 100 in Oak Creek

Figure 3.2: WisDOT KUAB FWD test system with GPR units used in this study.

3.2.3 Visual and Automated Pavement Surface Distress Surveys

Visual surveys were conducted to identify and quantify the various types of pavement surface distress exhibited at the investigated pavements and to obtain data needed to evaluate pavement performance in terms of a Pavement Condition Index (PCI). Each distress survey was conducted for one 528 ft section at each pavement site. The section was selected to be representative of the overall pavement condition. It should be noted that the WisDOT Pavement Data Unit conducts automated pavement surface distress surveys as part of pavement management of the state/national highway network. The collected data is compiled in the Pavement Information/Inventory Files (PIF) database where the performance indicators such as the PCI and the International Roughness Index (IRI) are calculated for the length of the fourth $\frac{1}{10}$

of a mile for each highway segment. The research team accessed the PIF database and analyze the data corresponding to pavement sections investigated in this study.

At the investigated pavement sites, surface distresses were visually identified, quantified, and recorded. Pavement distress types, extent, and levels of severity were identified and quantified according to the FHWA distress identification manual.

3.2.4 Pavement Surface Profile Measurements

Pavement surface profile measurements were conducted using the CS8800 Walking Profiler System provided by Surface Systems & Instruments, Inc. The profile measurements were conducted on the inside wheel path, center of the lane, and outside wheel path for a length of 600 ft at each investigated pavement test section. The system is equipped with GPS system and MS Windows based software that allows for real time display of measured profiles. The system also allows for the data files to be saved in formats consistent with MS Excel and ProVAL software. Figure 3.3 depicts the walking profiler system used in this study.



Figure 3.3: The CS8800 Walking Profiler System provided by Surface Systems & Instruments, Inc. used to measure pavement surface profiles.

3.3 Sampling of Base Layer Aggregates and Field Testing

3.3.1 Pavement Surface Coring

The research team used 8" wet core bit for drilling the HMA pavement surface and expose the base layer aggregates. The HMA cores were labeled and stored , while the hole in the HMA surface is prepared for drainability testing, DCP testing, and base aggregate sampling, in a chronological order. Only at STH 78 in Sauk County, three trenches were cut on the pavement surface rather than coring. Figure 3.4 depicts the coring process of HMA surface at STH 22 in Waupaca as well as the trench cutting at STH 78 in Sauk County.



(a) Coring HMA surface



(b) Excavating HMA surface

Figure 3.4: Coring of HMA surface at STH 22 in Waupaca and trench cutting at STH 78 in Sauk County.

3.3.2 Drainability Testing of Base Aggregates

Once the pavement surface core was removed, the hole in the HMA surface was filled with water and left for a period of about 10 to 45 minutes to stabilize, depending on the rate of water level decrease. Thereafter, the hole is refilled again with water to the top of the pavement surface and the level of water was recorded with time for a period ranging from few minutes to one hour. The research team attempted to use the core-hole permeameter (CHP) device in accordance with ASTM D6391: Standard Test Method for Field Measurement of Hydraulic Conductivity Using Borehole Infiltration. However, the time limitations of highway lane closures and the need to conduct DCP testing, aggregates sampling, FWD and GPR, refilling the hole with HMA, and traffic control made such attempts very difficult to execute. The research team instead filled the HMA hole with water as described earlier and observed and recorded the decrease in water level with time, as depicted in Figure 3.5.



Figure 3.5: Field drainability test conducted on the investigated aggregate base layers.

3.3.3 Dynamic Cone Penetration Test

The field testing program included aggregate base course layer and subgrade testing using the DCP. A dynamic cone penetrometer with a single-mass hammer was used to perform tests on the project sites. The DCP was driven into the aggregate base layer (through the HMA hole) by the impact of a single-mass 17.6 lb hammer dropped from a height of 22.6 in. The test was conducted according to the standard test procedure described by ASTM D6951: Standard Test Method for Use of the Dynamic Cone Penetrometer in Shallow Pavement Applications. For pavement test sites, DCP tests were conducted at the wheel path and lane center HMA holes in which the cone was driven through the whole aggregate base course layer and into the subgrade. Figure 3.6a depicts DCP test on the RCA base course layer of Calhoun Road in Waukesha County.

3.3.4 Sampling of Base Aggregates

The research team retrieved the base materials from the selected pavement sites after performing the previously described field tests. Base material samples with a volume of approximately one to two 5-gallon buckets (depending on the site condition) were collected from these sites by removing the base aggregate materials using hand tools by the research team as

shown in Figure 3.6b. After collecting the base materials the holes were filled with ready cold asphalt patch mix in accordance with WisDOT requirements as shown in Figure 3.6c.



(a) DCP testing



(b) Base aggregate sampling



(c) Filled cores

Figure 3.6: DCP field testing on Calhoun Road RCA base layer, aggregate sampling from STH 25 base layer, and holes filled with cold asphalt mix at STH 25 in Maxville.

3.4 Laboratory Testing of Base Aggregate

Representative aggregate samples were collected from the investigated pavement sites as described earlier. Table 3.2 presents the ASTM and AASHTO standard test procedures conducted on the base aggregates from each investigated pavement site.

3.4.1 Particle Size Analysis

Sieve analysis was used to determine the particle size distribution of the base course aggregate specimens. First, the sample was oven-dried to constant mass at 230°F. Then quartering was used to reduce the sample into a test sample that was at least 15 kg. The purpose was to prepare a test sample that was representative of the sampled project site location. Next, the sample was washed over a No. 200 sieve so that material finer than the No. 200 sieve would pass through the opening of the sieve. Then the sample was oven-dried to constant mass once again.

Afterwards, the following set of sieves were stacked: 1.25", 3/4", 3/8", No. 4, No. 10, No. 40, No. 200, and a pan. These sieve sizes are in compliance with the WisDOT specifications for the particle size distribution of 1¼ in dense graded base course aggregate layers described in Section 305.2.2.1 of WisDOT Standard Specifications for Highway and Structure Construction (2108). The stacked sieves were then placed onto an automatic sieve shaker and were agitated according to the standard procedures. The retained masses on each sieve were weighed and used to calculate the percentage of material passing each sieve and subsequently plot the particle size distribution curves.

Table 3.2: ASTM and AASHTO standard test methods employed.

Standard Test Procedure	Standard Designation	
	ASTM	AASHTO
Standard Test Method for Materials Finer than 75-µm (No. 200) Sieve in Mineral Aggregates by Washing	C117 - 17	T 11-05 (13)
ASTM: Standard Test Method for Relative Density (Specific Gravity) and Absorption of Coarse Aggregate AASHTO: Standard Method of Test for Specific Gravity and Absorption of Coarse Aggregate	C127 - 15	T 85-14
ASTM: Standard Test Method for Relative Density (Specific Gravity) and Absorption of Fine Aggregate AASHTO: Standard Method of Test for Specific Gravity and Absorption of Fine Aggregate	C128 - 15	T 84 - 13
Standard Test Method for Sieve Analysis of Fine and Coarse Aggregates	C136 - 14	T 27 - 14
Standard Practice for Reducing Samples of Aggregate to Testing Size	C702 - 11	T 248 - 14
Standard Practice for Sampling Aggregates	D75 - 14	T 2 - 91 (15)
Standard Test Method for Resistance of Coarse Aggregate to Degradation by Abrasion in the Micro-Deval Apparatus	D6928 - 17	T 327 - 12

3.4.2 Specific Gravity and Absorption

The absorption of aggregates is significant especially with respect to durability and resistance to harsh freeze-thaw deterioration. The specific gravity and absorption tests were used to measure the oven-dry specific gravity, saturated-surface-dry specific gravity, apparent specific gravity, and absorption of the aggregate specimens. Aggregate samples consisted of particles larger than the No. 8 sieve and were submerged in water for 24 hours so that they reached saturation. The aggregate samples were removed from the water and an absorbent towel was used to dry the surface of the aggregate particles so that they were in the saturated-surface-dry condition. The aggregate sample was then weighed to get the saturated-surface-dry weight. Next, the sample was placed into a wire basket and weighed while submerged in water to obtain the weight of the sample while in water. The sample was then dried to constant mass in the oven at 230°F and the weight of the dry sample was recorded. The oven-dry specific gravity, G_s (OD),

the saturated-surface-dry specific gravity, G_s (SSD), and the apparent specific gravity, G_s (Apparent), were then calculated. Absorption was also calculated from these measurements.

3.4.3 Micro-Deval Abrasion Test

The Micro-Deval abrasion test measures the resistance of aggregates to abrasion. As a brief overview of the test, a specimen is placed into a container that also includes stainless steel balls and water. The container is placed into the Micro-Deval apparatus and revolved to produce an abrasive charge. Because of the impact of the abrasive charge, the sample degrades. Water is used in the test because many aggregates are more susceptible to abrasion when wet than dry. The Micro-Deval abrasion test was run on both coarse aggregates and fine aggregates. The steps for the Micro-Deval abrasion test are explained for the coarse aggregate specimens. The steps for the fine aggregate specimens are the same except that the sieve sizes and masses retained, volume of water, mass of the steel balls, and number of revolutions are different from those used for coarse aggregates.

The coarse aggregate specimens consisted of the following fractions: 375 g passing the $\frac{3}{4}$ in sieve retained on the $\frac{5}{8}$ in sieve, 375 g passing the $\frac{5}{8}$ in sieve retained on the $\frac{1}{2}$ in sieve, and 750 g passing the $\frac{1}{2}$ in sieve retained on the $\frac{5}{8}$ in sieve. For a few of the coarse aggregate specimens, the following gradation was used: 750 g passing the $\frac{1}{2}$ in sieve retained on the $\frac{3}{8}$ in sieve, 375 g passing the $\frac{3}{8}$ in sieve retained on the $\frac{1}{4}$ in sieve, and 750 g passing the $\frac{1}{4}$ in sieve retained on the No. 4 sieve. The initial weight of the coarse specimens was 1,500 g. For each test, the specimen was placed into the Micro-Deval container and 2 L of water was added to the container. The specimen was immersed in water for at least one hour. Then 5 kg of steel balls were added to the container. The container was then placed into the Micro-Deval apparatus. The apparatus had a revolution counter, so the number of revolutions was set to 12,000 revolutions (10,500 revolutions for the alternate gradation). The container revolved at a rate of 100 revolutions per minute for two hours and then the container was taken out of the apparatus once the revolutions were completed. The specimen was then poured out of the container over a No. 4 sieve superimposed onto a No. 16 sieve and the specimen was washed over the sieves. Then the steel balls were removed with a magnet. Next, the sample was oven dried at a temperature of 230°F for 24 hours. The sample was weighed afterwards and the final mass was recorded. The percent loss was then calculated using the initial and final masses of the specimen.

Chapter 4

Laboratory Tests on Base Aggregate Materials – Analysis of Results

This chapter presents the results of the laboratory testing program on the crushed stone aggregate (CA) and recycled aggregate materials (RCA, and RAP) collected from the investigated pavement test sections. Laboratory test results are analyzed and critically evaluated.

4.1 Particle Size Distribution

The particle size distributions of the investigated CA, RCA, and RAP base materials are presented in Figure 4.1. Also shown in this figure are the current WisDOT specification limits for the particle size distribution of the 1¼ in dense graded base course aggregate layers (Section 305.2.2.1 of WisDOT Standard Specifications for Highway and Structure Construction, 2108). An inspection of Figure 4.1 shows that the particle size distributions of the base materials are generally within the WisDOT specification limits, but partly cross the upper and lower limits in the fine sand area and the lower limit in the gravel size zone. The percentages of gravel size, sand size and materials finer than 75 µm (No. 200 sieve) are summarized in Table 4.1 and depicted in Figures 4.2-4.5. Appendix B presents the particle size distribution plots for all investigated CA, RCA, and RAP base layer materials.

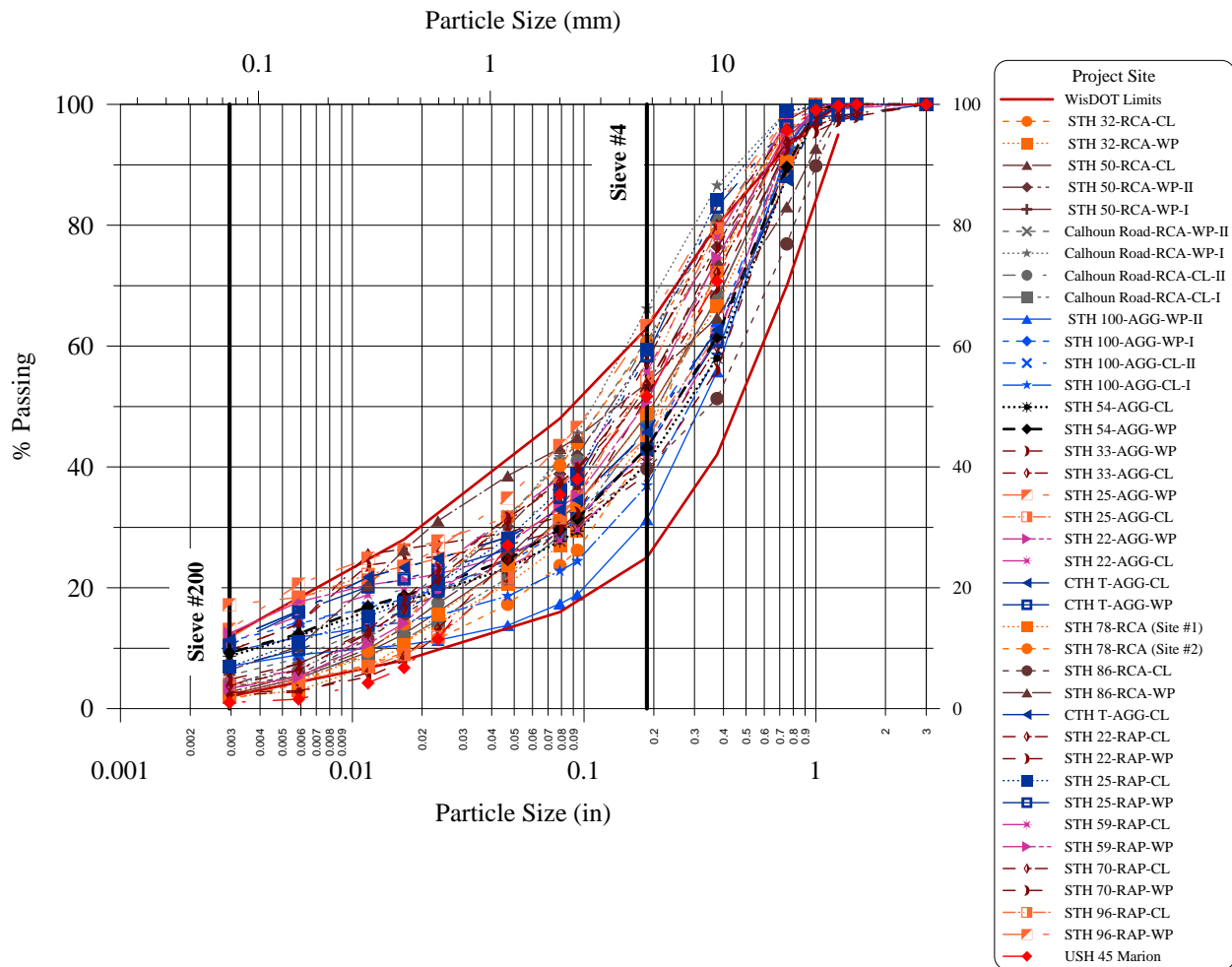
Examination of the particle size distribution data and Figures 4.2-4.3 shows significant differences among the CA, RCA and RAP size fractions. The CA base materials possessed the highest gravel size fractions (varying between 47.36 and 68.72% with an average of 57.73% and COV of 8.5%), and the highest fines size fractions (ranging from 7.02 to 13.10% with an average of 10.4% and COV of 15.4%) when compared with the RCA and RAP base materials. The gravel size fractions for both RCA and RAP base materials are comparable but the RCA base materials exhibited higher variability (ranging between 33.83 and 60.36% with an average of 47.17% and COV of 17.4%). The range of gravel size fractions for the RAP base materials is from 36.6 to 49.26% with an average of 44.65% and COV of 8.9%.

On the other hand, the CA base materials have the lowest sand size fractions (ranging between 24.26 and 39.53% with an average of 31.87% and COV of 11.4%) compared with RCA and RAP base materials. The sand size fractions for the RCA base materials ranged from 36.18 to 62.36% with an average of 49.45% and COV of 15.9%, and for the RAP base materials, the sand size fraction varied between 46.22 and 55.18% with an average of 50.12% and COV of 5.3%.

The RCA base materials contained the lowest fines size fractions ranging from 1.49 to 6.36% with an average of 3.38% and COV of 41.6% while the RAP base materials possessed

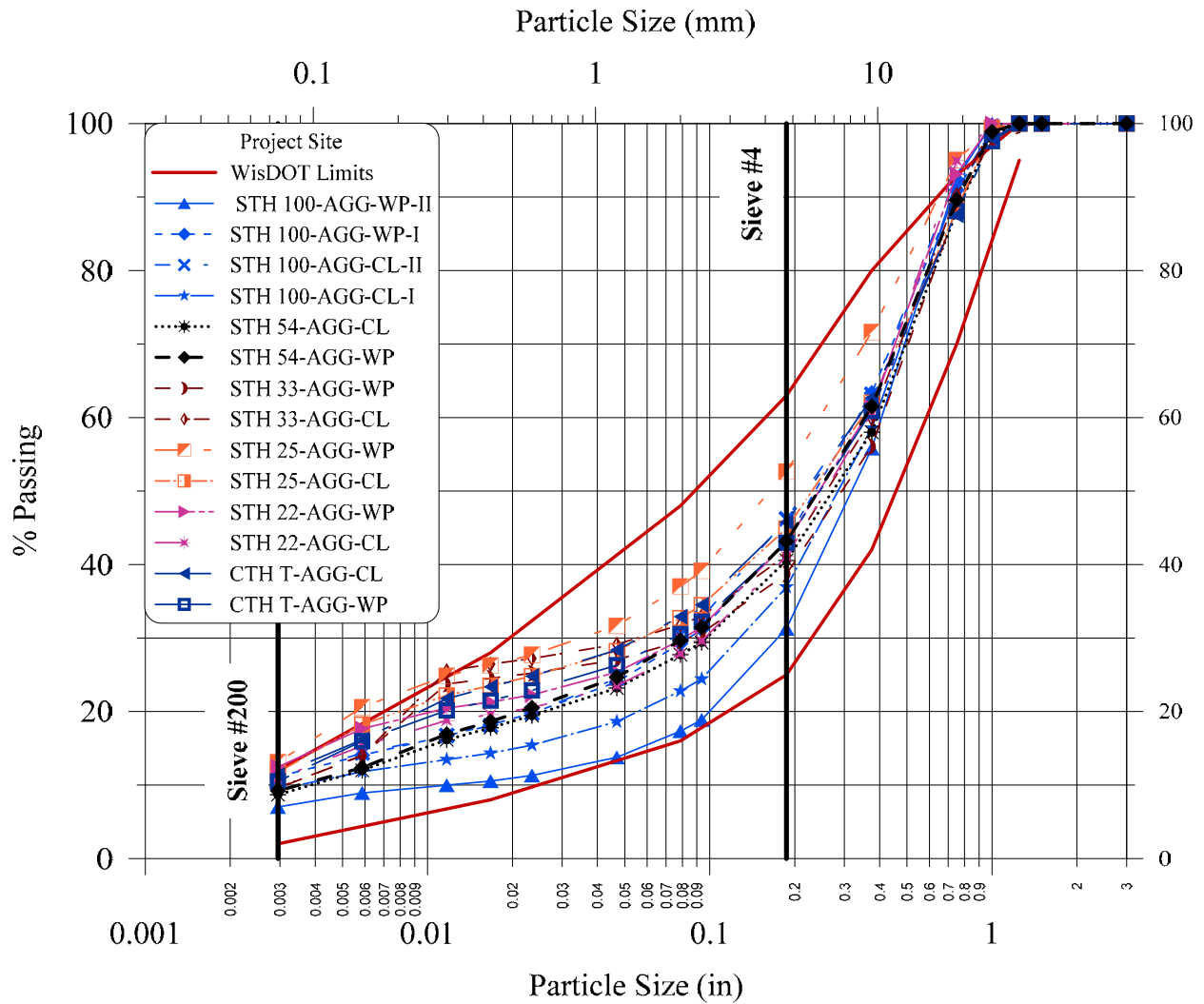
finer size fractions ranging from 0.99 to 17.18% with an average of 5.23% and COV of 83.2%. In total, two CA and one RAP base material samples exceeded the 12% upper limit specified by WisDOT for fines. It should be noted that the Unified Soil Classification System (USCS) was used to determine gravel, sand and fines size ranges.

Analysis of the particle size distributions of the investigated CA, RCA, and RAP base materials indicated that the most interesting point observed is the high sand size fractions for both RCA and RAP base materials with six out of thirteen RCA base samples exceeding the upper WisDOT specification limits.



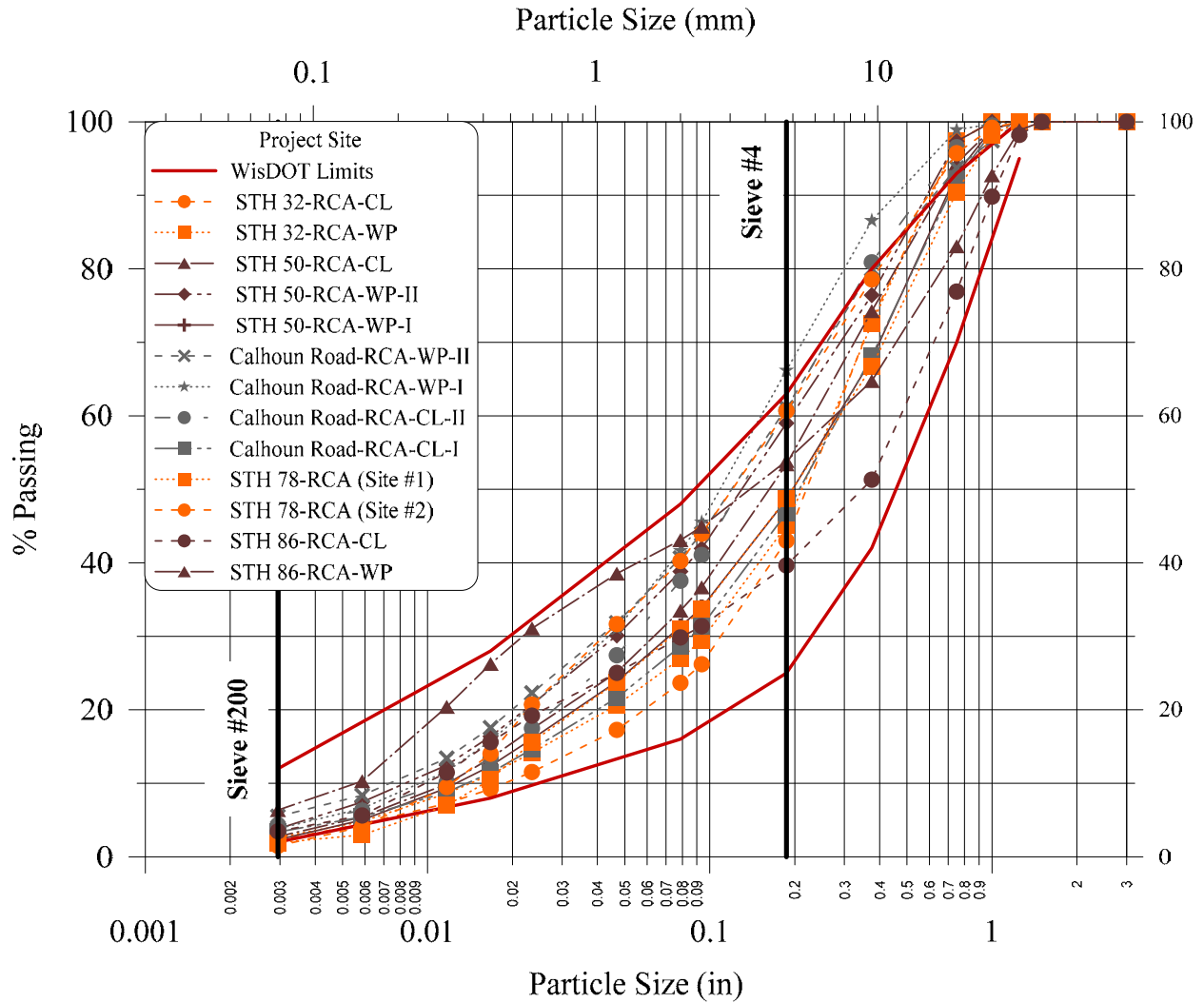
(a) All investigated CA, RCA, and RAP base materials

Figure 4.1: Particle size distribution of the investigated CA, RCA, and RAP base course materials and the current WisDOT gradation specification limits for the 1¼" dense graded base course materials.



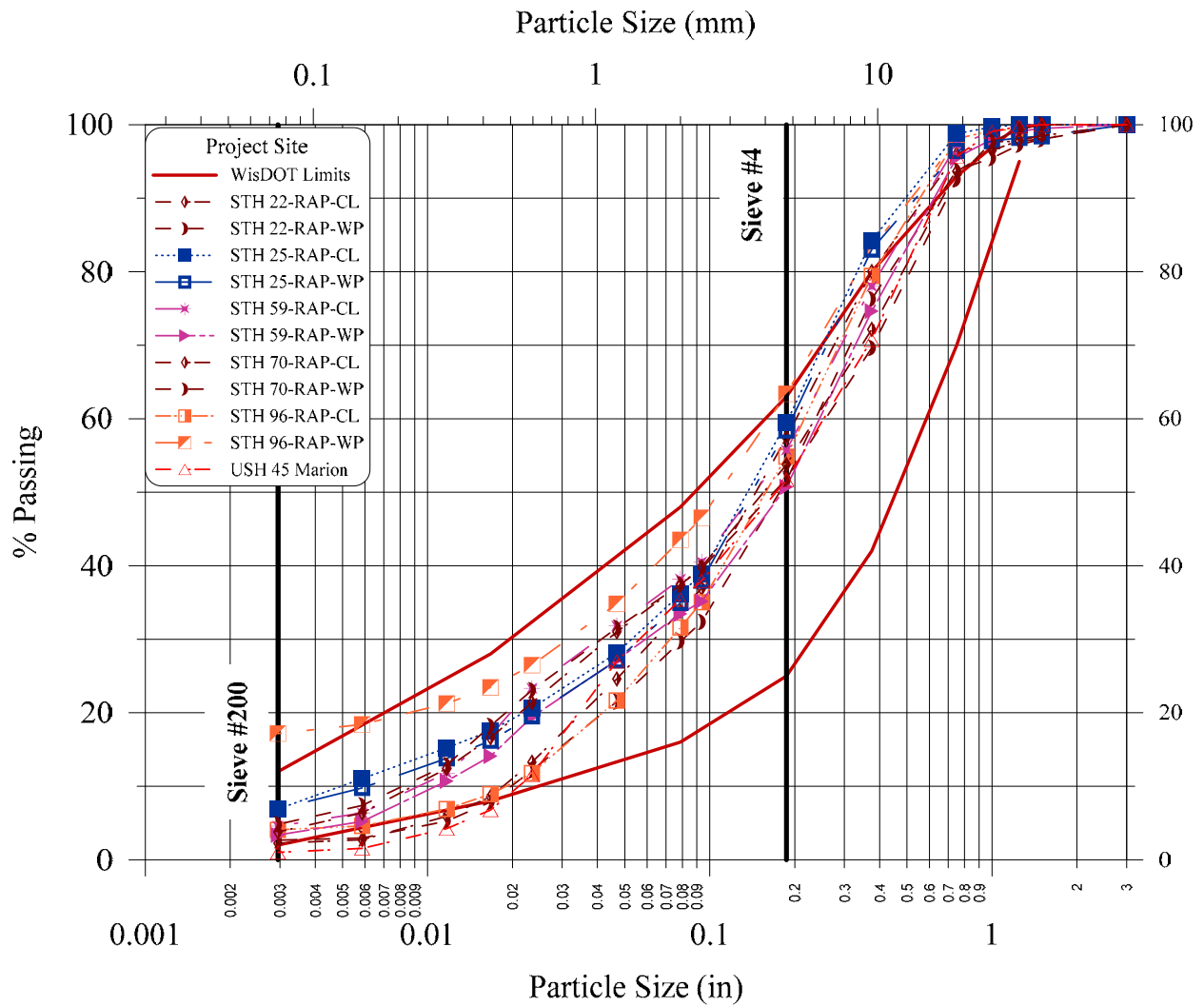
(b) Crushed aggregate samples (CA) versus the 2018 WisDOT gradation specification limits

Figure 4.1 (Cont.): Particle size distribution of the investigated CA, RCA, and RAP base course materials and the current WisDOT gradation specification limits for the 1 1/4" dense graded base course materials.



(c) Recycled concrete aggregate (RCA) versus the 2018 WisDOT gradation specification limits

Figure 4.1 (Cont.): Particle size distribution of the investigated CA, RCA, and RAP base course materials and the current WisDOT gradation specification limits for the 1¼" dense graded base course materials.

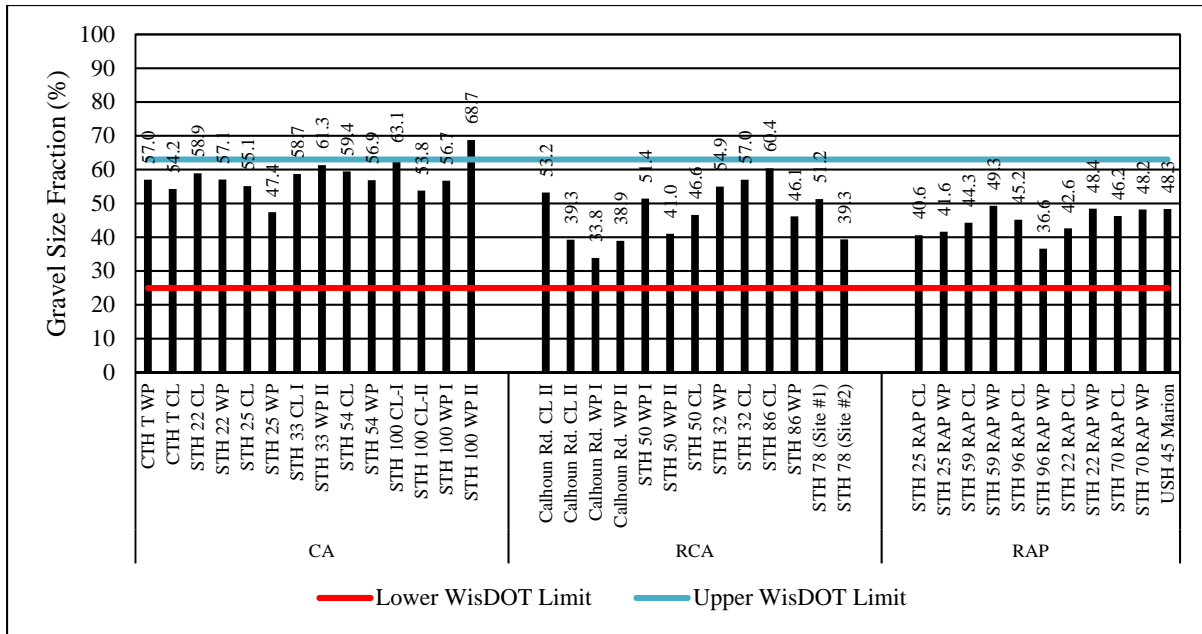


(d) Reclaimed asphalt pavement (RAP) versus the 2018 WisDOT gradation specification limits

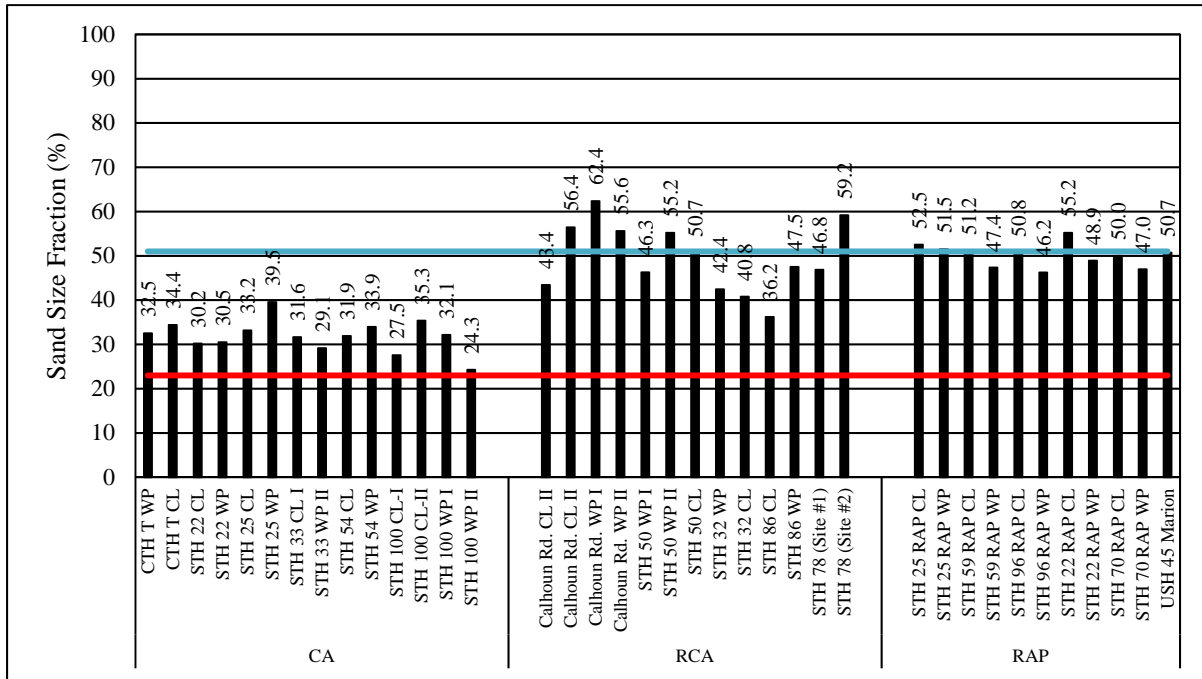
Figure 4.1 (Cont.): Particle size distribution of the investigated CA, RCA, and RAP base course materials and the current WisDOT gradation specification limits for the 1¼" dense graded base course materials.

Table 4.1: Particle size characteristics of the investigated base RCA, CA, and RAP base course.

Aggregate Source		Gravel (%)	Sand (%)	Fine (%)	Fineness Modulus (FM)	Grading Number (GN)
RCA	STH 78 (S1)	51.25	46.84	1.91	4.78	3.48
	STH 78 (S2)	39.34	59.17	1.49	4.34	3.90
	STH 32 CL	56.99	40.78	2.23	4.93	3.49
	STH 32 WP	54.94	42.44	2.62	4.80	3.56
	STH 50 CL	46.59	50.66	2.74	4.58	3.71
	STH 50 WP-1	51.39	46.28	2.34	4.70	3.54
	STH 50 WP-2	41.00	55.19	3.81	4.31	3.92
	Calhoun Rd WP I	33.83	62.36	3.81	4.20	4.13
	Calhoun Rd WP II	38.91	55.60	5.49	4.25	3.96
	Calhoun Rd CL I	53.22	43.41	3.37	4.79	3.49
	Calhoun Rd CL II	39.26	56.44	4.31	4.40	3.93
	STH 86 CL	60.36	36.18	3.46	4.91	3.07
STH 86 WP	46.13	47.51	6.36	4.18	3.70	
CA	STH 22 CL	58.90	30.20	10.90	4.56	3.55
	STH 22 WP	57.06	30.49	12.46	4.47	3.61
	STH 25 CL	55.11	33.17	11.72	4.39	3.63
	STH 25 WP	47.36	39.53	13.10	4.08	3.95
	STH 33 CL	58.71	31.64	9.65	4.40	3.59
	STH 33 WP II	61.29	29.15	9.56	4.52	3.45
	STH 22/54 CL	59.44	31.88	8.68	4.71	3.39
	STH 22/54 WP	56.85	33.93	9.22	4.61	3.51
	STH 100 CL I	63.06	27.55	9.39	4.88	3.33
	STH 100 CL II	53.78	35.35	10.88	4.53	3.62
	STH 100 WP I	56.73	32.13	11.14	4.60	3.54
	STH 100 WP II	68.72	24.26	7.02	5.13	3.14
	CTH T CL	54.24	34.40	11.40	4.41	3.62
CTH T WP	57.01	32.51	10.48	4.51	3.52	
RAP	STH 25 RAP CL	40.58	52.54	6.89	4.28	4.03
	STH 25 RAP WP	41.60	51.48	6.91	4.37	3.94
	STH 59 RAP CL	44.26	51.17	4.57	4.33	3.90
	STH 59 RAP WP	49.26	47.36	3.38	4.56	3.70
	STH 96 RAP CL	45.16	50.78	4.07	4.67	3.76
	STH 96 RAP WP	36.60	46.22	17.18	3.91	4.28
	STH 22 RAP CL	42.58	55.18	2.24	4.63	3.76
	STH 22 RAP WP	48.42	48.90	2.67	4.80	3.57
	STH 70 RAP CL	46.24	49.98	3.78	4.42	3.74
	STH 70 RAP WP	48.20	46.97	4.83	4.41	3.72
	USH 45	48.31	50.70	0.99	4.70	3.60

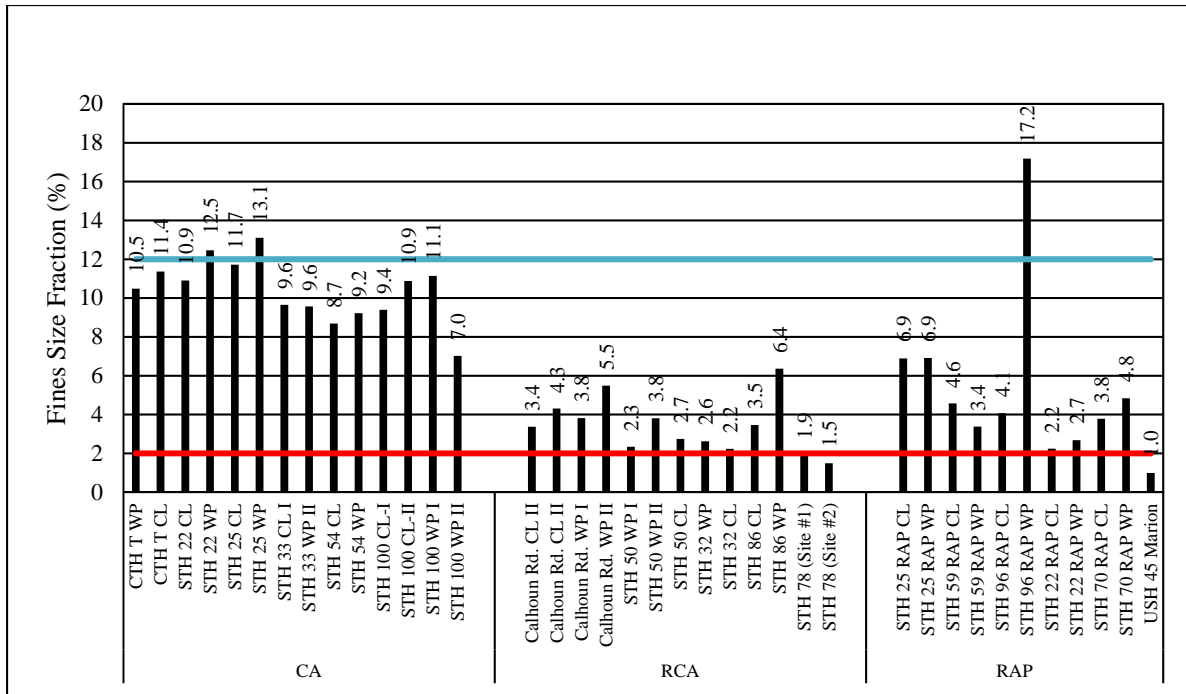


(a) Gravel size fraction

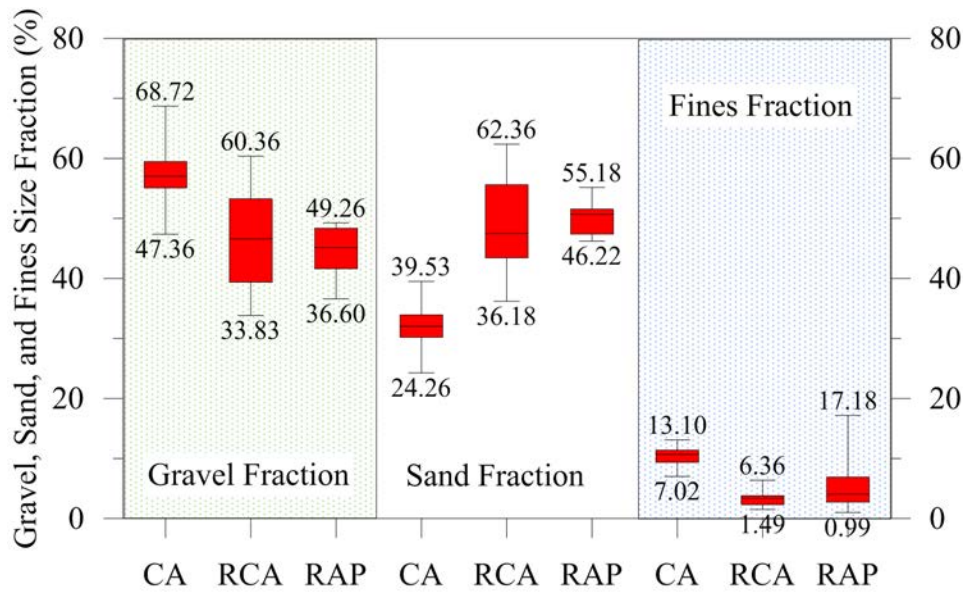


(b) Sand size fraction

Figure 4.2: Particle size characteristics of the investigated CA, RCA, and RAP base materials.

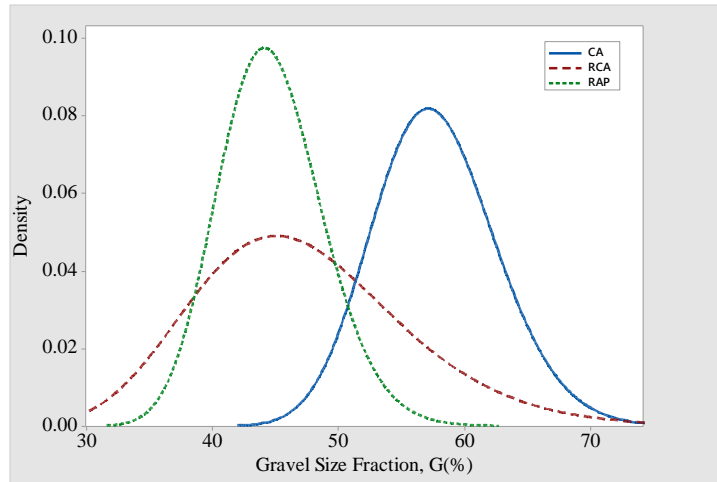


(c) Fines size fraction

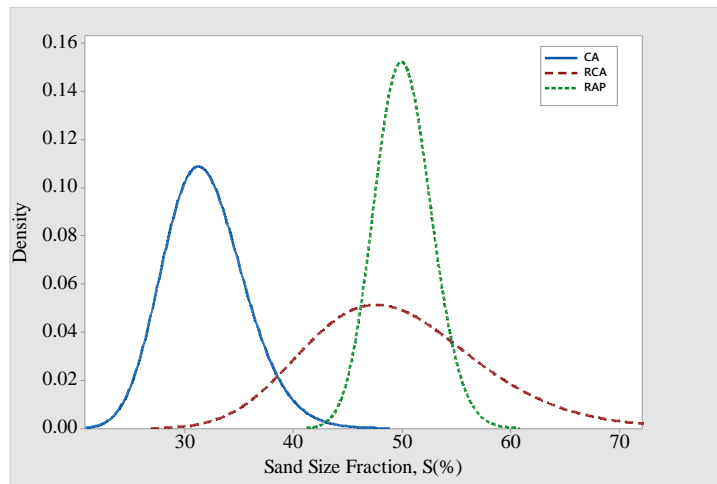


(d) Box-Whisker of the gravel, sand, and fines size fractions

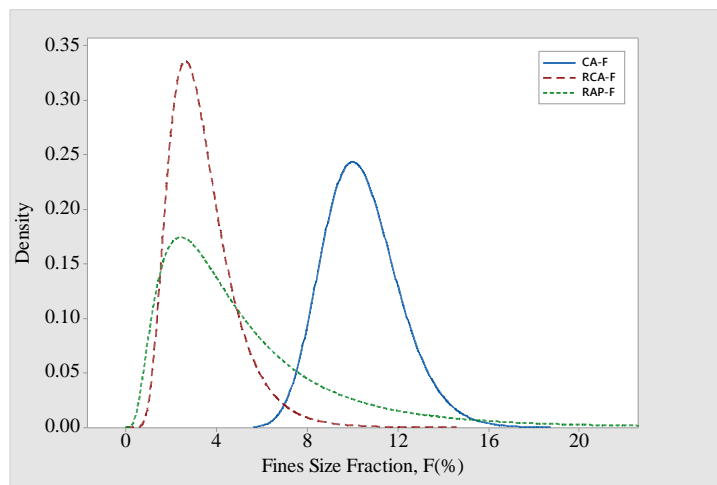
Figure 4.2 (Cont.): Particle size characteristics of the investigated CA, RCA, and RAP base materials.



(a) Gravel Size Fractions



(b) Sand Size Fractions



(c) Fines Size Fractions

Figure 4.3: Lognormal distribution representing the amount of gravel, sand, and fines materials in the investigated CA, RCA, and RAP base materials.

To further evaluate the gradation of base materials, the fineness modulus (FM) was calculated in accordance with the procedures in ASTM C125: Standard Terminology Relating to Concrete and Concrete Aggregates. The larger the FM, the coarser the aggregate is. Another way to evaluate the base materials gradation is by using the Grading Number (GN), which is an index introduced to represent the effect of gradation on DCP test results (Dai and Kremer, 2006). The GN concept is derived from the FM but it uses the percent passing rather than the percent retained. The maximum value of GN is 7 when 100% of the material passes the No. 200 sieve. This represents an extremely fine material (all silt and clay particles). On the other hand, the minimum value of GN is 0 when 0% of the material passes the largest sieve. This indicates a very coarse material. Figure 4.4 presents the FM and GN values for the investigated CA, RCA, and RAP base materials. The FM for the CA base materials ranged from 4.08 to 5.13 with an average of 4.56. For RCA, the FM values ranged from 4.18 to 4.93 with an average of 4.55 and for RAP, these values ranged from 3.91 to 4.80 with an average of 4.46. This indicates that the CA was the coarsest material followed by RCA and RAP, with RAP being the finest among all investigated materials. The same ranking is obtained when using the GN values for the investigated CA, RCA, and RAP base materials as depicted in Figure 4.4. The base materials with the lowest FM values possess the highest GN values, which consistently indicates finer materials. Figure 4.4d depicts the lognormal distributions representing the FM and GN values for the investigated CA, RCA, and RAP base materials. The average GN for the CA base materials is 3.53 (the coarsest) while the average GN for the RAP base materials is 3.82 (the finest). The GN average for the RCA base materials is 3.68. Figure 4.4d shows a clear difference among the three base layer materials when using the GN to express the state of coarseness or fineness of base materials compared with the FM.

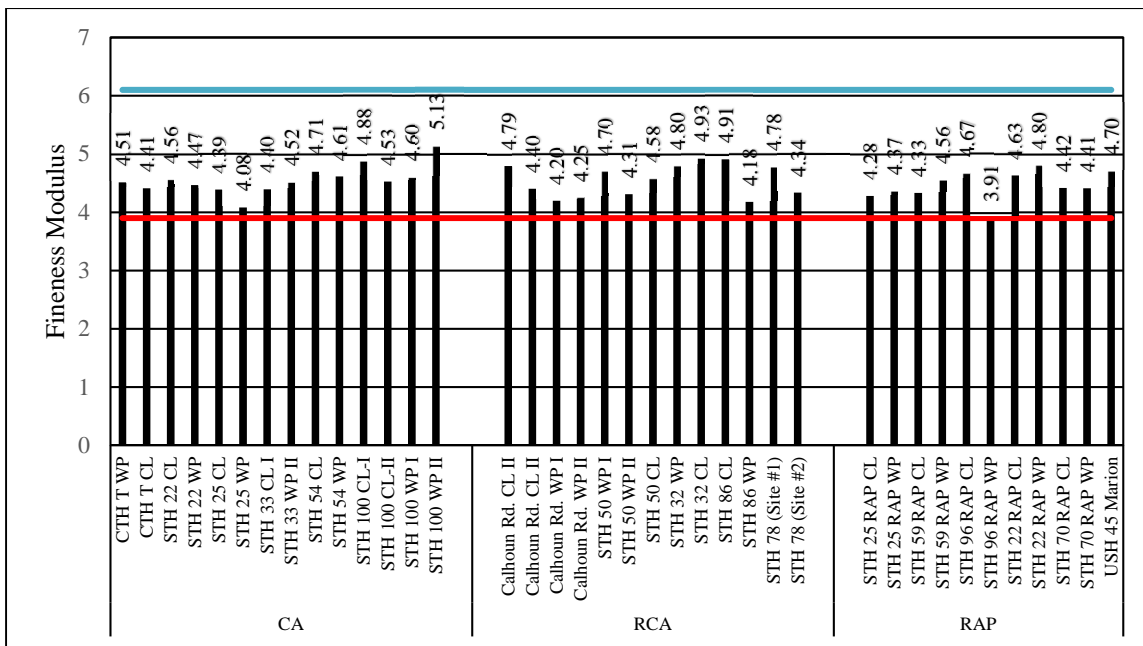
Table 4.2 presents the values of C_u and C_c obtained from the particle size distributions of the investigated CA, RCA, and RAP base materials along with the corresponding USCS classification of these materials. Majority of the CA base materials fell under “poorly-graded gravel with silt and sand” classification, while most of the RCA materials were classified as “well-graded sand with gravel” and “well-graded gravel with sand”. Majority of the RAP base material were classified as “well-graded sand with gravel” and “poorly-graded sand with gravel.” Figure 4.5 depicts the C_u and C_c values showing the C_u value of the CA base material are significantly higher than the C_u values of the RCA and RAP. Similarly, the C_u values of the CA base material are higher compared with the C_c values of the RCA and RAP base materials.

4.2 Specific Gravity and Absorption

The oven-dry (OD) specific gravity, saturated-surface dry (SSD) specific gravity, apparent specific gravity, and absorption of the coarse fraction for the investigated CA, RCA, and RAP base materials are summarized in Table 4.3 and depicted in Figures 4.6-4.7. The results of the oven dry specific gravity ranged from 2.12 to 2.44 with an average of 2.3 and COV of 4.4% for the RCA base materials, which was the lowest among all investigated base layer

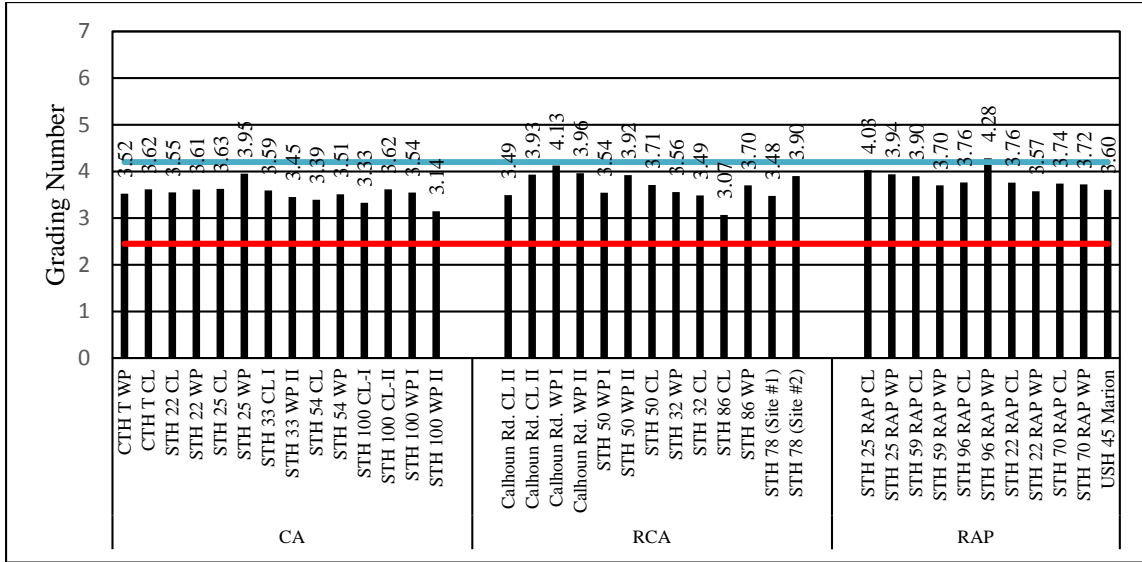
materials. The RAP base materials also possessed an average specific gravity of 2.43 (ranged from 2.17 to 2.60) with a COV of 4.8%, which is relatively lower than the specific gravity CA base materials, which had a range between 2.49 and 2.69 with an average of 2.62 and COV of 2.7%. The low specific gravity of RAP base material is influenced by the asphalt cement coating on the particles.

The absorption test results summarized in Table 4.3 and Figures 4.6-4.7 showed that the investigated RCA base materials exhibited values ranging from 2.67 to 8.2% with an average of 4.6% and COV of 41.9% indicating relatively high absorption characteristics when compared with CA and RAP base materials. On the other hand, the CA base materials showed absorption values ranging from 1.41 to 3.43% with an average of 2.13% and COV of 31.8%. The RAP base materials possessed the lowest absorption values ranging between 1.2 to 2.6% with an average of 1.68% and COV of 29%. Asphalt cement coating the RAP particles plugs their pores and reduces the intrusion of water into RAP particles and therefore reduces absorption. Tabatabai et al. (2013) conducted an analysis on various virgin Wisconsin coarse aggregates and found that the mean absorption value was 1.71%.

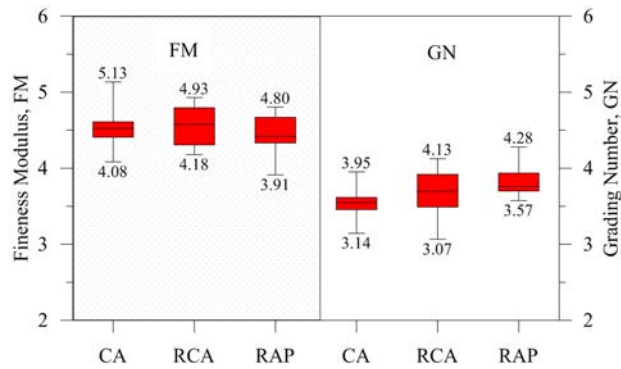


(a) Fineness Modulus (FM) of the investigated aggregates (WisDOT limits are 3.96 to 6.1)

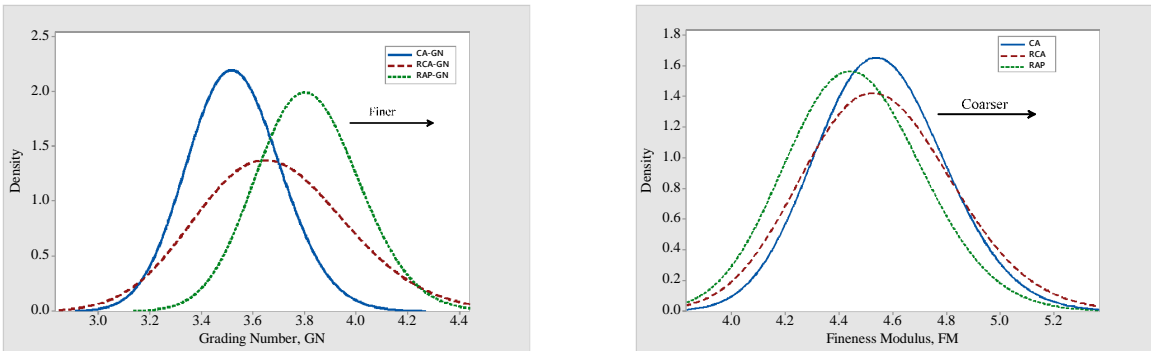
Figure 4.4: Particle size characteristics of the investigated aggregates.



(b) Grading Number (GN) of the investigated aggregates (WisDOT limits are 2.5 to 4.2)



(c) Box-Whisker of the gravel, sand, and fines size fractions

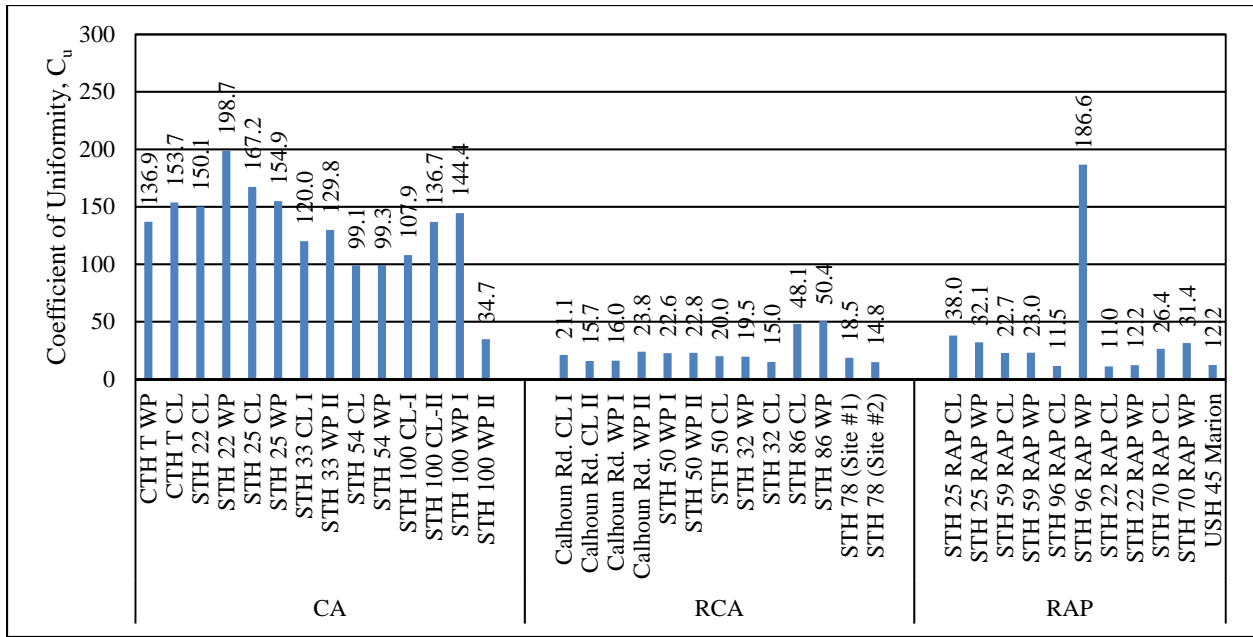


(d) Lognormal distribution of the FM and GN of CA, RCA, and RAP base materials

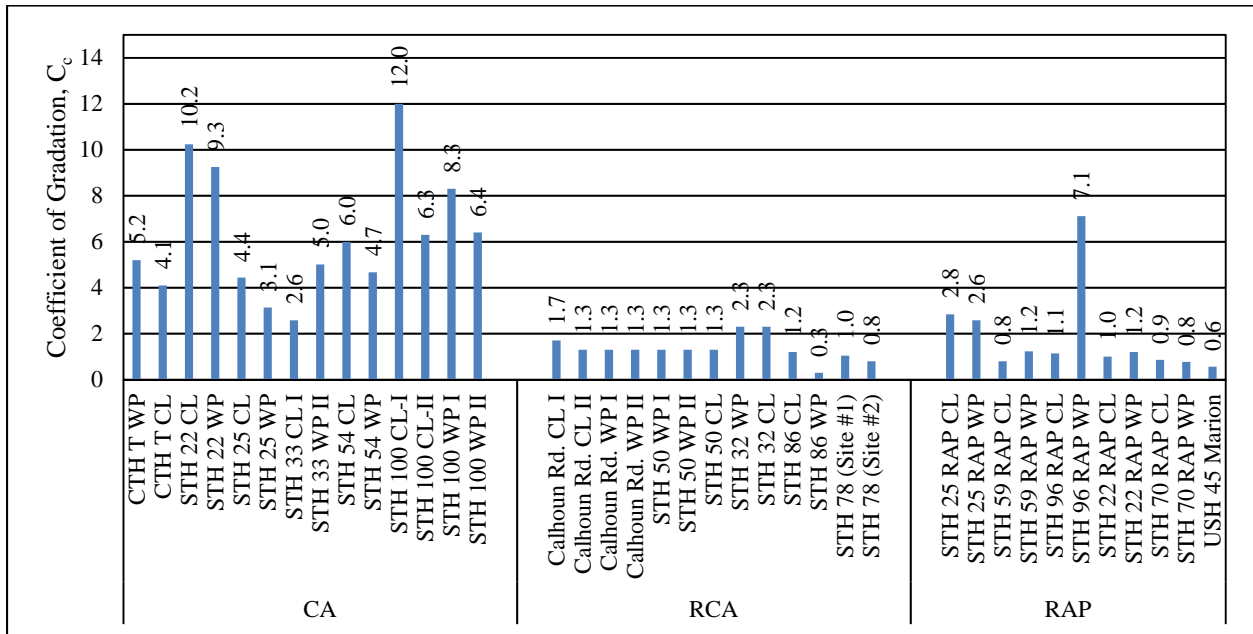
Figure 4.4 (Cont.): Particle size characteristics of the investigated aggregates.

Table 4.2: Classification of the investigated base layer materials according to the USCS.

Aggregate Source	C _u	C _c	Group Symbol	Group Name	
CA	CTH T WP	136.9	5.2	GP-GM	Poorly-graded gravel with silt and Sand
	CTH T CL	153.7	4.1	GP-GM	Poorly-graded gravel with silt and Sand
	STH 22 CL	150.1	10.2	GP-GM	Poorly-graded gravel with silt and Sand
	STH 22 WP	198.7	9.3	GP-GM	Poorly-graded gravel with silt and Sand
	STH 25 CL	167.2	4.4	GP-GM	Poorly-graded gravel with silt and Sand
	STH 25 WP	154.9	3.1	GC	Clayey gravel with sand
	STH 33 CL I	120.0	2.6	GW-GM	Well-graded gravel with silt and sand
	STH 33 WP II	129.8	5.0	GP-GM	Poorly-graded gravel with silt and Sand
	STH 54 CL	99.1	6.0	GP-GM	Poorly-graded gravel with silt and Sand
	STH 54 WP	99.3	4.7	GP-GM	Poorly-graded gravel with silt and Sand
	STH 100 CL-I	107.9	12.0	GP-GM	Poorly-graded gravel with silt and Sand
	STH 100 CL-II	136.7	6.3	GP-GM	Poorly-graded gravel with silt and Sand
	STH 100 WP I	144.4	8.3	GP-GM	Poorly-graded gravel with silt and Sand
STH 100 WP II	34.7	6.4	GP-GM	Poorly-graded gravel with silt and Sand	
RCA	Calhoun Rd. CL II	21.1	1.7	GW	Well-graded gravel with sand
	Calhoun Rd. CL II	15.7	1.3	SW	Well-graded sand with gravel
	Calhoun Rd. WP I	16.0	1.3	SW	Well-graded sand with gravel
	Calhoun Rd. WP II	23.8	1.3	SW-SM	Well-graded sand with silt and gravel
	STH 50 WP I	22.6	1.3	GW	Well-graded gravel with sand
	STH 50 WP II	22.8	1.3	SW	Well-graded sand with gravel
	STH 50 CL	20.0	1.3	SW	Well-graded sand with gravel
	STH 32 WP	19.5	2.3	GW	Well-graded gravel with sand
	STH 32 CL	15.0	2.3	GW	Well-graded gravel with sand
	STH 86 CL	48.1	1.2	GW	Well-graded gravel with sand
	STH 86 WP	50.4	0.3	SP-SM	Poorly-graded sand with silt and gravel
	STH 78 (Site #1)	18.5	1.0	GW	Well-graded gravel with sand
STH 78 (Site #2)	14.8	0.8	SP	Poorly-graded sand with gravel	
RAP	STH 25 RAP CL	38.0	2.8	SW-SM	Well-graded sand with silt and gravel
	STH 25 RAP WP	32.1	2.6	SW-SM	Well-graded sand with silt and gravel
	STH 59 RAP CL	22.7	0.8	SP	Poorly-graded sand with gravel
	STH 59 RAP WP	23.0	1.2	GW	Well-graded gravel with sand
	STH 96 RAP CL	11.5	1.1	SW	Well-graded sand with gravel
	STH 96 RAP WP	186.6	7.1	SC	Clayey sand with gravel
	STH 22 RAP CL	11.0	1.0	SW	Well-graded sand with gravel
	STH 22 RAP WP	12.2	1.2	SW	Well-graded sand with gravel
	STH 70 RAP CL	26.4	0.9	SP	Poorly-graded sand with gravel
	STH 70 RAP WP	31.4	0.8	SP	Poorly-graded sand with gravel
USH 45 Marion	12.2	0.6	SP	Poorly-graded sand with gravel	



(a) C_u

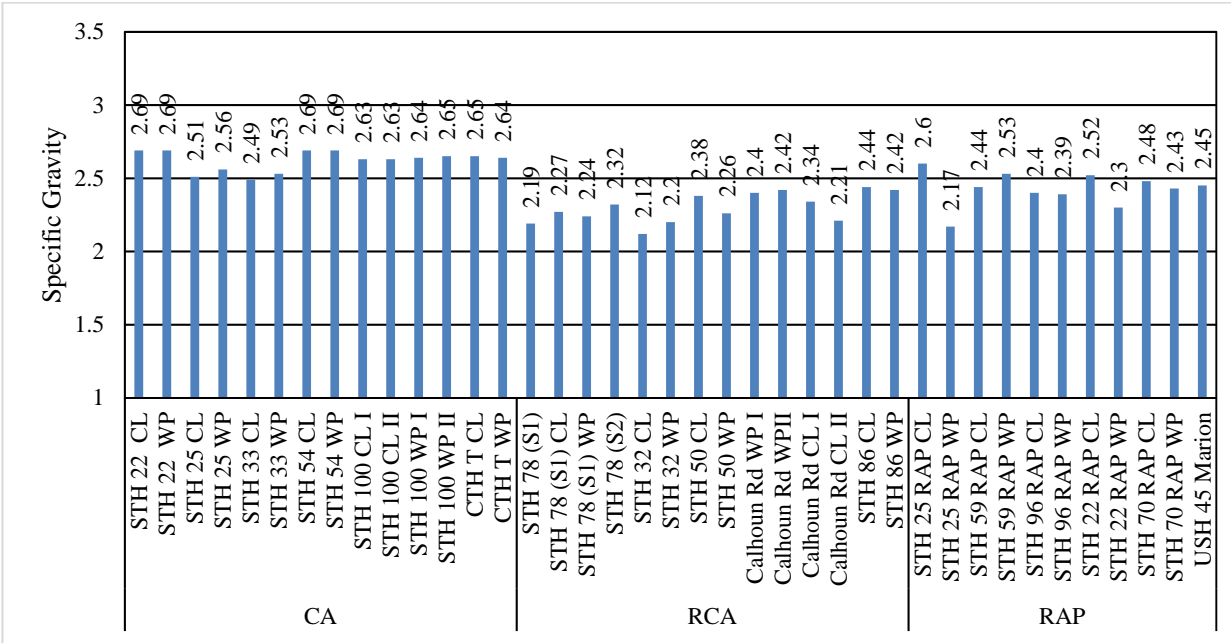


(b) C_c

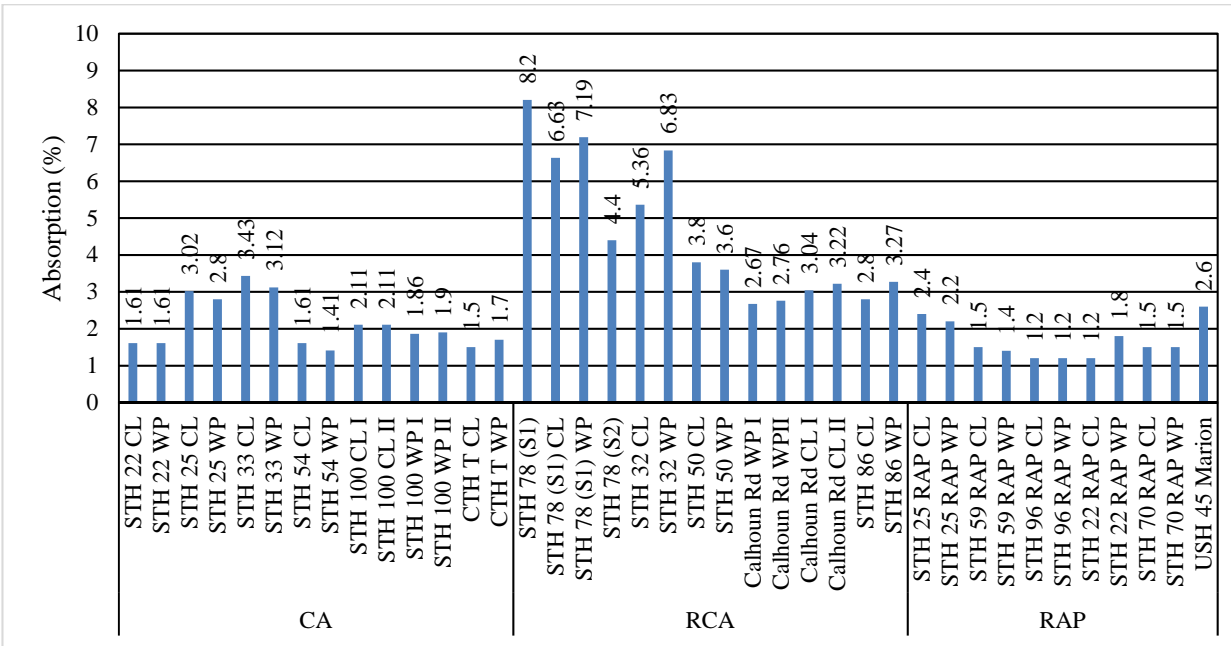
Figure 4.5: Coefficients of uniformity and gradation for the investigated CA, RCA, and RAP base layer materials.

Table 4.3: Results of specific gravity and absorption tests on the investigated RCA, CA, and RAP base materials (coarse fraction).

Base Materials Source		Specific Gravity			Absorption (%)
		OD	SSD	Apparent	
RCA	STH 78 (S1)	2.19	2.37	2.67	8.20
	STH 78 (S) CL	2.27	2.42	2.67	6.63
	STH 78 (S1) WP	2.24	2.40	2.67	7.19
	STH 78 (S2)	2.32	2.42	2.58	4.40
	STH 32 CL	2.12	2.23	2.39	5.36
	STH 32 WP	2.20	2.34	2.58	6.83
	STH 50 CL	2.38	2.47	2.61	3.80
	STH 50 WP	2.26	2.34	2.46	3.60
	Calhoun Rd WP I	2.40	2.47	2.57	2.67
	Calhoun Rd WP II	2.42	2.49	2.59	2.76
	Calhoun Rd CL I	2.34	2.41	2.51	3.04
	Calhoun Rd CL II	2.21	2.28	2.38	3.22
	STH 86 CL	2.44	2.51	2.62	2.80
	STH 86 WP	2.42	2.50	2.63	3.27
CA	STH 22 CL	2.69	2.74	2.82	1.61
	STH 22 WP	2.69	2.74	2.82	1.61
	STH 25 CL	2.51	2.58	2.71	3.02
	STH 25 WP	2.56	2.64	2.76	2.80
	STH 33 CL	2.49	2.58	2.73	3.43
	STH 33 WP	2.53	2.61	2.75	3.12
	STH 22/54 CL	2.69	2.73	2.81	1.61
	STH 22/54 WP	2.69	2.73	2.80	1.41
	STH 100 CL I	2.63	2.68	2.78	2.11
	STH 100 CL II	2.63	2.69	2.79	2.11
	STH 100 WP I	2.64	2.69	2.78	1.86
	STH 100 WP II	2.65	2.70	2.79	1.90
	CTH T CL	2.65	2.69	2.76	1.50
	CTH T WP	2.64	2.68	2.76	1.70
RAP	STH 25 RAP CL	2.60	2.66	2.77	2.40
	STH 25 RAP WP	2.17	2.22	2.28	2.20
	STH 59 RAP CL	2.44	2.48	2.53	1.50
	STH 59 RAP WP	2.53	2.57	2.62	1.40
	STH 96 RAP CL	2.40	2.43	2.48	1.20
	STH 96 RAP WP	2.39	2.42	2.46	1.20
	STH 22 RAP CL	2.52	2.55	2.60	1.20
	STH 22 RAP WP	2.30	2.35	2.40	1.80
	STH 70 RAP CL	2.48	2.52	2.58	1.50
	STH 70 RAP WP	2.43	2.47	2.53	1.50
	USH 45	2.45	2.51	2.62	2.60

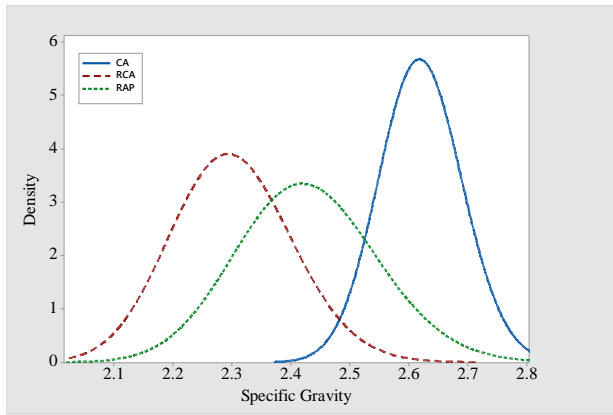


(a) Specific gravity

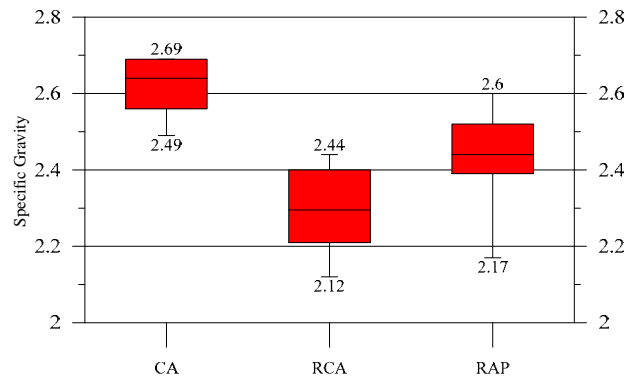


(b) Absorption

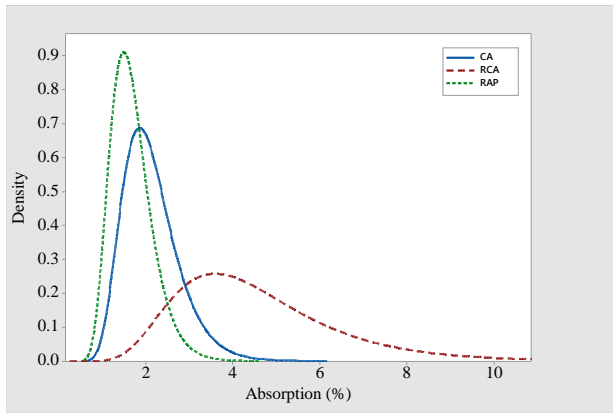
Figure 4.6: Specific gravity and absorption test results for investigated CA, RCA, and RAP base materials.



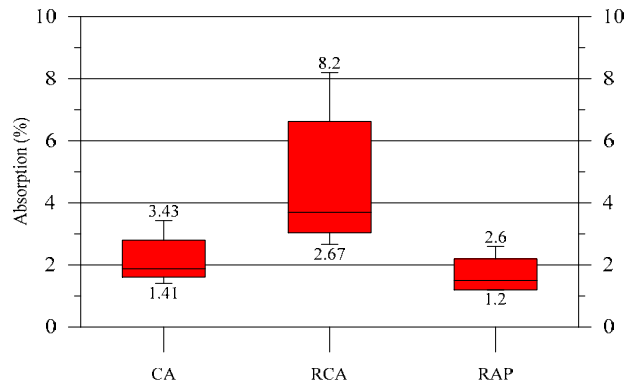
(a) Lognormal distribution of specific gravity



(b) Box-Whisker plot of specific gravity



(c) Lognormal distribution of absorption



(d) Box-Whisker plot of absorption

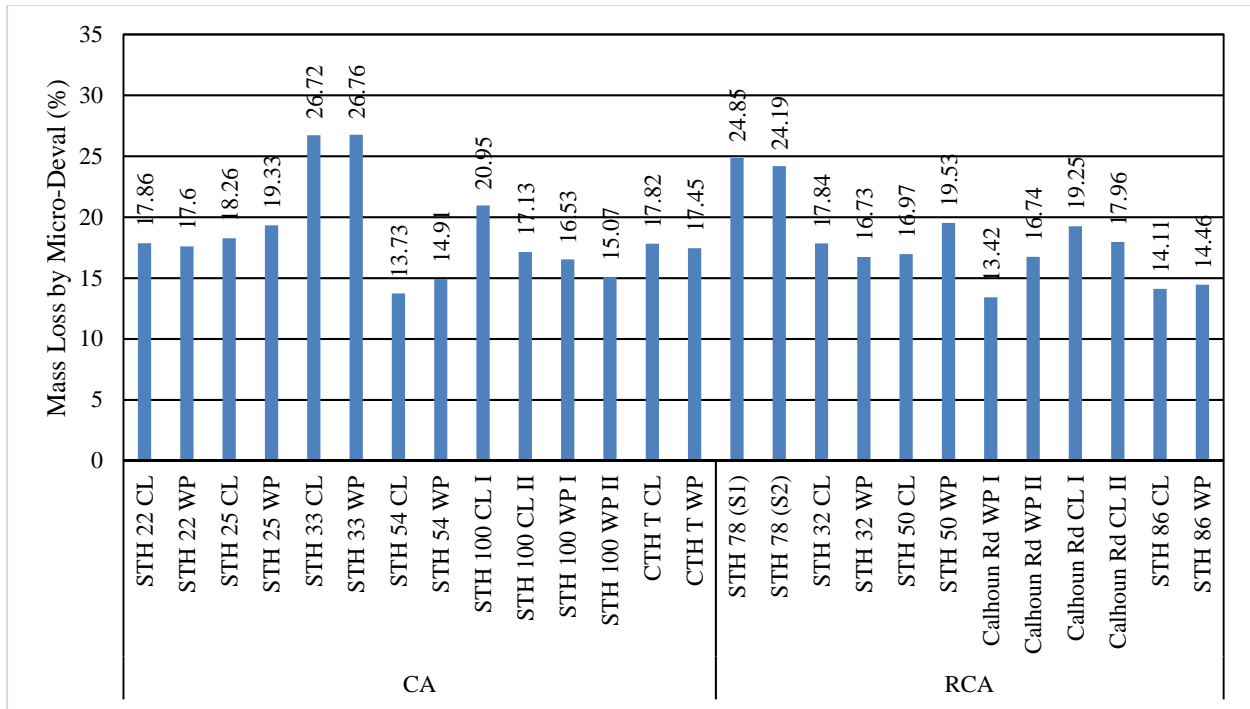
Figure 4.7: Variability of specific gravity and absorption test results for investigated CA, RCA, and RAP base materials.

4.3 Micro-Deval Abrasion

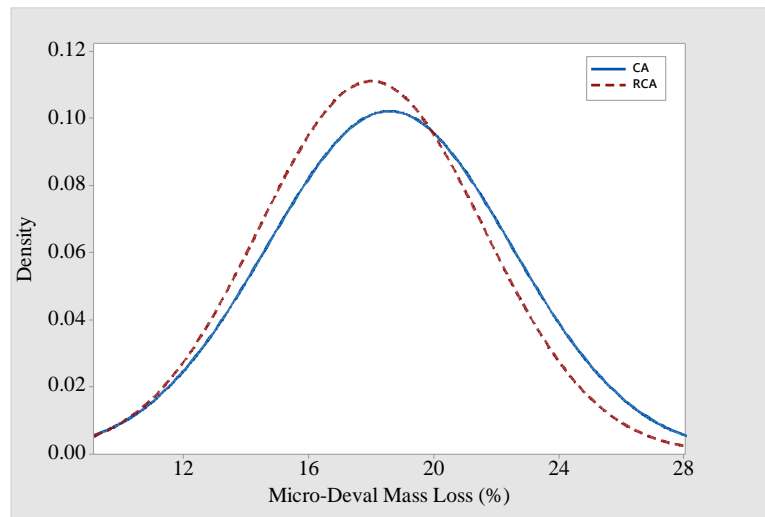
The results of the Micro-Deval abrasion tests on the coarse-aggregate fractions for the CA and RCA base materials are presented in Table 4.4 and Figure 4.8. The percent mass loss by Micro-Deval abrasion test for both base material types are comparable. The mass loss for the CA base materials ranged from 13.7 to 26.8% with an average of 18.6% and COV of 21%. For the RCA base materials, the mass loss varied between 13.4 and 24.9% with an average of 18% and COV of 20%. Tabatabai et al. (2013) conducted an analysis on Micro-Deval test results on various Wisconsin coarse aggregates and reported the mean Micro-Deval mass loss was 15.05% for coarse aggregates. The investigated CA and RCA base materials exhibited mass loss percentages that are generally high compared with crushed stone natural aggregates.

Table 4.4: Mass loss of coarse aggregates by Micro-Deval abrasion test for the investigated CA, and RCA base materials.

Base Layer Aggregate Source		Mass Loss (%)	
RCA	STH 78 (S1)	24.85	
	STH 78 (S2)	24.19	
	STH 32 CL	17.84	
	STH 32 WP	16.73	
	STH 50 CL	16.97	
	STH 50 WP	19.53	
	Calhoun Rd WP I	13.42	
	Calhoun Rd WP II	16.74	
	Calhoun Rd CL I	19.25	
	Calhoun Rd CL II	17.96	
	STH 86 CL	14.11	
	STH 86 WP	14.46	
	CA	STH 22 CL	17.86
		STH 22 WP	17.60
STH 25 CL		18.26	
STH 25 WP		19.33	
STH 33 CL		26.72	
STH 33 WP		26.76	
STH 54 CL		13.73	
STH 54 WP		14.91	
STH 100 CL I		20.95	
STH 100 CL II		17.13	
STH 100 WP I		16.53	
STH 100 WP II		15.07	
CTH T CL		17.82	
CTH T WP		17.45	

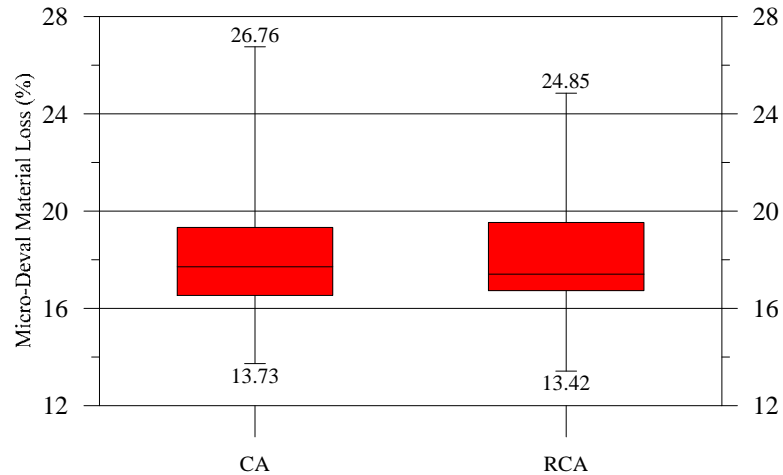


(a) Bar chart of Micro-Deval mass loss



(b) Lognormal distribution

Figure 4.8: Mass loss of coarse aggregates fraction for CA and RCA base materials due to the Micro-Deval test.



(c) Box-Whisker plot of Micro-Deval mass loss

Figure 4.8 (Cont.): Mass loss of coarse aggregates fraction for CA and RCA base materials due to the Micro-Deval test.

For the durability evaluation of CA and RCA base materials, analysis of the Micro-Deval abrasion and absorption data were conducted and combined with data obtained from other studies, namely: WHRP-1 (Weyers et al., 2005), WHRP-2 (Tabatabai et al., 2013), WHRP-3, WHRP-4 (data obtained from WisDOT materials testing files/database via personal communications with the research team), and the aggregate durability study WHRP-5 (Titi et al., 2018). The mass losses of coarse fractions of CA and RCA quantified by the Micro-Deval abrasion test are plotted against absorption in Figure 4.9a for various Wisconsin aggregates tests reported in the WHRP-1, WHRP-2, WHRP-3, WHRP-4, and WHRP-5 studies.

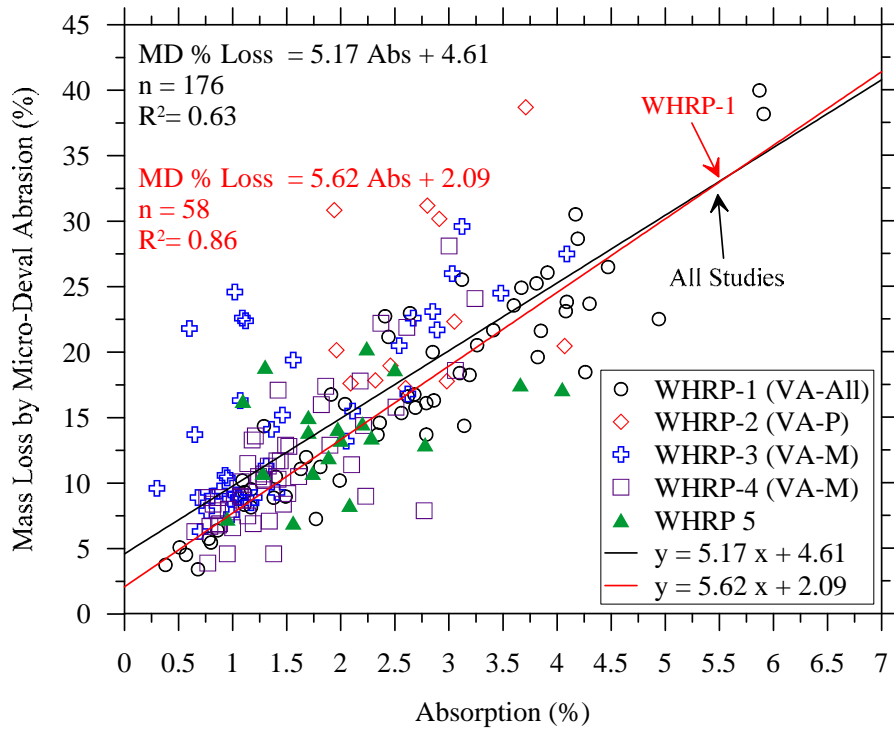
For the WHRP-1 results presented in Figure 4.9a, the aggregates were obtained from Wisconsin pits and quarries (i.e., crushed stone and natural gravel) and included virgin aggregates of good, intermediate, and poor performance quality as specified in Weyers et al. (2005). For these aggregates, mass loss during the Micro-Deval abrasion test ranged between 3.42% (for coarse aggregate with 0.68% absorption) and 39.98% (for coarse aggregate with 5.87% absorption). This is consistent with the results reported by Rismantojo (2000) which indicated that there was a significant relationship between Micro-Deval abrasion and aggregate absorption.

When separating the coarse aggregate test results from the WHRP-1 study into groups based on performance, the virgin aggregates with good performance quality exhibited a mass loss ranging from 3.76% (for coarse aggregate with 0.38% absorption) and 23.57% (for coarse aggregate with 3.6% absorption). For the virgin aggregates with intermediate performance quality, the mass loss varied between 3.42% (for the coarse aggregate with 0.68% absorption) to 26.5% (for the coarse aggregate with 4.47% absorption). Finally, for the virgin aggregates with

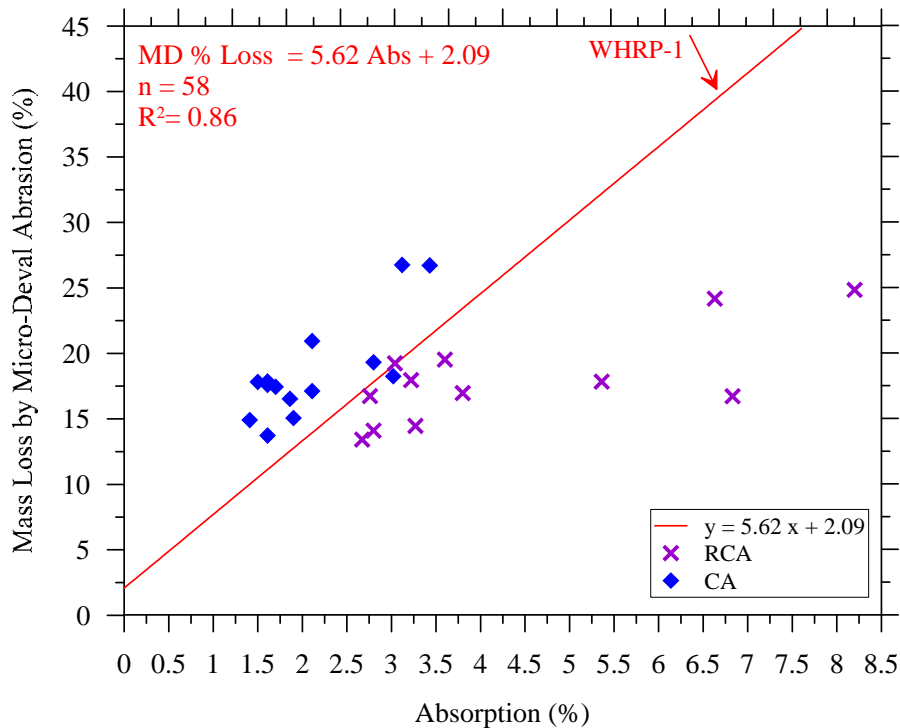
poor performance quality, the mass loss ranged between 5.09% (for the coarse aggregate with 0.51% absorption) and 39.98% (for the coarse aggregate with 5.87 % absorption).

Tabatabai et al. (2013 and 2018) conducted Micro-Deval abrasion and absorption tests on Wisconsin aggregates with poor performance (WHRP-2 study) and reported that the mass loss ranged between 17.26% (for coarse aggregate with 2.6% absorption) and 38.7% (for coarse aggregate with 3.71% absorption). For WHRP-3 data, test results on virgin aggregates with mixed performance showed the mass loss ranging between 6.3% (for coarse aggregate with 0.7% absorption) and 27.5% (for coarse aggregate with 4.09% absorption). For the WHRP-4 data with aggregates of mixed performance, the mass loss of coarse aggregate ranged between 3.9% (for coarse aggregate with 0.77% absorption) and 28.1% (for coarse aggregate with 3.9% absorption). The preceding analysis considered only Wisconsin virgin aggregates. However, the current study is investigating recycled materials base layer aggregates but can use the results on Wisconsin various aggregates as a reference for performance comparison.

Inspection of Figure 4.9b does not lead to solid conclusions with respect to predicting the Micro-Deval abrasion test results from the absorption or identifying the performance of base aggregate layers based solely on the results of the Micro-Deval test. However, both the Micro-Deval abrasion and absorption tests provided important information on the durability of recycled aggregate base materials.



(a) Best fit for all WHRP studies



(b) Current study with respect to best fit model (WHRP-1)

Figure 4.9: Comparison of mass loss of coarse aggregates from Micro-Deval abrasion versus absorption for various Wisconsin virgin aggregates.

4.4 Case Study – RCA Base Layer Material at STH 78

The HMA pavement of STH 78 between Merrimac and Prairie du Sac was constructed on RCA base layer with materials obtained from deconstruction of building. Pavement performance in terms of cracking and ride quality was low compared with expected HMA pavement performance with similar number of service years. The research team joined WisDOT field investigation and conducted field and laboratory tests to characterize the RCA materials. The objective is to search for reasons behind this unsatisfactory performance.

Figure 4.10 depicts the particle size distribution plots of the RCA base material from tests conducted in 2009 (by WisDOT and contractors) and in 2018 (by WisDOT and the research team). The figure also depicts the current and the 2009 WisDOT specification limits for dense graded base.

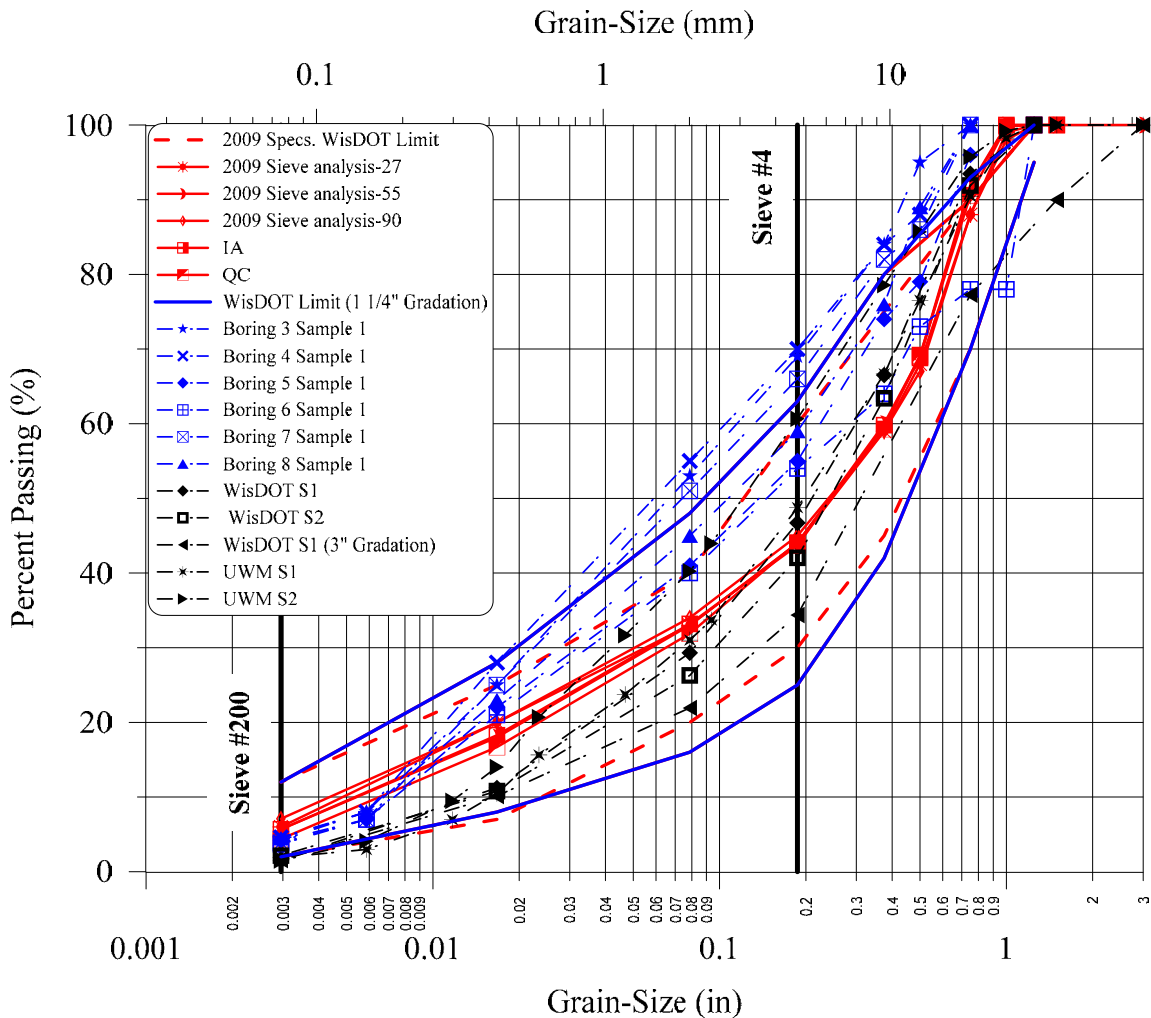
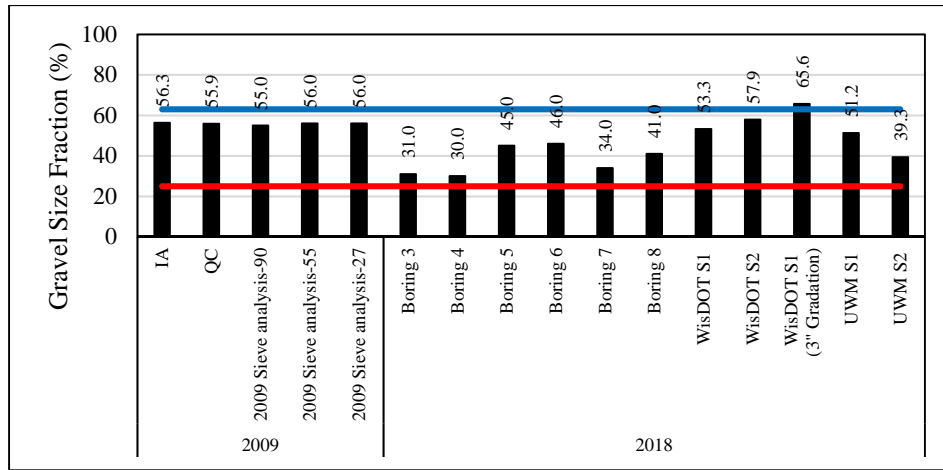


Figure 4.10: Particle size distribution of the investigated RCA base course material at STH 78 with data from 2009 and 2018.

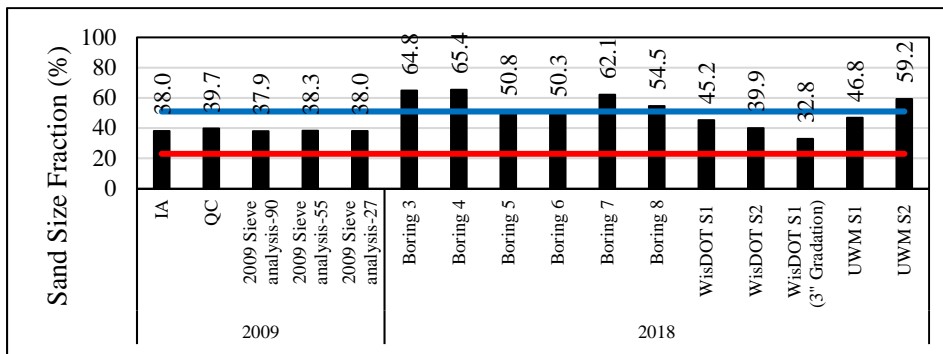
The particle size distribution plots in solid red lines are pertaining the 2009 tests while the dashed blue and black lines denote the 2018 tests. Visual examination of the figure shows that there is a shift in the particle size distributions towards the finer fraction from 2009 to 2018. To quantify such observation, the gravel, sand, and fines size fractions are calculated and presented in Table 4.5 and Figure 4.11. An examination of Table 4.5 and Figure 4.11 shows that, in general, the gravel size fractions were higher, and the sand size fractions were lower in 2009 but after nine years of service the test results showed lower gravel size fractions and higher sand size fractions. Such observation indicates degradation of base layer materials that could be attributed to freeze-thaw cycles. An opposite trend pertaining to the fines size fractions can be seen in Figure 4.11.

Table 4.5: Particle size characteristics of the investigated RCA base course of STH 78.

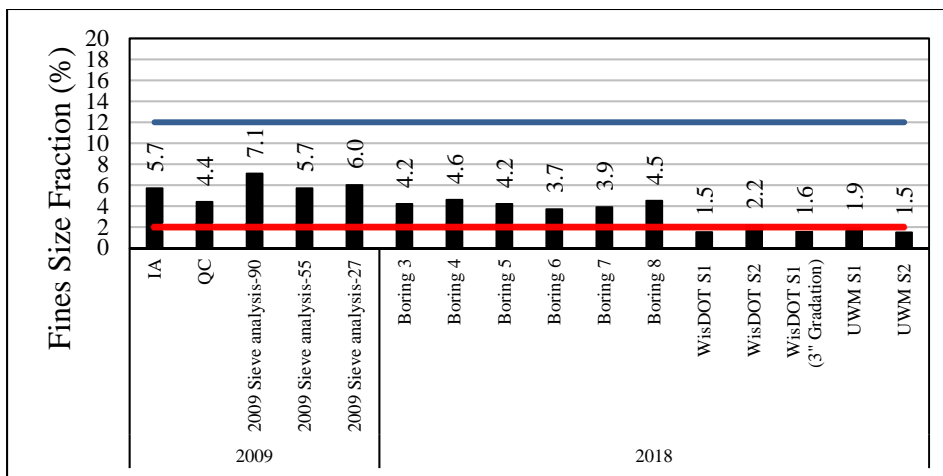
Aggregate Source		Gravel (%)	Sand (%)	Fine (%)	Fineness Modulus	Grading Number
2009	IA	56.3	38.0	5.7	4.53	3.52
	QC	55.9	39.7	4.4	4.61	3.47
	2009 Sieve analysis-90	55.0	37.9	7.1	4.49	3.52
	2009 Sieve analysis-55	56.0	38.3	5.7	4.54	3.53
	2009 Sieve analysis-27	56.0	38.0	6.0	4.53	3.48
2018	Boring 3	31.0	64.8	4.2	3.73	3.35
	Boring 4	30.0	65.4	4.6	3.63	3.42
	Boring 5	45.0	50.8	4.2	4.21	2.92
	Boring 6	46.0	50.3	3.7	4.43	3.39
	Boring 7	34.0	62.1	3.9	3.81	3.28
	Boring 8	41.0	54.5	4.5	4.02	3.08
	WisDOT S1	53.3	45.2	1.5	4.74	3.46
	WisDOT S2	57.9	39.9	2.2	4.87	3.33
	WisDOT S1 (3" Gradation)	65.6	32.8	1.6	5.20	2.84
	UWM S1	51.2	46.8	1.9	4.74	3.48
	UWM S2	39.3	59.2	1.5	4.34	3.90



(a) Gravel size fraction



(b) Sand size fraction



(c) Fines size fraction

Figure 4.11: Particle size characteristics of the investigated RCA base material for STH 78.

The results of LA abrasion, freeze-thaw, and Micro-Deval tests on the RCA base material from the stockpile and STH 78 base layer are depicted in Figure 4.12. The percent mass loss from all tests are generally high. The mass loss from LA abrasion test ranged from 33.8 to 37.9% compared with 30% reported for MnDOT RCA, 23% for MnDOT class 5 aggregate, 36% for recycled clay brick, and 20 to 45% reported by FHWA as typical range. The mass loss from AASHTO T 103 (soundness of aggregates by freezing and thawing) ranged between 36.1 and 53.5%. The mass loss values from the Micro-Deval abrasion were 24.2 and 24.9% compared with 11% reported for MnDOT class 5 materials (after 30 wet/dry cycles), 16% for RCA from California (after 30 wet/dry cycles), and 21% for RCA from Texas (after 30 wet/dry cycles). The absorption values for the STH 78 RCA ranged from 4.4 to 8.2% with an average of 6.6%.

Tabatabai et al. (2013 and 2018) conducted tests on 12 marginal (poor) crushed aggregate samples from Wisconsin. Test results showed that the LA abrasion the mass loss ranged from 21 to 41% with an average of 35%, the Micro-Deval mass loss ranged between 17.3 and 38.7 with an average of 23.62%, the freeze-thaw mass loss ranged from 0.5 to 31.8% with an average of 12.12. It should be noted that the absorption for these samples varied between 1.94 and 4.07% with an average of 2.65%. Comparison of the test results in Figure 4.12 for the RCA base materials and the aggregate marginal values presented above shows that mass loss from LA abrasion and Micro-Deval tests are comparable. The mass loss and absorption of the RCA base materials were higher than the corresponding values for the marginal aggregates, indicating poor performance of the RCA base materials in these tests. The pictures in Figure 4.13 show the RCA base material before and after Micro-Deval abrasion test demonstrating the poor quality of such material where the RCA cement paste were lost during the test leaving just the original gravel used in the original PCC mix.

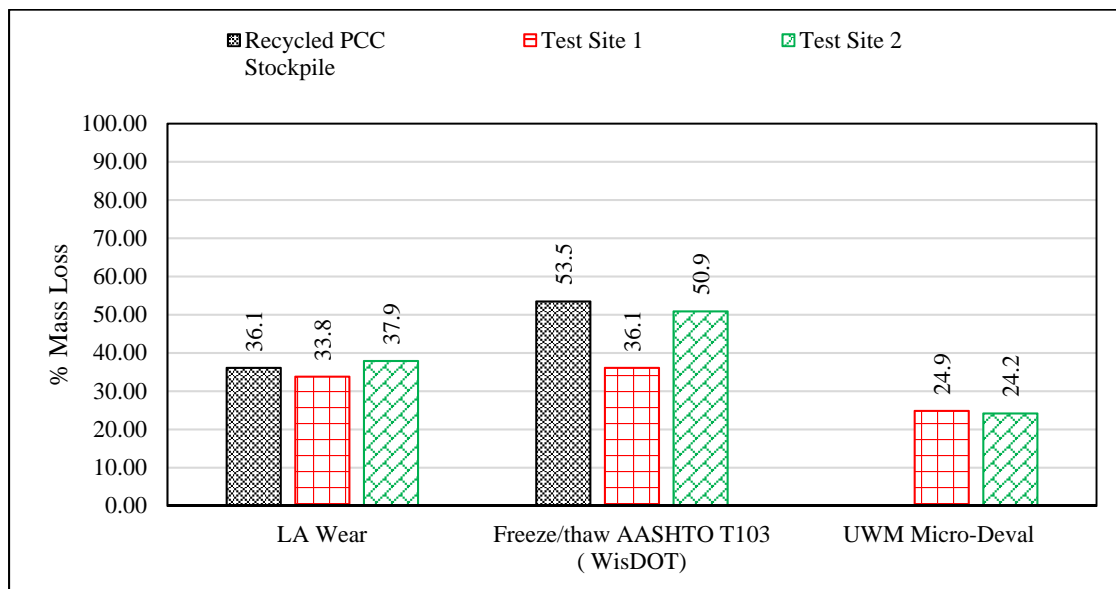


Figure 4.12: Mass loss of the RCA base material at STH 78.

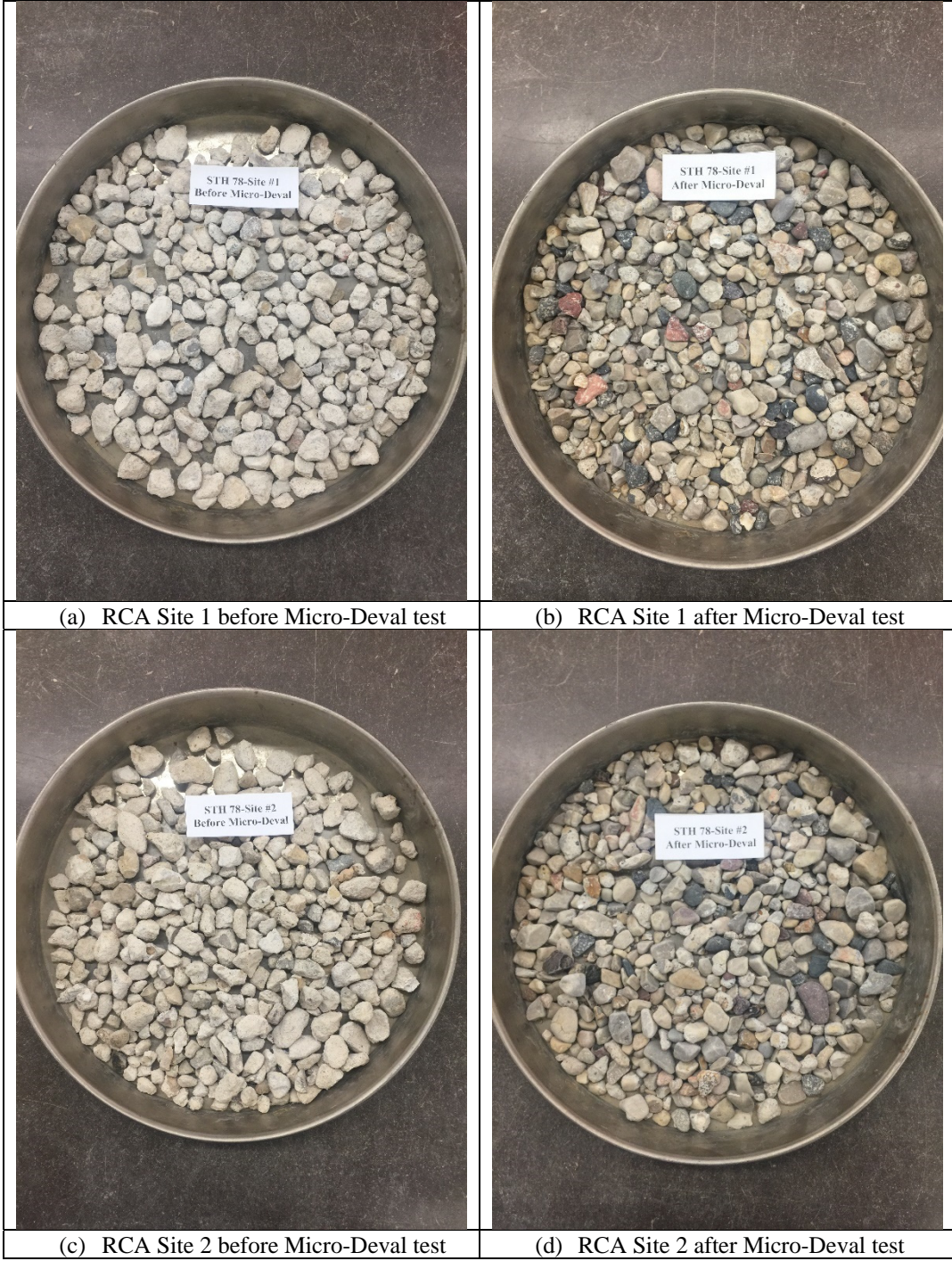


Figure 4.13: Pictures of the RCA base material from STH 78 before and after Micro-Deval abrasion test.

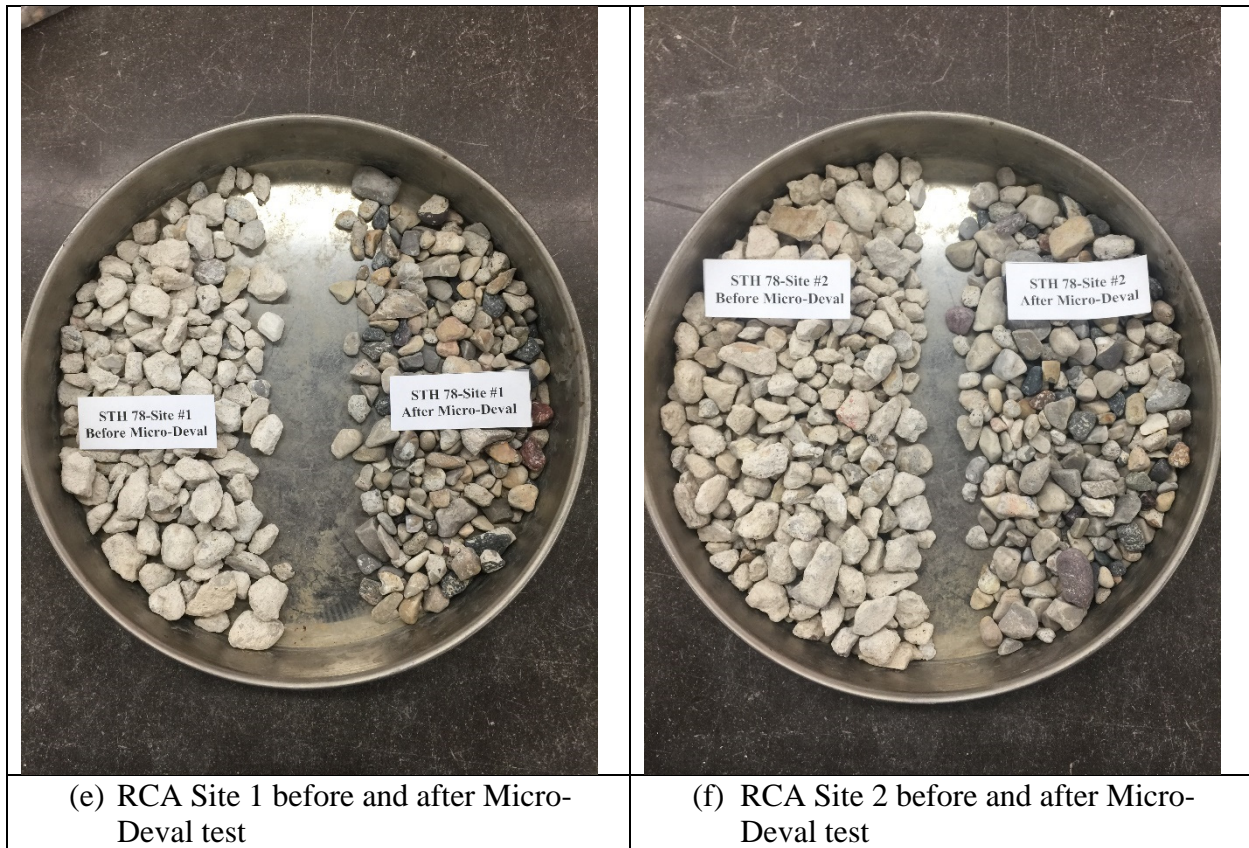


Figure 4.13 (Cont.): Pictures of the RCA base material from STH 78 before and after Micro-Deval abrasion test.

The poor performance of the STH 78 pavement in terms of pavement condition and ride quality is presented and discussed in detail in Chapter 7 based on the field measurements of pavement performance indicators by WisDOT and the research team. Such performance could be attributed in part to the poor performance of the RCA base layer materials where the field moisture content values were relatively high ranging from 3.66 to 19.93% with an average of 10.47% (Figure 4.14). The higher than normal absorption characteristics and sand size fraction increase the chance to retain moisture resulting in pavement surface heave/movement due to freeze thaw effect.

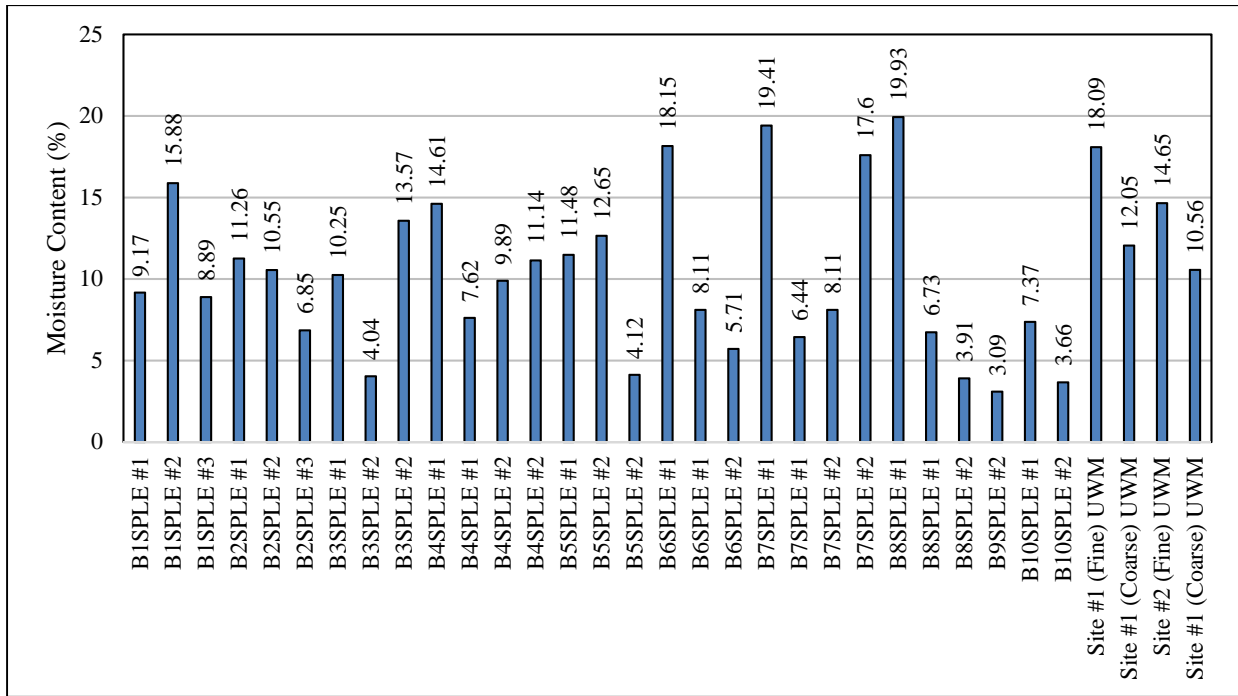


Figure 4.14: Moisture content of the investigated RCA base course layer of STH 78 at several locations.

Chapter 5

Field Tests on Aggregate Base Layers – Analysis of Results

This chapter presents the results of the field tests on the CA, RCA, and RAP base layers of the investigated pavement sections. Results of the DCP, FWD, GPR, drainability, visual distress survey, and walking profiler tests and measurements are analyzed and critically evaluated.

5.1 Dynamic Cone Penetration Test Results

Multiple DCP tests were conducted at each pavement test site on both the wheel path and the lane center whenever possible. DCP test results were not possible to obtain from the RCA base layer at STH 78 between Merrimac and Prairie du Sac due to refusal. A significant number of drops (~270 drops per test) were performed during several attempts with no penetration recorded. No DCP tests were performed on the RCA base layer of STH 86 in Tomahawk due to field limitations. The results of the DCP test on the investigated RCA base layer of STH 50 in Kenosha are shown in Figure 5.1. The penetration rate profile (in/blow) is presented with depth. Figure 5.1a indicates very high resistance to penetration (<0.16 in/blow) through the 10-inch RCA base layer (at the lane center) followed by less penetration resistance (> 1.25 in/blow) when the DCP went through the subgrade soil. The DCP test was stopped at about 5 inches of depth due to penetration refusal at the wheel path of the RCA base layer.

The DCP tests on the RCA and CA base layers were used to estimate the CBR variation with depth using the formula proposed by Webster et al. (1992, 1994):

$$CBR = \frac{292}{DCPI^{1.12}} \quad \text{Equation 5.1}$$

where DCPI is the penetration index in mm/blow. The estimated CBR are then averaged over one inch of base layer thickness to provide profiles of CBR with depth, as shown in Figure 5.1c for the RCA base layer of STH 50 in Kenosha. An inspection of this figure demonstrates variability in the RCA base materials strength with depth as well as between locations corresponding to the wheel path and the lane center. The average estimated CBR values for the 10-inch-thick RCA base layer ranged from 93.9% for the lane center to 98% for the wheel path, indicating a high-strength base. Such high strength was clearly evident during the penetration tests and the removal of the RCA samples from the base layer through HMA surface layer coring.

Moreover, the DCP test results are used to predict the distribution of the base layer modulus with depth using the formula proposed by Powell et al. (1984):

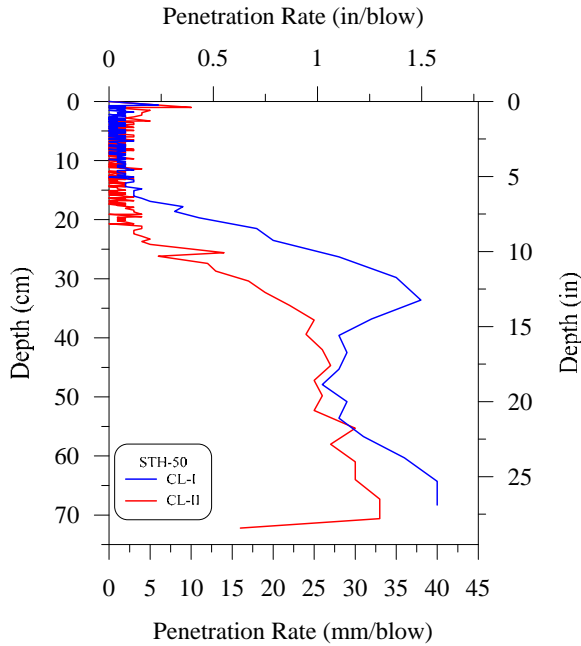
$$M_r = 17.58CBR^{0.64} \quad \text{Equation 5.2}$$

where M_r is the resilient modulus in MPa. Figure 5.1d depicts the distribution with depth of the estimated RCA base layer modulus for STH 50 in Kenosha. The average estimated layer modulus values for the 10-inch RCA base layer vary between 46.7 ksi for the lane center and 48 ksi for the wheel path, indicating relatively high layer moduli values.

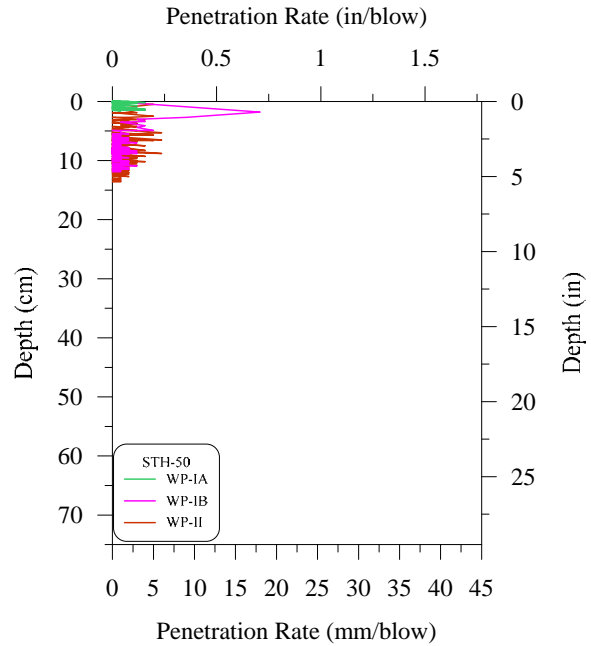
The results of the DCP tests of the corresponding estimated distributions of CBR and layer modulus for the CA base of STH 25 in Maxville are presented in Figure 5.2. An examination of this figure shows penetration resistance exceeding 0.25 in/blow for the top 2 inches of the CA base layer followed by a higher penetration resistance of <0.1 in/blow. The average estimated CBR values ranged from 88.5% for the lane center to 91.9% for the wheel path. The variation of the corresponding average estimated base layer modulus ranged from 44.9 to 46 ksi.

Figure 5.3 presents the results of the DCP test on the RAP base layer of STH 25 near Maxville. The penetration resistance showed high variability among the four test locations with average penetration resistance of 0.1 and 0.23 in/blow for test locations CL I and CL II, respectively. On the other hand, the average penetration resistance for test locations WP I and WP II were 0.1 and 0.14 in/blow, respectively. The average estimated CBR values for the RAP test section of STH 25 varied between 47.9% for test location CL II and 89.2% for test location WP I, with the corresponding average estimated base layer modulus ranging from 30 to 45.2 ksi.

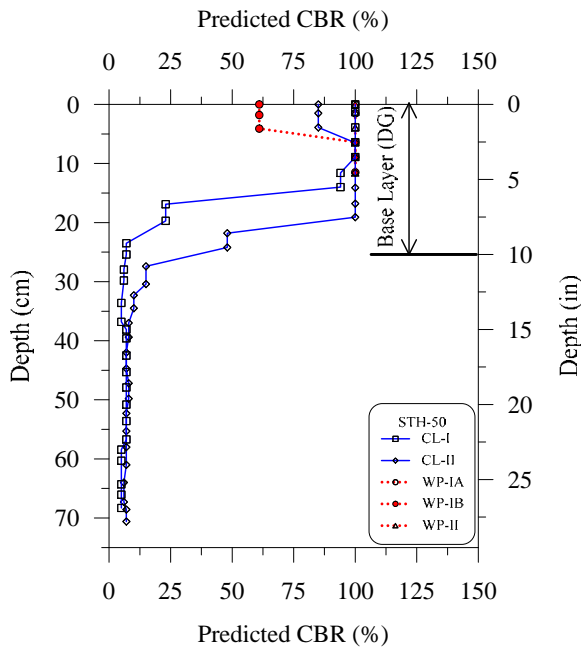
The results of the DCP tests and the corresponding estimated CBR and layer modulus values for the CA, RCA, and RAP base layers are presented in Appendix C.



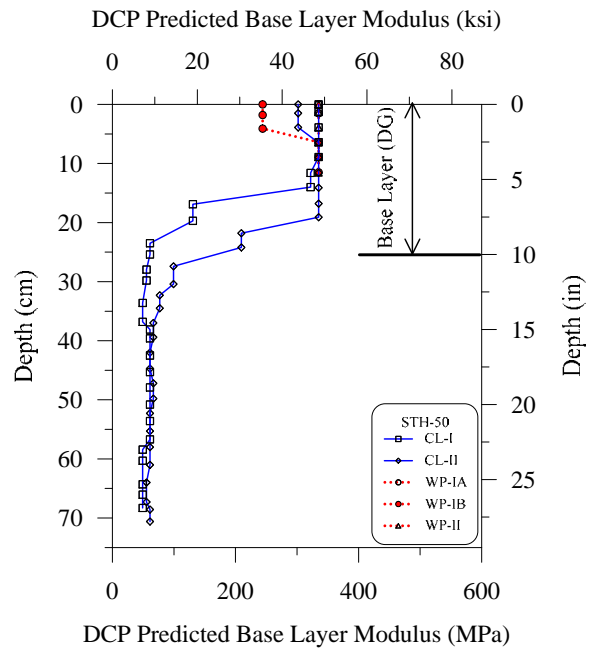
(a) DCP tests STH 50, CL-I, CL-II



(b) DCP tests STH 50, WP-IA, WP-IB, WP-II

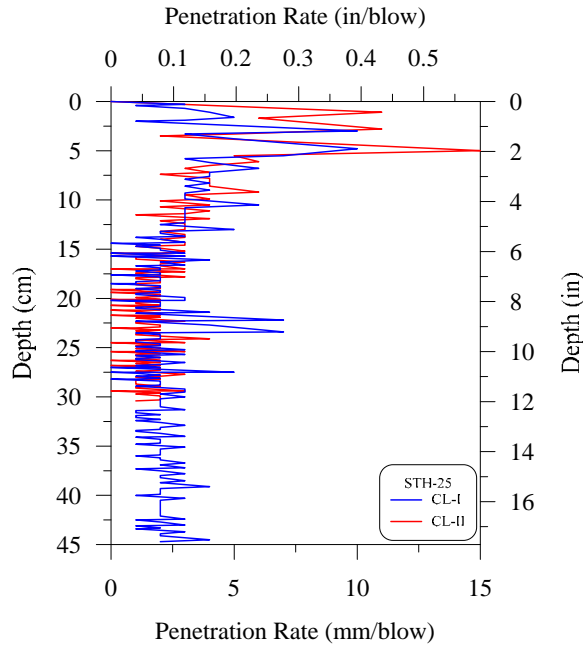


(c) Predicted CBR (%) STH 50

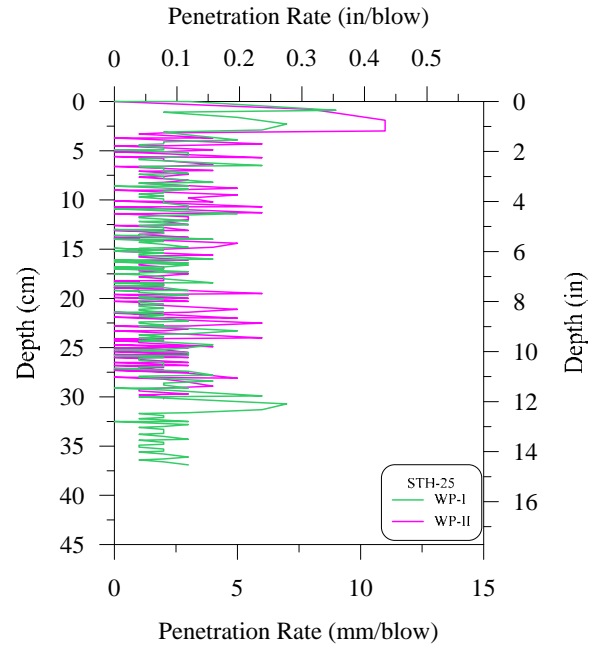


(d) Base layer modulus by DCP test STH 50

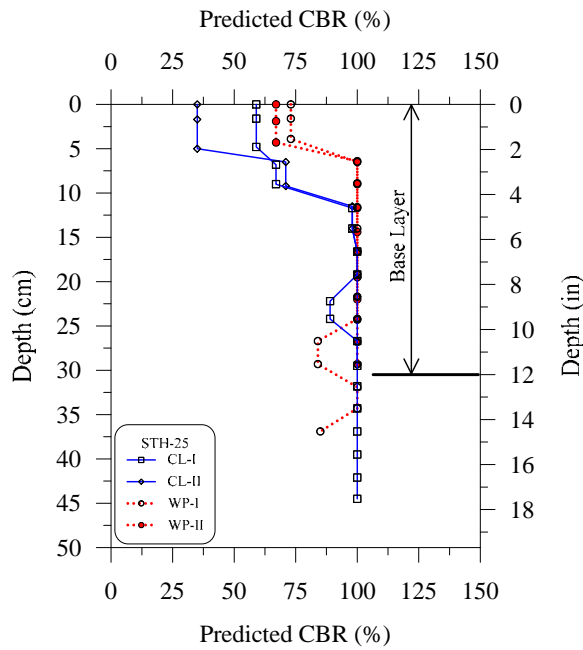
Figure 5.1: Penetration resistance with depth from DCP test and distribution with depth of the corresponding estimated CBR and base layer modulus for the RCA base at STH 50, Kenosha.



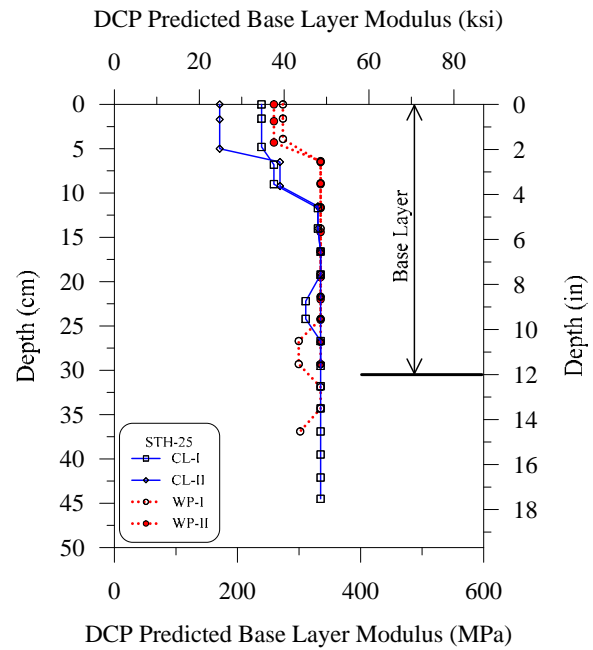
(a) DCP tests STH 25, CL-I, CL-II



(b) DCP tests STH 25, WP-I, WP-II

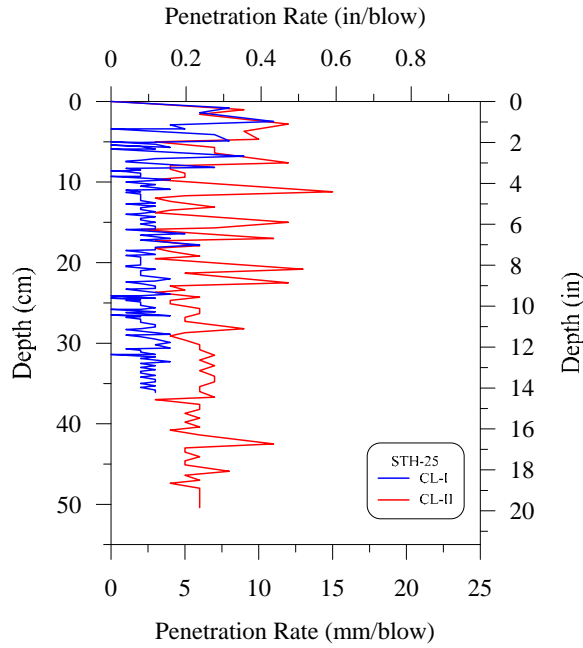


(c) Predicted CBR (%) STH 25

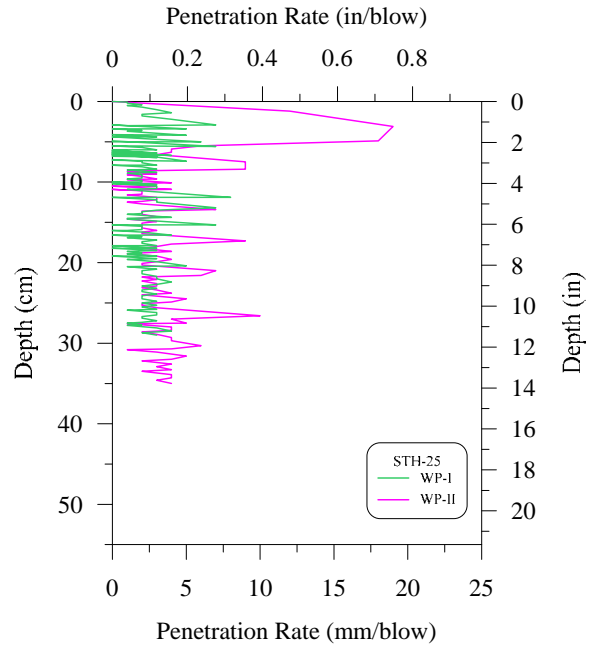


(d) Base layer modulus by DCP test STH 25

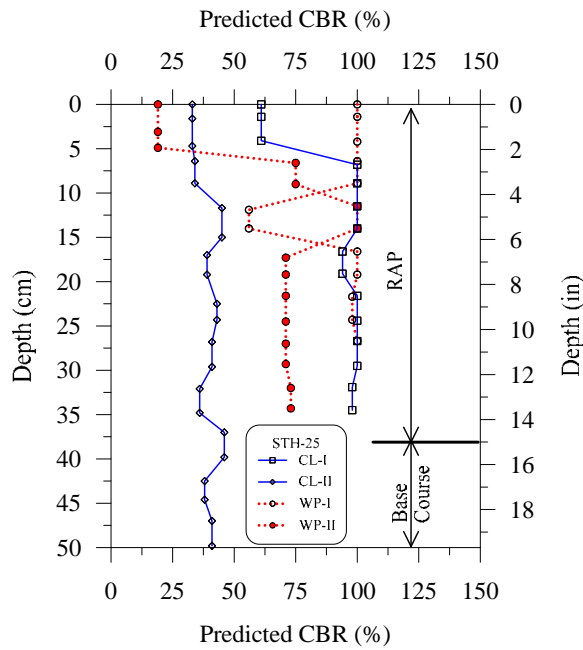
Figure 5.2: Penetration resistance with depth from DCP test and distribution with depth of the corresponding estimated CBR and base layer modulus for the CA base at STH 25, Maxville.



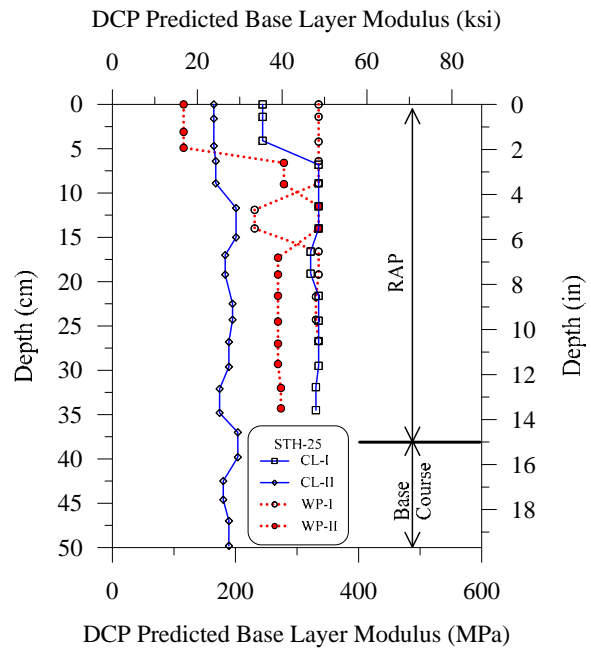
(a) DCP tests STH 25, CL-I, CL-II



(b) DCP tests STH 25, WP-I, WP-II



(c) Predicted CBR (%) STH 25



(d) Base layer modulus by DCP test STH 25

Figure 5.3: Penetration resistance with depth from DCP test and distribution with depth of the corresponding estimated CBR and base layer modulus for the RAP base at STH 25, Maxville.

Saeed (2008) investigated the performance related tests of recycled aggregates including RCA for use in unbound pavement layers. In an NCHRP report, Saeed (2008) identified the relevance of recycled material mass properties for various base layer applications. Saeed (2008) identified the resilient or compressive strength modulus and California Bearing Ratio (CBR) among the properties that are relevant to the use of the recycled aggregates as unbound structural base layers. Therefore, a summary and evaluation of the results of the CBR and base layer moduli estimated from the DCP tests on CA, RCA, and RAP is presented herein. Tables 5.1-5.3 present layer thicknesses, layer type (e.g., 1¼" dense graded), number of layers, average predicted CBR, and average predicted layer moduli for the CA, RCA, and RAP base layers, respectively. The test results summarized in Tables 5.1-5.3 are also presented in Figures 5.4 and 5.5 for performance comparison between CA, RCA, and RAP base layers. A visual examination of Figures 5.4 and 5.5 shows that the predicted CBR and resilient modulus values of the investigated base layer types are comparable. In order to express this comparison in numbers, simple statistical analyses were conducted to calculate averages, identify ranges, and determine variations.

The results of the statistical analyses are presented in Table 5.4 as well as in Figures 5.6 and 5.7. Examination of the statistical summary shows that the average predicted CBR ranged from 65 to 98% for the RCA base layers, between 64% and 90% for the CA base layers, and from 68% to 84% for RAP base layers. The coefficient of variation for the predicted CBR values was higher for the CA base layers (from 2 to 32%) compared with both the RCA (from 2 to 20%) and RAP (from 3 to 23%) base layers. A similar trend is observed for the predicted resilient modulus with an average ranging between 37 and 48 ksi for the RCA base layers, between 36 and 46 ksi for the CA base layers, and between 38 and 43 ksi for the RAP base layers. The CBR and base layer modulus values predicted from the results of the DCP tests indicated, in general, high strength and modulus properties of the investigated base layers.

In general, there were difficulties in retrieving RCA base materials from STH 78 (with higher than normal strength as well as moisture content), STH 32, and STH 50. The research team believes that was due to the self-cementing effects where the process and formation of Calcium Silicate Hydrates (C-S-H) or secondary rehydration from the fine cementitious material is typically reported to occur in RCA materials.

Table 5.1: Summary of CA base layer thicknesses and the corresponding estimated CBR and layer modulus for the investigated pavements.

Pavement Test Section and Location	Base Course and Subbase Layers							
	Pavement Age (year)	WisDOT			Predicted CBR (%)		Predicted M _r (ksi)	
		Base Layer Thickness (in.)			Layer 1	Layer 2	Layer 1	Layer 2
		Layer 1	Layer 2	Layer 3				
CTH T CL I	11	6 (DG)	8 (BR)	NA	49.6	53.9	31.0	32.7
CTH T CL II					65.3	60.9	37.0	35.4
CTH T WP I					67.3	53.1	37.7	32.4
CTH T WP II					73.2	84.7	39.8	43.7
STH 25 CL I	14	12 (DG)	NA	NA	88.5	-	44.9	-
STH 25 CL II					90.8	-	45.7	-
STH 25 WP I					91.9	-	46.0	-
STH 25 WP-II					89.3	-	45.2	-
STH 33 CL I	11	9 (DG)	12 (SC)	NA	77.1	65.1	41.1	36.9
STH 33 CL II					84.8	66.6	43.7	37.5
STH 33 CL III					76.0	60.4	40.8	35.2
STH 33 WP I					67.6	68.8	37.8	38.2
STH 33 WP II					74.5	68.2	40.2	38.0
STH 33 WP III					59.8	57.2	35.0	34.0
STH 22 CL I	22	13 (DG)	NA	NA	85.7	-	44.0	-
STH 22 CL II					78.3	-	41.5	-
STH 22 WP I					70.1	-	38.7	-
STH 22 WP II					78.2	-	41.5	-
STH-54 CL I	10	14 (DG)	30 (SC)	NA	81.2	-	42.5	-
STH 54 CL II					86.0	-	44.1	-
STH 54 WP I					83.6	-	43.3	-
STH-54-WP-II					37.7	-	26.0	-
STH 100 CL	12	4 (OG)	8.5 RCA (DG)	18 (SC)	36.6	90.5	25.5	45.6
STH 100 WP					35.0	68.4	24.8	38.1
STH 59	16	8 (DG)	15 (BR)	-	-	-	-	-

DG = 1 ¼" Dense Graded, OG = Open Graded, BR = Breaker Run, SC = Select Crushed, GB = Granular Backfill, SB = Select Borrow, WP = Wheel Path, CL = Center of Lane

Table 5.2: Summary of RCA base layer thicknesses and the corresponding estimated CBR and layer modulus for the investigated pavements.

Pavement Test Section and Location	Base Course and Subbase Layers							
	Pavement Age (year)	WisDOT Plans			Predicted CBR (%)		Predicted M _r (ksi)	
		Base Layer Thickness (in.)			Layer 1	Layer 2	Layer 1	Layer 2
		Layer 1	Layer 2	Layer 3				
Calhoun CL I	13	15 RCA (DG)	18 (GB)	NA	49.5	-	31.0	-
Calhoun CL II					71.2	-	39.1	-
Calhoun WP I					72.2	-	39.5	-
Calhoun WP II					65.7	-	37.1	-
STH 32 CL I	13	4 RCA (OG)	10 RCA (DG)	12-16 (BR)	90.1	98.9	45.5	48.3
STH 32 CL II					94.2	99.7	46.7	48.5
STH 32 WP I					93.5	98.1	46.5	48.0
STH 32 WP II					56.0	94.2	33.5	46.8
STH 50 CL I	13	10 RCA (DG)	NA	NA	93.9	-	46.7	-
STH 50 CL II					94.9	-	47.0	-
STH 50 WP I					96.1	-	47.4	-
STH 50 WP IB					98.0	-	48.0	-
STH 50 WP II					96.3	-	47.4	-
STH 78 Site 1	9	4-6 RCA (DG)	8 RCA (3" DG)	NA	DCP Refusal			
STH 78 Site 2	9	4-6 RCA (DG)	8 RCA (3" DG)	NA				
STH 86	14	11 (DG)	NA	NA	N/A			
STH 100 CL	12	4 (OG)	8.5 RCA (DG)	18 (SC)	36.6	90.5	25.5	45.6
STH 100 WP					35.0	68.4	24.8	38.1

DG = 1¼" Dense Graded, OG = Open Graded, BR = Breaker Run, SC = Select Crushed, GB = Granular Backfill
WP = Wheel Path, CL = Center of Lane

Table 5.3: Summary of RAP base layer thicknesses and the corresponding estimated CBR and layer modulus for the investigated pavements.

Pavement Test Section and Location	Base Course and Subbase Layers							
	Pavement Age (year)	WisDOT Base Layer Thickness (in.)			Predicted CBR (%)		Predicted M _r (ksi)	
		Layer 1	Layer 2	Layer 3	Layer 1	Layer 2	Layer 1	Layer 2
STH 22 WP II	18	4	8		67.9	49.4	37.9	30.9
STH 25 CL I	14	15	8	N/A	85.4	91.4	43.9	45.9
STH 25 CL II					47.9	44.4	30.3	28.9
STH 25 WP I					89.2	-	45.2	-
STH 25 WP II					78.5	-	41.6	-
STH 59 CL I	9	3	6	N/A	85.6	98	44	48
STH 59 CL II					82.9	95.8	43.1	47.3
STH 59 WP I					80.8	77.1	42.4	41.2
STH 59 WP II					86.6	73.2	44.3	39.8
STH 70 CL I	18	4	6	N/A	47.1	66.3	30	37.3
STH 70 CL II					80.6	72.6	42.3	39.6
STH 70 WP I					78.7	87.5	41.7	44.6
STH 70 WP II					79.9	85	42.1	43.8
STH 96 CL I	24 (16 after overlay)	4	6	N/A	81.7	71.8	42.7	39.3
STH 96 CL II					82.6	80.8	43	42.4
STH 96 WP-I					67.3	54.8	37.7	33
STH 96 WP II					78.7	66.6	41.7	37.5

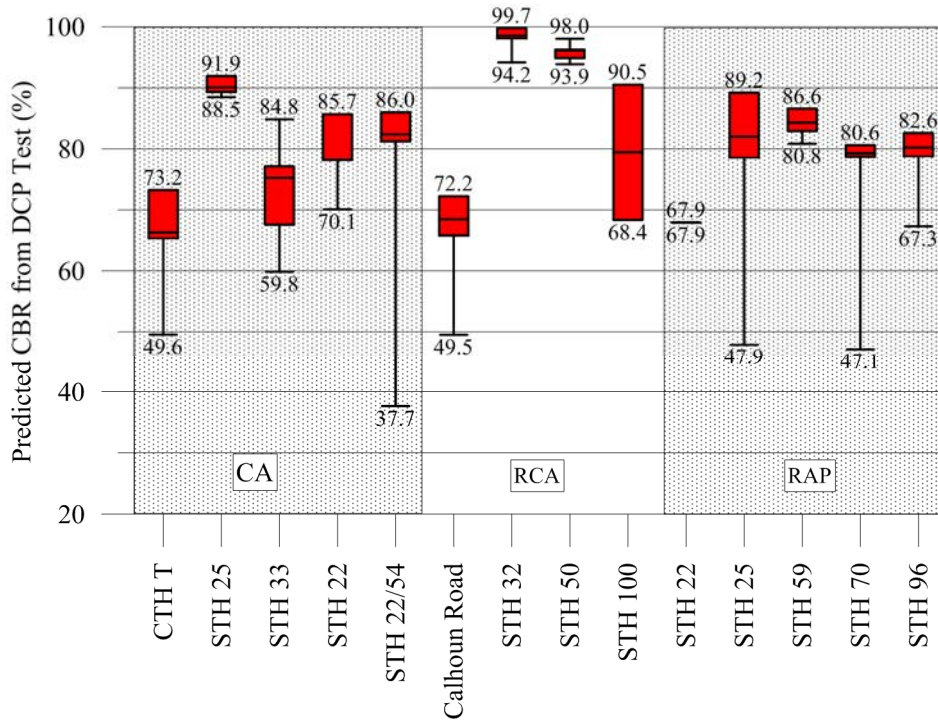


Figure 5.4: Box-Whisker comparison of the average predicted CBR values from DCP tests for RCA, CA, and RAP base layers for the investigated pavement.

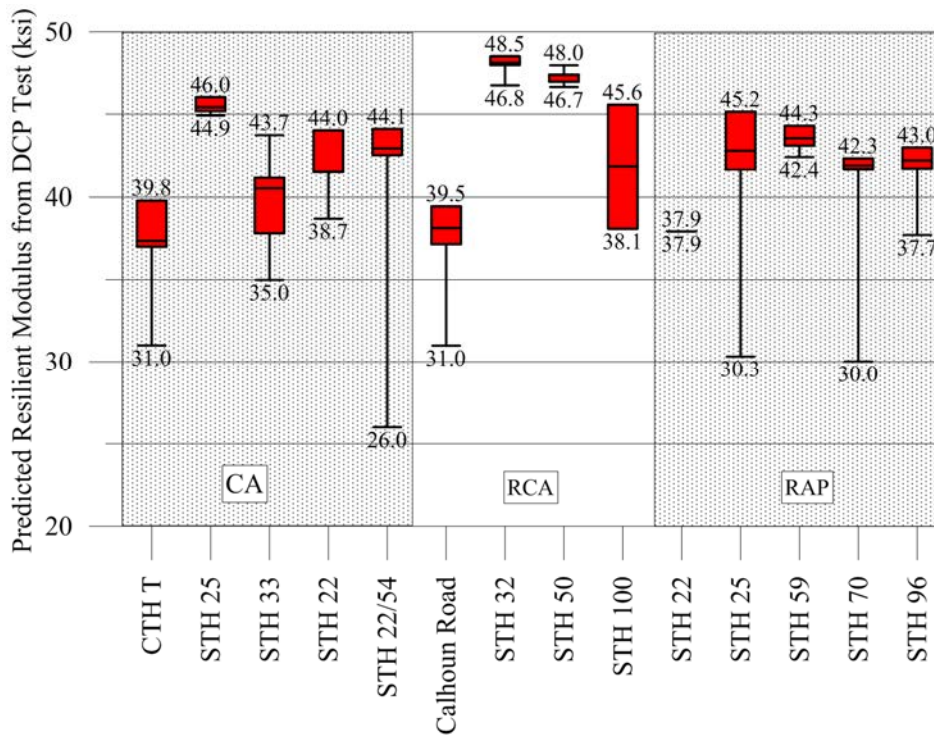


Figure 5.5: Box-Whisker comparison of the average predicted layer modulus values from DCP tests for RCA, CA, and RAP base layers for the investigated pavement.

Table 5.4: Statistical summary of predicted CBR and layer modulus of the RCA and CA base layer materials.

Base Layer Material	Pavement Test Section	Predicted CBR (%)				Predicted Layer Modulus (ksi)			
		Average	COV (%)	Min.	Max.	Average	COV (%)	Min.	Max.
CA	CTH T	63.8	15.8	49.6	73.2	36.4	10.4	31.0	39.8
	STH 25	90.1	1.7	88.5	91.9	45.5	1.1	44.9	46.0
	STH 33	73.3	11.7	59.8	84.8	39.8	7.6	35.0	43.7
	STH 22	78.1	8.2	70.1	85.7	41.4	5.2	38.7	44.0
	STH 22/54	72.1	32.0	37.7	86.0	39.0	22.3	26.0	44.1
RCA	Calhoun Road	64.7	16.2	49.5	72.2	36.7	10.7	31.0	39.5
	STH 32	97.5	2.4	94.2	99.7	47.9	1.6	46.8	48.5
	STH 50	95.8	1.6	93.9	98.0	47.3	1.1	46.7	48.0
	STH 100	79.5	19.7	68.4	90.5	41.8	12.7	38.1	45.6
	STH 78	Refusal							
	STH 86	N/A							
RAP	STH 22	67.9	-	67.9	67.9	37.9	-	37.9	37.9
	STH 25	75.3	25.0	47.9	89.2	40.3	16.9	30.3	45.2
	STH 59	84.0	3.1	80.8	86.6	43.4	2.0	42.4	44.3
	STH 70	71.6	22.8	47.1	80.6	39.0	15.4	30.0	42.3
	STH 96	77.6	9.1	67.3	82.6	41.3	5.9	37.7	43.0

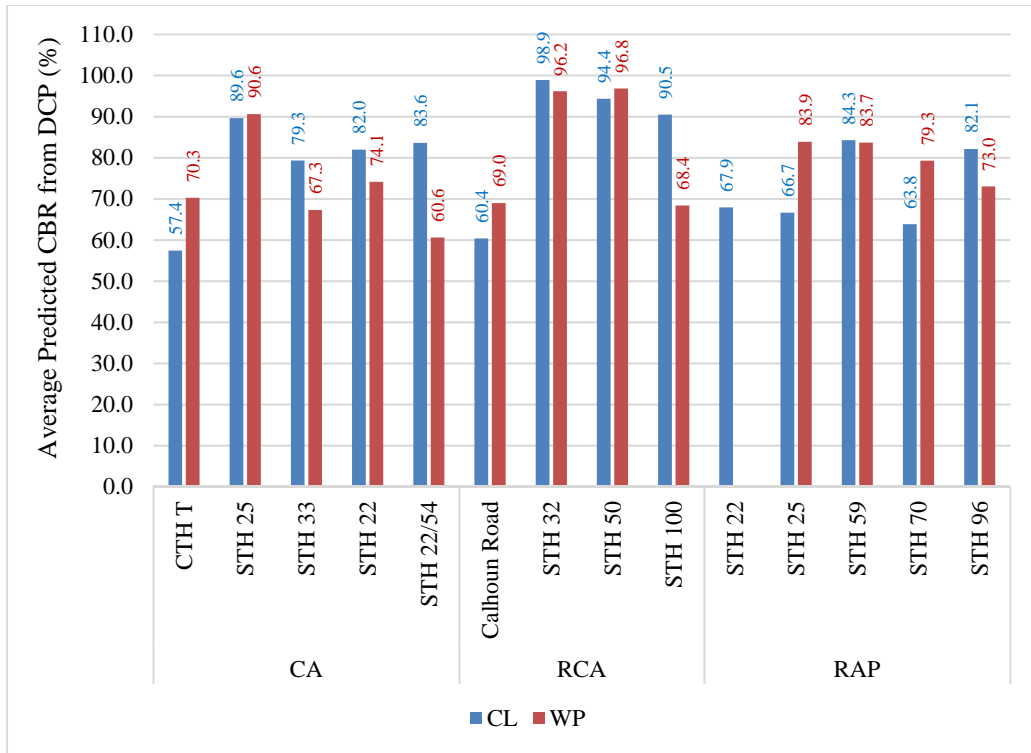


Figure 5.6: Comparison of the average predicted CBR from DCP for the RCA, CA, and RAP base layers of the investigated pavements.

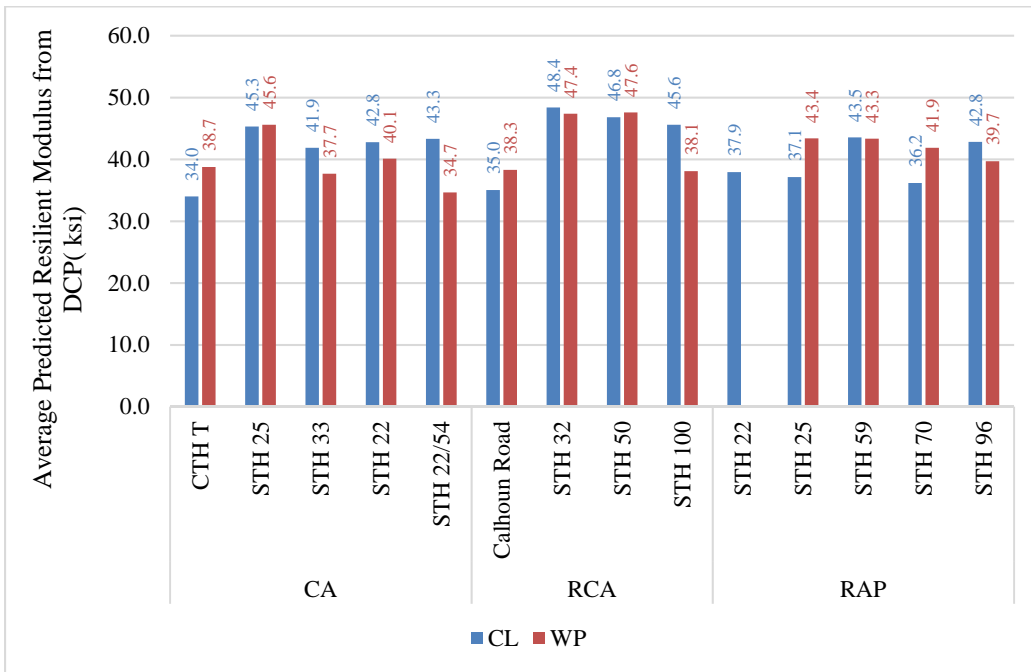


Figure 5.7: Comparison of the average predicted layer modulus from DCP for the RCA, CA, and RAP base layers of the investigated pavements.

5.2 Falling Weight Deflectometer Test Results

The FWD test data was analyzed using the pavement layer moduli back-calculation software developed by ERI, Inc. The back-calculation program is widely used to estimate the pavement layer moduli from FWD test results. The analysis was conducted using pavement layer thicknesses obtained from the WisDOT project plans, existing soils reports/pavement coring by WisDOT and consultants, and measurement by the research team during pavement coring. Typical sections of all investigated pavement test sections and core thickness measurements are presented in Appendix D. All analysis steps necessary to predict layer moduli values were executed. For example, pavement deflections were normalized to the 9,000 lb load and then adjusted for temperature variations.

The variation of the deflection under the loading plate (D_0) along the distance for the investigated HMA pavements test sections is presented in Table 5.5 and depicted in Figures 5.8-5.10. The adjusted normalized D_0 ranged between 2.9 and 25.1 mils for pavements with CA base layers, from 3.9 to 16.7 mils for pavements with RCA base layers, and between 4.4 and 32.7 mils for pavements with RAP base layers. An inspection of Figures 5.8-5.10 shows that, in general, the pavements with CA base layers exhibited the highest deflection with averages ranging from 8.6 to 18.8 mils but with the lowest variability (COV varying between 5.1 and 22.1%). On the other hand, the pavements with RCA base layers have the lowest deflection with averages ranging from 5.5 to 9.6 mils with higher variability (COV varying between 13.7 and 33.1%). Deflection averages for the pavements with RAP base layers varied between 7.6 and 18.6 mils with COV ranging from 3.2 to 53.3%.

Table 5.5 and Figures 5.11-5.13 present the values of the effective structural number (SN_{eff}) for the investigated HMA pavement test sections. The effective structural number represents the structural capacity of the pavement system (all layers) estimated from the FWD test results. The investigated HMA pavement test sections with RCA base layers exhibited the highest average SN_{eff} values ranging between 5.8 and 10.1 (COV varying from 8.9 to 17.1), while the pavement test sections with CA base layers had the lowest average SN_{eff} values ranging from 4.6 to 6.1 (COV ranging from 2.5 to 15.5%). The pavement test sections with RAP base layers exhibit an intermediate behavior with SN_{eff} averages ranging between 4.3 and 7.4 (COV varying between 1.6 and 23.5%).

The results of the FWD analyses pertaining to D_0 and SN_{eff} demonstrate that, in general, the investigated HMA pavement sections with RCA base layers exhibited the lowest deflections and the highest structural capacity (SN_{eff}) compared with the investigated HMA pavement sections with CA and RAP base layers. The pavement sections with CA base layers exhibited the highest deflection and the lowest structural capacity.

Table 5.5: Statistical summary of adjusted deflection under loading plate (D₀) normalized to 9,000 lb load for investigated HMA pavement test sections with CA, RCA, and RAP base layers.

Pavement Test Section		Adjusted Normalized Deflection, D ₀				Effective Structural Number SN _{eff}			
		Avg.	COV	Min.	Max.	Avg.	COV	Min.	Max.
		(mils)	(%)	(mils)	(mils)	(mils)	(%)	(mils)	(mils)
CA	STH 33 WB RWP St. Joseph 2011	11.4	17.8	8.4	16.4	6.1	7.0	5.1	7.0
	STH 33 EB RWP St. Joseph 2011	11.7	19.9	8.0	15.3	5.9	7.8	5.2	6.6
	STH 77 EB RWP Burnett 2011	12.9	6.0	11.5	14.9	5.3	2.5	5.1	5.6
	STH 22/54 NB RWP Waupaca 2011	10.5	18.0	6.3	16.9	6.0	10.4	4.6	7.8
	CTH T SB RWP S1 Blue River 2011	11.0	16.4	7.2	15.8	5.5	7.2	4.5	6.4
	CTH T SB RWP S2Blue River 2011	11.2	21.5	5.9	16.5	5.5	11.5	4.6	6.9
	STH 33 EB CL Core Area St. Joseph	11.6	5.1	10.7	12.5	5.7	3.9	5.2	6.2
	STH 33 EB RWP Core Area St. Joseph	12.7	16.9	7.8	18.2	5.8	8.6	4.9	7.6
	CTH T SB RWP Core Area Blue River	10.6	15.4	6.6	13.7	5.4	7.3	4.8	6.4
	CTH T NB RWP Distressed Area Blue River	13.3	5.9	12.3	14.9	4.6	2.8	4.4	4.8
	STH 22 NB RWP Shawano	10.3	18.6	7.4	14.1	6.0	15.2	4.6	8.0
	STH 22/54 NB RWP S1 Shawano	14.0	18.6	10.3	19.6	5.5	8.5	4.6	6.5
	STH 22/54 NB RWP S2 Waupaca	13.3	19.9	9.8	19.6	5.7	10.6	4.5	6.5
	STH 22/54 NB RWP Core Area Waupaca	10.6	8.6	9.3	11.8	6.0	8.1	5.3	6.7
	STH 25 SB RWP Core Area Maxville	11.1	11.6	7.6	12.7	5.1	9.3	4.6	6.5
	STH 25 SB CL Core Area Maxville	8.8	7.8	7.7	10.0	5.9	6.5	5.2	6.4
	STH 25 SB RWP S1 Maxville	8.6	22.1	2.9	10.2	5.7	4.0	5.4	6.2
	STH 59 EB RWP S1 Riley Rd 2009	12.8	13.8	9.6	15.8	5.2	7.5	4.8	6.1
	STH 59 EB RWP S2 Riley Rd2009	12.9	21.6	9.7	17.7	5.1	4.3	4.6	5.3
	STH 59 EB RWP S3 Riley Rd 2009	18.1	7.3	16.1	20.3	4.6	3.7	4.4	4.9
	STH 59 EB RWP S1 Riley Rd2010	12.0	15.0	9.8	15.3	5.1	4.3	4.7	5.4
	STH 59 EB RWP S2 Riley Rd2010	15.8	8.6	13.0	18.4	4.9	4.1	4.5	5.2
	STH 59 EB RWP S3 Riley Rd 2010	16.1	10.0	14.2	18.4	5.0	5.3	4.6	5.4
	STH 59 EB RWP S1 Riley Rd2017	13.7	22.1	9.6	20.6	5.4	15.5	4.2	6.6
	STH 59 EB RWP JY 2009	16.0	16.4	11.9	21.0	5.1	8.0	4.4	5.8
	STH 59 EB LWP JY 2009	12.2	9.5	10.7	15.7	5.8	5.6	5.0	6.3
	STH 59 WB RWP JY 2009	18.8	14.7	15.1	25.1	5.0	11.2	3.9	5.9
	STH 59 WB LWP JY 2009	15.9	8.9	13.9	18.5	5.0	7.2	4.4	5.5
RCA	STH 50 EB RWP S1	6.2	32.3	4.1	16.7	10.1	14.3	5.2	12.7
	STH 50 EB RWP Core Area	9.5	26.6	6.6	16.6	8.2	15.2	5.3	10.3
	STH 100 EB RWP S1	8.8	19.2	7.0	14.6	6.6	9.5	4.6	7.4
	STH 100 EB RWP Core Area	8.5	19.5	6.3	12.6	6.5	8.9	5.2	7.2
	STH 100 EB LWP Core Area	7.9	23.4	5.8	12.8	7.0	11.6	4.9	7.8
	STH 86 NB RWP	8.4	26.6	4.6	11.8	7.0	15.9	5.7	9.8
	STH 86 SB RWP	6.7	22.4	3.9	11.7	7.3	12.1	5.5	9.5
	STH 78 NB RWP Trench Area	8.8	26.6	6.3	14.3	6.7	14.5	4.9	7.9
	STH 78 NB RWP S1	8.4	33.1	4.9	15.7	7.2	17.1	4.9	9.1
	STH 78 SB RWP Trench Area II	9.6	25.0	7.2	16.0	5.8	11.9	4.2	6.8
	Calhoun Road NB RWP	5.5	23.4	4.1	7.8	8.5	13.2	6.8	10.2
	STH 32 NB RWP S1	6.3	20.3	4.1	9.9	9.9	15.1	6.8	14.3
	STH 32 NB RWP Core Area	6.6	13.7	5.4	8.9	9.0	10.2	6.9	10.6
	STH 32 NB LWP Core Area	5.6	26.9	4.5	10.5	9.9	12.5	6.5	11.6

Table 5.5 (Cont.): Statistical summary of adjusted deflection under loading plate (D_0) normalized to 9,000 lb. load for investigated HMA pavement test sections with CA, RCA, and RAP base layers.

Pavement Test Section		Adjusted Deflection				Effective Structural Number			
		D_0				SN_{eff}			
		Avg.	COV	Min.	Max.	Avg.	COV	Min.	Max.
		(mils)	(%)	(mils)	(mils)	(mils)	(%)	(mils)	(mils)
RAP	STH 22 NB RWP S1 Shawano	7.6	20.4	5.4	12.5	6.9	8.4	5.3	8.0
	STH 22 NB RWP S2 Shawano	11.7	19.5	8.7	16.4	6.2	12.3	5.3	7.5
	STH 22 NB RWP Core Area Shawano	10.7	15.9	8.2	13.6	5.9	9.8	5.0	6.9
	STH 25 SB RWP Core Area Maxville	9.0	11.9	7.2	11.6	6.1	6.2	5.4	7.0
	STH 25 SB RWP S1 Maxville	8.3	14.6	6.1	11.1	6.5	8.8	5.5	7.8
	STH 59 EB RWP Core Area	16.4	15.4	12.8	20.9	5.0	10.8	4.3	6.4
	STH 59 EB RWP Riley Road	9.6	13.6	7.5	11.5	6.0	20.9	3.7	9.0
	STH 59 EB RWP 2010	8.0	6.8	7.2	9.1	6.4	9.1	5.6	7.4
	STH 59 EB LWP 2010	10.4	17.1	8.1	13.0	7.0	4.2	6.4	7.4
	STH 59 WB RWP 2010	8.8	8.5	7.7	10.3	6.7	12.4	5.5	7.8
	STH 59 WB LWP 2010	11.9	19.9	6.9	15.1	6.8	6.2	6.1	7.4
	STH 59 EB RWP 2017	8.4	14.6	6.4	11.1	6.0	14.4	5.1	8.1
	STH 59 EB LWP 2017	11.5	53.3	6.7	32.7	7.1	12.4	6.1	9.1
	STH 59 WB RWP 2017	8.0	16.2	5.4	10.0	7.0	23.5	3.0	8.5
	STH 59 WB LWP 2017	12.8	38.4	4.4	21.6	7.4	10.1	6.5	8.8
	STH 70 EB RWP DL Minocqua	14.0	21.0	11.2	20.4	5.5	11.8	4.2	6.1
	STH 70 EB RWP PL Minocqua	10.8	18.5	6.1	15.9	6.4	13.6	4.9	9.9
	USH 45 NB RWP S1 Tigerton	9.2	7.6	8.3	10.5	5.8	2.3	5.6	6.1
	USH 45 NB RWP S2 Tigerton	9.2	3.2	8.8	9.7	5.8	1.6	5.7	6.0
	STH 96 NB RWP S1 Lark	18.6	22.9	9.9	28.3	5.5	16.4	4.4	8.0
STH 96 NB RWP Core Area Lark	17.4	12.3	14.3	21.0	4.3	6.0	3.9	4.8	
STH 96 NB LWP Core Area Lark	15.5	12.1	13.6	21.0	4.5	5.2	4.0	4.9	

Table 5.6: Statistical summary of back-calculated layer moduli for the investigated HMA pavement test sections with CA, RCA, and RAP base layers.

Pavement Test Section		E _{HMA}				E _{Base}				E _{Subgrade}			
		Avg.	COV	Min.	Max.	Avg.	COV	Min.	Max.	Avg.	COV	Min.	Max.
		(ksi)	(%)	(ksi)	(ksi)	(ksi)	(%)	(ksi)	(ksi)	(ksi)	(%)	(ksi)	(ksi)
CA	STH 33 WB RWP St. Joseph 2011	349	25	146	522	34	24	18	51	15	23	10	22
	STH 33 EB RWP St. Joseph 2011	322	23	209	459	34	24	16	46	16	22	11	24
	STH 77 EB RWP Burnett 2011	700	18	466	1034	29	16	16	39	20	12	15	24
	STH 22/54 NB RWP Waupaca 2011	819	38	242	1813	27	42	12	76	20	23	12	38
	CTH T SB RWP S1 Blue River 2011	201	19	144	325	50	11	35	58	30	28	20	53
	CTH T SB RWP S2 Blue River 2011	213	16	155	281	49	18	34	76	28	36	15	62
	STH 33 EB CL Core Area St. Joseph	321	19	192	428	31	10	26	40	22	9	18	24
	STH 33 EB RWP Core Area St. Joseph	427	25	291	858	26	23	16	46	18	24	9	31
	CTH T SB RWP Core Area Blue River	405	18	273	544	34	11	27	40	26	9	22	31
	CTH T NB RWP Distressed Area Blue River	1,035	26	438	1470	46	33	28	73	27	23	19	43
	STH 22 NB RWP Shawano	673	54	218	1494	34	36	19	70	23	22	17	32
	STH 22/54 NB RWP S1 Shawano	989	27	599	1941	63	31	19	101	17	16	11	25
	STH 22/54 NB RWP S2 Waupaca	276	26	185	401	33	38	15	57	19	21	16	29
	STH 22/54 NB RWP Core Area Waupaca	294	20	212	377	46	18	34	60	22	9	19	26
	STH 25 SB RWP Core Area Maxville	377	71	197	1384	31	24	13	43	35	18	28	52
	STH 25 SB CL Core Area Maxville	422	18	311	592	47	22	32	76	35	7	32	40
	STH 25 SB RWP S1 Maxville	282	23	197	368	54	11	48	67	36	12	31	48
	STH 59 EB RWP S1 Riley Rd 2009	320	66	207	1000	27	17	22	37	23	32	16	33
	STH 59 EB RWP S2 Riley Rd 2009	220	14	177	283	34	24	19	45	31	44	15	50
	STH 59 EB RWP S3 Riley Rd 2009	360	101	225	1806	22	18	17	29	14	7	12	15
	STH 59 EB RWP S1 Riley Rd 2017	225	24	157	311	47	48	20	86	17	43	12	33
	STH 59 EB RWP JY 2009	846	38	368	1338	36	32	26	76	13	19	10	19
	STH 59 EB LWP JY 2009	882	29	377	1272	28	19	18	37	18	12	14	22
	STH 59 WB RWP JY 2009	543	55	100	1003	42	29	30	68	11	12	8	13
STH 59 WB LWP JY 2009	454	44	166	785	36	20	30	53	14	11	11	16	
RCA	STH 50 EB RWP S1	1,280	35	452	1923	91	31	21	146	18	17	12	24
	STH 50 EB RWP Core Area	727	44	181	1442	70	43	21	147	15	14	11	18
	STH 100 EB RWP S1	975	42	357	1876	53	24	31	85	20	13	15	26
	STH 100 EB RWP Core Area	873	41	266	1520	52	37	20	91	23	18	17	34
	STH 100 EB LWP Core Area	1,115	35	591	1788	46	31	27	69	26	23	20	37
	STH 86 NB RWP	1,050	27	670	1694	94	53	20	185	21	20	15	30
	STH 86 SB RWP	1,073	34	509	1651	115	42	28	195	27	21	22	41
	STH 78 NB RWP Trench Area	467	35	239	820	63	51	21	113	26	6	23	29
	STH 78 NB RWP S1	387	56	102	1135	96	73	23	330	26	16	18	35
	STH 78 SB RWP Trench Area II	608	41	227	1186	56	40	17	84	28	13	20	37
	Calhoun Road NB RWP	1,445	26	879	2000	118	53	47	240	27	22	20	43
	STH 32 NB RWP S1	829	46	266	2000	105	57	25	256	30	25	16	48
	STH 32 NB RWP Core Area	752	22	532	1082	111	44	47	203	28	16	18	33
	STH 32 NB LWP Core Area	766	52	388	2000	182	36	25	293	29	16	19	38

Table 5.6 (Cont.): Statistical summary of back-calculated layer moduli for the investigated HMA pavement test sections with CA, RCA, and RAP base layers.

Pavement Test Section		E _{HMA}				E _{Base}				E _{Subgrade}			
		Avg.	COV	Min.	Max.	Avg.	COV	Min.	Max.	Avg.	COV	Min.	Max.
		(ksi)	(%)	(ksi)	(ksi)	(ksi)	(%)	(ksi)	(ksi)	(ksi)	(%)	(ksi)	(ksi)
RAP	STH 22 NB RWP S1 Shawano	512	22	267	773	92	37	42	189	26	21	17	39
	STH 22 NB RWP S2 Shawano	457	47	105	876	36	48	15	73	19	23	12	27
	STH 22 NB RWP Core Area Shawano	396	26	208	531	52	31	26	76	20	10	17	24
	STH 25 SB RWP Core Area Maxville	403	27	235	636	79	25	48	116	28	14	19	31
	STH 25 SB RWP S1 Maxville	439	35	236	869	80	35	38	149	30	9	24	36
	STH 59 EB RWP Core Area	633	44	286	1385	35	38	18	80	12	7	11	14
	STH 59 EB RWP Riley Road	935	69	100	2000	78	87	11	274	17	34	9	32
	STH 59 EB RWP 2017	622	37	288	1000	81	46	18	152	15	17	12	23
	STH 59 EB LWP 2017	764	51	306	1985	181	38	47	297	17	6	16	19
	STH 70 EB RWP DL Minocqua	1,143	44	349	1829	49	33	29	82	16	10	11	18
	STH 70 EB RWP PL Minocqua	961	38	334	1582	46	19	33	67	17	11	12	20
	USH 45 NB RWP S1 Tigerton	248	17	196	329	76	13	61	94	28	11	23	31
	USH 45 NB RWP S2 Tigerton	230	17	167	297	76	10	66	90	29	10	23	34
	STH 96 NB RWP S1 Lark	191	59	63	467	33	95	11	169	15	21	10	24
	STH 96 NB RWP Core Area Lark	174	30	103	257	27	13	20	33	13	8	12	16
	STH 96 NB LWP Core Area Lark	201	28	122	282	29	21	19	43	15	8	13	18

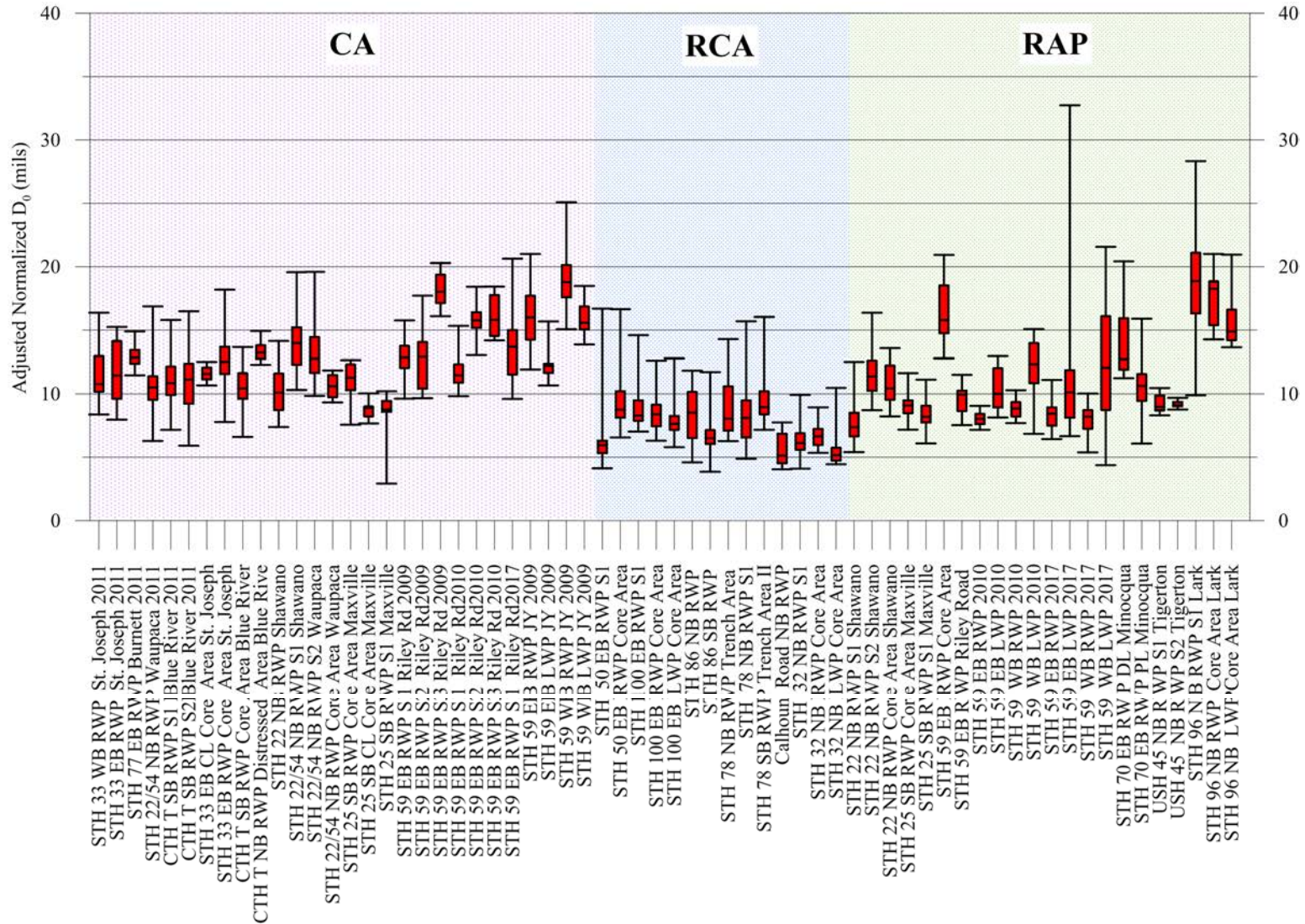


Figure 5.8: Box-Whisker plot of the measured adjusted deflection under loading plate (D_0) normalized to 9,000 lb load for the investigated pavement test sections with crushed aggregate, recycled concrete aggregate, and reclaimed asphalt pavement base layers.

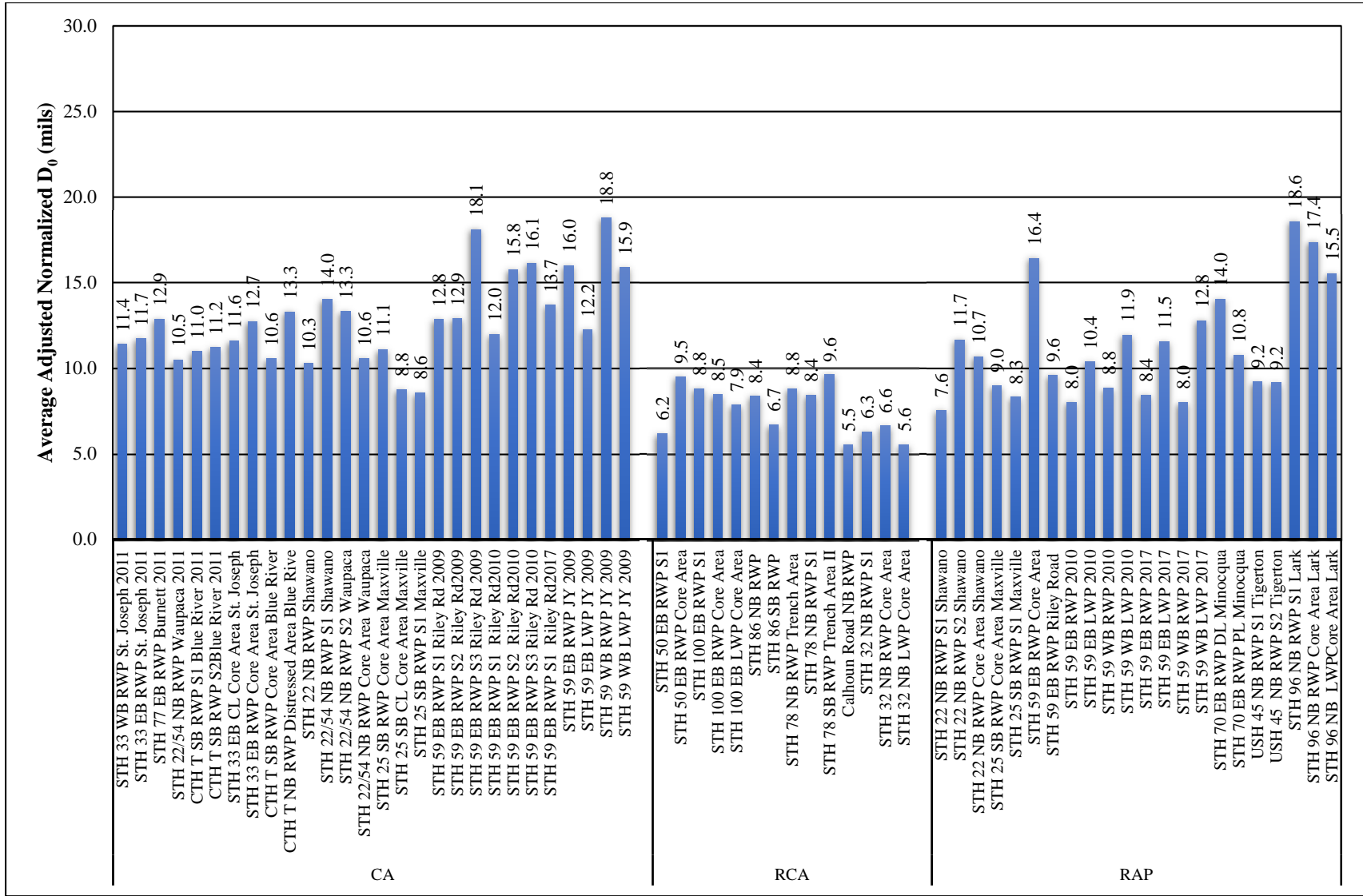


Figure 5.9: Average adjusted deflection under loading plate (D_0) normalized to 9,000 lb load for the investigated HMA pavement test sections with crushed aggregate, recycled concrete aggregate, and reclaimed asphalt pavement base layers.

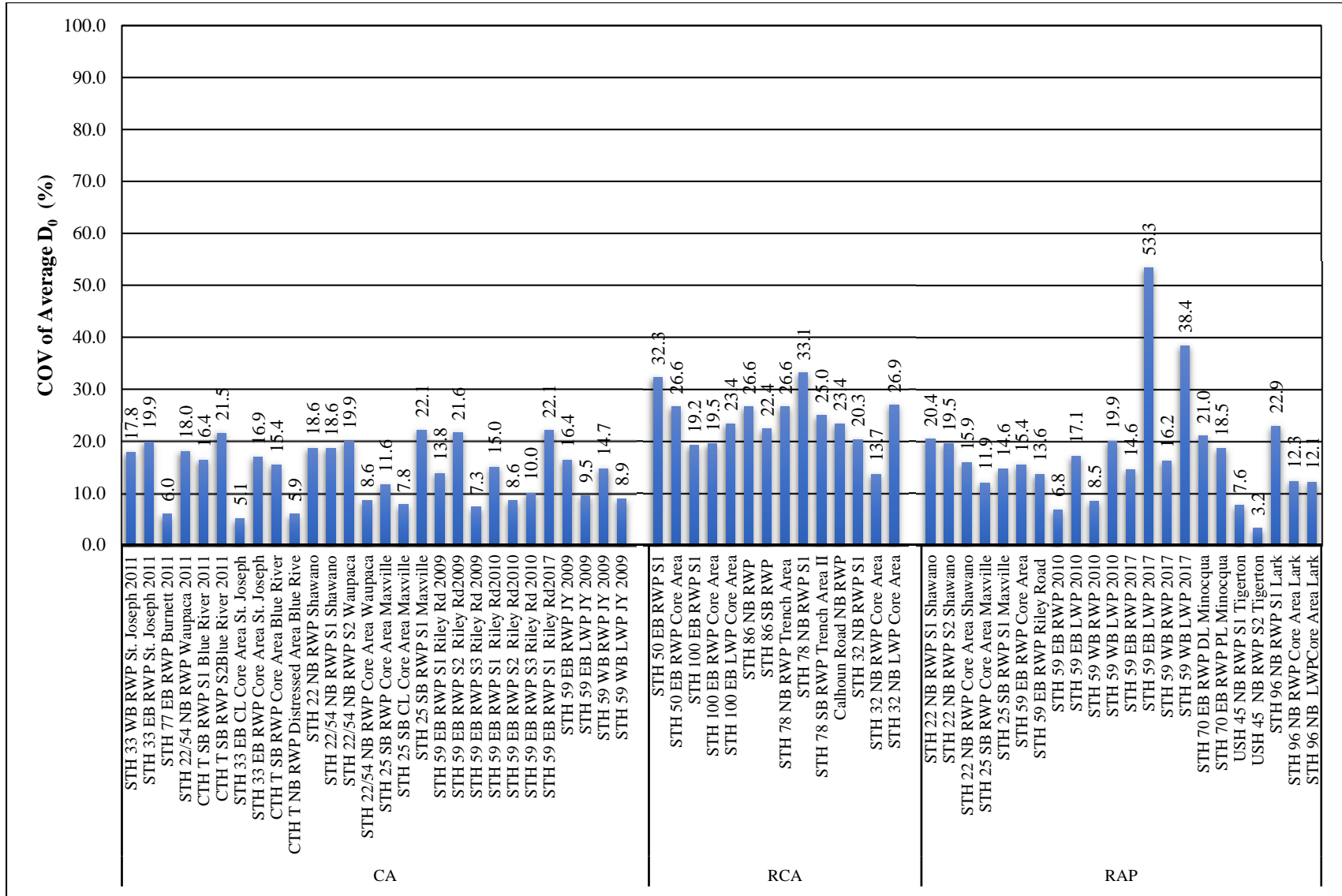


Figure 5.10: Coefficient of variation of back-calculated HMA layer modulus for the investigated pavement test sections with crushed aggregate, recycled concrete aggregate, and reclaimed asphalt pavement base layers.

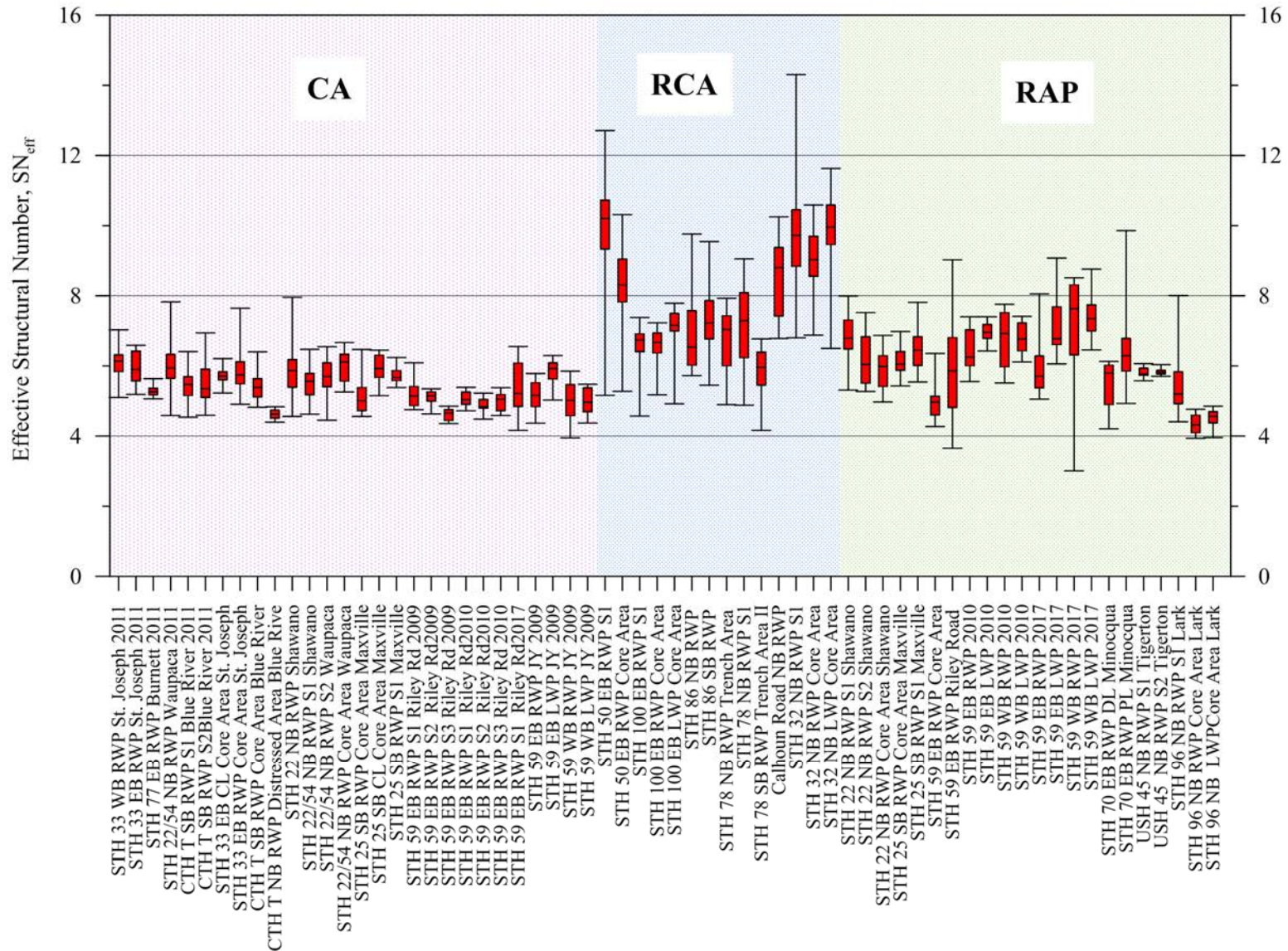


Figure 5.11: Box-Whisker plot of the effective structural number for the investigated pavement test sections with crushed aggregate, recycled concrete aggregate, and reclaimed asphalt pavement base layers.

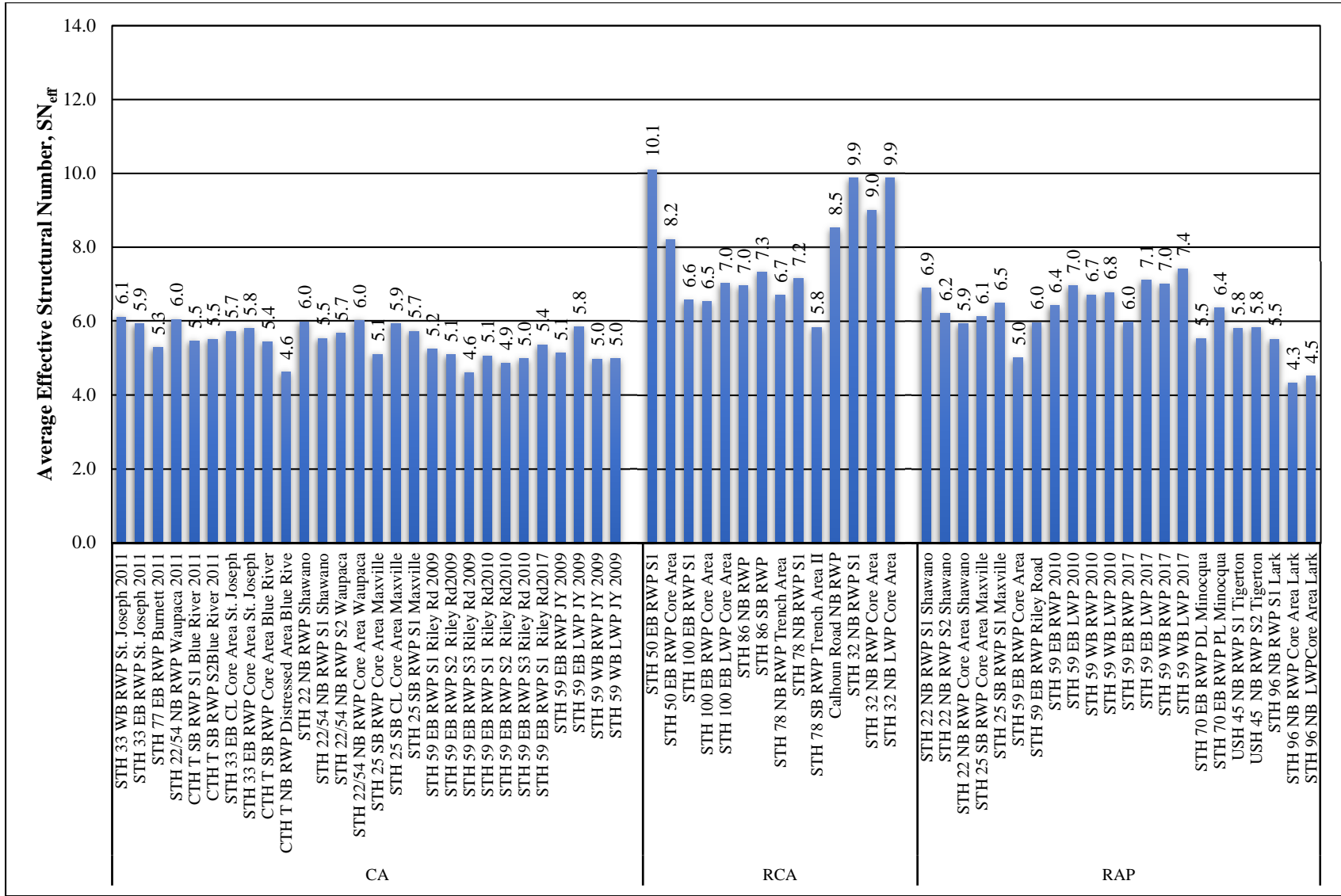


Figure 5.12: Average effective structural number for the investigated HMA pavement test sections with crushed aggregate, recycled concrete aggregate, and reclaimed asphalt pavement base layers.

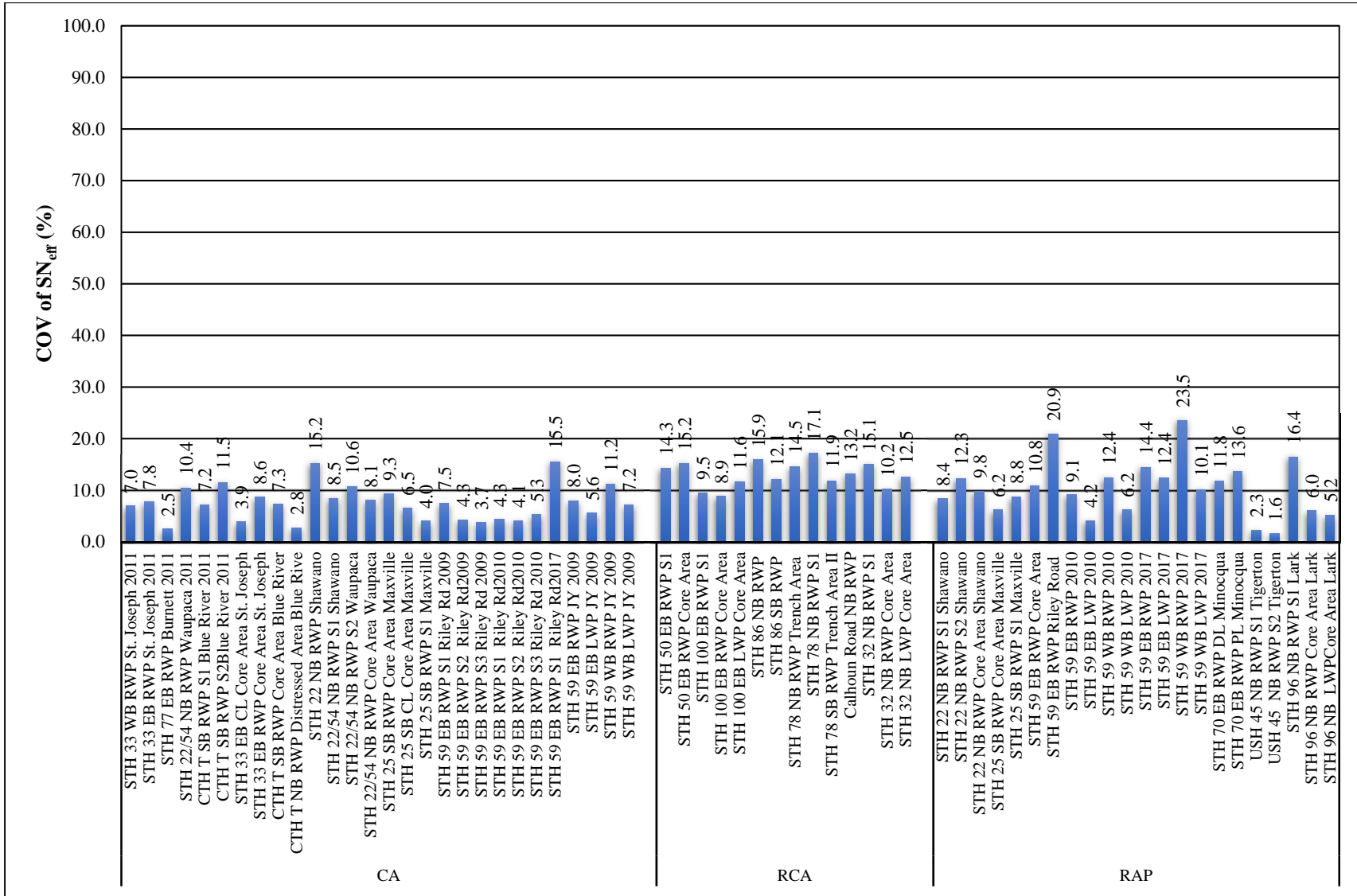


Figure 5.13: Coefficient of variation of effective structural number for the investigated pavement test sections with crushed aggregate, recycled concrete aggregate, and reclaimed asphalt pavement base layers.

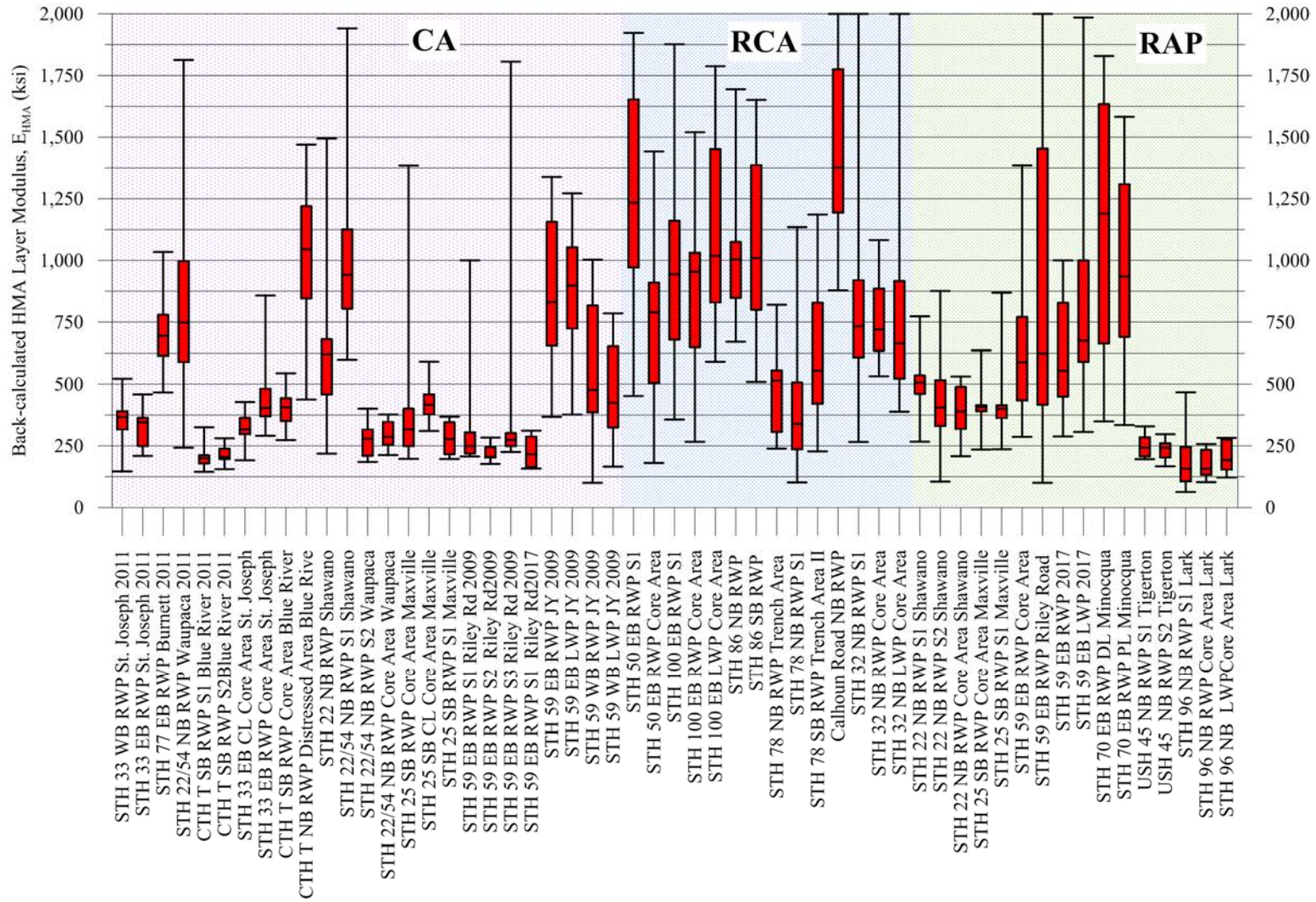


Figure 5.14: Box-Whisker plot of the back-calculated HMA layer modulus for the investigated pavement test sections with crushed aggregate, recycled concrete aggregate, and reclaimed asphalt pavement base layers.

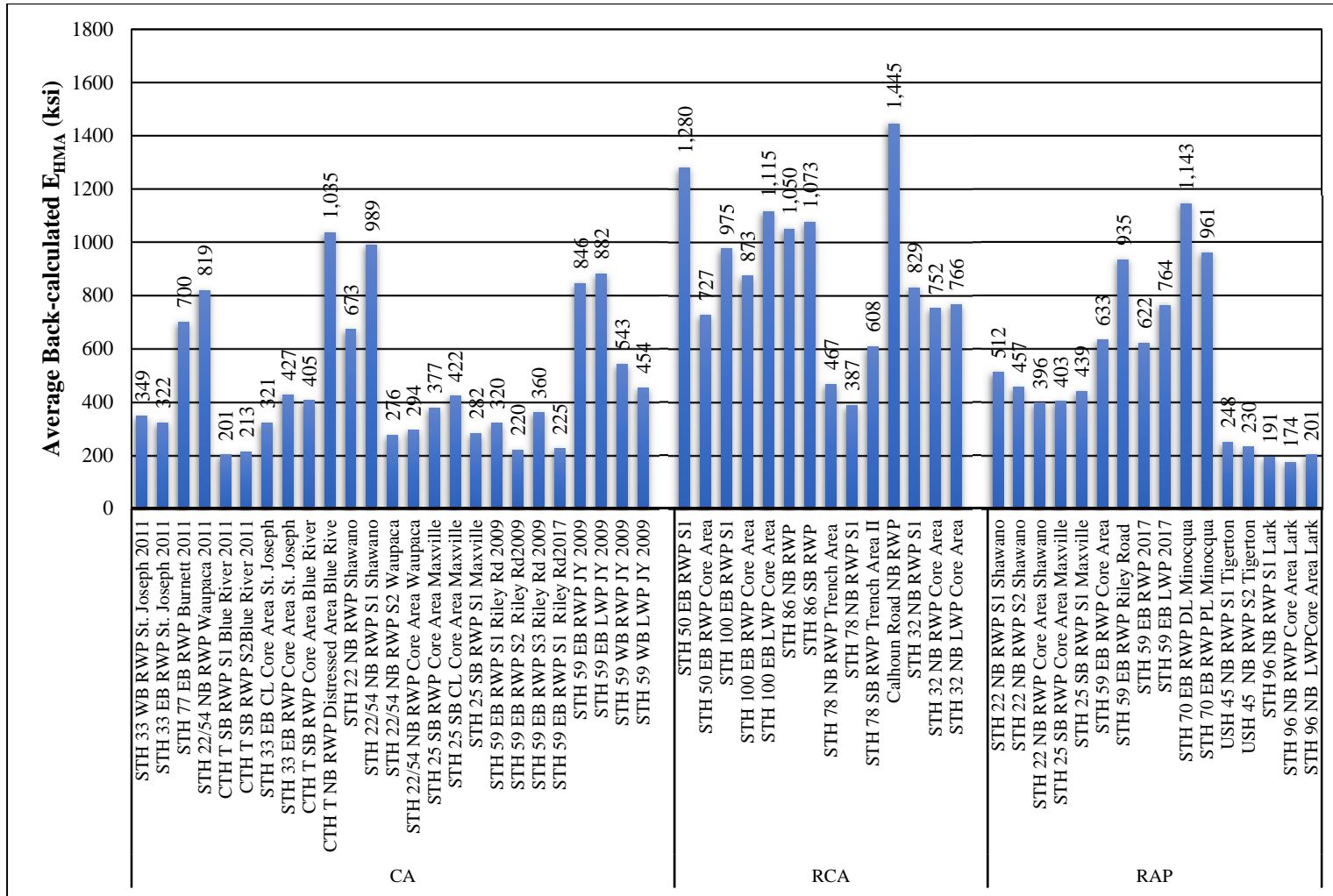


Figure 5.15: Average back-calculated HMA layer modulus for the investigated pavement test sections with crushed aggregate, recycled concrete aggregate, and reclaimed asphalt pavement base layers.

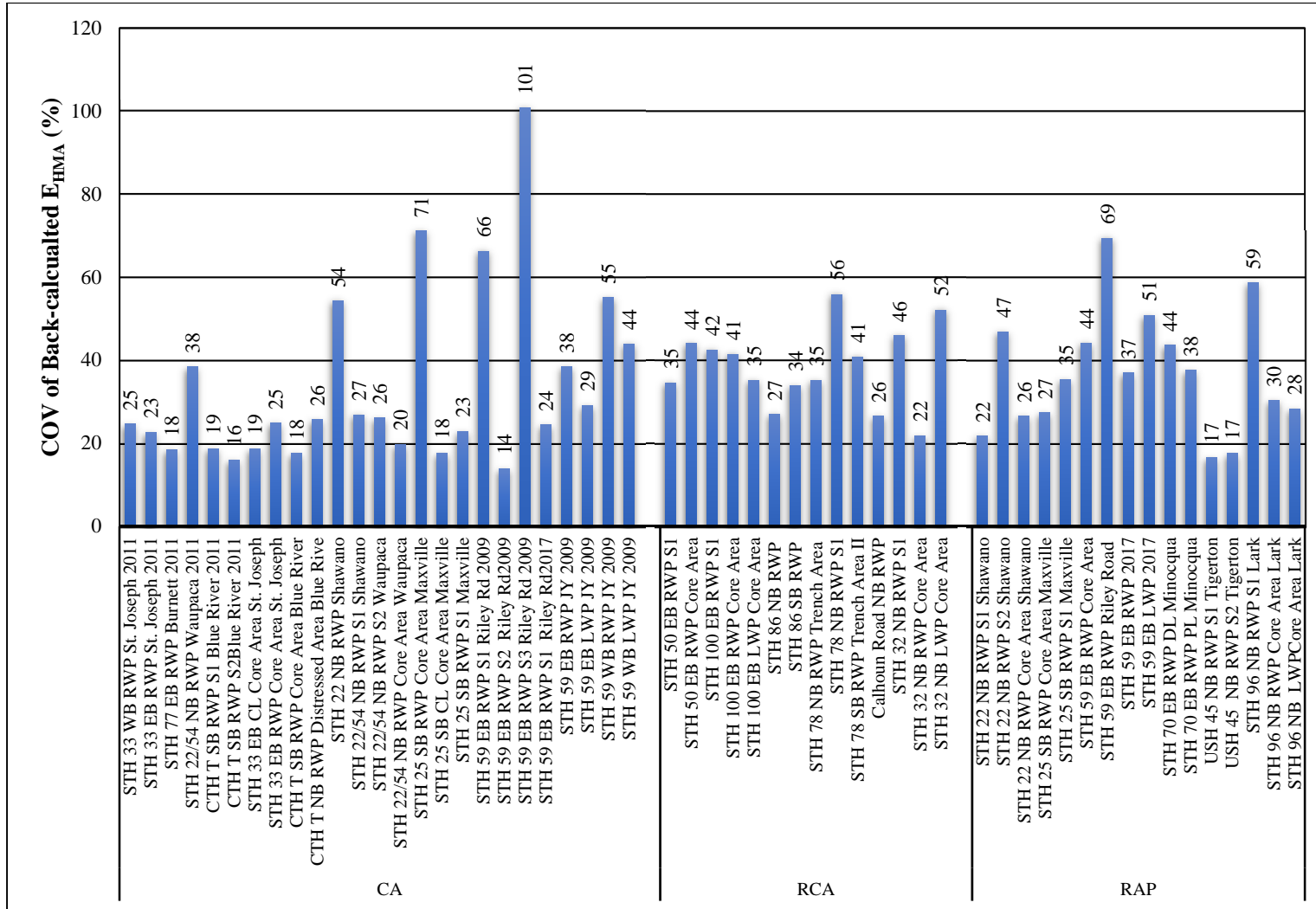


Figure 5.16: Coefficient of variation of back-calculated HMA layer modulus for the investigated pavement test sections with crushed aggregate, recycled concrete aggregate, and reclaimed asphalt pavement base layers.

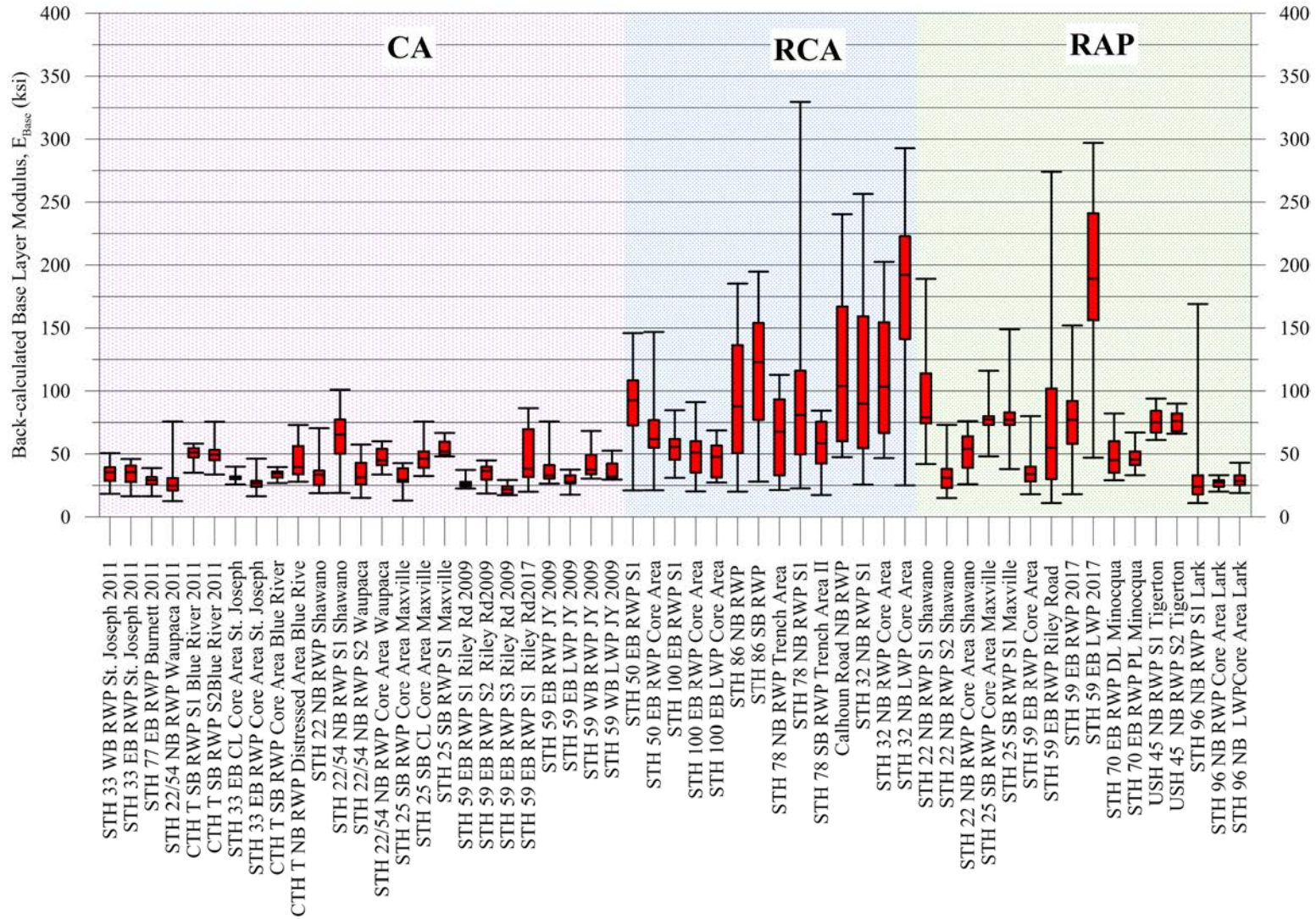


Figure 5.17: Box-Whisker plot of the back-calculated base layer modulus for the investigated pavement test sections with crushed aggregate, recycled concrete aggregate, and reclaimed asphalt pavement base layers.

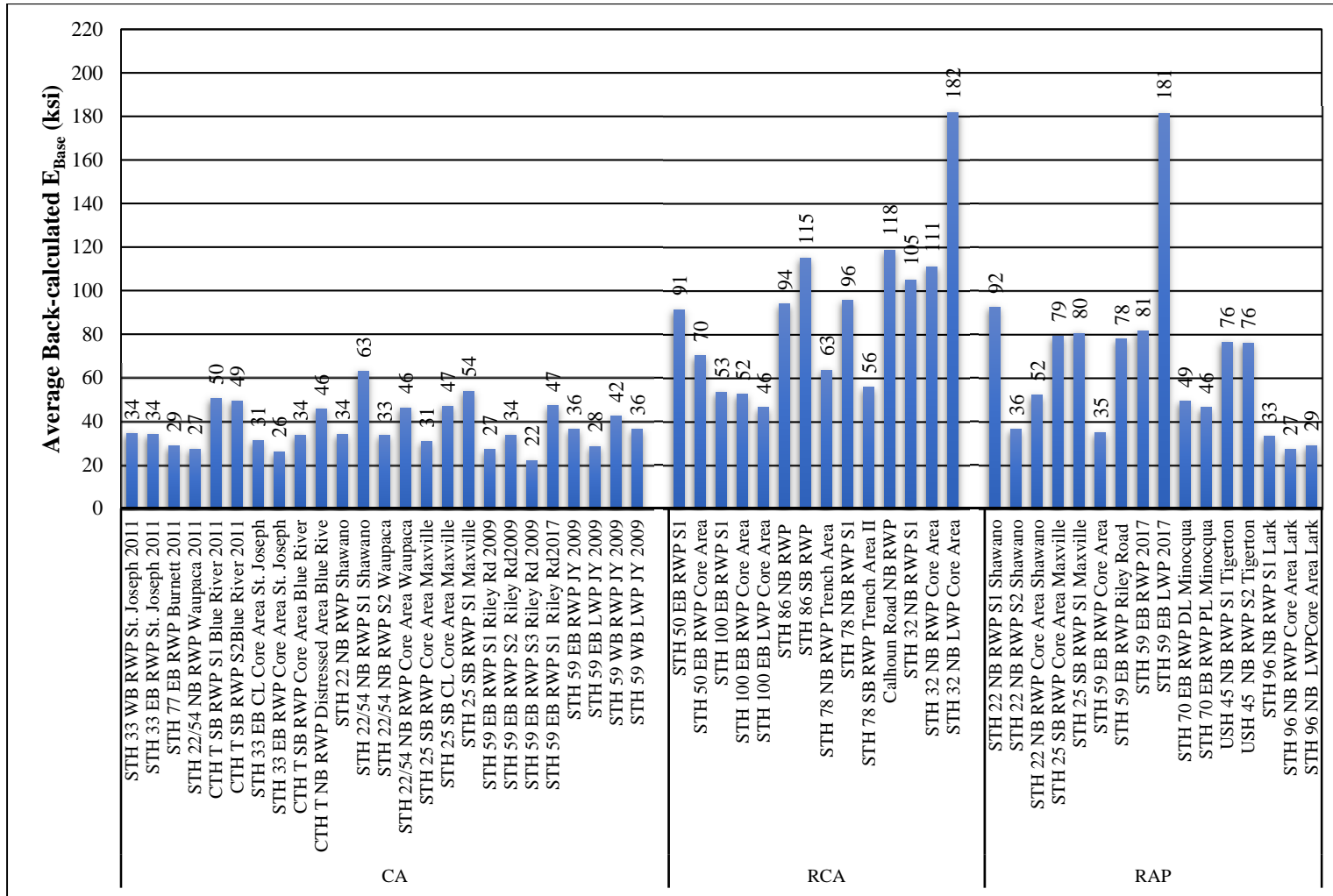


Figure 5.18: Average back-calculated base layer modulus for the investigated pavement test sections with crushed aggregate, recycled concrete aggregate, and reclaimed asphalt pavement base layers.

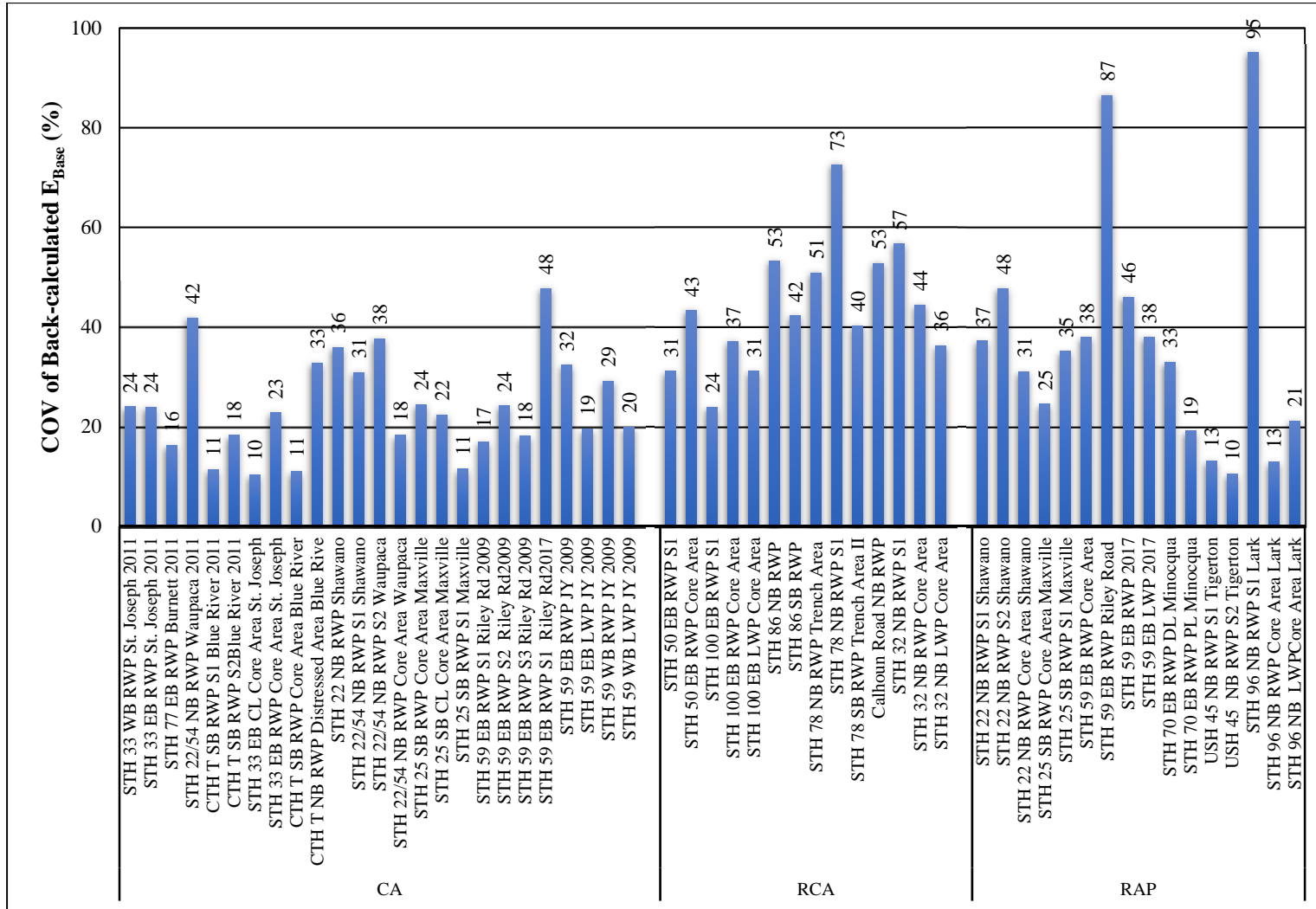


Figure 5.19: Coefficient of variation of back-calculated base layer modulus for the investigated pavement test sections with crushed aggregate, recycled concrete aggregate, and reclaimed asphalt pavement base layers.

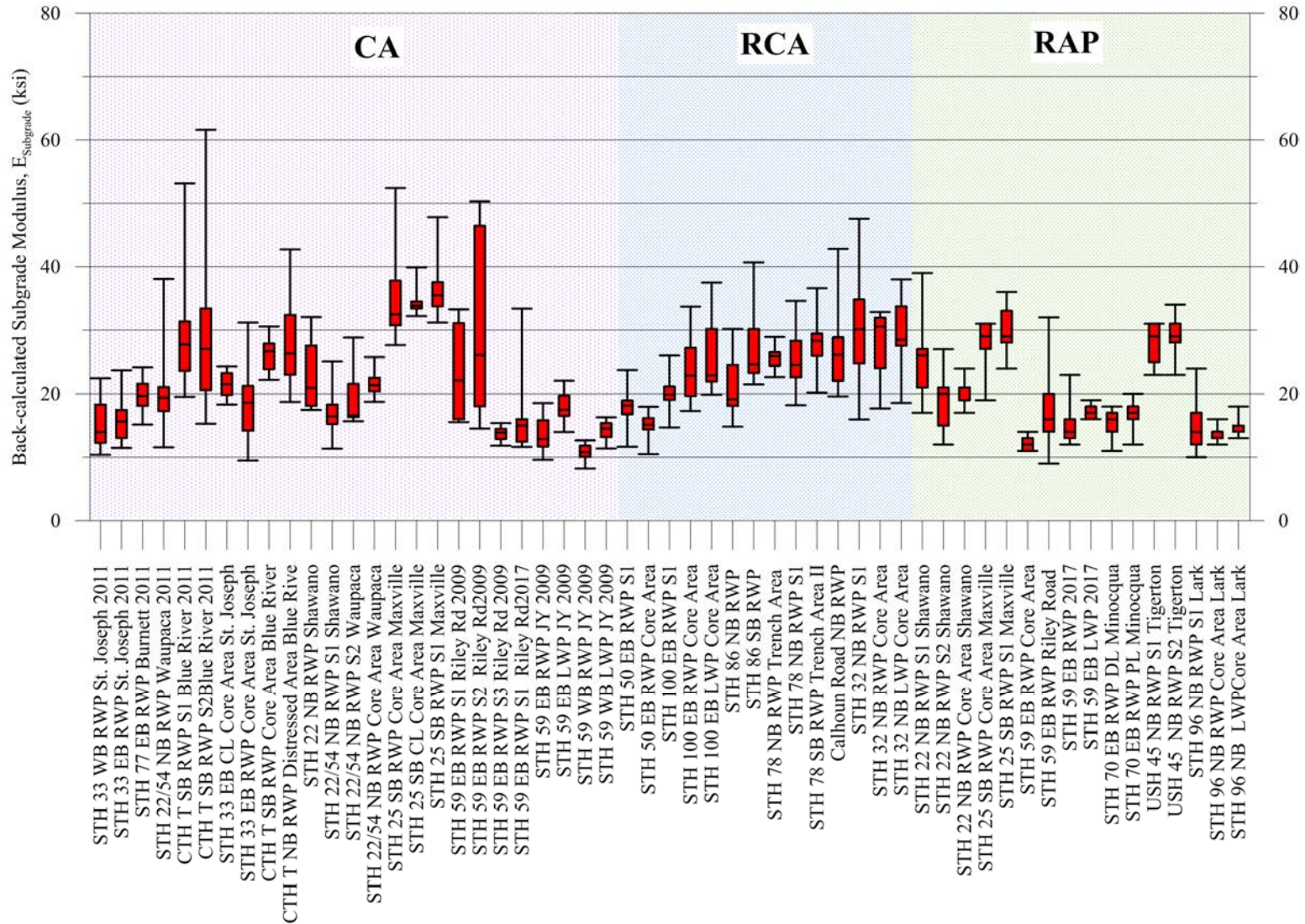


Figure 5.20: Box-Whisker plot of the back-calculated subgrade modulus for the investigated pavement test sections with crushed aggregate, recycled concrete aggregate, and reclaimed asphalt pavement base layers.

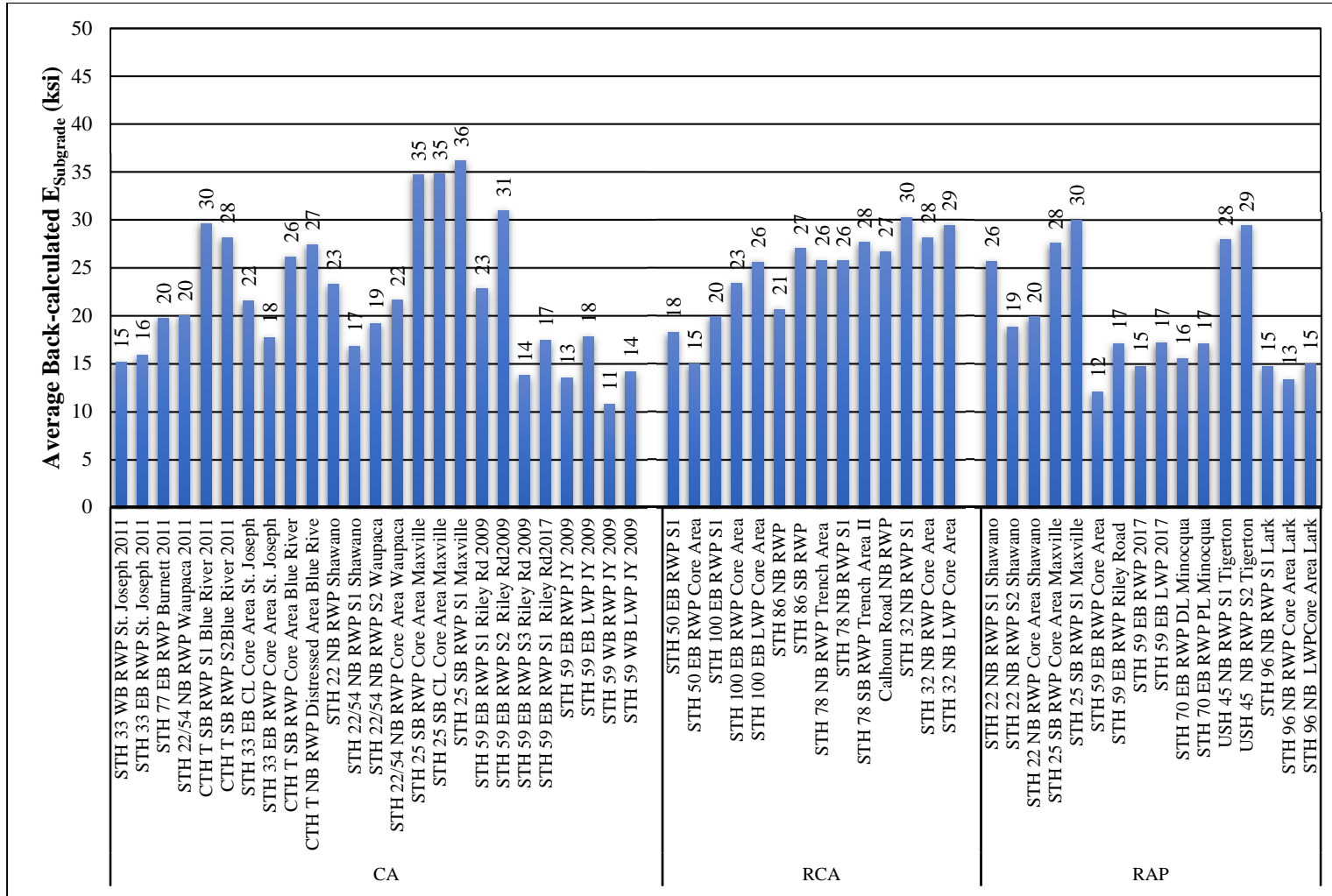


Figure 5.21: Average back-calculated subgrade modulus for the investigated pavement test sections with crushed aggregate, recycled concrete aggregate, and reclaimed asphalt pavement base layers.

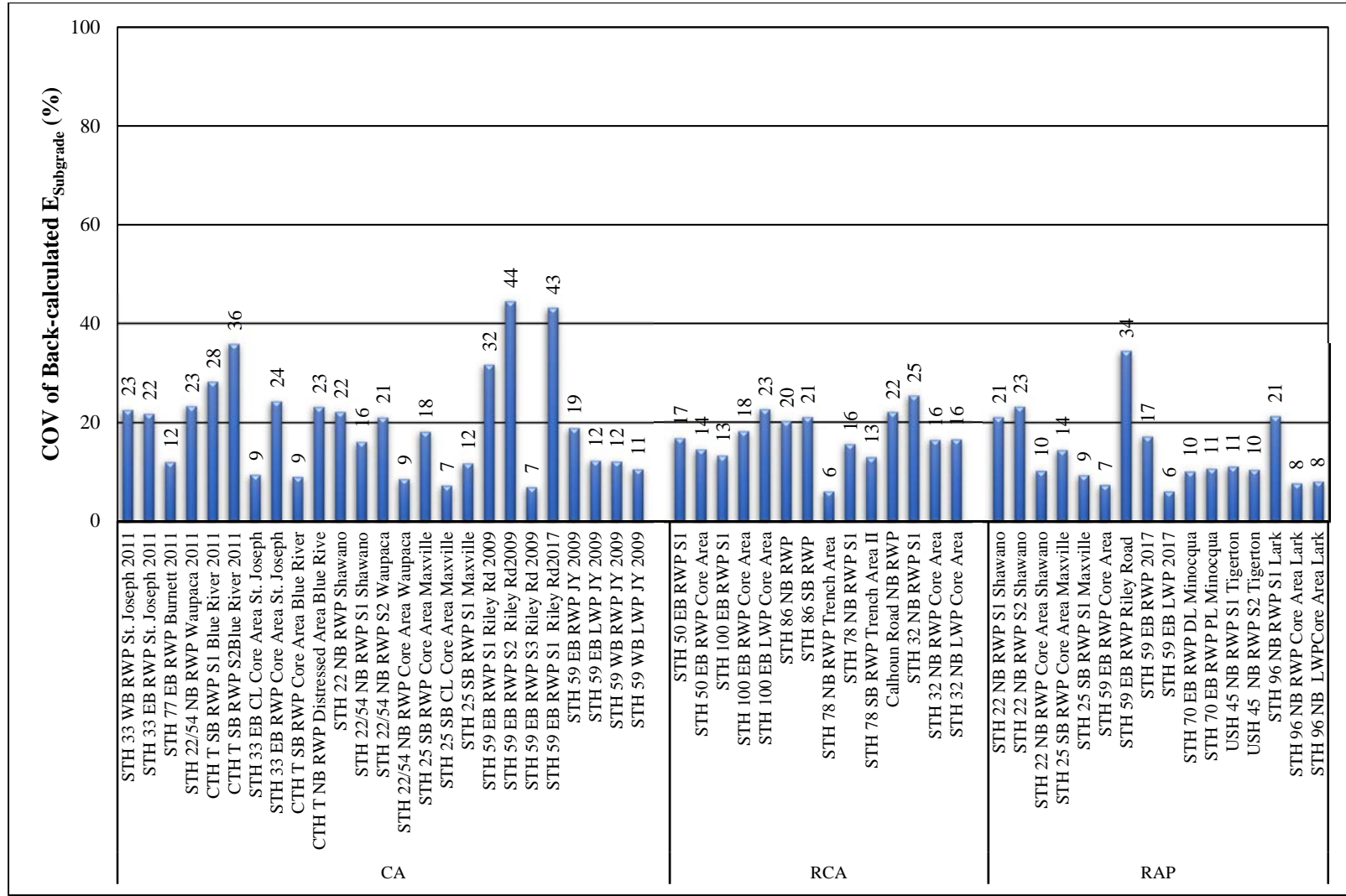


Figure 5.22: Coefficient of variation of back-calculated subgrade modulus for the investigated pavement test sections with crushed aggregate, recycled concrete aggregate, and reclaimed asphalt pavement base layers.

The back-calculation analysis conducted on the FWD test results for all investigated pavement sections are summarized in Table 5.6 and Figures 5.14-5.22. The back-calculated moduli for the HMA layer (E_{HMA}) for all investigated pavement sections varied significantly among the pavement test sections (and within the individual pavement sections) with COV ranging between 51.4% (for pavement sections with RCA base layers) and 75.8% (for pavement sections with RAP base layers). For pavement sections with CA base layers, E_{HMA} averages ranged from 201 to 1,035 ksi, while E_{HMA} averages varied between 387 and 1,445 ksi for pavement section with RCA base layers. For pavement sections with RAP base layers, E_{HMA} averages varied between 174 to 1,134 ksi. The averages for the back-calculated E_{HMA} are 523, 845, and 560 ksi for pavement sections with CA, RCA, and RAP base layers, respectively. Consequently, the back-calculated E_{HMA} average for the pavement sections with CA and RAP base layers are lower than the corresponding average for pavement sections with RCA base layers. The variability in back-calculated E_{HMA} is not necessarily exclusively dependent on the base course layer variability. There are other factors that may influence the mechanical stability of HMA (mix design, compaction temperature, compaction effort, density, pavement surface age, pavement surface temperature and exposure to UV, and, most importantly, variability in layer thickness (as demonstrated by measured core thicknesses presented in Appendix D and GPR profiles).

The back-calculated base layer modulus values (E_{Base}) for all investigated pavement test sections are summarized in Table 5.6 and Figures 5.17-5.19. The results indicate significant variability in the back-calculated E_{Base} with averages ranging from 22 to 63 ksi for CA base layers, between 46 and 182 ksi for RCA base layers, and from 27 to 181 ksi for RAP base layers. An inspection of the back-calculated E_{Base} results in Figures 5.17-5.19 indicates that, in general, the RCA base layers exhibited the highest average values (87 ksi with COV of 63%), followed by the RAP base layers (63 ksi with COV of 72%), while the CA base layers possessed the lowest average values (37 ksi with COV of 40%).

The results of the back-calculated subgrade modulus ($E_{Subgrade}$) are presented in Table 5.6 and Figures 5.20-5.22. For pavement sections with CA base layers, the averages of $E_{Subgrade}$ ranged from 11 to 36 ksi with an overall average of 21 ksi and COV of 39%. $E_{Subgrade}$ averages, for pavement sections with RCA base layers, varied between 15 and 30 ksi with an average of 25 ksi and COV of 26%. For RAP base layers, these values ranged between 12 and 30 ksi with an average of 18 and COV of 35%. Generally, $E_{Subgrade}$ values for all investigated pavement sections (with base layers of CA, RCA, and RAP) were all comparable and fell within a close range of values.

Appendix E presents the details of the FWD test results and back-calculation results for all investigated HMA pavement test sections with CA, RCA, and RAP base layers.

5.3 Ground Penetrating Radar

The GPR scan files were obtained from WisDOT and analyzed by the research team using the RADAN® Software (a GSSI GPR Post Processing Software) utilizing the RoadScan Module. The RoadScan Module uses a signal calibration technique that measures significant layer interface amplitudes from the pavement data and calculates the propagation velocity of the GPR signal through the pavement layer (GSSI, 2018).

For this study, 400 MHz and 1 GHz antennae were used to image the thickness profiles of HMA pavements, including surface, base, and subbase layers. Because GPR systems only capture signal amplitudes versus time, two different calibrations were implemented during the data analysis. The first calibration was needed to determine the reflection at the top of the pavement and to correct the GPR signatures for the changes in antenna height as the vehicle moves along the road. The second calibration was required to convert the travel time obtained from the GPR records to the thickness of different layers. There are two alternatives for this calibration. The first alternative is to measure the electromagnetic wave velocity in the pavement structure while the second alternative involves calibrating the data using pavement cores. The second alternative was used in this study. It should be noted that the quality of the profiles can be improved if several cores are collected along the length of the profile. If a limited number of cores were collected, the analysis assumed that the material properties were uniform. Using cores and assuming constant profile properties along road sections, the thicknesses of the layers in pavement substructures were delineated for the investigated pavement test sections.

As an example, GPR testing and analysis for STH 59 (west of Edgerton) is presented in which the pavement has two sections: one with a CA base layer; and the other with RAP base layer. The location, track of GPR testing, and pavement surface cores for the STH 59 pavement west of Edgerton (Riley Road and STH 59) are shown in Figure 5.23. The GPR scan began on Riley Road about 84 m before the intersection of STH 59 (distance 0 to 84 m). The GPR scan for STH 59 EB began from the distance log of 84 to 1,226 m in which the pavement section with CA base layer extended from 84 to 418 m and the RAP base layer extended from 418 to 1,226 m. Analyses of the test data (using a relative dielectric permittivity k' of 4) indicated the existence of two HMA layers with the bottom of the first layer shown in yellow dots and the bottom of the second layer shown in red dots in Figure 5.23. The next two layers appeared to be base layers with depth down to 0.4 m; however, the thicknesses of these layers appeared to be thinner than the thicknesses presented in the typical cross-section as well as the thicknesses measured by the research team during pavement coring and aggregate sampling.

For the CA base layer section of STH 59, the GPR profiles showed that the average thickness of HMA pavement layer I was 2.43 in with COV of 27% and the average thickness of HMA layer II was 2.24 in with COV 13.4%. The average total thickness of the HMA layer was 4.67 compared with 4 in described in WisDOT pavement plans and 3.75 in average core thickness. The average thickness of the upper base layer was 1.81 in with COV of 31%, and the

average thickness of the lower base layer was 6.05 in with COV of 25%. The average total thickness of the base layer was estimated to be 7.86 in compared with the 8 in CA base layer described by WisDOT pavement typical sections. The GPR test results demonstrated the existence of high variability in the thickness of pavement layers, which is also evident from the core thickness measurements obtained for all investigated test sections.

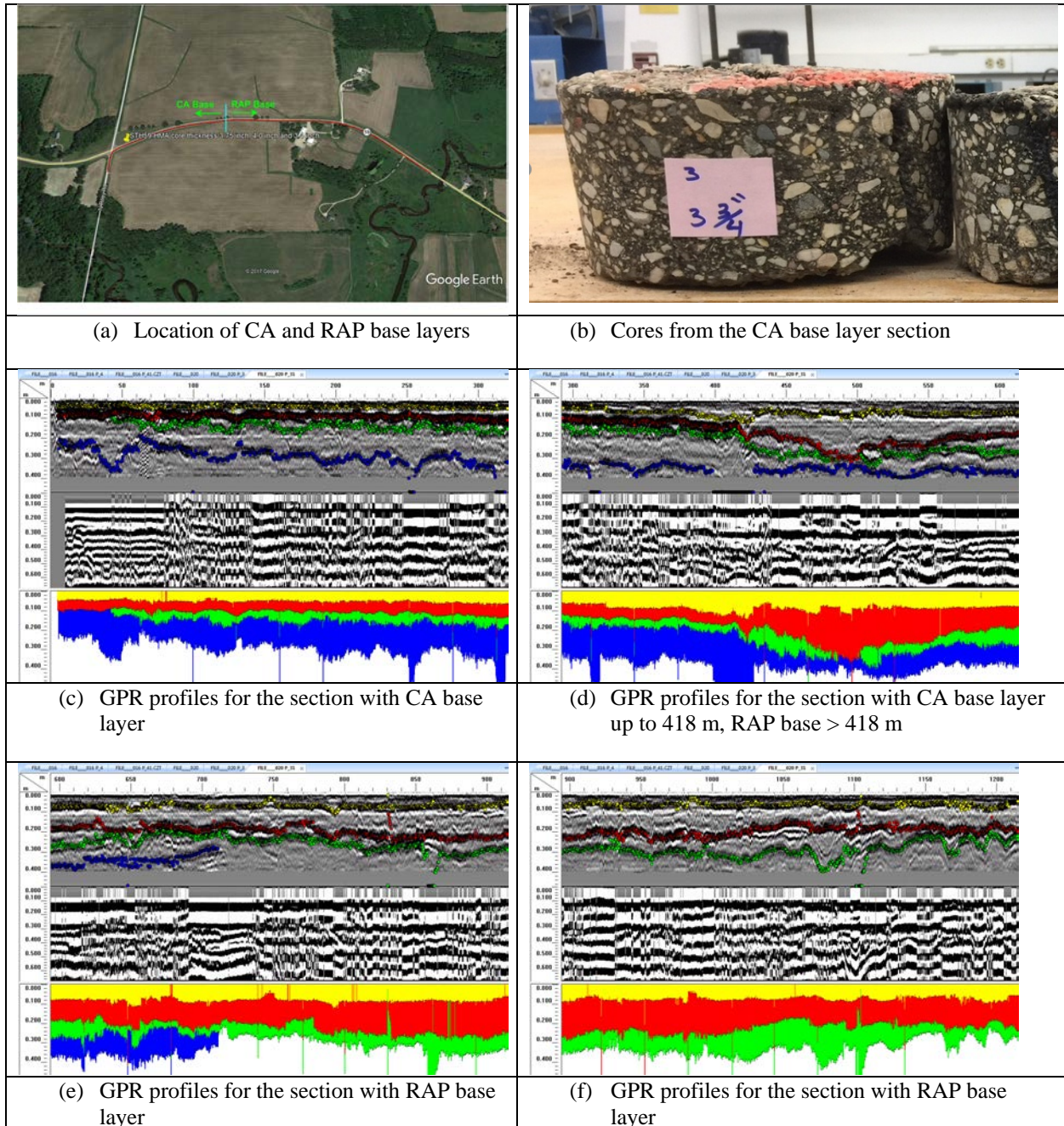


Figure 5.23: Location and pavement layer profiles for STH 59 with CA and RAP base layers obtained from analysis.

5.4 Base Layers Drainability Test Results

The results of the field drainability tests on the investigated base layers (CA, RCA, and RAP) are presented in Tables 5.7-5.8 and Figure 5.24. Test results indicated that RCA base layers had higher drainability characteristics with values ranging from 3.1 to 43.3 ft/day for the base layers on STH 50. This demonstrates the high variability since both numbers are for the wheel path locations within the test section. The coefficient of permeability values for the RCA base materials retrieved from STH 50 were 6.8 ft/day for the location at the center of the lane and 10.7 ft/day for the wheel path location (Figure 5.25). The drainability values for CA base layers are the lowest among all base layer types with values ranging between 0.7 and 16.6 ft/day. The coefficient of permeability for the CA base materials varied from 5.5 to 52.8 ft/day. The drainability test results for the RAP base layers ranged between 0.3 and 26.9 ft/day. No permeability tests were conducted on the RAP base materials in the laboratory.

The field drainability test results are influenced by many factors including the thickness of the base layer, particle size distribution of base materials, amount of fines, density of base materials, properties of the subbase layers, subgrade type and properties, the climatic conditions, seasonal variations in moisture within pavement layers and subgrade, pavement geometry/slopes, drainage infrastructure around the pavement, etc. Therefore, the comparison and evaluation of the drainability of base layers is more complicated than presented herein.

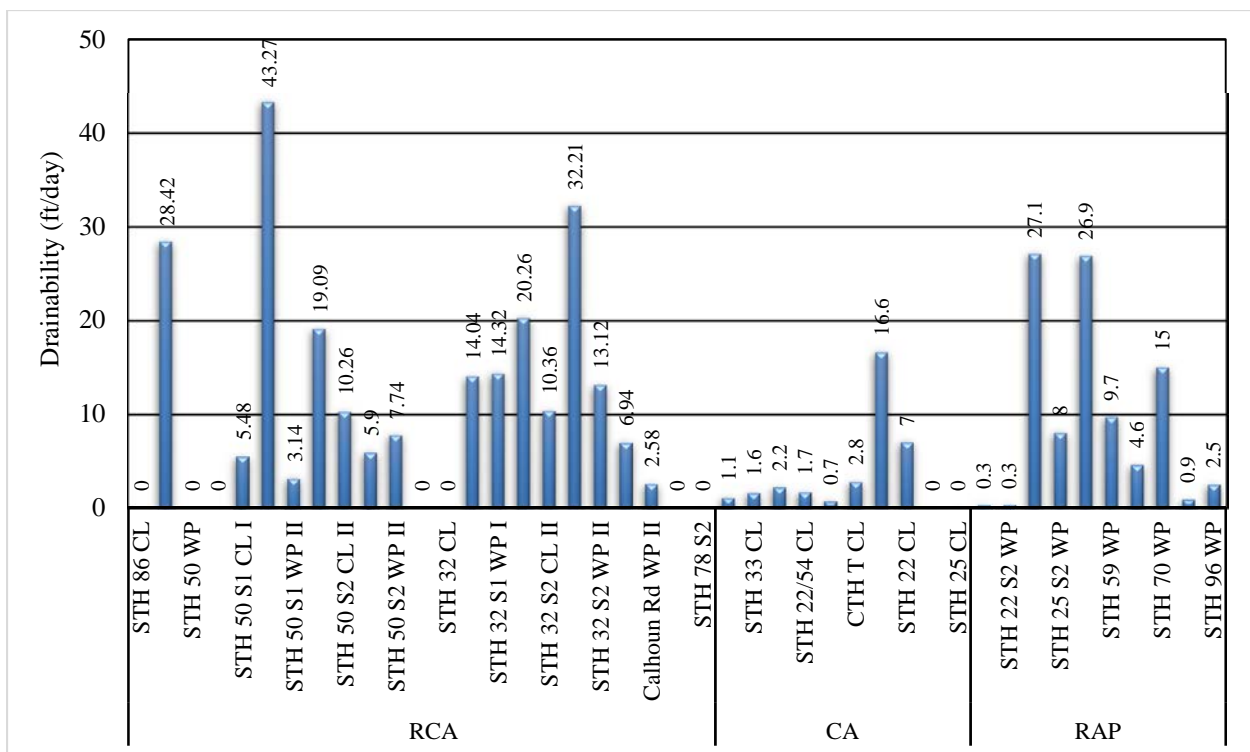
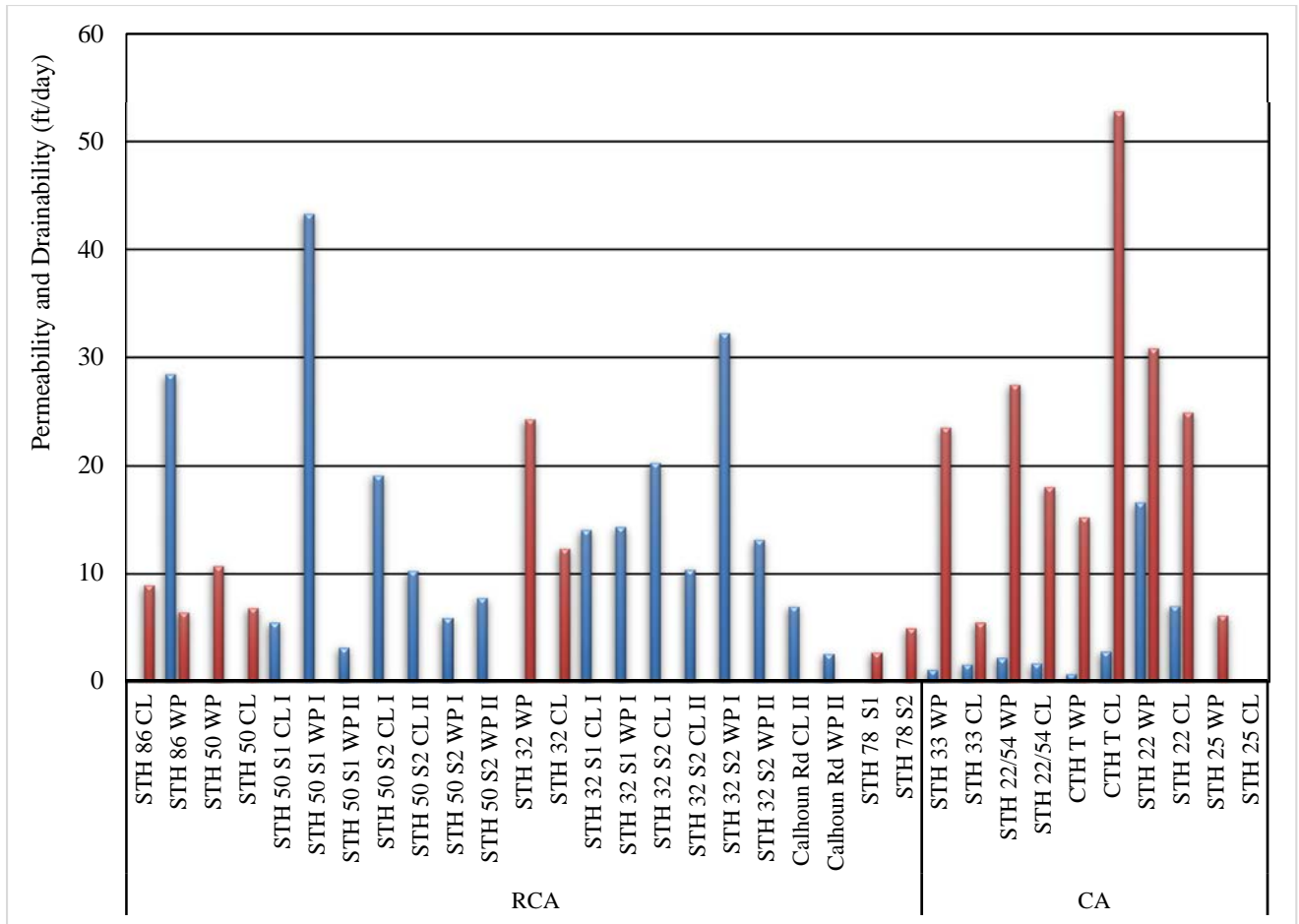


Figure 5.24: Field drainability of the investigated RCA, CA, and RAP base course layers.



■ Constant-head permeability test ■ Field drainability test

Figure 5.25: Field drainability and laboratory hydraulic conductivity of the investigated RCA and CA base course materials.

Table 5.7: Field drainability test results on CA and RCA base layers and laboratory permeability tests on RCA and CA base materials.

Base Type	Base Test Section and Location		Field Drainability (ft/day)	Laboratory Coefficient of Permeability (ft/day)
RCA	STH 86	CL	-	8.93
		WP	28.42	6.40
	STH 50	WP	-	10.69
		CL	-	6.81
		S1 CL I	5.48	-
		S1 WP I	43.27	-
		S1 WP II	3.14	-
		S2 CL I	19.09	-
		S2 CL II	10.26	-
		S2 WP I	5.90	-
		S2 WP II	7.74	-
		STH 32	WP	-
	CL		-	12.30
	S1 CL I		14.04	-
	S1 WP I		14.32	-
	S2 CL I		20.26	-
	S2 CL II		10.36	-
	S2 WP I		32.21	-
	S2 WP II		13.12	-
	Calhoun Road	CL II	6.94	-
WP II		2.58	-	
STH 78	S1	-	2.71	
	S2	-	4.95	
CA	STH 33	WP	1.10	23.52
		CL	1.60	5.46
	STH 22/54	WP	2.20	27.43
		CL	1.70	18.01
	CTH T	WP	0.70	15.19
		CL	2.80	52.77
	STH 22	WP	16.60	30.81
		CL	7.00	24.93
STH 25	WP	0.00	6.12	
	CL	0.00	-	

Table 5.8: Field drainability test results on RAP base layers.

Base Type	Base Test Section and Location		Field Drainability (ft/day)
RAP	STH 22	STH 22 S2 CL	0.3
		STH 22 S2 WP	0.3
	STH 25	STH 25 S2 CL	27.1
		STH 25 S2 WP	8.0
	STH 59	STH 59 CL	26.9
		STH 59 WP	9.7
	STH 70	STH 70 CL	4.6
		STH 70 WP	15.0
	STH 96	STH 96 CL	0.9
		STH 96 WP	2.5

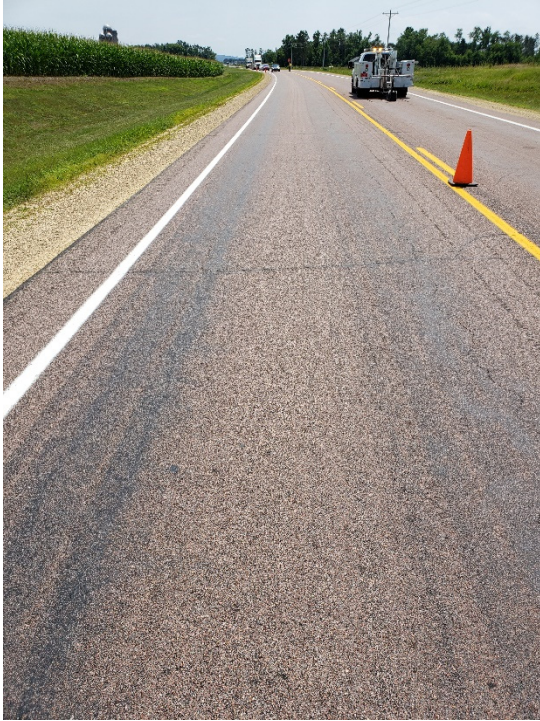
5.5 Pavement Surface Visual Distress Surveys and Profile Measurements

The research team conducted a visual distress survey analysis on all investigated pavement test sections with CA, RCA, and RAP base layer. The goal was to calculate the pavement condition index (PCI) values for 25-ft-long subsections along the 528 ft pavement test section representing each investigated pavement. The most commonly observed pavement surface distress in the investigated pavement test sections included: transverse cracking, longitudinal cracking, alligator (fatigue) cracking, rutting, bleeding, edge cracking, pavement edge heave, and block cracking. Figures 5.26-5.28 depict various pavement surface distress observed during the field investigation.

Based on the visual distress survey of the investigated pavement sections, fatigue cracking is the most commonly observed surface distress associated with CA and RAP base layers as depicted in Figures 5.27 and 5.28. Transverse and longitudinal cracks were commonly observed on pavement sections with RCA base layers.

The visual distress survey data were analyzed using the computer program MicroPAVER and the corresponding PCI values were calculated. Figure 5.29 presents the results of the analysis and the corresponding classification of the pavement condition for the pavement test sections at STH 22/54 with CA base layer, STH 86 with RCA base layer, and STH 22 with RAP base layer. The pavement surface description based on PCI evaluation is also presented on each figure. As an example, the PCI values ranged from 30 to 73% for STH 22/54 with the designation varying between very poor to satisfactory. The average PCI for the 528-ft pavement section on STH 22/54 was 54% with a general classification of fair. The PCI scale consists of good (PCI 70 to 100), fair (PCI from 55 to <70), and poor (PCI < 55). It should be noted that the PCI values calculated herein are based on the 528-ft pavement test section that included pavement surface coring and base layer sampling as well as other field tests. The section was selected to represent the whole pavement project based on the judgment and experience of the research team. The variation of PCI values with distance along the investigated pavement test sections are presented in Appendix F.

The variation of the PCI and the average values for the investigated pavement test sections are presented in Figure 5.30. The PCI values are highly variable in all sections and among the pavements with CA, RCA, and RAP base layers with a minimum of 7% and a maximum of 100%. The pavement sections with CA base layers exhibited PCI averages ranging between 28 and 92% with overall average of 58% and COV of 44.3% (pavement age: 9 to 14 years). The PCI averages for the pavement sections with RCA base layers varied between 27 and 86% with overall average of 65.5% and COV of 34.3% (pavement age: 10 to 22 years). Finally, the PCI averages for the pavement sections with RAP base layers ranged from 38 to 100% with overall average of 62.8% and COV of 34.9% (pavement age: 1 to 18 years). It should be noted that USH 45 with RAP base layer was investigated during construction and one year after construction to serve as control section for future performance evaluation.



(a) Bleeding and fatigue cracking – STH 25



(b) Fatigue and transverse cracking – STH 33



(c) Fatigue cracking – STH 25



(e) Fatigue cracking – CTH T



(d) Transverse and Longitudinal cracking – STH 22

Figure 5.26: Pavement surface distress observed on pavements with CA base layers.



(a) Rutting – STH 86



(b) Longitudinal and transverse cracking – STH 86



(c) Edge heave– STH 78



(d) Longitudinal and transverse cracking – STH 86



(e) Longitudinal and transverse cracking – STH 78



(f) Longitudinal and transverse cracking – STH 100

Figure 5.27: Pavement surface distress observed on pavements with RCA base layers.



(a) Fatigue cracking – STH 96



(b) Fatigue cracking STH 70



(c) Bleeding – STH 25

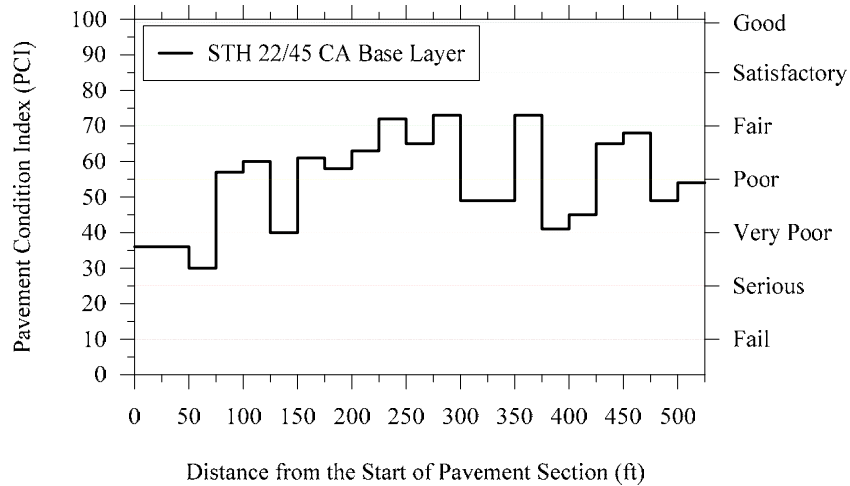


(d) Longitudinal cracking – STH 59

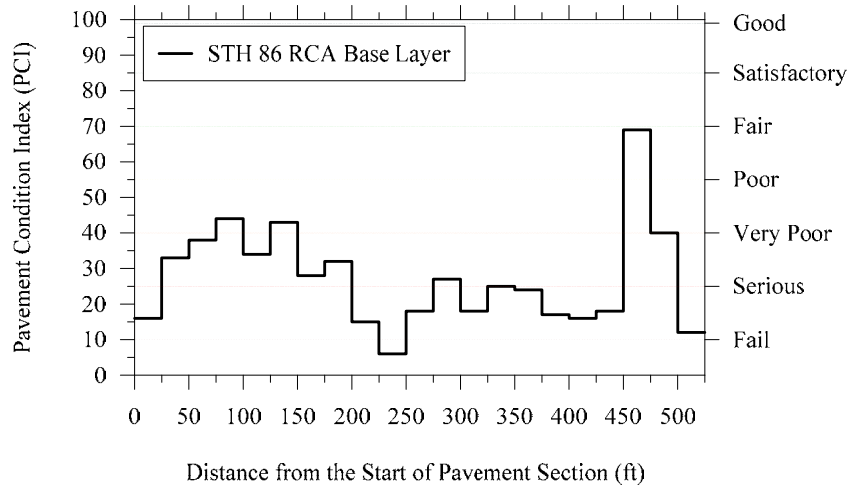


(e) Fatigue and transverse cracking – STH 22

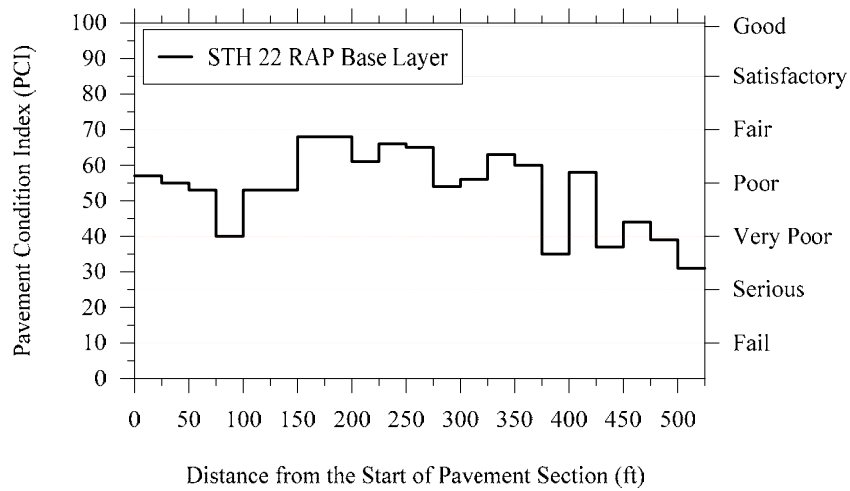
Figure 5.28: Pavement surface distress observed on pavements with RAP base layers.



(a) STH 22/54 with CA base layer

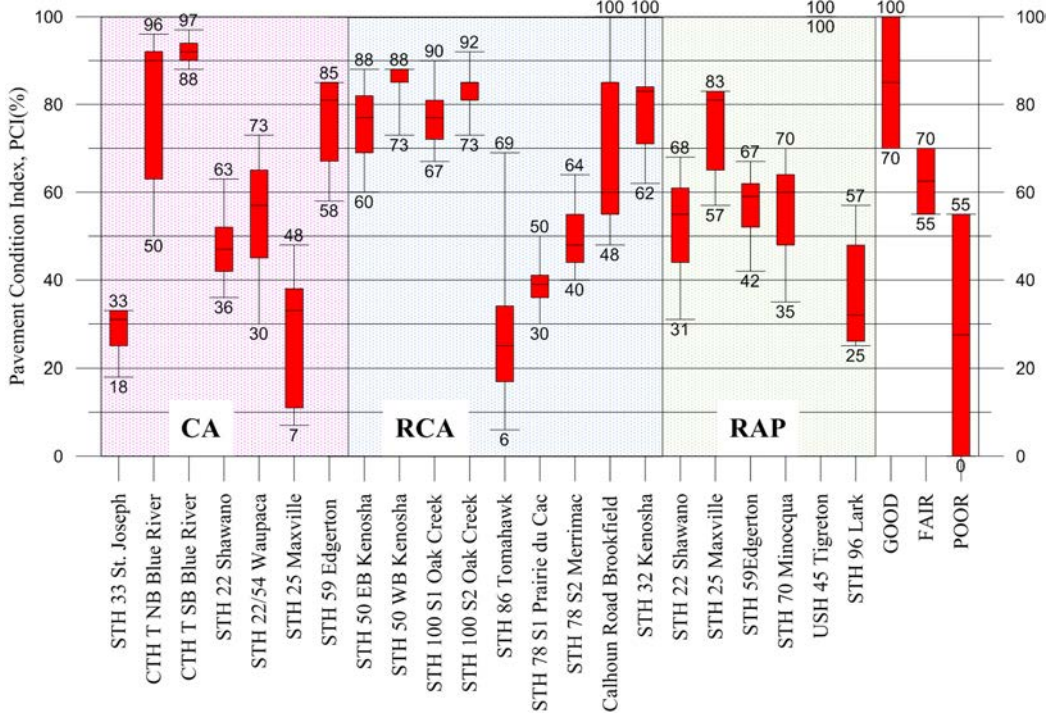


(b) STH 86 with RCA base layer

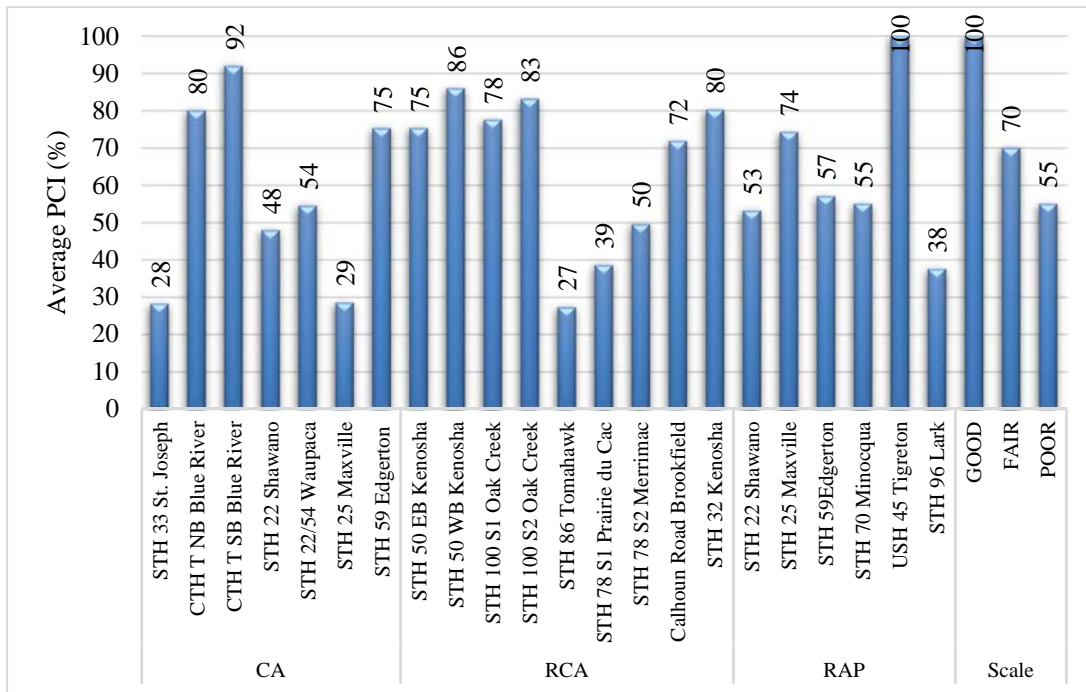


(c) STH 22 with RAP base layer

Figure 5.29: PCI calculated from the visual distress survey data along the 528 ft pavement test sections.



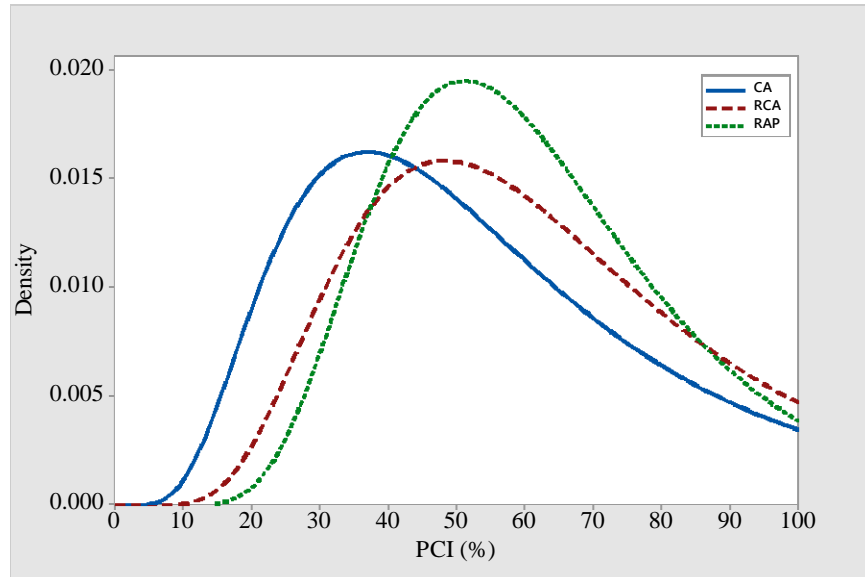
(a) Box-Whisker plot of calculated PCI



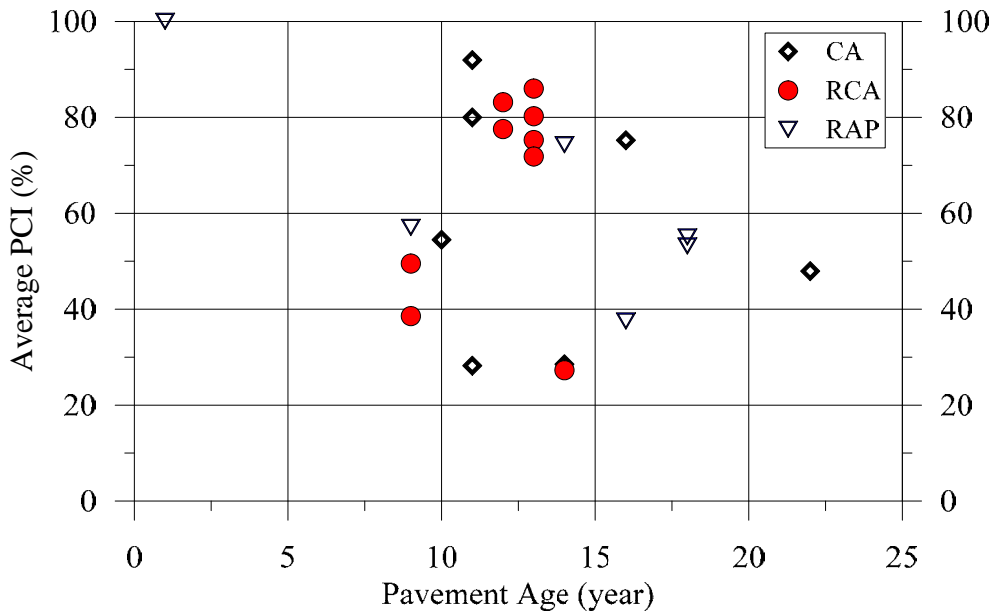
(b) Average PCI for the 528 ft pavement test section

Figure 5.30: Variation of PCI along the 528 ft surveyed test sections.

The lognormal distribution of PCI values for each 25-ft test section within the pavement sections with similar base material type (i.e., CA, RCA, and RAP) are presented in Figure 5.31. The figure (Figure) 5.31 shows the general ranking of the investigated pavements based on the overall average described earlier but it does not account for the pavement age. An attempt to correlate the calculated PCI average values with pavement age is presented in Figure 5.31, but it did not lead to reliable trend.



(a) Lognormal distribution of PCI values obtained for the 25 ft sections



(b) Average PCI values versus pavement age for the investigated 528 ft test sections

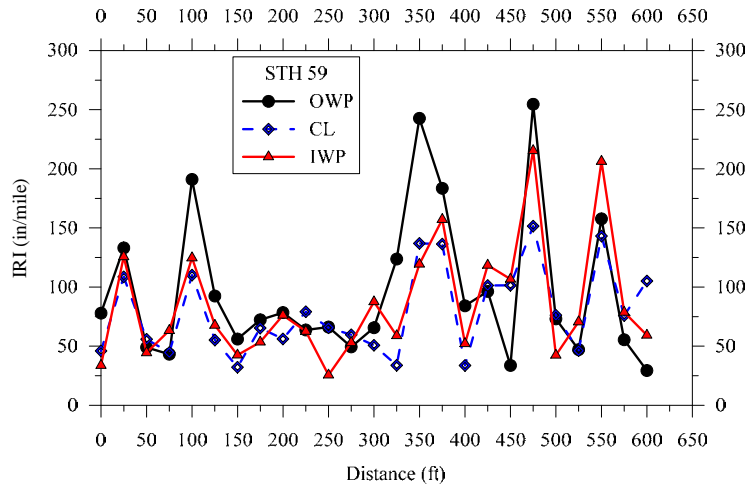
Figure 5.31: Analysis of PCI values for the investigated pavement test sections.

The pavement surface profile measurements were conducted on the outside (right) wheel path (OWP), center of the lane (CL), and the inside (left) wheel path (IWP) for all investigated pavement test sections. The length of each pavement test section was 600 ft and the International Roughness Index values were calculated for 25-ft subsections using the program ProVAL. Figure 5.32 depicts the IRI values in inch per mile unit for three pavement test sections with CA, RCA, and RAP base layers. An inspection of Figure 5.32 indicates very high variability in the IRI values within the tracks (such as the outside wheel path) of the same pavement test section as well as among the pavement test sections. For STH 59 with a CA base layer, the IRI ranged from 29 to 255 in/mile for the OWP, between 32 and 152 in/mile for the CL, and from 26 to 215 for the IWP. The corresponding average IRI values were 97, 79, and 86 in/mile for the OWP, CL, and IWP respectively. Generally, the OWP profile measurement showed higher IRI values compared with the CL and IWP for the same pavement test section. The outside wheel path is near the pavement edge/shoulder and usually lacks adequate lateral support when compared with the inside wheel path and lane center. This would lead to higher rutting and roughness values, which was observed by the research team during field work. The IRI variation with distance along the test section for all investigated pavements are presented in Appendix G.

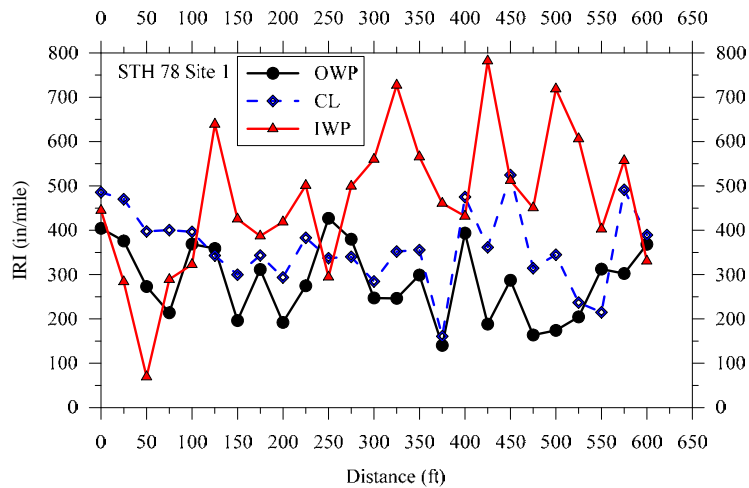
In order to provide an evaluation of the pavement performance based on the base layer materials type (CA, RCA, and RAP), the IRI values and the associated variability for all investigated test sections are shown in Figure 5.33. An examination of the figure indicates relatively high IRI values and high variability exhibited by the pavement sections on RCA base layer materials, particularly for STH 78 test sections S1 and S2. The IRI averages for the investigated pavements ranged from 71 to 153 in/mile for sections with CA base layers, between 66 and 467 in/mile for sections with RCA base layers, and from 42 to 204 in/mile for sections with RAP base layers.

The FHWA document on pavement ride quality performance specifies the IRI threshold values of 95 in/mile for good ride quality and 170 in/mile for acceptable ride quality (FHWA 2008). For newly constructed HMA pavements, typical acceptable IRI values range from 52 to 66 in/mile as reported by Merritt et al. (2015). For newly constructed HMA I pavements in Wisconsin, the incentive table suggests that the acceptable average IRI values vary between 35 and 60 in/mile ($35 \leq \text{IRI} < 60$). The specifications also call for corrective action to achieve 60 in/mile when the average IRI exceeds 140 in/mile. For newly constructed HMA II pavements, the WisDOT incentive table specifies IRI be between 55 and 85 in/mile for \$0 incentive (expected range of performance). The corrective action to achieve 85 in/mile is required for HMA II pavement when IRI is greater than 140 in/mile.

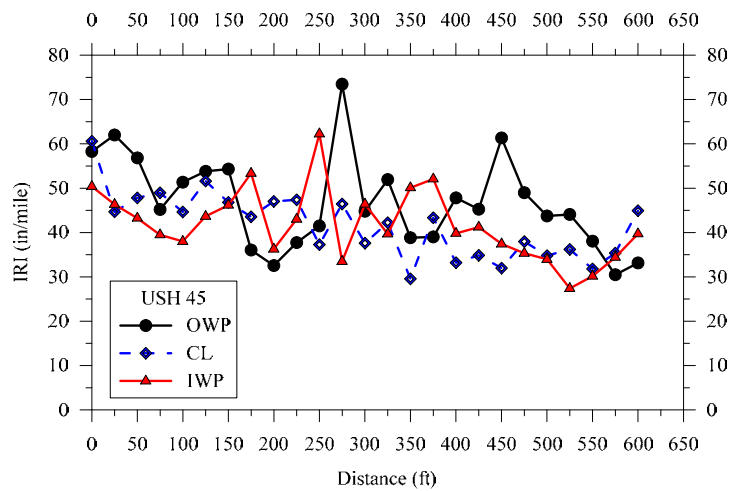
Based on WisDOT requirement to perform a corrective action for a newly constructed HMA pavement when the $\text{IRI} > 140$ in/mile, two sections with CA base layers, five sections with RCA base layers, and two sections with RAP base layers exhibited IRI values that exceeded the threshold limit of 140 in/mile.



(a) STH 59 west of Edgerton nine years after construction (CA base)

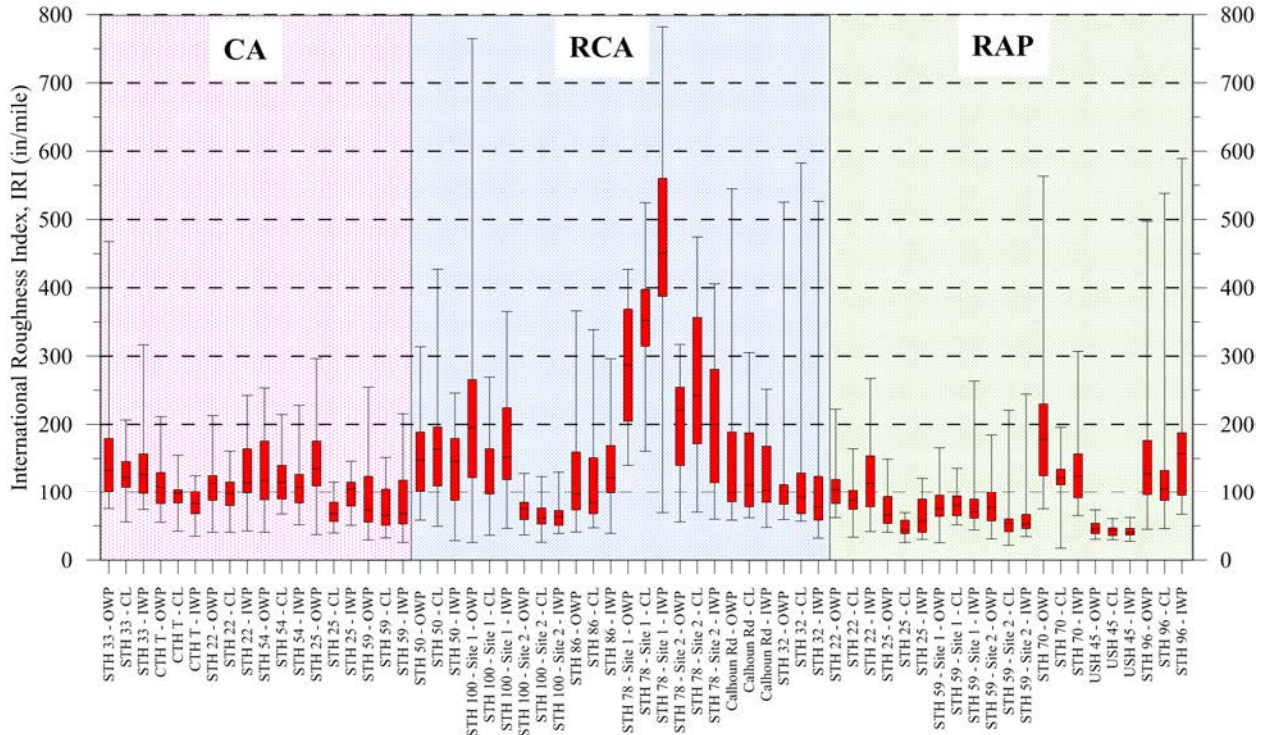


(b) STH 78 in Prairie du Sac nine years after construction (RCA base)

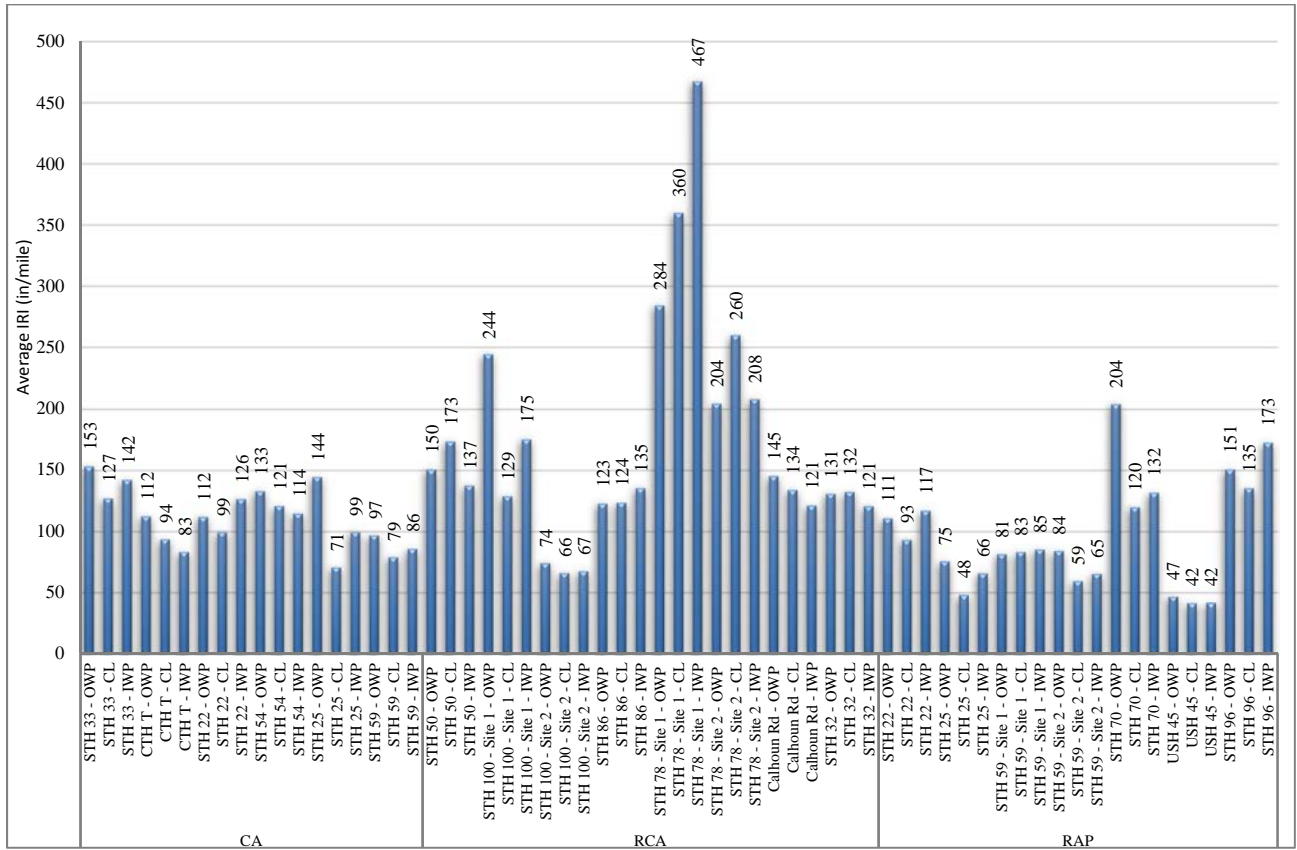


(c) USH 45 in Tigerton one year after construction (RAP base)

Figure 5.32: Pavement surface ride quality expressed as IRI and calculated based on the walking profiler measurements.



(a) Box-Whisker plot of the calculated IRI



(b) Average IRI for the 528 ft pavement test section

Figure 5.33: Variation of IRI along the 600-ft test sections.

Figure 5.34 presents the histogram and corresponding lognormal distribution for the IRI values based on the 25-ft subsections for the investigated pavement sections grouped based on the base layer material types: CA, RCA, and RAP. The average IRI for all pavement sections with CA base layers is 110.7 in/mile with COV of 46.5%. This is lower than the average IRI of 173.5 in/mile (COV of 75%) for the pavement test sections with RCA base layers. The pavement test sections with RAP base layers exhibited the smoothest ride quality with an average of 95.8 in/mile with COV of 70.1%.

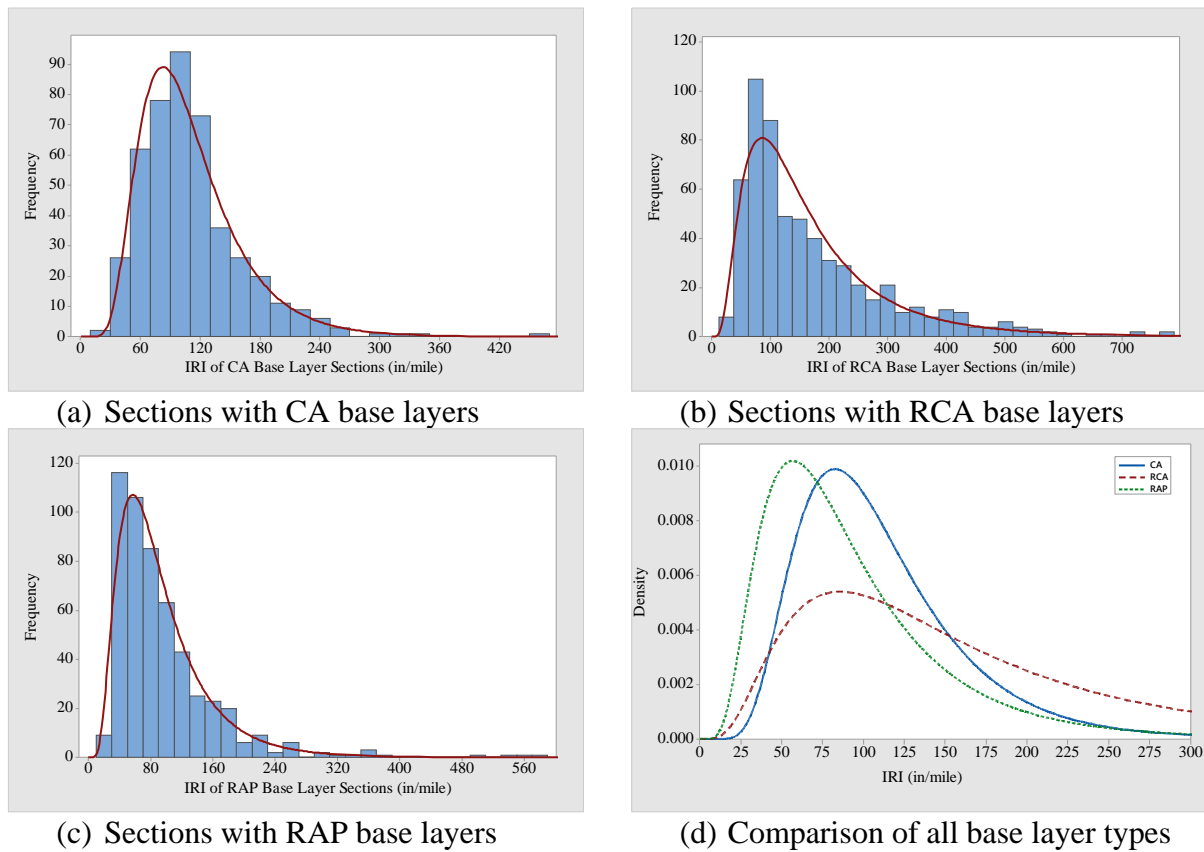


Figure 5.34: Histogram and the corresponding lognormal distribution representation of the IRI values based on the 25 ft subsection for the investigated pavement test sections with CA, RCA, and RAP base layers.

Chapter 6

Long Term Performance of HMA Pavements Constructed on Recycled Base Layers

This chapter presents the results of the analyses conducted to evaluate the long-term performance of the HMA pavements constructed on CA, RCA, and RAP base layers in Wisconsin. The data analyzed herein were obtained from laboratory and field testing by the research team, from the Pavement Data Unit of WisDOT (Pavement Inventory/Information Files - PIF), and from the archives of various other field tests conducted by the research team on HMA pavements in Wisconsin since 2009.

The objective of this chapter is to document the actual performance of existing pavements in WI based on the available NDT testing (current study and data available to the research team from previous studies and WisDOT files), pavement distress surveys, and pavement surface smoothness/ride quality evaluation.

6.1 Case Studies – CA versus RAP Base Layer

6.1.1 STH 59 West of Edgerton, Rock County

This project consists of two sections: (1) pavement section I with a RAP base layer that was reconstructed in 2009 with an original CA base layer before 2009) and (2) pavement section II with a CA base layer that was milled and resurfaced in 2009. The total length of the project is 11.7 miles of which approximately one mile has a CA base layer and the remainder has a RAP base layer. The location of the project on Google Maps is given by:

<https://www.google.com/maps/dir/42.826053,-89.3035136/42.832782,-89.0941356/@42.8379362,-89.1453492,12.7z/data=!4m9!4m8!1m5!3m4!1m2!1d-89.2770578!2d42.8315678!3s0x880637a55a8bafbf:0xcb5abece79dccac7!1m0!3e0?hl=en>

The research team conducted field work on both pavement sections in 2009, 2010, 2011, 2017, and 2018 that included visual distress surveys, FWD, GPR, and DCP test. The results of the field tests as well as the analyses conducted on pavement data obtained from WisDOT are presented herein. Figure 6.1 depicts pictures of the pavement surface condition at both test sections.

The results from the analysis of FWD tests on STH 59 pavement section I are presented in Figure 6.2. The FWD testing was conducted on a 150-ft long section with measurements taken at every 10-ft interval on both lanes (EB and WB) at right and left wheel paths. Such a testing configuration provided detailed data pertaining to pavement surface deflection and structural

capacity. Figure 6.2 indicated relatively high pavement surface deflection (with D_0 ranging approximately from 10 to 24 mils), which was expected due to the pavement surface deterioration as depicted in Figure 6.1 a. An inspection of Figure 6.2a shows higher pavement surface deflections at the pavement edges compared with the pavement centerline. The figure also shows high variability in the back-calculated E_{HMA} , E_{bas} , $E_{Subgrade}$. Figure 6.3 shows a comparison between the pavement structural capacities of section I with a CA base layer (before reconstruction in 2009) and the same section with a RAP base layer after reconstruction in 2010. The contour maps of SN_{eff} presented in Figure 6.3 (under the similar color scale) indicated higher structural capacity one year after reconstruction of the pavement with a RAP base layer (SN_{eff} from 4.1 to 6.0) compared with the same pavement section with a CA base layer (SN_{eff} from 5.6 to 7.4). It should be noted that the pavement section before reconstruction had a CA base layer of unknown age (according to WisDOT files) and the testing on the same section with a RAP base layer was conducted one year after reconstruction.

Figure 6.4 presents box-whisker plots of the pavement surface deflection and structural capacity variation with time for the CA and RAP base layer sections at STH 59 from 2009 to 2017. An examination of the figure demonstrates that (on average) the pavement section with a RAP base layer exhibited lower deflections and higher structural capacity compared with the same section before reconstruction.

The results of the long-term pavement performance analysis for STH 59 with RAP and CA base layers are presented in Figure 6.5. The results indicate that the pavement section with CA exhibited lower rutting at the left wheel path, had no longitudinal cracking, and had lower transverse cracking compared with the pavement segments with a RAP base layer. It should be noted that, for all segments (CA and RAP), rut depth was less than 0.2 in. In general, the performance of the pavement segments with CA and RAP base layers are comparable with IRI values less than 90 in/mile (except for the pavement segment 80780 with a RAP base that exhibited high IRI values).

The change in pavement performance indicators with time is depicted in Figures 6.6 and 6.7. The PCI variation for the pavement segments is depicted in Figure 6.6a, showing good performance level for all segments with PCI greater than 70%. The change in the average PCI for each pavement section (CA and RAP base layer sections) is depicted in Figure 6.6b with a comparably good performance, noticing that the CA base has a slightly higher average PCI. The average increase in IRI with time is comparable for both pavement sections, while the pavement section with RAP exhibited slightly higher rutting but less than an average of 0.18 inch as presented in Figure 6.7. The analysis of STH 59 pavement performance data shows that, on average, the pavement segment with a CA base layer slightly outperformed the pavement segments with a RAP base layer; however, both pavement sections can be given a good performance rating.



(a) Pavement section I with CA base layer in 2009 before mill and relay



(b) Pavement section II with CA base layer in 2009 before mill and overlay



(c) Mill and relay in 2009

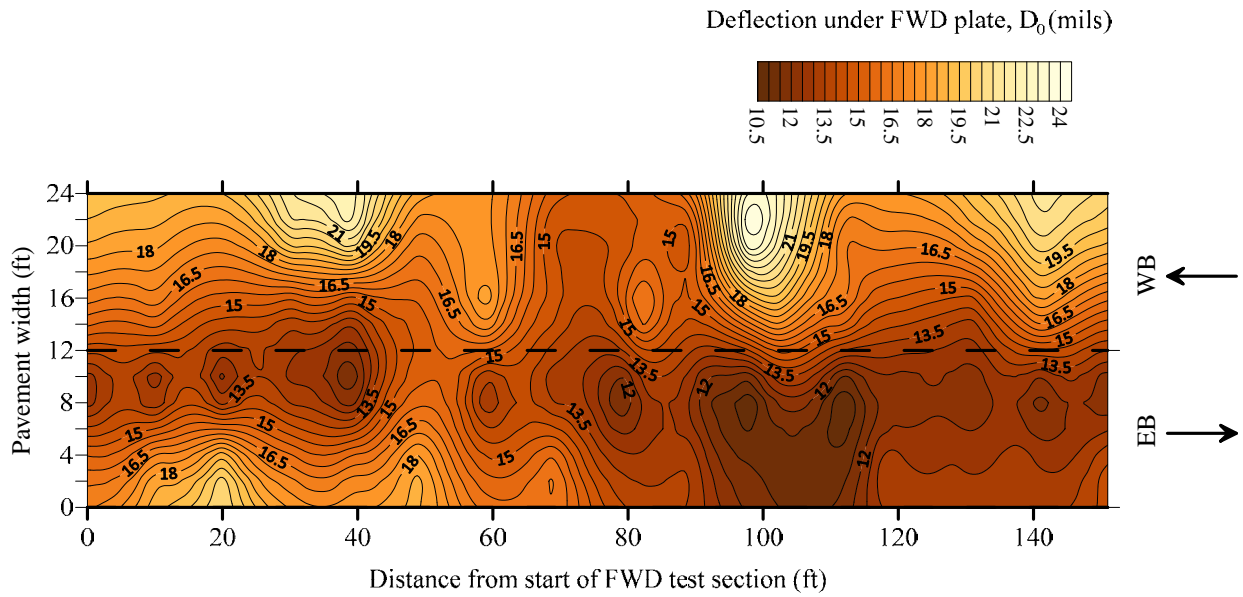


(e) Longitudinal cracking in RAP base layer section in 2018

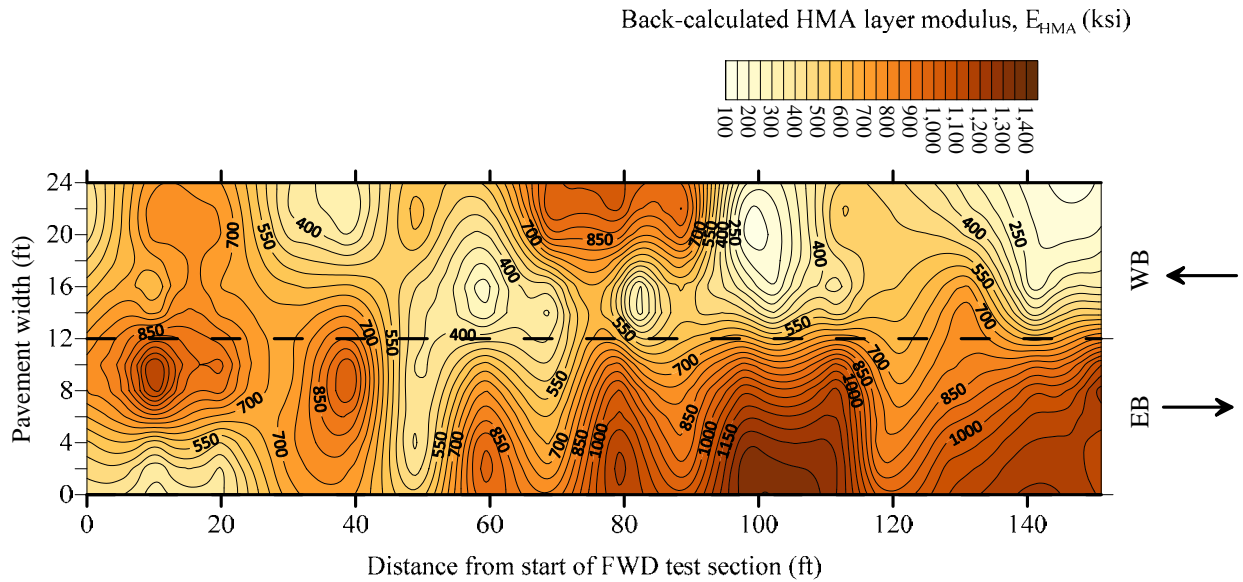


(d) Transvers cracking in 2011 in pavement section II with CA base layer section

Figure 6.1: STH 59 pavement sections with RAP and CA base layers in 2009 before reconstruction and in 2011 and 2018 after reconstruction.

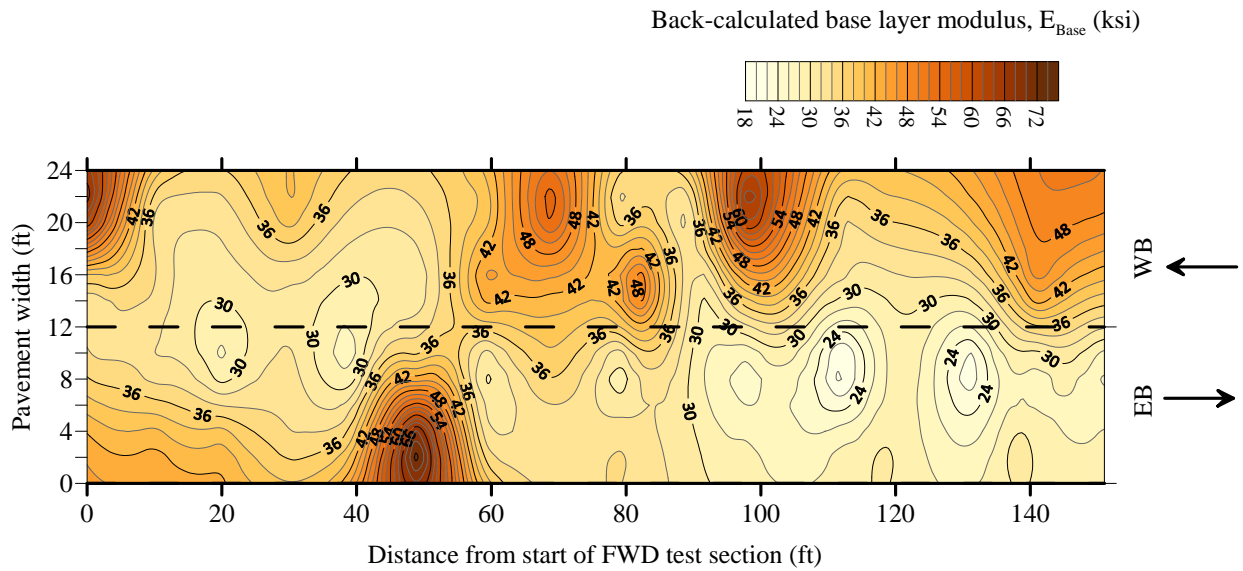


(a) Adjusted normalized deflection under FWD plate

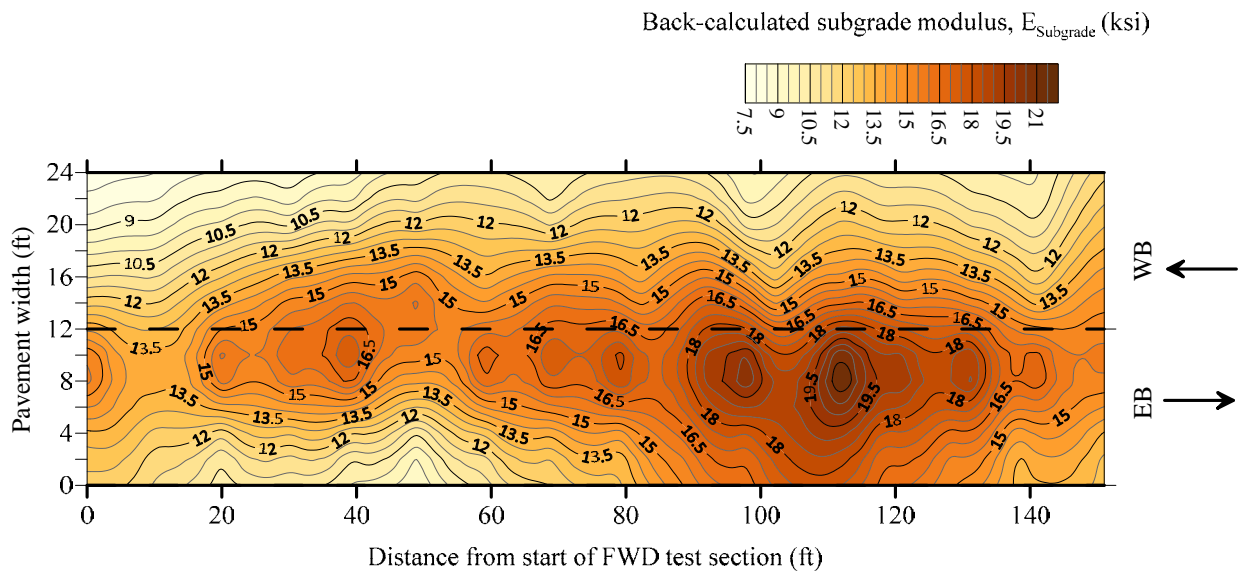


(b) Back-calculated HMA layer modulus

Figure 6.2: Results of FWD test conducted in 2009 on STH 59 pavement section I (pictured in Figure 6.1 a) with crushed aggregate base just before milling and relay of the 5-inch-thick HMA layer.

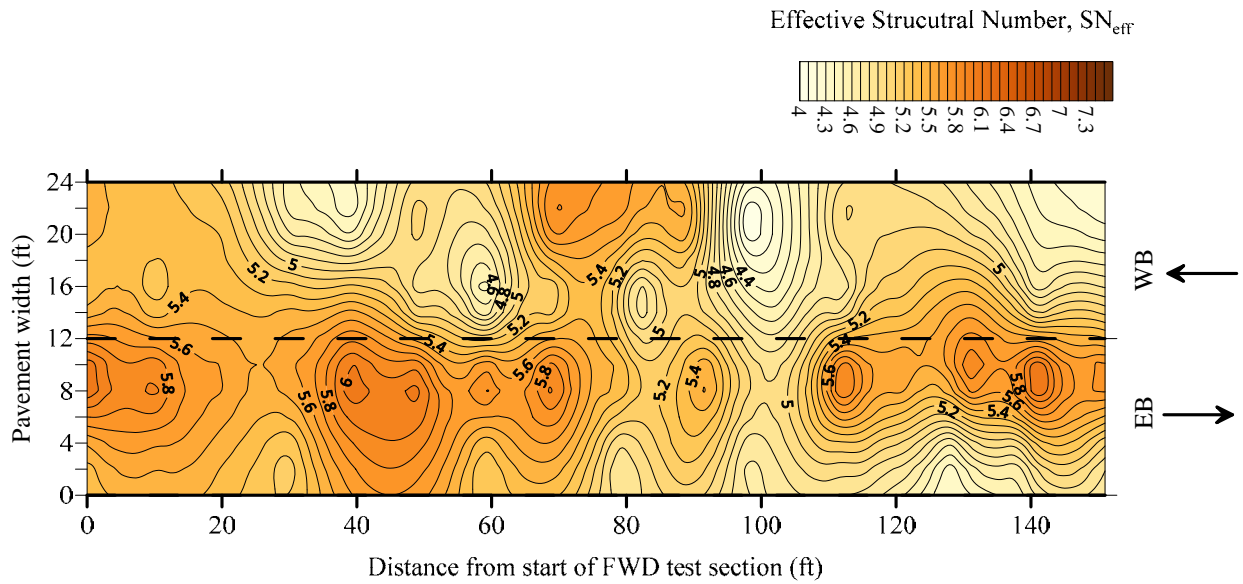


(c) Back-calculated HMA layer modulus

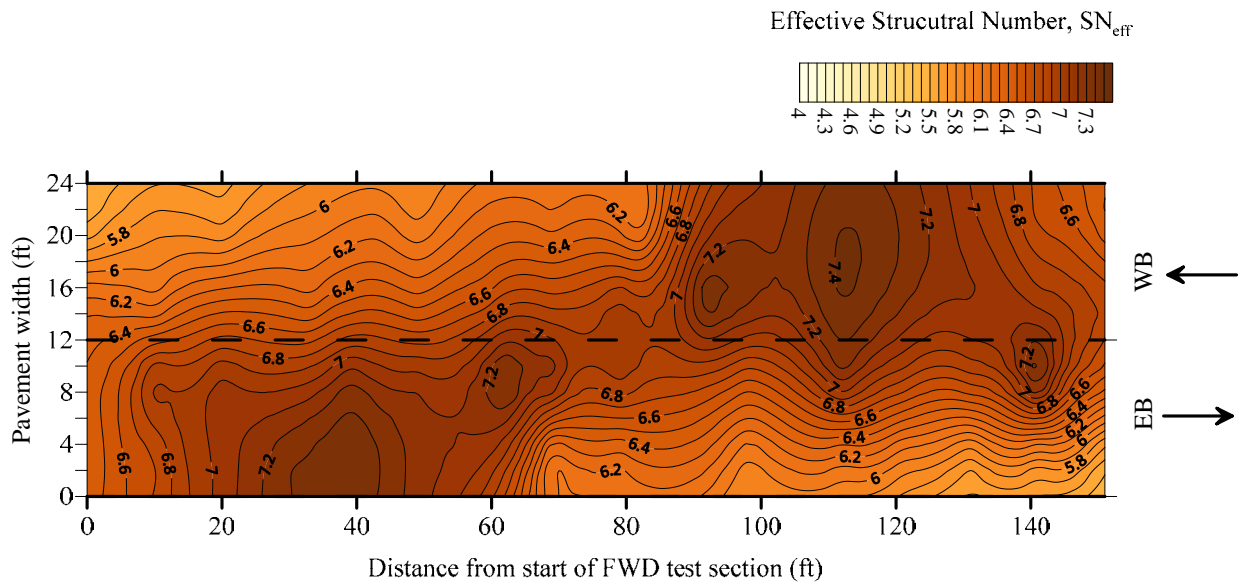


(d) Back-calculated subgrade modulus

Figure 6.2 (Cont.): Results of FWD test conducted in 2009 on STH 59 with crushed aggregate base just before milling and relay of the 5-inch-thick HMA layer.



(a) Structural capacity of pavement section I in 2009 when the base was CA



(b) Structural capacity of section I in 2010 when the base was reconstructed into RAP

Figure 6.3: Comparison of structural capacity of pavement section I on STH 59 before reconstruction (pavement had a CA base layer in 2009) and one year after reconstruction (RAP base layer – mill and relay 2009).

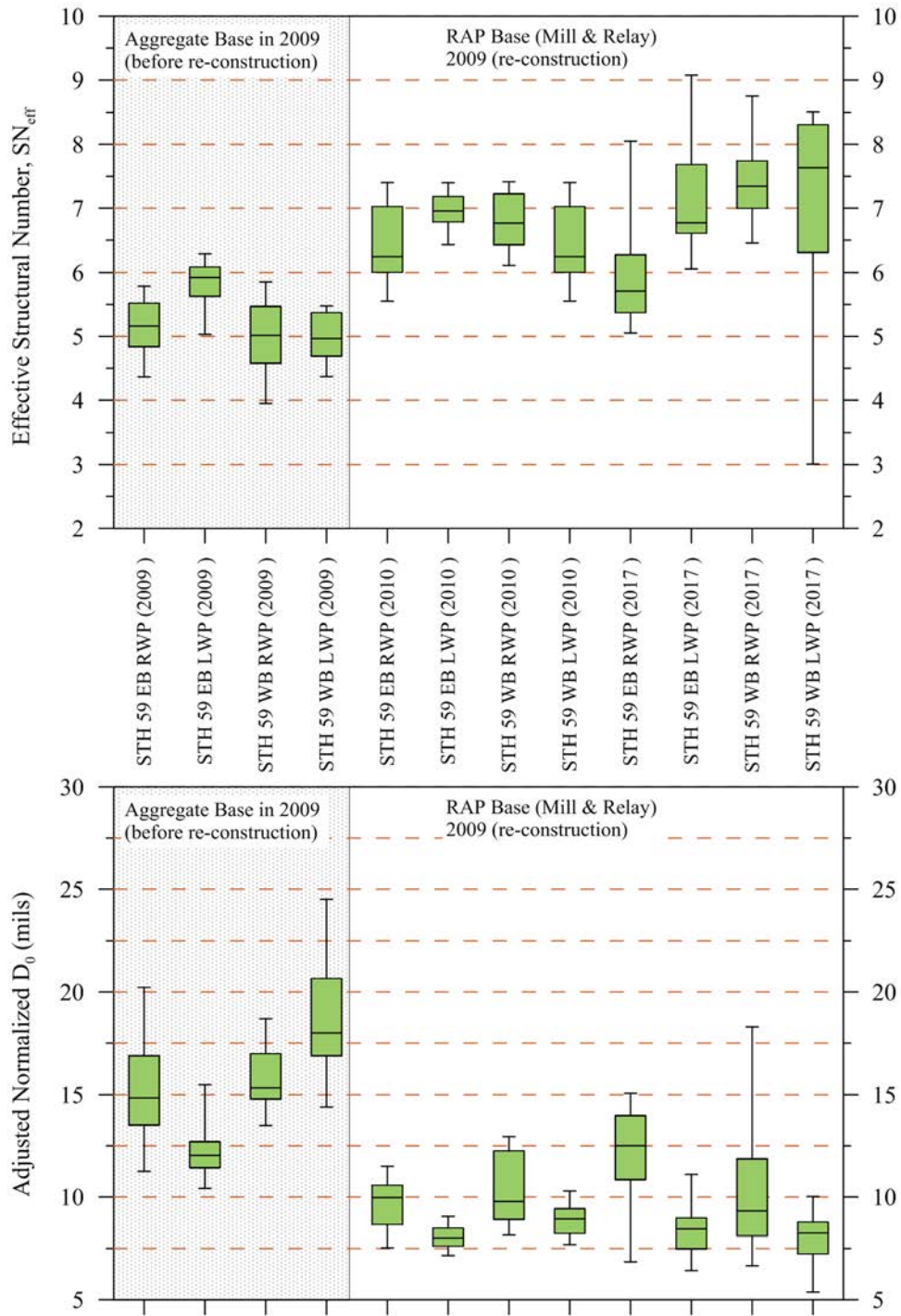
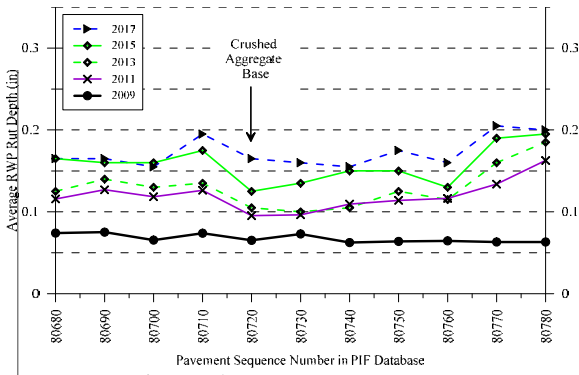
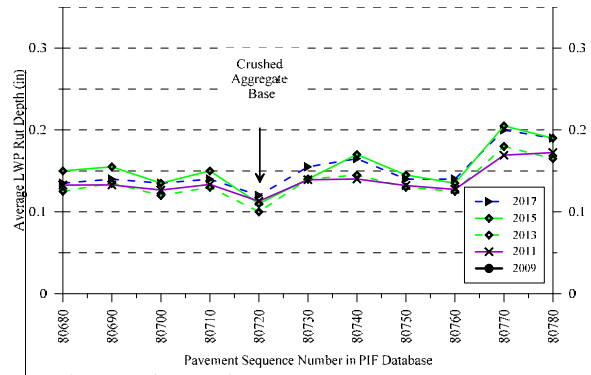


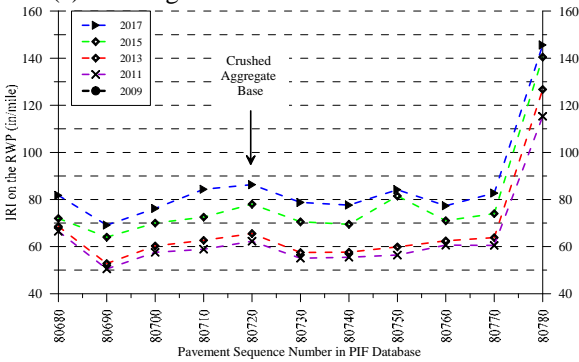
Figure 6.4: Pavement structural capacity and surface deflection for STH 59 with a CA base layer before re-construction to a RAP base layer.



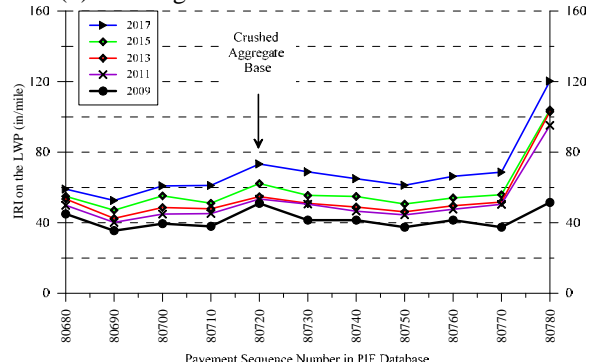
(a) Rutting at the RWP



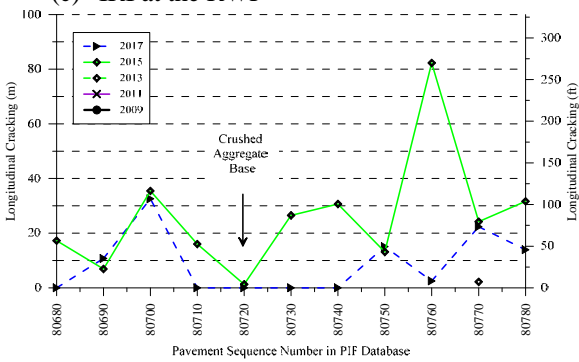
(b) Rutting at the LWP



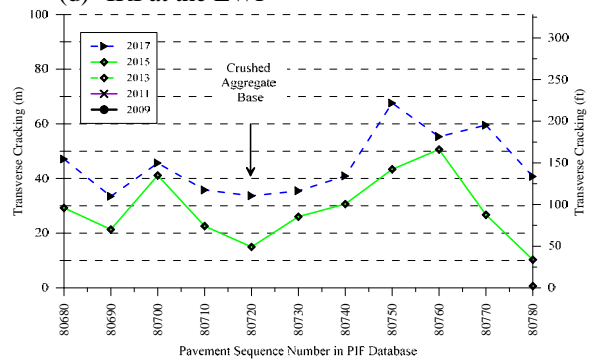
(c) IRI at the RWP



(d) IRI at the LWP

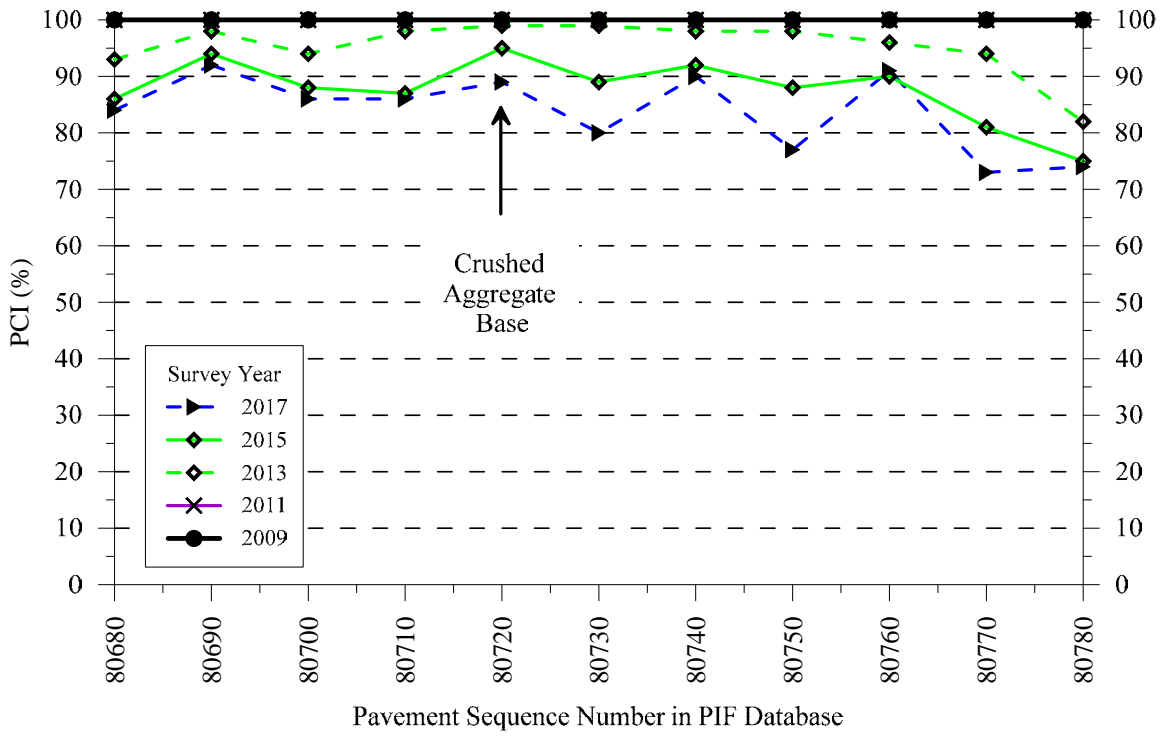


(e) Longitudinal cracking

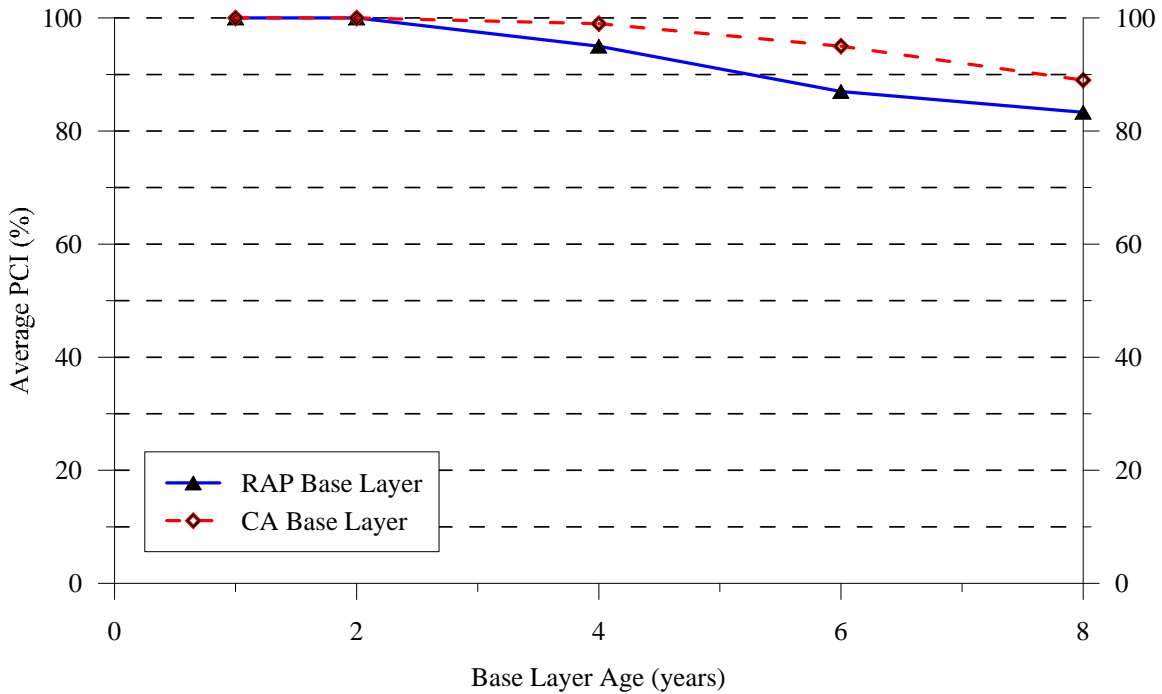


(f) Transverse cracking

Figure 6.5: Comparison of rutting, ride quality and cracking performance for STH 59 segments with CA and RAP base layers.

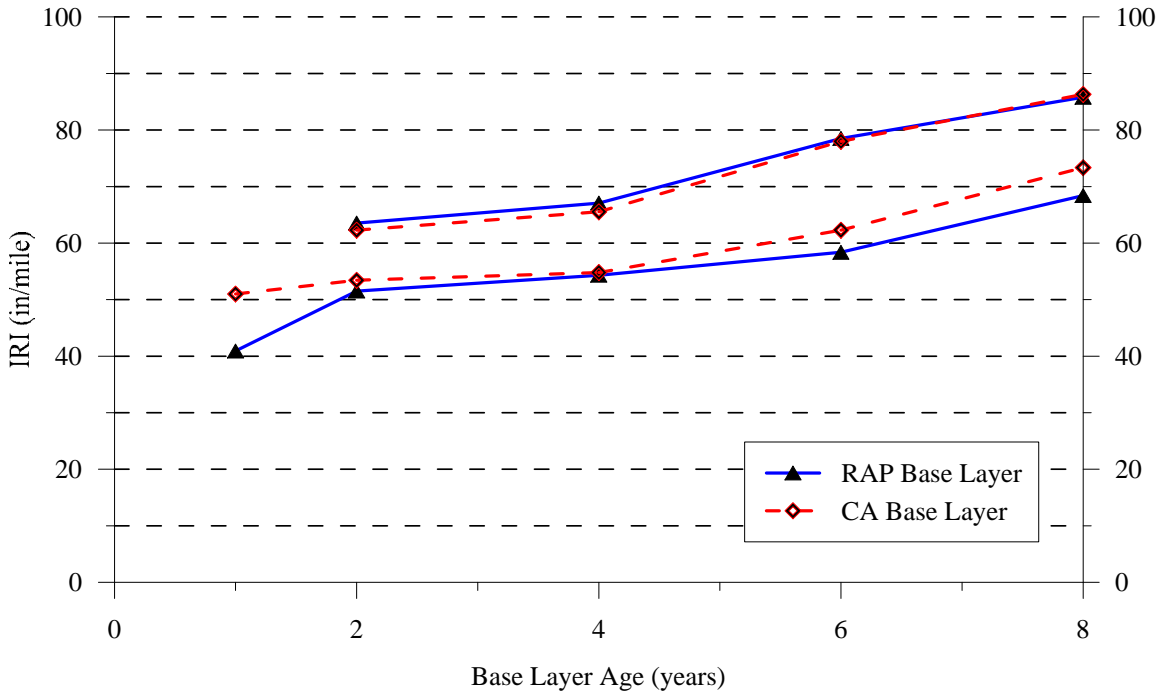


(a) Average PCI for all segments over the pavement life

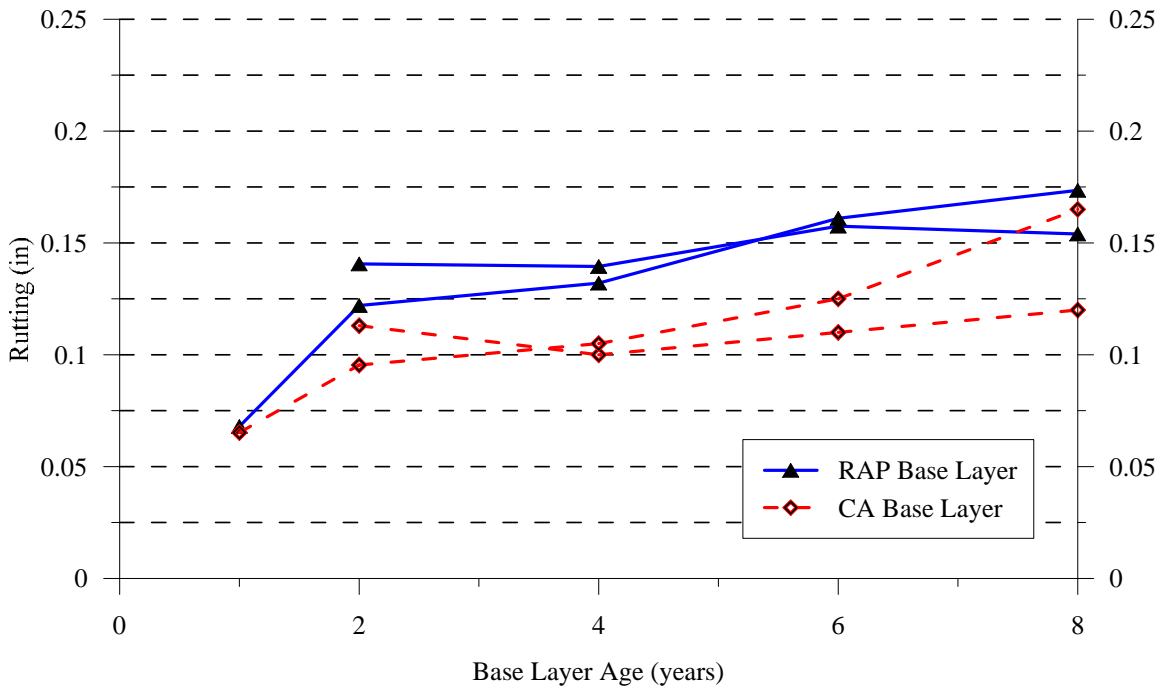


(b) Overall average of PCI segments with CA and RAP base layers over the pavement life

Figure 6.6: Comparison of average PCI variation with time for the HMA pavement segments of STH 59 constructed on CA and RAP base layers.



(a) Ride quality – International Roughness Index, IRI(in/mile) versus age



(b) Rutting versus pavement age

Figure 6.7: Comparison of average IRI and rutting for the STH 59 segments with CA and RAP base layers.

6.1.2 STH 25 near Maxville, Buffalo County

The pavement test section at STH 25 near Maxville in Buffalo County consists of 11.7 miles with a RAP base course layer and one 2,394-ft-long section with a crushed stone aggregate base built in 2004. A comparison of pavement test sections on STH 25 provides an excellent example since both CA and RAP sections have similar climatic condition, age, subgrade, traffic, etc. The exact locations of the pavement sections are shown below in Figure 6.8 and given by the following Google Maps links:

<https://www.google.com/maps/place/WI-25,+Durand,+WI+54736/@44.5181844,-91.9977896,11.3z/data=!4m16!1m10!4m9!1m3!2m2!1d-92.019258!2d44.4341553!1m3!2m2!1d-91.999482!2d44.5967227!3e0!3m4!1s0x87f844bba929b209:0x5426d524bd144745!8m2!3d44.595896!4d-92.0007417?hl=en>

<https://www.google.com/maps/place/WI-25,+Durand,+WI+54736/@44.5181844,-91.9977896,11.3z/data=!4m16!1m10!4m9!1m3!2m2!1d-92.019258!2d44.4341553!1m3!2m2!1d-91.999482!2d44.5967227!3e0!3m4!1s0x87f844bba929b209:0x5426d524bd144745!8m2!3d44.595896!4d-92.0007417?hl=en>

<https://www.google.com/maps/place/Maxville/@44.5623556,-92.0149591,15.4z/data=!4m16!1m10!4m9!1m3!2m2!1d-92.0090266!2d44.5680053!1m3!2m2!1d-92.0085907!2d44.5614712!3e0!3m4!1s0x87f84526faae02f7:0xd296d5110530d982!8m2!3d44.5674679!4d-92.0009794?hl=en>

The results of the laboratory tests on base layer materials (CA and RAP) and field tests on pavement sections were given and discussed earlier. The particle size distribution showed that the STH 25 CA materials had higher gravel size and fines fractions and lower sand size fraction than STH 25 RAP materials. The CA materials showed an average mass loss of 18.8% in a Micro-Deval abrasion test and an average absorption of 2.91%. The average absorption for the RAP material was 2.3%. A Micro-Deval test was not conducted on the RAP base materials.

The strength and modulus characterization showed that the CA base layer had higher values compared with the corresponding values for the RAP section. The average predicted CBR (by DCP test) for the CA layer was 90.1% with a layer modulus of 45.5 ksi with corresponding values of 75.3% and 40.3 ksi for the RAP layer. On the other hand, the pavement section with the RAP base layer had a lower average D_0 (8.7 mils) and higher average SN_{eff} (6.3) compared with average D_0 of 9.5 mils and SN_{eff} of 5.6 for the CA section. These results are consistent with the back-calculated base layer modulus where the average E_{base} was 79.5 ksi for the RAP base and 44 ksi for the CA base layer. The test section with the CA base showed significant fatigue cracking, resulting in an average PCI of 29% compared with 74% for the test RAP section. The same trend was observed when calculating the IRI from the walking profiles on both test sections with an average IRI of 104.6 in/mile for the CA base layer section and 63 in/mile for the RAP base layer section.

The long-term pavement performance evaluated herein is based on data collected by WisDOT pavement data unit and analyzed by the research team; data include pavement surface

condition (PCI), ride quality/smoothness of ride (IRI), rutting, and cracking (fatigue, longitudinal, transverse, edge, and block cracking).

Figure 6.9 depicted the performance of pavement segments (sequences in PIF database) with age showing the CA and RAP base layer segments. A chip seal treatment was applied in 2017 (at pavement age of 13 years) that neither improved the ride quality nor reduced the rutting of the right wheel path for all RAP and CA base layer segments at the time of measurement, as shown in Figure 6.9. An inspection of the pavement performance indicators in Figure 6.9 shows that the pavement segment with a CA base layer (29140) had a comparable performance with the RAP base layer segments (29130, 29150, and 29160) located within close proximity, but outperformed the other segments located at the beginning of the pavement project. Figure 6.10 summarizes all pavement surface distress indices in the PCI value indicating the overall pavement surface condition. The pavement performance indicators that change with time are depicted in Figures 6.10 and 6.11. This figure shows that the pavement segment with a CA base layer outperformed the pavement segments with a RAP base layer on average; however, the difference is not very significant. It should be noted that there is only one pavement segment with a CA base layer that is approximately 0.5 mile in length compared with about 11 miles of pavement with a RAP base layer. Based on the visual observation along the total length of the project, the research team believes that the pavement with the RAP base showed good performance comparable with the CA base, if not better, when considering the 528 ft section of the CA base layer surveyed (see pictures of test sections of STH 25 with the CA base layer in Figures 5.26-5.28 in Chapter 5).

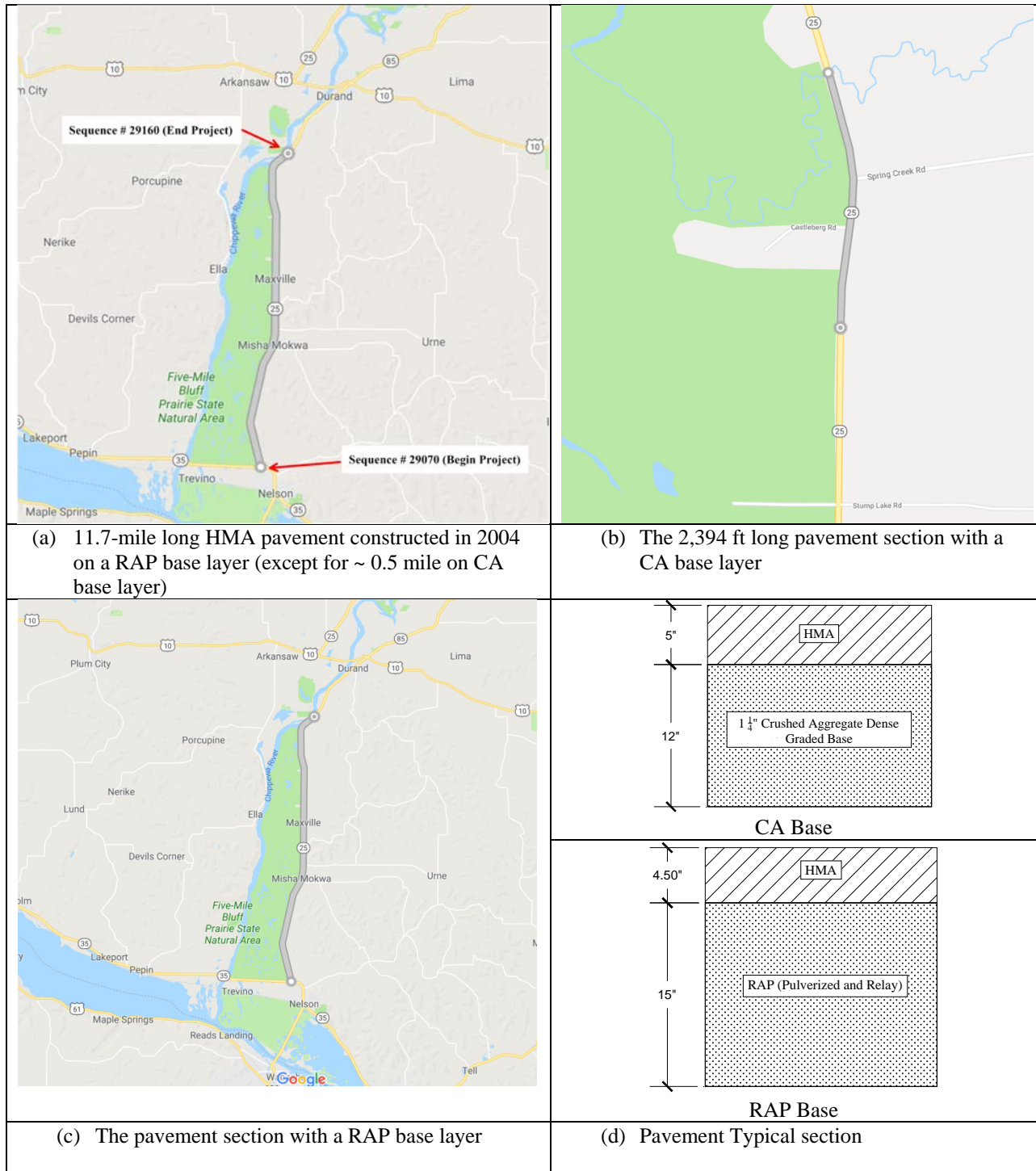


Figure 6.8: Pavement test sections at STH 25 near Maxville.

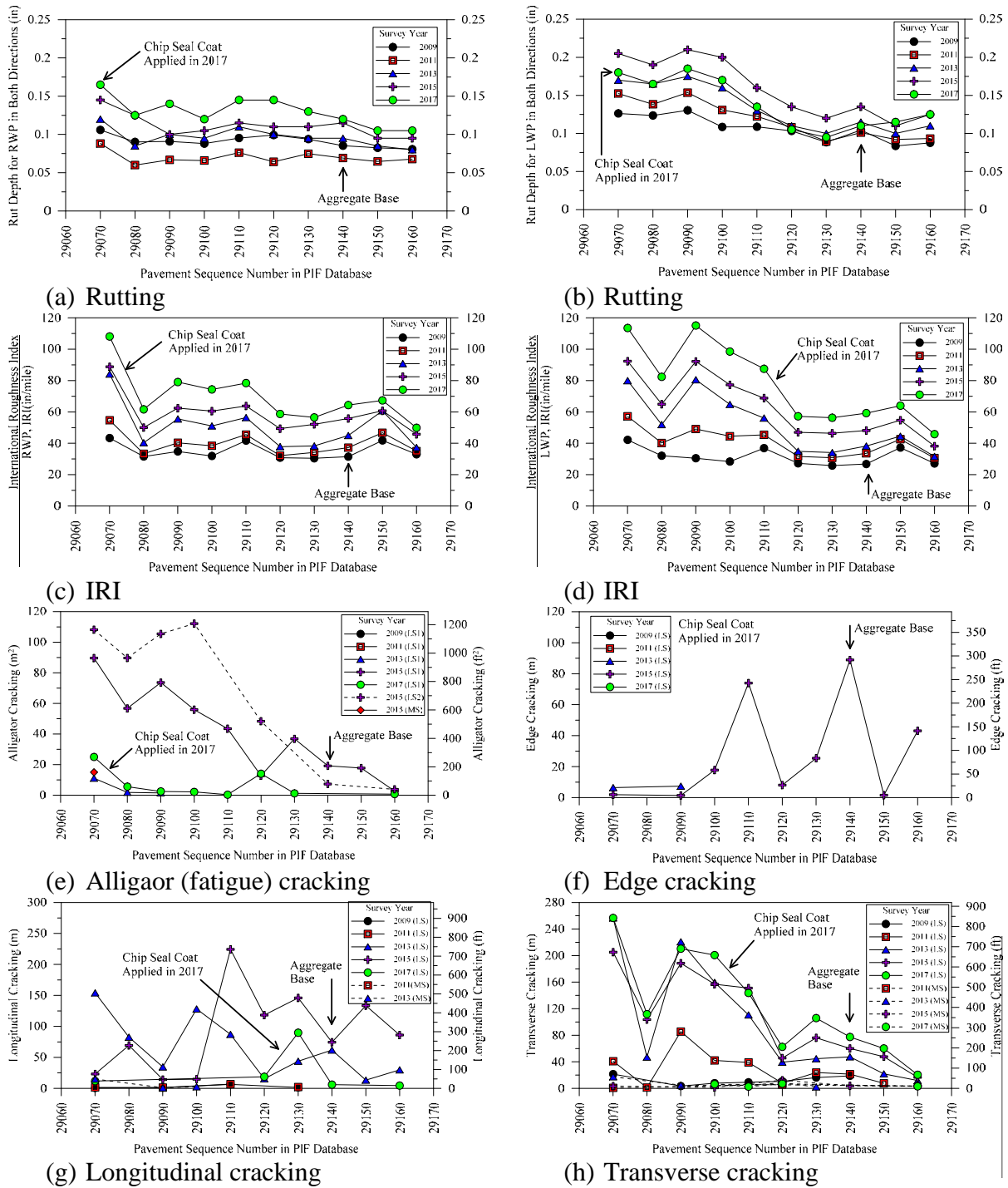
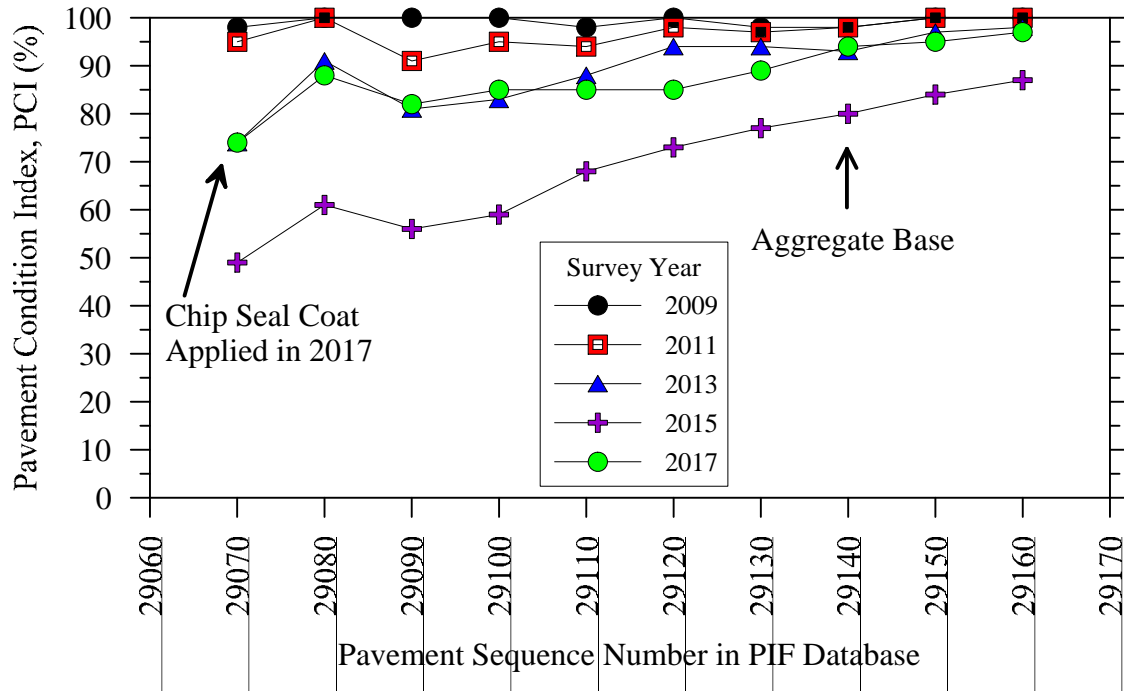
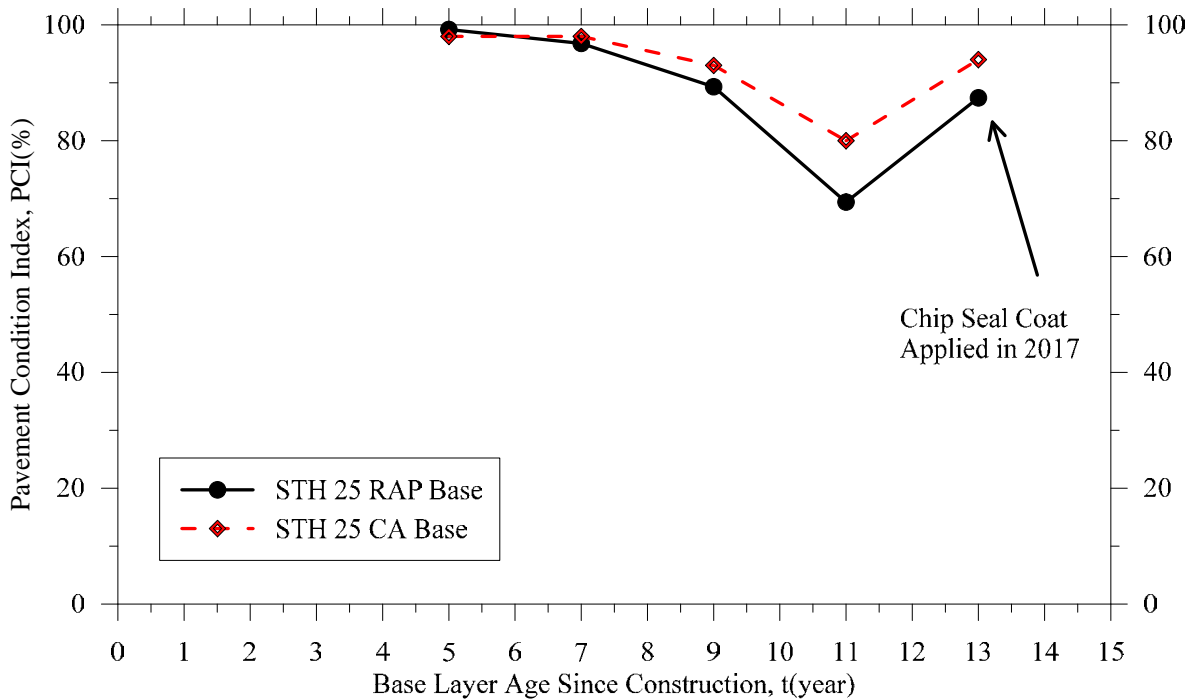


Figure 6.9: Comparison of ride quality and cracking performance for STH 25 segments with CA and RAP base layers.

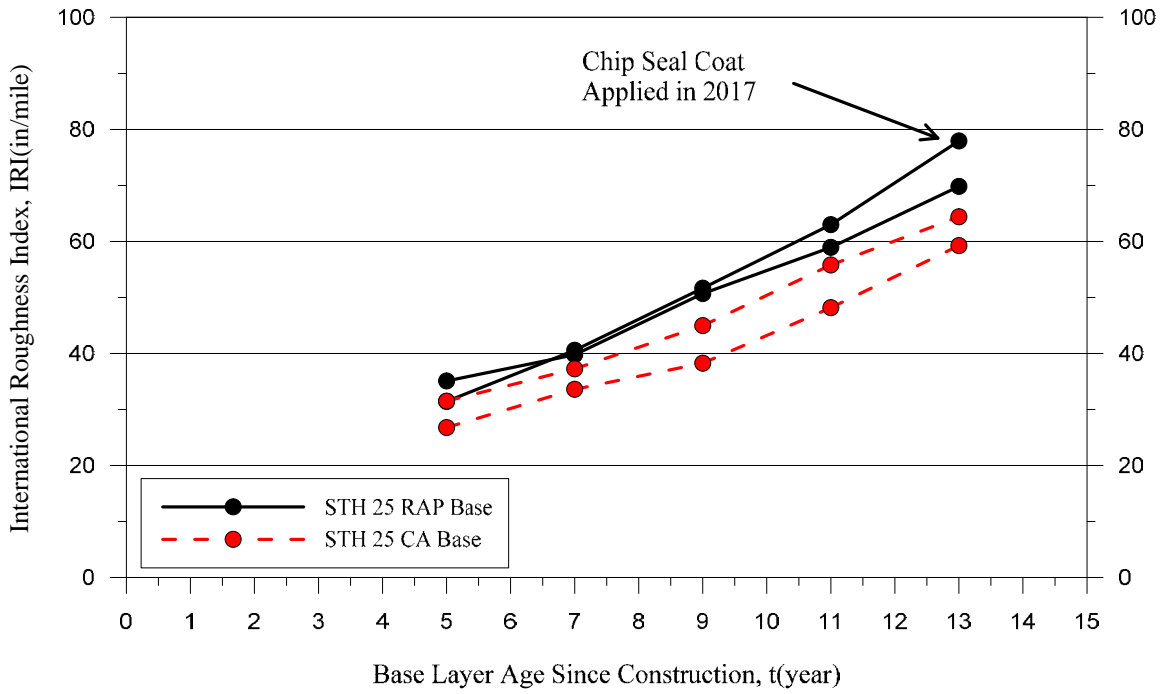


(a) PCI average per segment

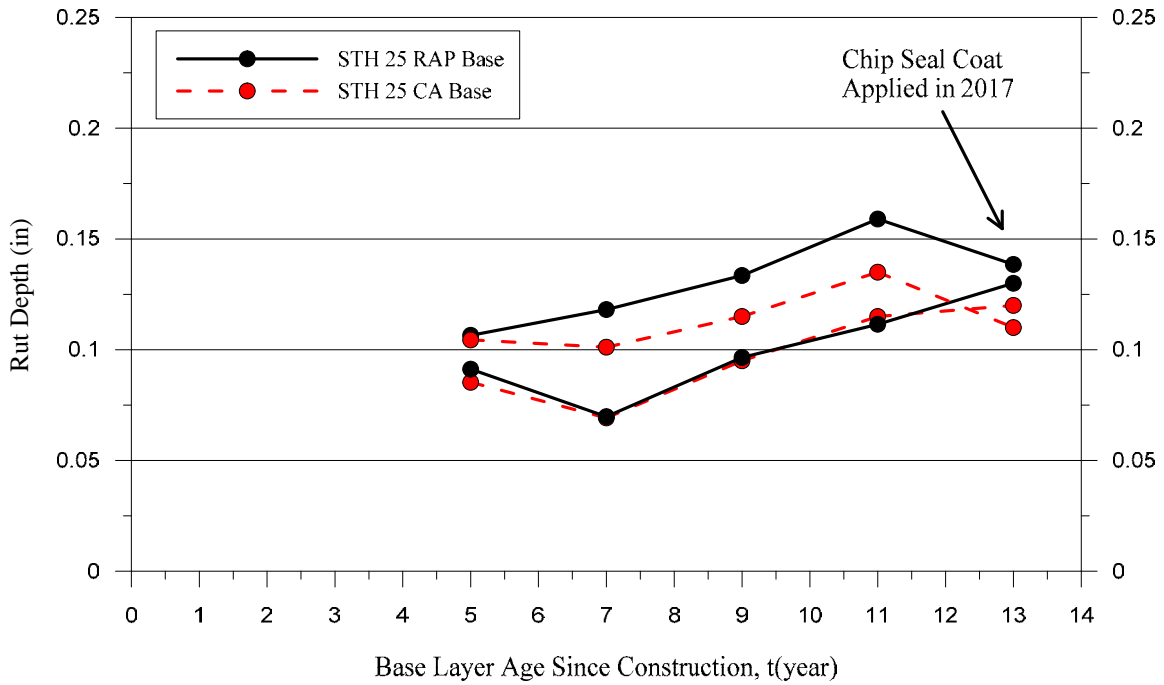


(b) PCI average versus age

Figure 6.10: Comparison of average PCI for the STH 25 segments with CA and RAP base layers.



(a) Ride quality – International Roughness Index, IRI(in/mile) versus age



(b) Rutting versus pavement age

Figure 6.11: Comparison of average IRI and rutting for the STH 25 segments with CA and RAP base layers.

6.1.2 STH 77 near Webb Lake, Burnett County

The flexible pavement segments of STH 77 near Webb Lake consist of two parts: a 9.2-mile segment with 4.5 in a HMA surface layer constructed on 6 in a RAP base layer followed (on the east direction) by a 4.6-mile pavement segment with a 5 in thick HMA surface layer constructed on a 10-in dense graded CA base layer. The project consisted of pavement reconstruction of CA base layer segments in the year 2011 followed by the reconstruction of the pavement with a RAP base layer in the year 2012. The exact locations of the pavement sections are given by the following Google Maps links:

STH 77 with a CA base layer:

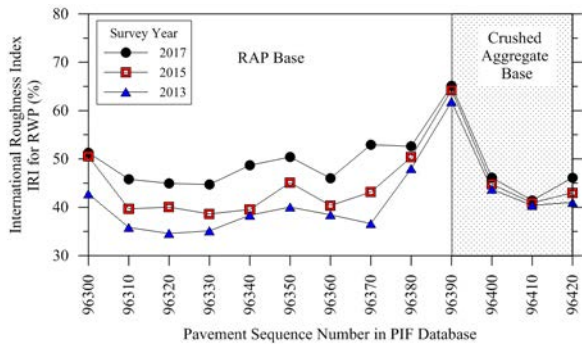
<https://www.google.com/maps/dir/46.03084,-92.1642833/46.036542,-92.0707264/@46.0138531,-92.1900952,12.6z/data=!4m2!4m1!3e0?hl=en>

STH 77 with a RAP base layer:

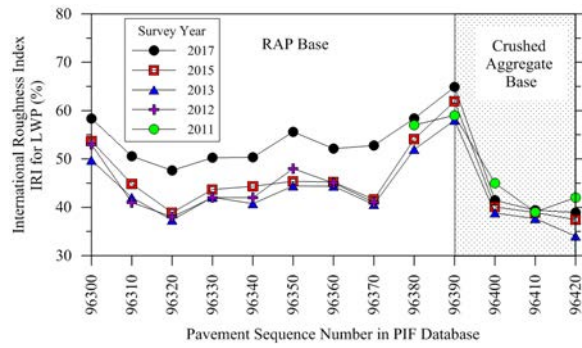
<https://www.google.com/maps/dir/46.03084,-92.1642833/46.0274091,-92.3305107/@46.0096718,-92.2025148,12.3z/data=!4m2!4m1!3e0?hl=en>

The long-term pavement performance indicators in terms of ride quality, cracking, and rutting are depicted for pavement segments with both CA and RAP base layers in Figure 6.12. Generally, both pavement types performed well since they are relatively newly constructed and showed insignificant rutting and good ride quality. However, the pavement segments with a RAP base layer developed a fair amount of longitudinal and transverse cracking compared with the pavement segments constructed on a CA base layer. The variation of the average PCI for the pavement segments over the life of the pavement is depicted in Figure 6.13. Inspection of the figure indicates the good performance of the pavement segments constructed on a CA base layer; however, the average PCI values for the pavement segments with a RAP base layer still falls within the good range of PCI.

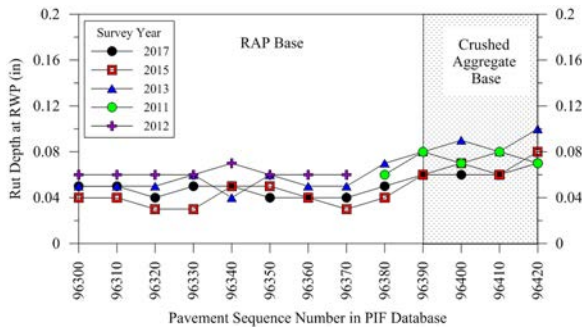
Figure 6.14 depicts comparisons of average IRI and rutting for the STH 77 segments with CA and RAP base layers. Inspection of the plots in the figure shows that the pavement sections on Ca and RAP base layers have comparable ride quality that is considered very good and very small measured rutting that considered insignificant. It should be noted that the research team noticed a fair volume of logging trucks using this route.



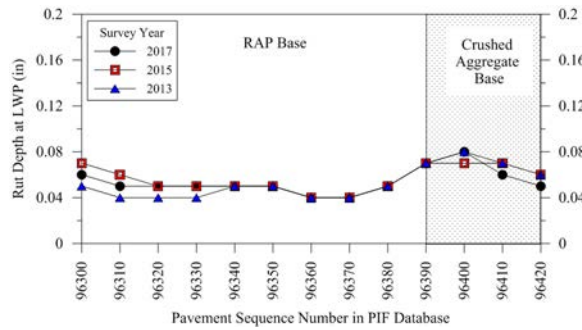
(a) Ride Quality of the RWP



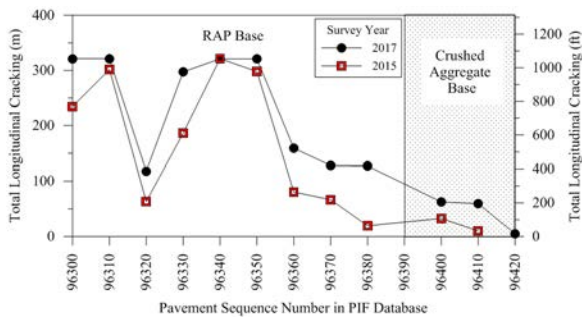
(b) Ride Quality of the LWP



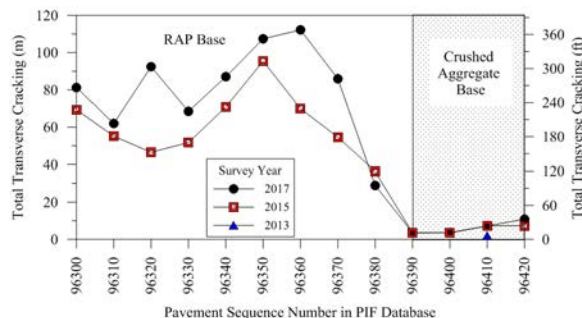
(c) Rutting at the RWP



(d) Rutting at the LWP

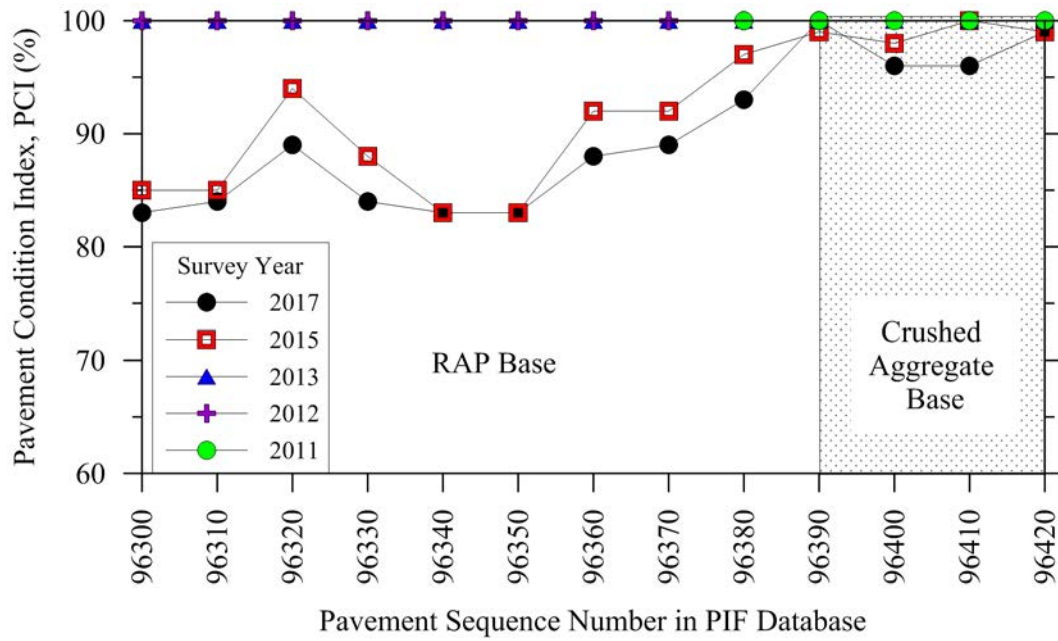


(e) Total longitudinal cracks (low severity)

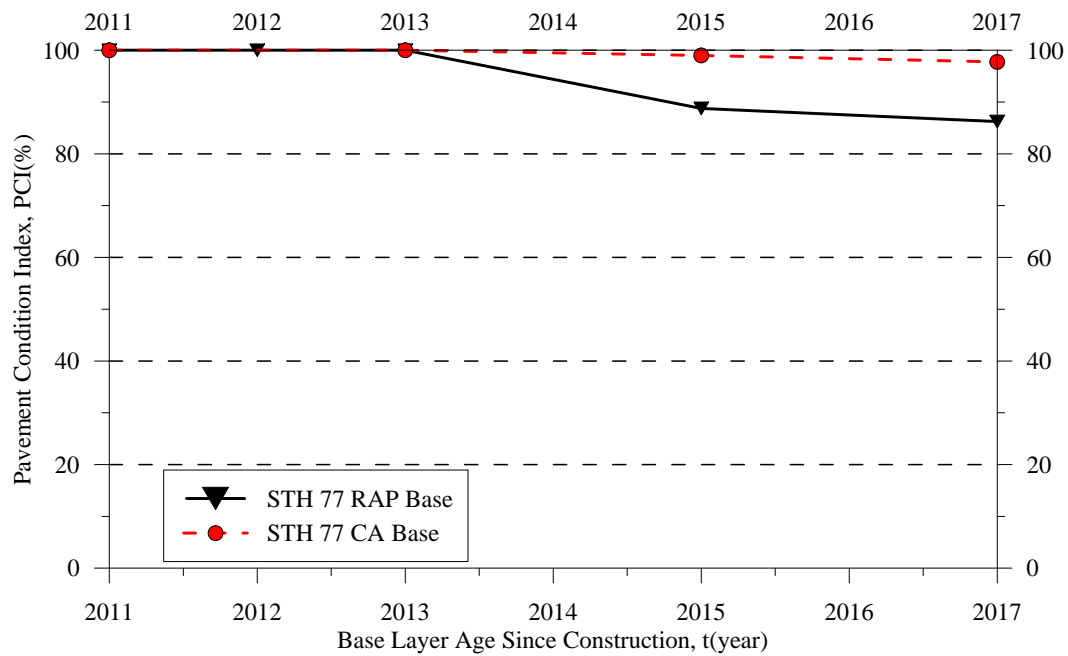


(f) Total transverse cracks (low severity)

Figure 6.12: Comparison of ride quality and cracking performance for STH 77 segments with CA and RAP base layers (segments constructed on CA and RAP base layers in the years 2011 and 2012, respectively).

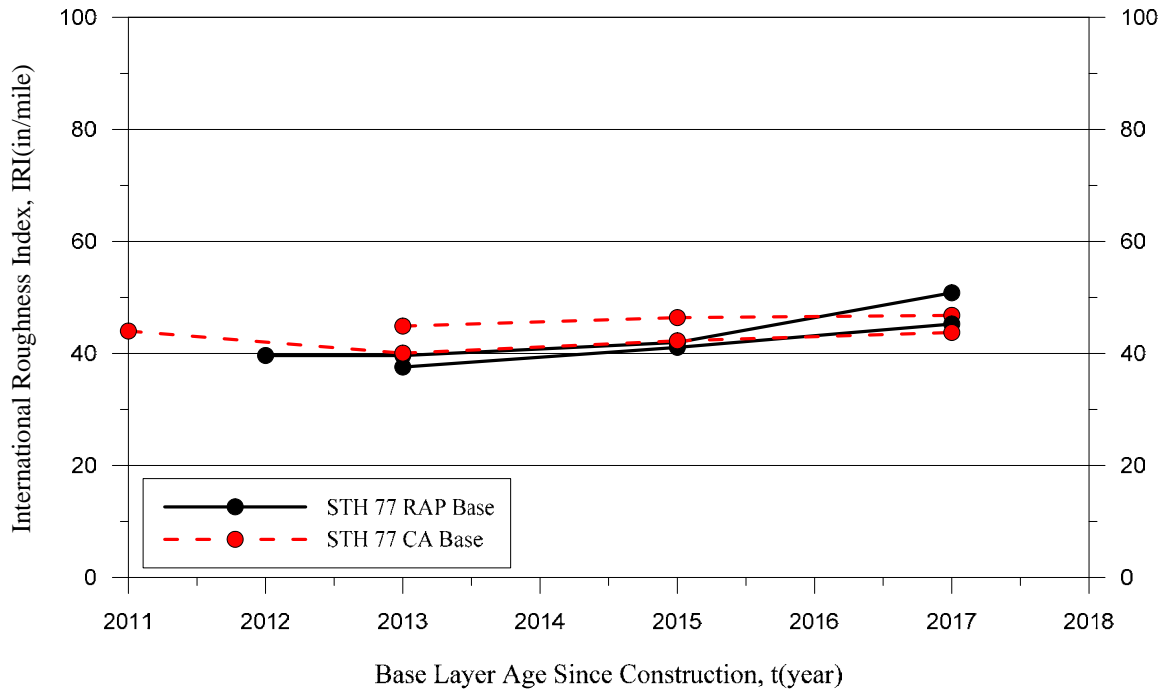


(a) Average PCI for all segments over the pavement life

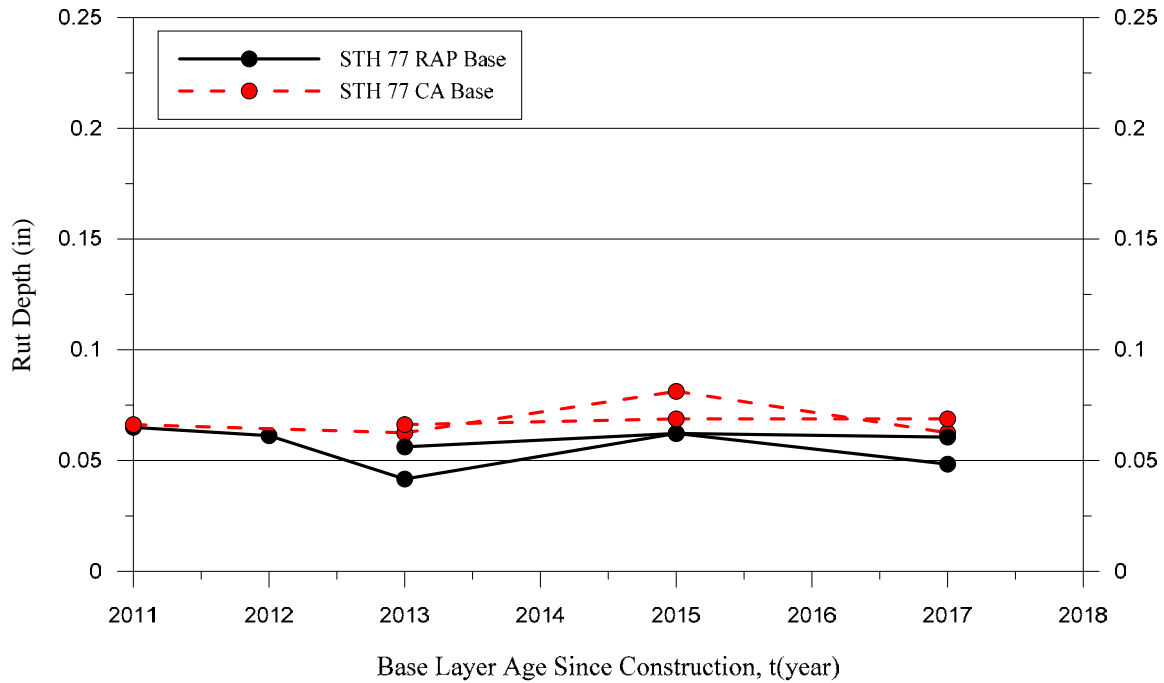


(b) Overall average of PCI segments with CA and RAP base layers over the pavement life

Figure 6.13: Comparison of average PCI variation with time for the HMA pavement segments of STH 77 constructed on CA and RAP base layers in the years 2011 and 2012.



(a) Ride quality – International Roughness Index, IRI(in/mile) versus age



(b) Rutting versus pavement age

Figure 6.14: Comparison of average IRI and rutting for the STH 77 segments with CA and RAP base layers.

6.2 Case Studies – HMA Pavement with RCA Base Layer

6.2.1 STH 78 from Prairie du Sac to Merrimac

Details of this project were presented in Chapter 4. Figure 6.15 presents the pavement performance indicators over the length of the project. An inspection of the figure indicates that the pavement surface deteriorated at a very high rate in the past few years with a significant amount of longitudinal and transverse cracking as well as a decrease in ride quality, demonstrated by the high increase in the IRI values. The change in the pavement condition index along the project length as well as the variation of the average PCI with time for the whole project are presented in Figure 6.16. The decrease in the PCI index is generally uniform for the length of the project with values greater than 60%. However, the significant decline in the ride quality with time depicted in Figure 6.17 with an average of 140 in/mile measured in 2017 (the IRI measured by the research team in 2018 using the walking profiler ranged from 204 to 467 in/mile) coupled with the average values of the PCI shows the poor performance rating for this pavement. Figure 6.17 depicts the variation of the average rutting with time, which remained constant with time with a rut depth less than 0.15 in.

6.3 Comparisons of All Investigated Pavement Sections

The results of the analysis of the PIF database pertaining to all investigated pavement sections with CA, RCA, and RAP base layers are presented in Figures 6.18-6.24. The RCA base layer pavement sections' performance indicators are compared in Figure 6.18. The performance of all investigated pavement sections with RCA indicated different performances. Pavement sections at STH 86 and STH 50 exhibited the highest IRI while the pavement section at STH 78 had the lowest PCI rating.

An inspection of the data in Figures 6.20 to 6.24 indicated that the PCI variation with time did not show a clear trend among the pavement test sections with CA, RCA, and RAP base layers. However, a pavement section with a CA base layer exhibited the lowest PCI rating 20 years after construction. The ride quality data demonstrated that the base sections with RAP base layers performed better compared with the pavement sections with RCA and CA base layers. Regarding the average rutting, the pavement sections with RCA base layers exhibited the lowest rut depth at a younger age while the sections with RAP base materials exhibited the highest rut depth. Alligator (fatigue) cracking was observed in higher quantities in pavement sections with RAP and CA base materials compared with the sections with RCA base layers. Transverse cracking occurred more often in pavement sections with RAP base layers at an older age compared with pavement sections with RCA base materials. Longitudinal cracking was more visible in the pavement sections with RCA base layers at a younger age compared with pavement sections with CA and RAP base layers.

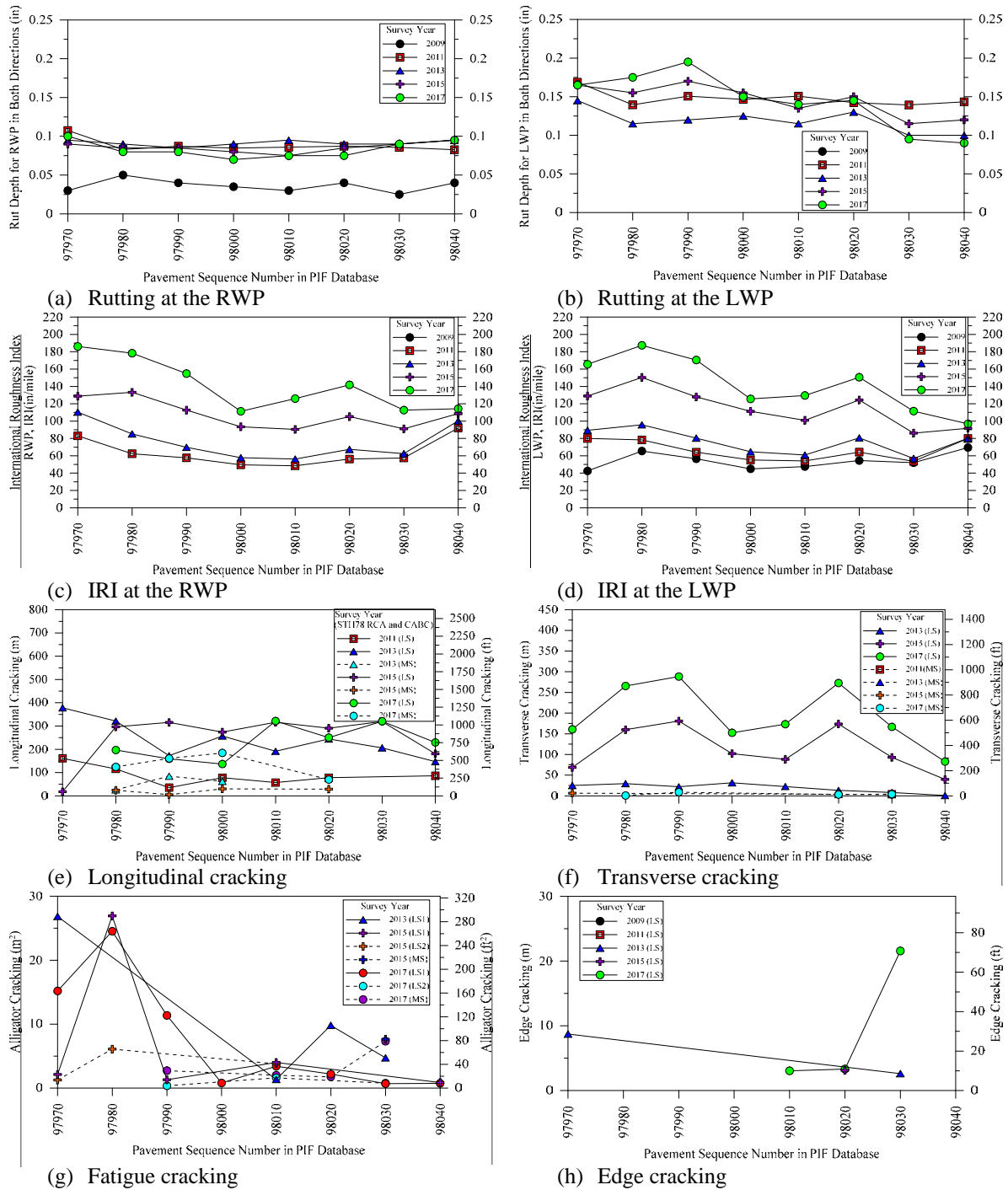
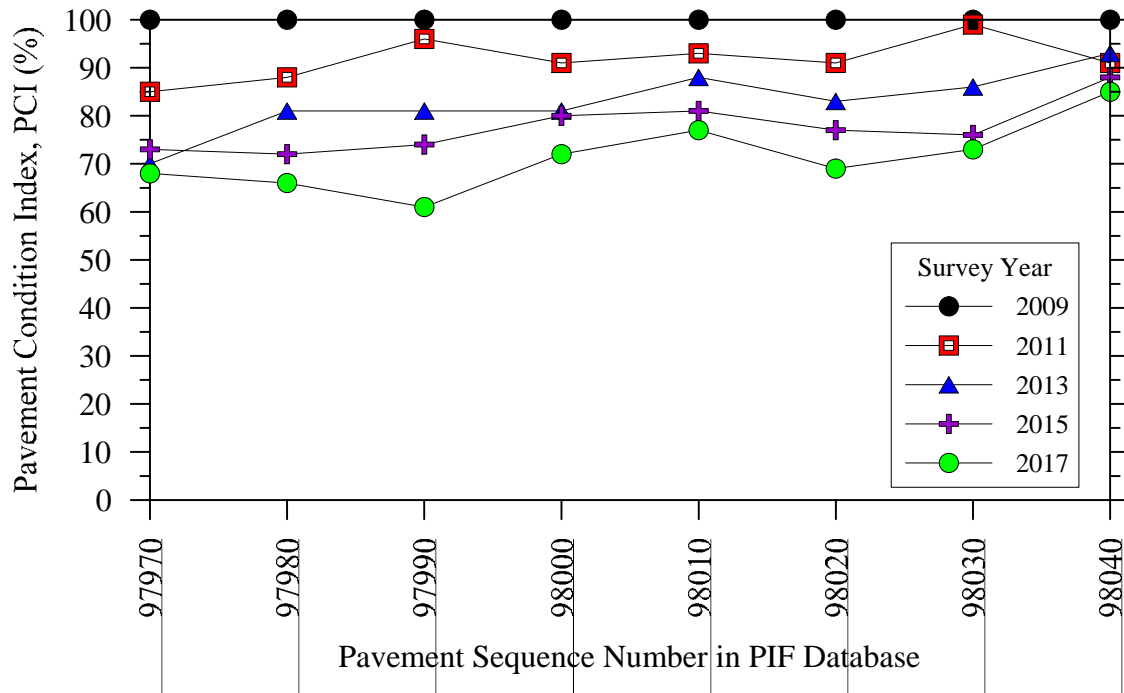
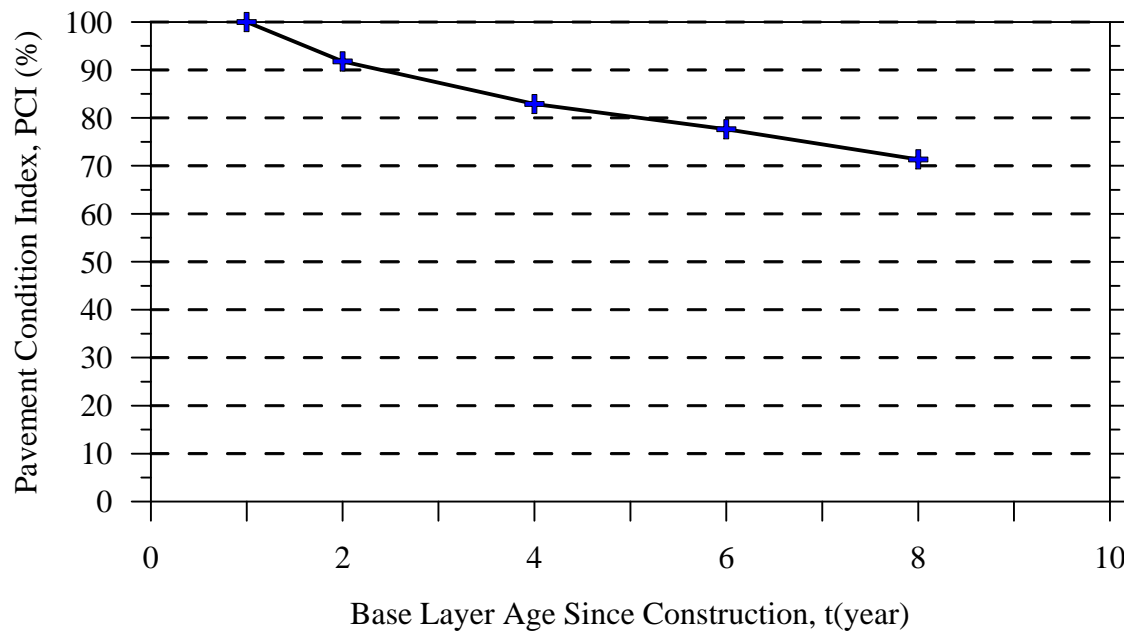


Figure 6.15: Comparison of rutting, ride quality and cracking performance for STH 78 segments with a RCA base layer.

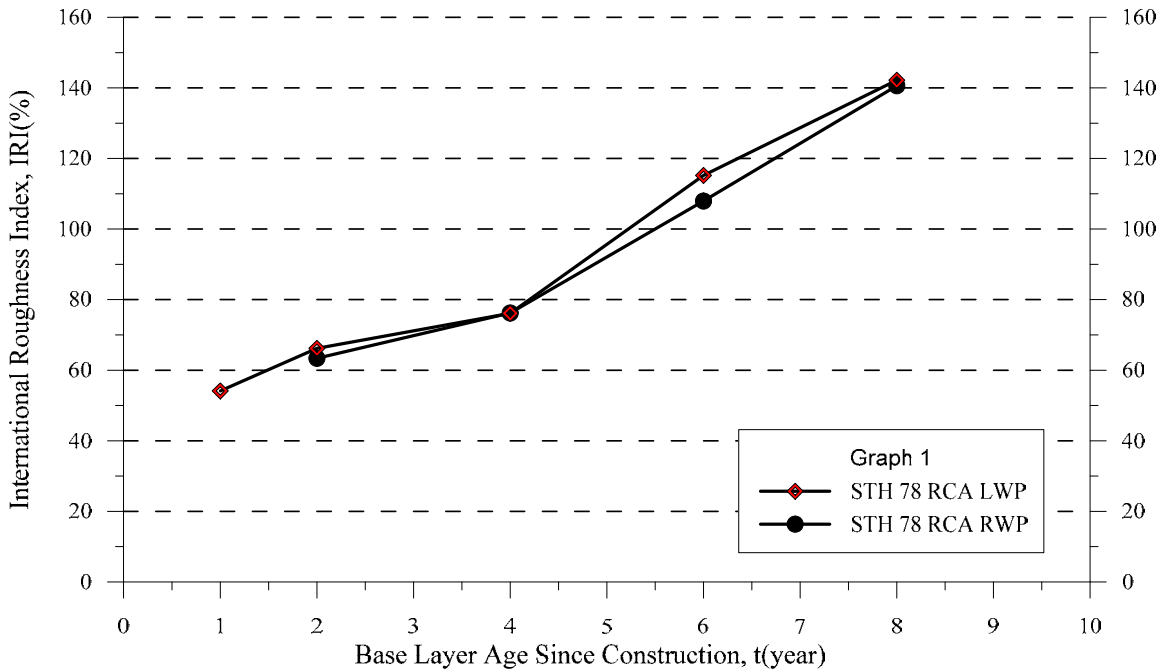


(a) Average PCI for all segments over the pavement life

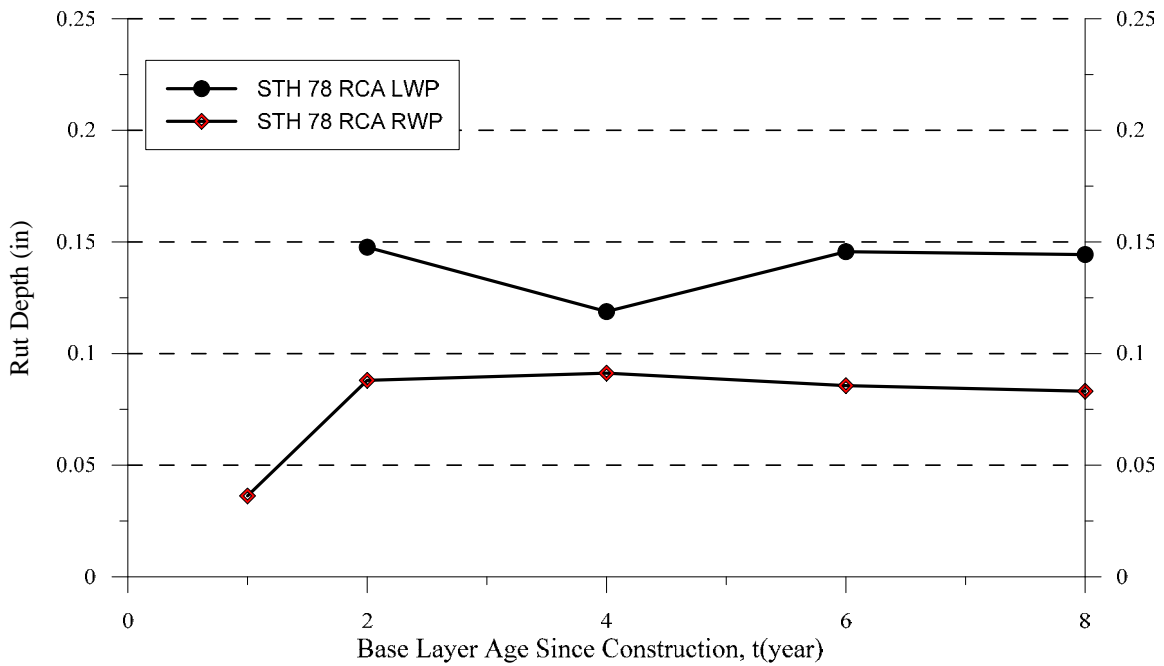


(b) Overall average of PCI segments with CA and RAP base layers over the pavement life

Figure 6.16: Comparison of average PCI variation with time for the HMA pavement segments of STH 78 constructed on a RCA base layer.

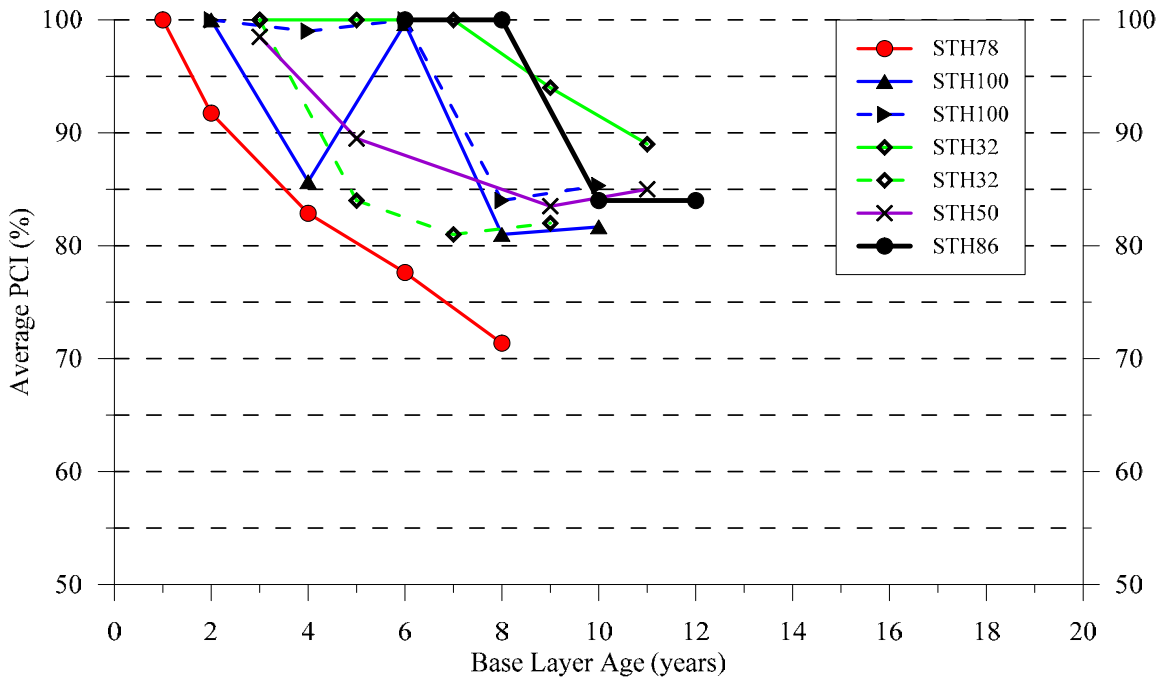


(a) Ride quality – International Roughness Index, IRI(in/mile) versus age

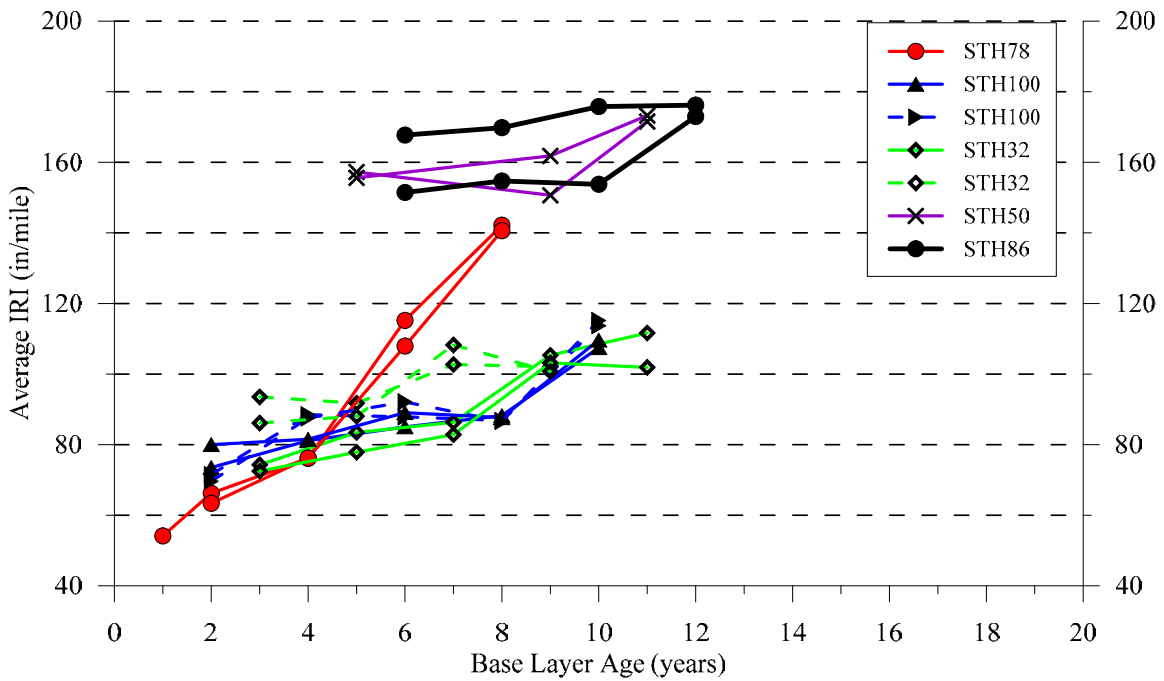


(b) Rutting versus pavement age

Figure 6.17: Comparison of average IRI and rutting for the STH 78 segments with RCA base layers.

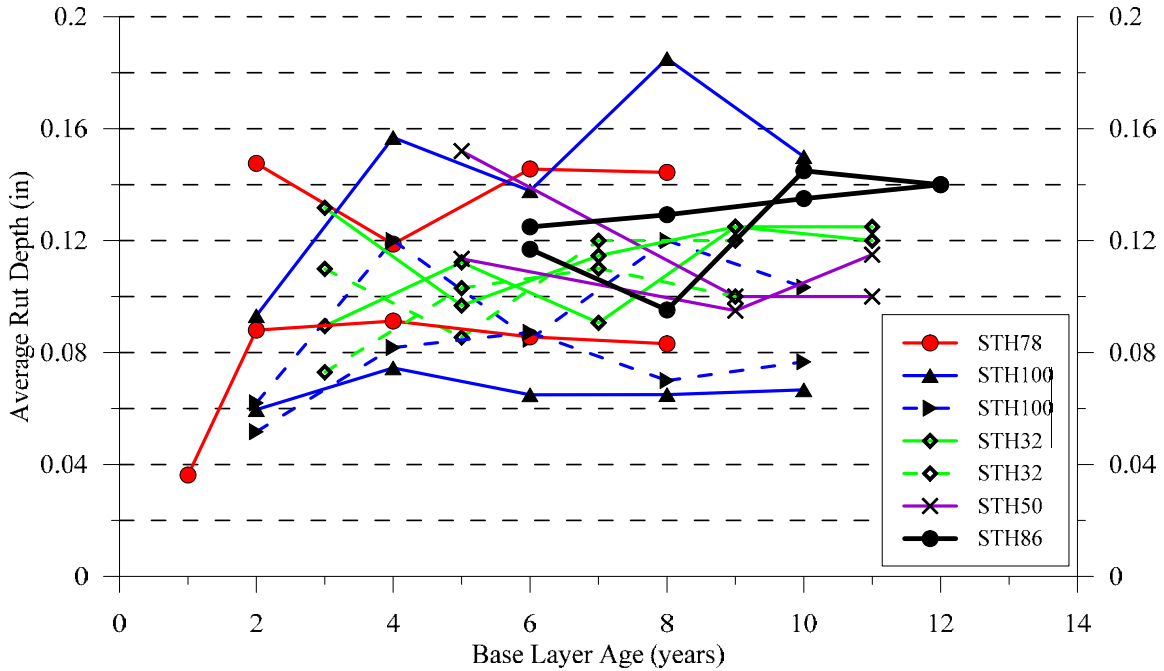


(a) Average pavement condition over the life of the pavement

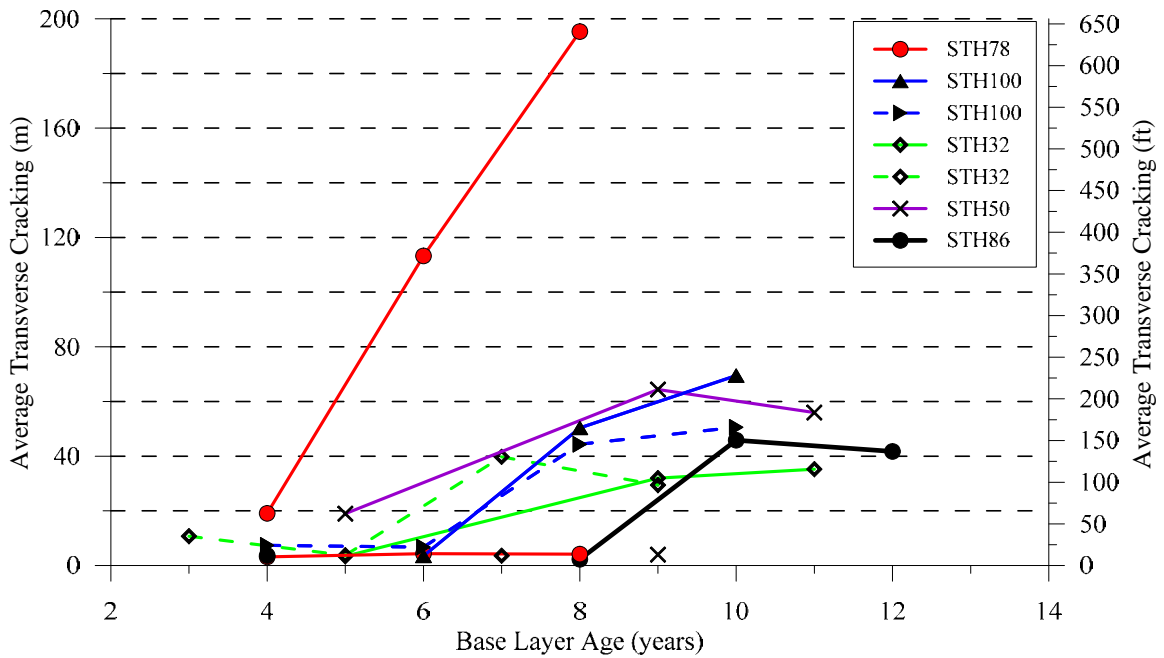


(b) Average pavement ride quality over the life of the pavement

Figure 6.18: Long-term pavement performance indicators for HMA pavements with RCA base layers.

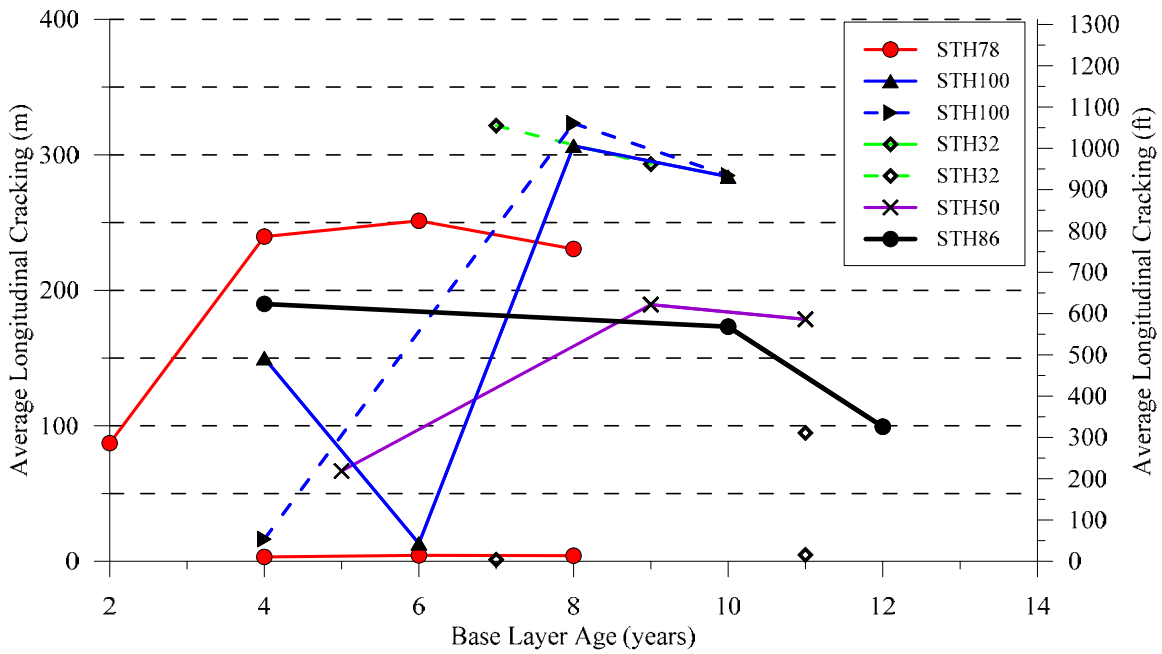


(c) Average pavement rutting over the life of the pavement

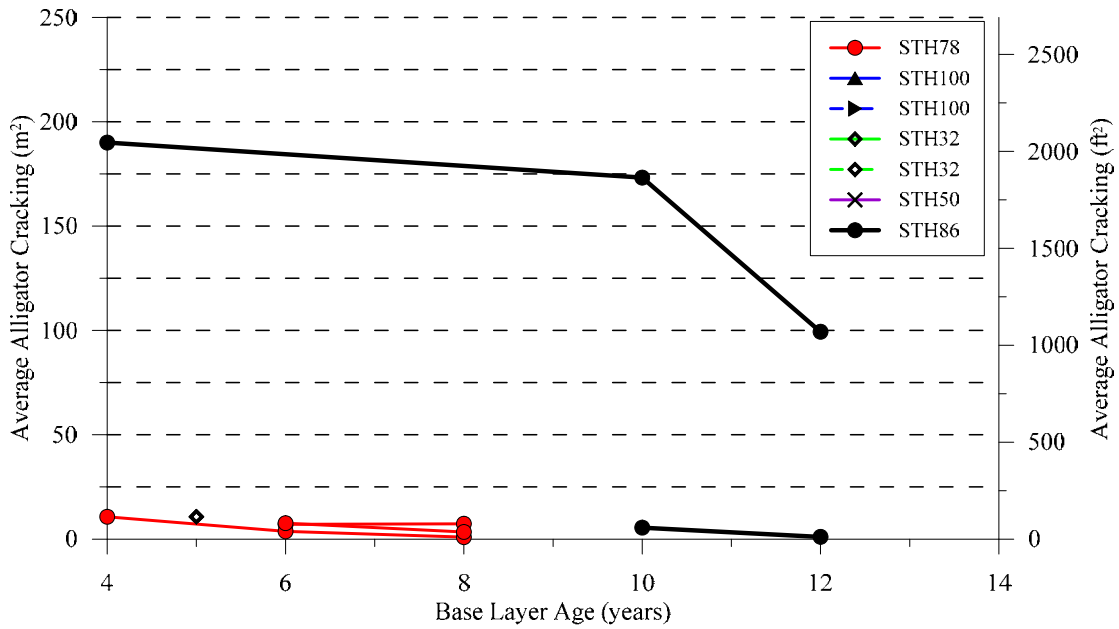


(d) Average pavement transverse cracking over the life of the pavement

Figure 6.18 (Cont.): Long-term pavement performance indicators for HMA pavements with RCA base layers.



(e) Average pavement longitudinal cracking over the life of the pavement



(f) Average pavement fatigue cracking over the life of the pavement

Figure 6.18 (Cont.): Long-term pavement performance indicators for HMA pavements with RCA base layers.

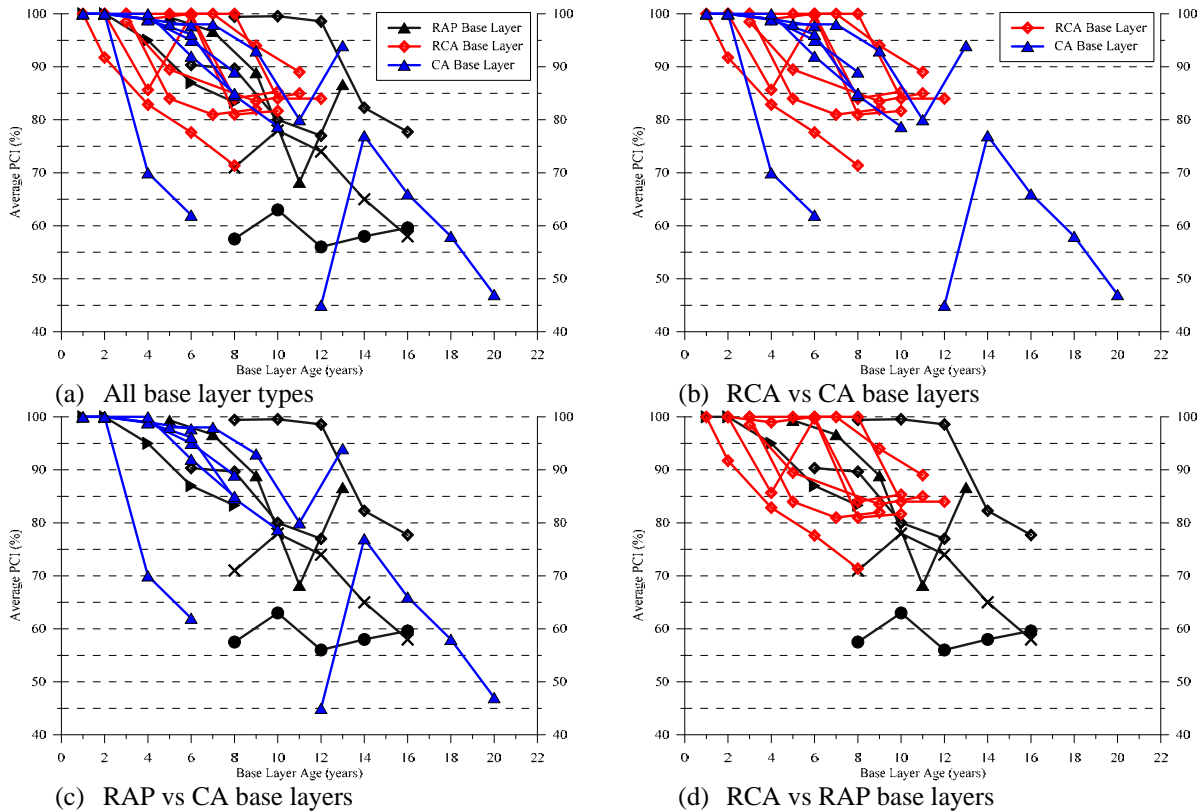


Figure 6.19: Comparison of the investigated pavement performance based on the type of base layer (average PCI for the total length of the project vs. pavement age).

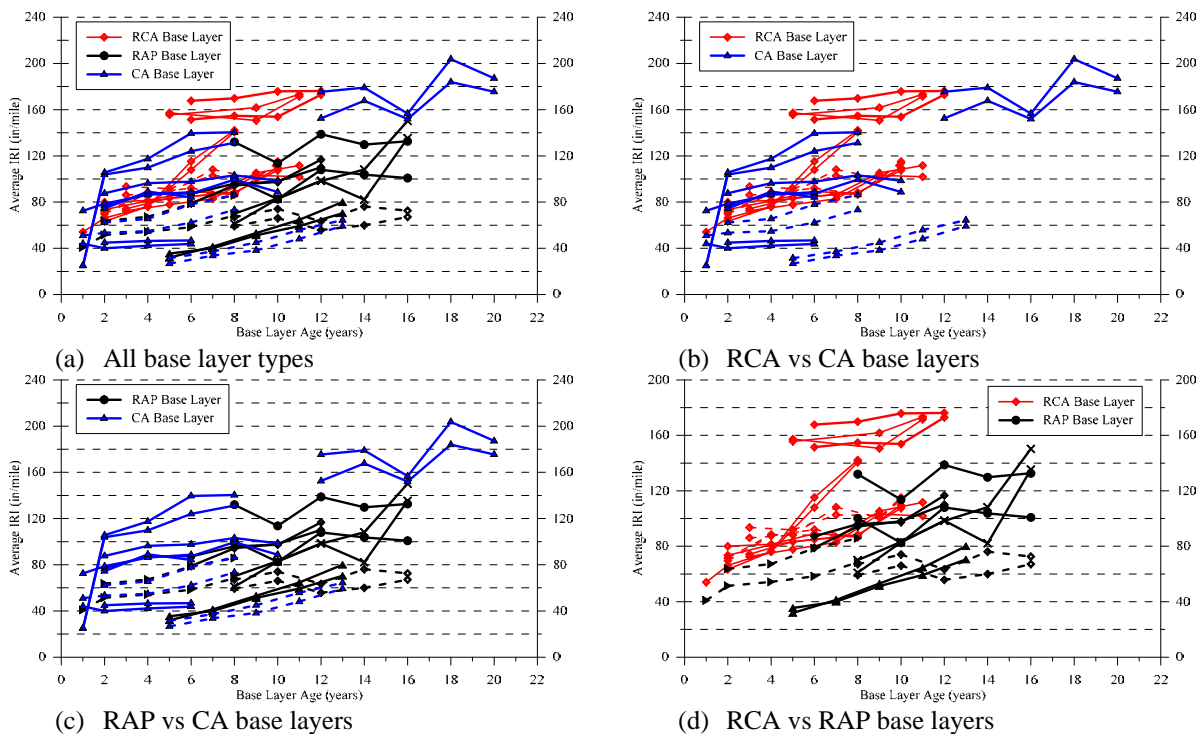


Figure 6.20: Comparison of the investigated pavement performance based on the type of base layer (average IRI for the total length of the project vs. pavement age).

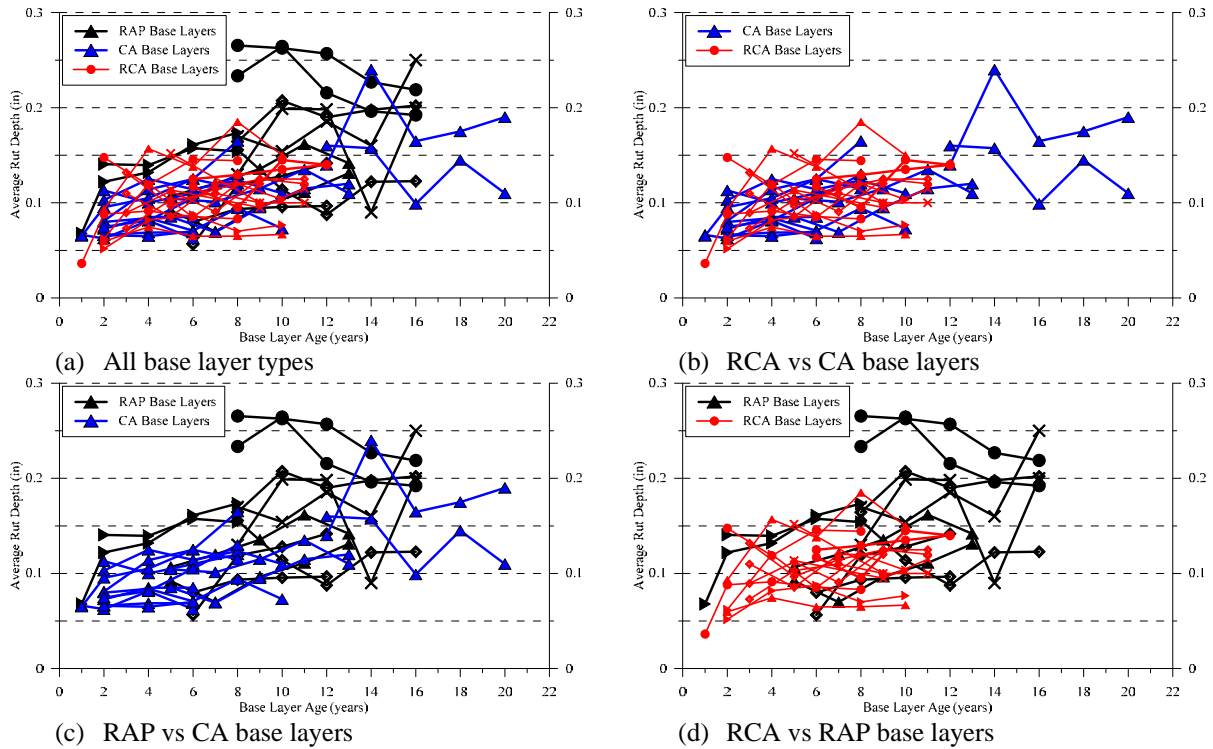


Figure 6.21: Comparison of the investigated pavement performance based on the type of base layer (average rut depth for the total length of the project vs. pavement age).

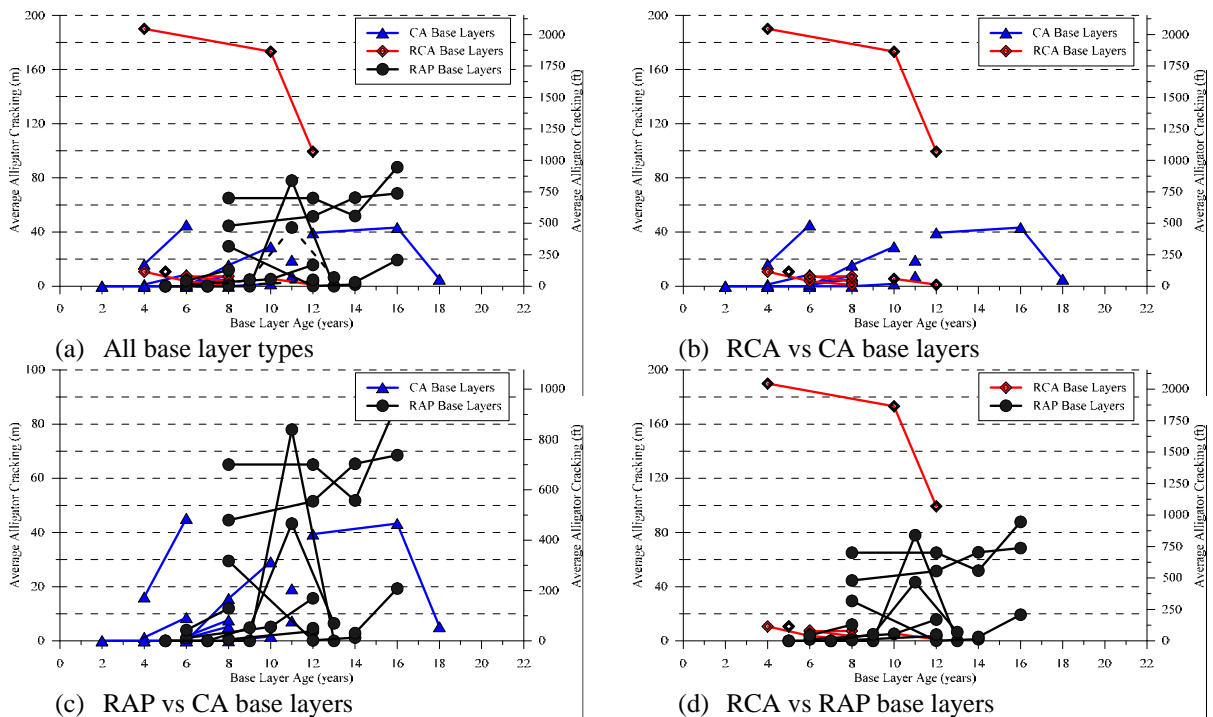
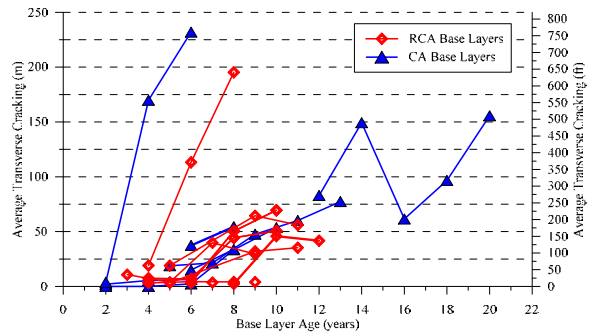
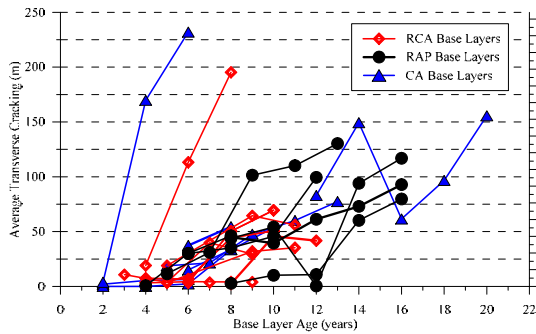
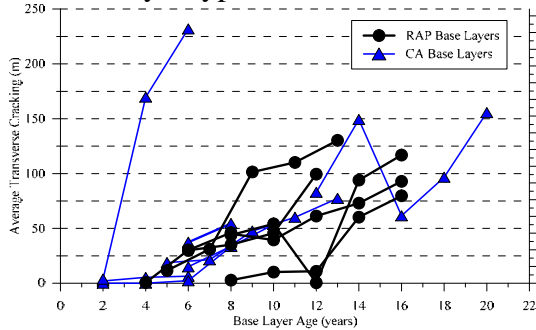


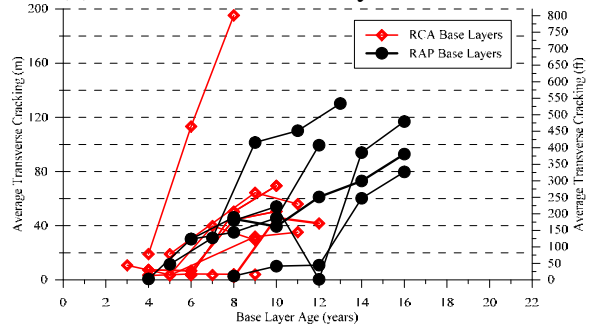
Figure 6.22: Comparison of the investigated pavement performance based on the type of base layer (average fatigue cracking for the total length of the project vs. pavement age).



All base layer types



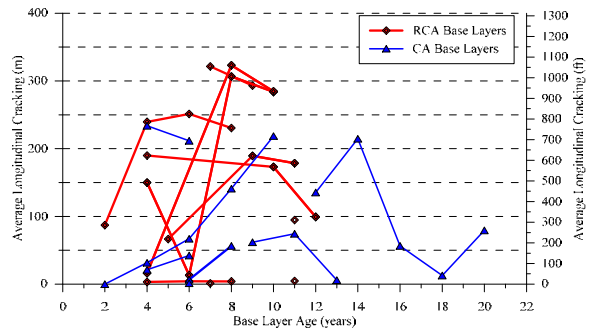
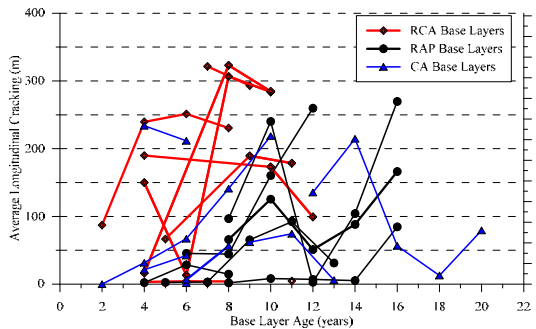
(e) RCA vs CA base layers



RAP vs CA base layers

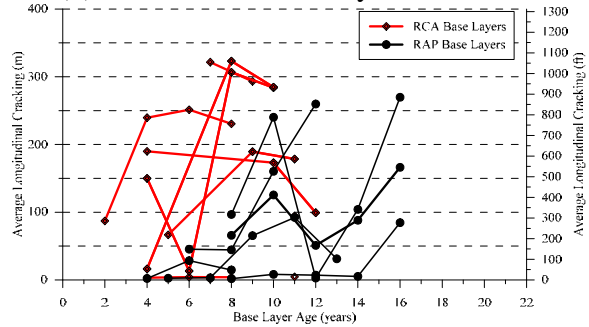
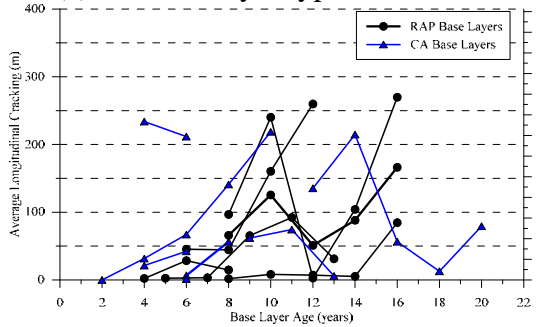
(f) RCA vs RAP base layers

Figure 6.23: Comparison of the investigated pavement performance based on the type of base layer (average transverse cracking for the total length of the project vs. pavement age).



(a) All base layer types

(b) RCA vs CA base layers



(c) RAP vs CA base layers

(d) RCA vs RAP base layers

Figure 6.24: Comparison of the investigated pavement performance based on the type of base layer (average longitudinal cracking for the total length of the project vs. pavement age).

Figures 6.25 to 6.28 present the variations of the averages of pavement performance indicators (PCI, IRI, rutting, and cracking) with HMA pavement age for all investigated pavements with CA, RCA, and RAP base layers. The results of long-term pavement performance analyses conducted herein using WisDOT PIF database (averages presented in Figures 6.25 to 6.28) demonstrated that the performance of the HMA pavements with RCA (with the exception of STH 78) and RAP is comparable with the performance of the HMA pavements with CA base course layers (commonly used in WisDOT projects).

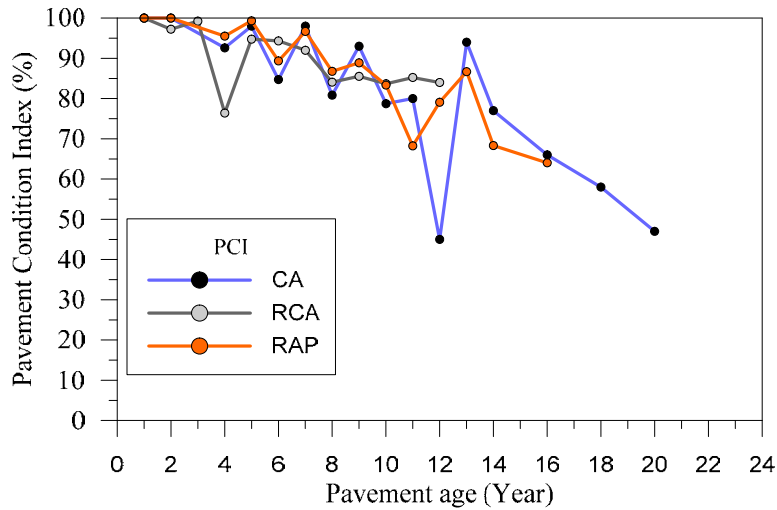


Figure 6.25: Comparison of the investigated pavement performance based on the type of base layer (average PCI for all pavement sections vs. pavement age).

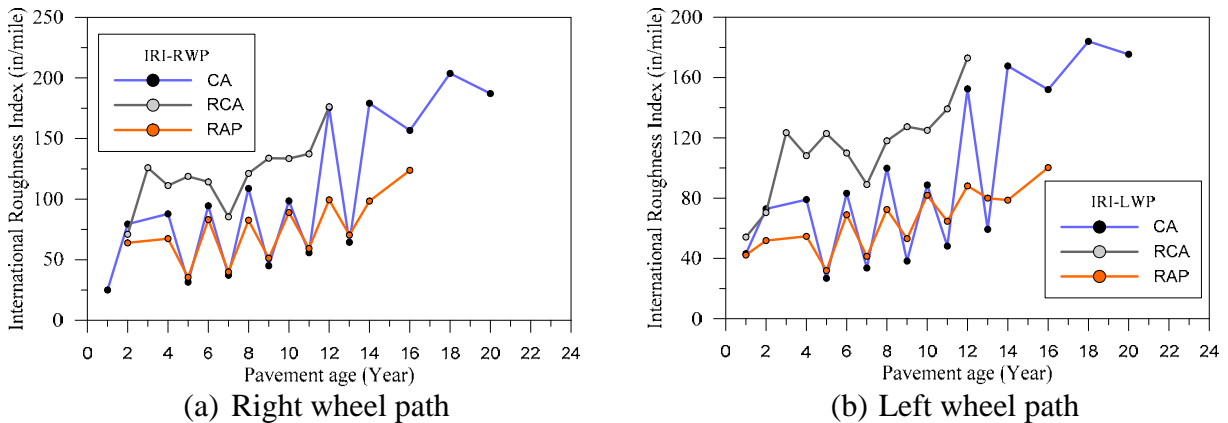
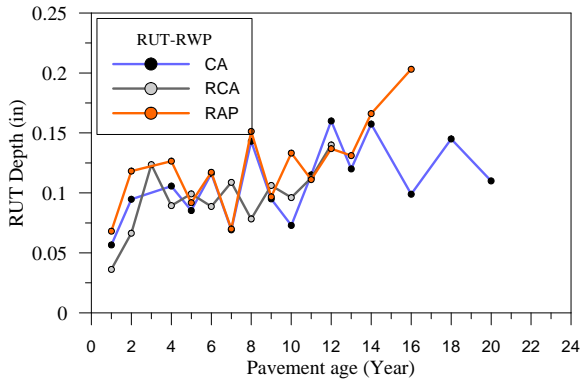
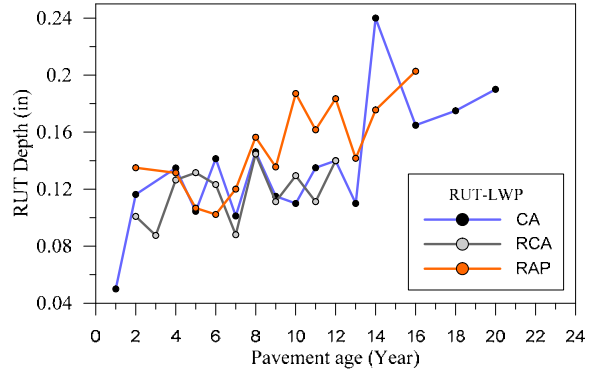


Figure 6.26: Comparison of the investigated pavement performance based on the type of base layer (average IRI for all pavement sections vs. pavement age).

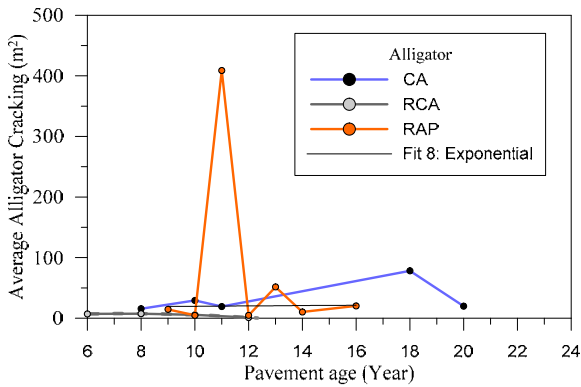


(a) Right wheel path

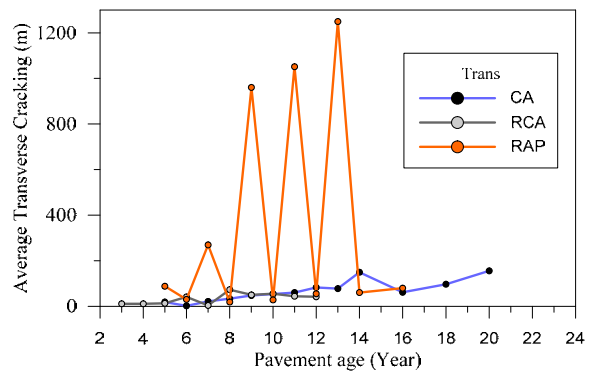


(b) Left wheel path

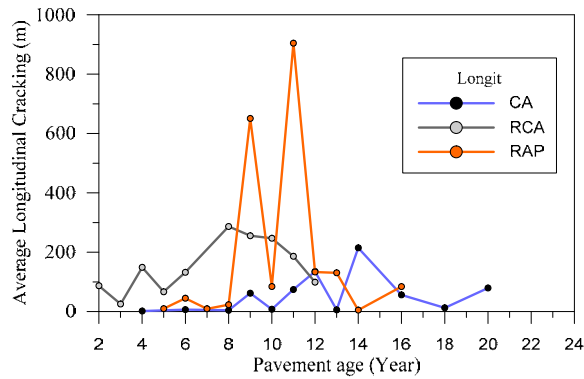
Figure 6.27: Comparison of the investigated pavement performance based on the type of base layer (average rutting for all pavement sections vs. pavement age).



(a) Alligator Cracking



(b) Transverse Cracking



(c) Longitudinal Cracking

Figure 6.28: Comparison of the investigated pavement performance based on the type of base layer (average cracking for all pavement sections vs. pavement age).

Chapter 7

Summary, Conclusions, and Recommendations

The Wisconsin Department of Transportation has been using RAP and RCA as a base course for over thirty years. The qualitative assessment of WisDOT roads constructed with RAP and RCA base layers with an HMA surface is that they are performing adequately. This study intended to provide quantitative evaluation of the use of RAP and RCA as base layers in HMA pavements. The study used the following to collect data via field and laboratory testing programs on pavement sections and materials from HMA pavements with CA, RCA, and RAP base layers of:

1. Falling Weight Deflectometer and Ground Penetrating Radar
2. Pavement surface profile measurements using a walking profiler
3. Visual pavement distress surveys
4. Field drainability and laboratory permeability tests
5. Dynamic Cone Penetrometer test
6. Particle size analysis
7. Micro-Deval abrasion test
8. Absorption and specific gravity tests
9. Analysis of pavement performance data from WisDOT PIF database for the investigated pavement sections
10. Reviewing and summarizing the State DOT's specifications on the use of RCA and RAP in base layers for HMA pavements
11. Conducting a survey of state DOTs on the use of RCA and RAP in base layers for HMA pavements.

Based on the work conducted herein, the collected measurements, data and information were analyzed and critically evaluated. The CA base materials possessed the highest gravel size fractions and the highest fines size fractions when compared with the RCA and RAP base materials. The gravel size fractions for both RCA and RAP base materials are comparable but the RCA base materials exhibited higher variability. On the other hand, the CA base materials have the lowest sand size fractions compared with RCA and RAP base materials. The RCA base materials contained the lowest fines size fractions. Analysis of the particle size distributions for the investigated CA, RCA, and RAP base materials indicated high sand size fractions in both RCA and RAP base materials with six out of thirteen RCA base samples exceeding the upper WisDOT specification limit.

The average GN for the CA base materials is lower than that of the RAP base materials while the average GN for RCA falls between CA and RAP. This indicates that the CA was the coarsest material, followed by RCA and RAP, with RAP being the finest among all investigated materials.

The C_u and C_c values of the CA base material are significantly higher than with the corresponding values for RCA and RAP materials. This is because the majority of the CA base materials fell under “Poorly-graded gravel with silt and sand” while most of the RCA materials were classified as “well-graded sand with gravel” and “well-graded gravel with sand.” Also, the majority of the RAP base materials were classified as “well-graded sand with gravel” and “poorly-graded sand with gravel.”

According to a study by Edil et al. (2012) on the particle size distribution (PSD) of RCA and RAP, five out of seven RCA base materials have less than 50% sand fraction while five out of seven RAP base materials have more than 50% sand fraction.

Based on the FHWA test typical results, RCA base materials exhibited absorption values ranging from 2.67 to 8.2% with an average that was higher than the corresponding values for CA and RAP base materials. The RAP base materials possessed the lowest absorption, ranging between 1.2 and 2.6% with an average of 1.68%. Tabatabai et al. (2013) conducted analyses on various virgin Wisconsin coarse aggregates and found that the mean absorption value was 1.71%. The absorption value reported by Edil et Al. (2012) ranged between 5 and 6.5% for RCA, and 0.6 to 3% for RAP. Our research shows the absorption ranging between 2.67 and 8.2% for RCA, and 1.2 to 2.6% for RAP. The oven dry specific gravity for the RCA base materials was the lowest among all investigated base layer materials.

The results of Micro-Deval abrasion tests on the coarse-aggregate fractions for the CA and RCA base materials show that the percent mass loss for both base materials are comparable. Tabatabai et al. (2013) conducted an analysis on Micro-Deval test results on various Wisconsin coarse aggregates and reported that the mean Micro-Deval mass loss was 15.05% for coarse aggregates. The investigated CA and RCA base materials exhibited mass loss percentages that are generally high compared with crushed stone natural aggregates. This observation is consistent with the results was reported by White et al. (2008).

Our study indicates that the predicted CBR and resilient modulus values for the investigated base layer types are comparable. The average predicted resilient moduli ranged between 37 and 48 ksi for the RCA base layers, between 36 and 46 ksi for the CA base layers, and between 38 and 43 ksi for the RAP base layers. In general, the CBR and base layer moduli predicted from the results of the DCP tests indicated high strength and modulus properties for the investigated base layers. Difficulties were noted in retrieving RCA base materials from STH 78 (with higher than normal strength as well as moisture content), STH 32, and STH 50. The research team believes this is due to self-cementing effects where the process and formation of Calcium Silicate Hydrates (C-S-H) or secondary rehydration from the fine cementitious material could occur in RCA materials.

The pavements with CA base layers exhibited the highest deflection and the least variability. On the other hand, pavements with RCA base layers had the lowest deflection with higher variability. The effective structural number represents the structural capacity of the pavement system (all layers) estimated from the FWD test results. The investigated HMA

pavement test sections with RCA base layers exhibited the highest average SN_{eff} values, while the pavement test sections with CA base layers had the lowest average SN_{eff} values. The pavement test sections with RAP base layers exhibited intermediate SN_{eff} values. The results of the FWD analyses pertaining to D_0 and SN_{eff} demonstrate that, in general, the investigated HMA pavement sections with RCA base layers exhibited the lowest deflections and the highest structural capacity (SN_{eff}) compared with those pavement sections with CA and RAP base layers. The pavement sections with CA base layers exhibited the highest deflection and the lowest structural capacity.

The back-calculated moduli for the HMA layer (E_{HMA}) for all investigated pavement sections varied significantly among the pavement test sections (and within the individual pavement sections). The averages for the back-calculated E_{HMA} are 523, 845, and 560 ksi for pavement sections with CA, RCA, and RAP base layers, respectively. Consequently, the back-calculated average E_{HMA} for the pavement sections with CA and RAP base layers are lower than the corresponding average for pavement sections with RCA base layers. The variability in back-calculated E_{HMA} is not necessarily dependent exclusively on the base course layer variability. There are other factors that may influence the mechanical stability of HMA. In general, the back-calculated base layer moduli (E_{Base}) for all investigated pavement tests indicate the highest average values for RCA base layers, followed by the RAP base layers, while the CA base layers possessed the lowest average values. The results of the back-calculated subgrade modulus ($E_{Subgrade}$) indicate that, generally, $E_{Subgrade}$ values for all investigated pavement sections (with base layers of CA, RCA, and RAP) were comparable and fell within a close range of values.

Test results indicated that RCA base layers had higher drainability characteristics with values ranging from 3.1 to 43.3 ft/day for the base layers on STH 50. This demonstrates the high variability since both numbers are for the wheel path locations within the test section. The coefficient of permeability for the RCA base materials was retrieved from STH 50. The drainability values for CA base layers were the lowest among all base layer types with values ranging between 0.7 and 16.6 ft/day. The field drainability test results are influenced by many factors, including the thickness of the base layer, the particle size distribution of base materials, the amount of fines, the density of base materials, the properties of the subbase layers, the subgrade type and properties, the climatic conditions, and the seasonal variations.

The research team conducted visual distress survey analyses on all investigated pavement test sections. The most commonly observed pavement surface distress in the investigated pavement test sections included: transverse cracking, longitudinal cracking, alligator (fatigue) cracking, rutting, bleeding, edge cracking, pavement edge heave, and block cracking. Based on the visual distress survey of the investigated pavement sections, fatigue cracking is the most commonly observed surface distress associated with CA and RAP base layers. Transverse and longitudinal cracks were commonly observed on pavement sections with RCA base layers.

It should be noted that the PCI values calculated in this study are based on the 528-ft pavement test sections. The PCI values are highly variable in all sections and among the pavements with CA, RCA, and RAP base layers. The general ranking of the investigated pavements was based on the overall average and does not account for the pavement age. An

attempt to correlate the calculated PCI average values with pavement age did not lead to a reliable trend.

The pavement surface profile measurements were conducted on the outside (right) wheel path (OWP), center of the lane (CL), and the inside (left) wheel path (IWP) for all investigated pavement test sections (the length of each pavement test section was 600 ft). Results indicated very high variability in the IRI values within the tracks (such as the outside wheel path) of the same pavement test section as well as among different pavement test sections. Generally, the OWP profile measurement showed higher IRI values compared with the CL and IWP for the same pavement test section. The outside wheel path is near the pavement edge/shoulder. Results show relatively high IRI values and high variability exhibited by the pavement sections on RCA base layer materials, particularly for STH 78 test sections S1 and S2.

Two HMA pavement sections with CA base layers, five sections with RCA base layers, and two sections with RAP base layers exhibited IRI values that exceeded the threshold limit of 140 in/mile. The average IRI value for all pavement sections indicates the pavement test sections with RAP base layers exhibited the smoothest ride quality with an average IRI of 95.8 in/mile.

Based on the results of this study, the research team believes that the performance of the HMA pavements with RCA (with the exception of STH 78) and RAP is satisfactory/adequate and comparable with the performance of the HMA pavements with CA base course layers. The research team recommends that WisDOT continues the practice of using the RCA and RAP in base course layers of HMA pavements, but recommends implementing the all or part of the following:

1. Source variability and approval (allow RCA from pavements but limit RCA from buildings, brick, etc. to $\leq 10\%$ or require rigorous durability/soundness laboratory testing such as absorption, freeze-thaw, Micro-Deval, LA abrasion, and sodium sulfate soundness).
2. Visual inspection of RCA and RAP materials to identify and removal rebars, dowel bars, wire mesh, aluminum pavement markings, and any other harmful materials.
3. Check for deleterious materials and soil/debris fed into crushers on site.
4. Gradation requirements (require maximum limits for sand fraction for RAP and RCA).
5. Limit the self-cementing fractions in RCA (may allow maximum percentage of RCA ≤ 70)
6. Durability testing requirements (absorption, Micro-Deval, LA abrasion, freeze-thaw).
7. Include blending proportions of RAP/CA and RCA/CA, 50/50 could be used.
8. Limit the lift thickness during RAP construction to 6 inches to achieve a proper compaction and require field compaction measurements.
9. Implement construction requirements (density, DCP, LWD, compaction test sections, etc.).

References

- 1) American Association of State Highway and Transportation Officials (2018). AASHTOWare Pavement ME Design, <http://me-design.com/MEDesign/>.
- 2) American Association of State Highway and Transportation Officials, (2017). Standard Specifications for Transportation Materials and Methods of Sampling and Testing and Provisional Standards.
- 3) ASTM Standard Specification (2018). Road and Paving Materials; Vehicle-Pavement Systems for Concrete Aggregates. vol. 04.03. West Conshohocken, PA: ASTM International.
- 4) ASTM Standard Specification (2018). Soil and Rock (II). vol. 04.09. West Conshohocken, PA: ASTM International.
- 5) Alam, T.B., Abdelrahman, M., and Schram, S.A. (2010). "Laboratory Characterisation of Recycled Asphalt Pavement as a Base Layer." *International Journal of Pavement Engineering* , No. 2, pp. 123-131.
- 6) Arshad, M., and Ahmed, M. (2017). "Potential use of Reclaimed Asphalt Pavement and Recycled Concrete Aggregate in Base/Subbase Layers of Flexible Pavements," *Construction and Building Materials*, Volume 151, pp. 83-97.
- 7) Attia, M. and Abdelrahman, M. (2010). "Modeling the Effect of Moisture on Resilient Modulus of Untreated Reclaimed Asphalt Pavement." *Transportation Research Record, Journal of the Transportation Research Board*, No. 1981, pp. 30-40.
- 8) Attia, M., and Abdelrahman, M. (2010). "Sensitivity of Untreated Reclaimed Asphalt Pavement to Moisture, Density, and Freeze Thaw". *Journal of Materials in Civil Engineering. American Society of Civil Engineers*. 22(12). pp 1260-1269.
- 9) Bejorano, M., Harvey, J., Lane, L. (2003). "In-Situ Recycling of Asphalt Concrete as Base Material in California". *Proc. 82nd Annual Meeting, Transportation Research Board, Washington, D.C.*
- 10) Bennert, T., W. Papp Jr, A. Maher, and N. Gucunski, (2000). "Utilization of Construction and Demolition Debris under Traffic-Type Loading in Base and Subbase Applications," *Transportation Research Record, Journal of the Transportation Research Board*, Vol. 1714, pp. 33-39.
- 11) Blankenagel, B. (2005). "Characterization of Recycled Concrete for use as Pavement Base Material," MS Thesis, Brigham Young University, p. 66.
- 12) Blankenagel, B.J., and Guthrie, W.S. (2006). "Laboratory Characterization of Recycled Concrete for use as Pavement Base Material." *Transport. Res. Rec.*, No. 1952, Washington, D.C., pp. 1-27.
- 13) Bleakley, A., Cosentino, P (2013). "Improving Properties of Reclaimed Asphalt Pavement for Roadway Base Applications Through Blending and Chemical Stabilization". *Transportation Research Record: Journal of the Transportation Research Board*, No. 2335. pp. 20-28.

- 14) Bozyurt, O. (2011). Behavior of Recycled Asphalt Pavement and Recycled Concrete Aggregate as Unbound Road Base. MS Thesis, Department of Civil and Environmental Engineering, University of Wisconsin-Madison.
- 15) Bozyurt, O., Tinjum, J.M., Son, Y.H., Edil, T.B. and Benson, C.H. (2012). “Resilient Modulus of Recycled Asphalt Pavement and Recycled Concrete Aggregate,” GeoCongress 2012, American Society of Civil Engineers, GSP No. 225, Oakland, CA, pp. 3901-3910.
- 16) Bradshaw, A., Costa, J. and Giampa, J. (2016). “Resilient Moduli of Reclaimed Asphalt Pavement Aggregate Subbase Blends,” ASCE Journal of Materials in Civil, DOI: 10.1061/(ASCE)MT.1943-5533.0001508.
- 17) Butler, L., Tighe, S., West, J. (2013). “Guidelines for Selection and Use of Coarse Recycled-Concrete Aggregates in Structural Concrete”. Transportation Research Record: Journal of the Transportation Research Board, No. 2335. pp. 3-12.
- 18) Ceylan, H. (2014). “Use of Crushed/Recycled Concrete as Drainable Base/Subbase and Possible Future Plugging of Pavement Systems,” Presentation, ASCE Iowa Geotechnical Engineering Conference.
- 19) Ceylan, H., Kim, S., Gopalakrishnan, K., (2014). “Use of Crushed/Recycled Concrete as Drainable Base/Subbase and Possible Future Plugging of Pavement Systems” Program for Sustainable Pavement Engineering and Research (PROSPER), Institute for Transportation, Iowa State University.
- 20) Cerni, G. and Colagrande, S. (2012). “Resilient Modulus of Recycled Aggregates Obtained by Means of Dynamic Tests in a Triaxial Apparatus,” Procedia - Social and Behavioral Sciences Volume 53, 3 October 2012, pp. 475-484.
- 21) Cooley, A., Brumfield, J., Easterling, J. and Kandhal, P. (2007). “Evaluation of Recycled Portland Cement Concrete Pavements for Base Course and Gravel Cushion Material,” Research Report SD05-07, South Dakota Department of Transportation, p 88.
- 22) Dai, S., and Kremer, C., (2006). Improvement and Validation of Mn/DOT DCP Specifications for Aggregate Base Materials and Select Granular (No. MN/RC-2005-32). Office of Materials Minnesota Department of Transportation.
- 23) Dong, Q., and Huang, B. (2014), “Laboratory Evaluation on Resilient Modulus and Rate Dependencies of RAP Used as Unbound Base Material,” ASCE Journal of Materials in Civil Engineering, Vol. 26, No. 2, DOI: 10.1061/(ASCE)MT.1943-5533, pp. 379-383.
- 24) Dong, Z., Ye, S., Gao, Y., Fang, G., Zhang, X., Xue, Z. and Zhang, T., (2016). ‘Rapid Detection Methods for Asphalt Pavement Thicknesses and Defects by a Vehicle-Mounted Ground Penetrating Radar (GPR) System’. Sensors, 16;
<https://doi.org/10.3390/s16122067>
- 25) Edil, T., Benson, C., Tinjum, J., Scheartle, G., Bozyurt, O., Nokkaew, K., Chen, J., Bradshaw, S. (2011). “Engineering Properties of Recycled Materials for Unbound Applications,” Minnesota Department of Transportation Contract No. 89264.

- 26) Edil, T., Tinjum, J., and Benson, C., (2012). "Recycled Unbound Materials". Research Report # 2012-35, Minnesota Department of Transportation, p. 340.
- 27) Federal Highway Administration (FHWA), (2008). "User Guideline for Byproducts and Secondary Use Materials in Pavement Construction," FHWA Report FHWA-RD-97-148, FHWA, VA.
- 28) Federal Highway Administration (FHWA), (2018). The Long-Term Pavement Performance (LTPP) Program.
- 29) Gabr, A., and Cameron, D. (2012). "Properties of Recycled Concrete Aggregate for Unbound Pavement Construction," ASCE Journal of Materials in Civil Engineering, Vol. 24, No. 6, DOI: 10.1061/(ASCE)MT.1943-5533.0000447. pp. 754-764.
- 30) Gabr, A., Mills, K., and Cameron, D. (2013). "Repeated Load Triaxial Testing of Recycled Concrete Aggregate for Pavement Base Construction," Geotech Geol Eng, Volume 31, DOI 10.1007/s10706-012-9572-8, pp. 119-132.
- 31) Gupta, N., Kluge, M., Chadik, P. and Townsend, T. (2018). "Recycled Concrete Aggregate as Road Base: Leaching Constituents and Neutralization By Soil Interactions And Dilution," Waste Management, 72, pp. 354-361.
- 32) Guthrie, W., Dane Cooley, and Dennis Eggett. (2007) "Effects of Reclaimed Asphalt Pavement on Mechanical Properties of Base Materials," Transportation Research Record: Journal of the Transportation Research Board 2005, <https://doi.org/10.3141/2005-06>, pp. 44-52.
- 33) GSSI (2018). RADAN (GPR Road Scan), <https://www.geophysical.com/>
- 34) Huesemann, M., Huesemann, T., and Fortman, T., (2005). "Leaching of BTEX from Aged Crude Oil Contaminated Model Soils: Experimental and Modeling Results," Soil & Sediment Contamination, 14, 545–585.
- 35) Jayakody, S. (2014). "Investigation on Characteristics and Performance or Recycled Concrete Aggregates as Granular Materials for Unbound Pavements". PhD Dissertation, Queensland University of Technology. pp 1-203.
- 36) Jitsangiam, P., Boonserm, K., Phenrat, T., P., Chummuneerat, S., Chindaprasirt, P. and Nikraz, H. (2015). "Recycled Concrete Aggregates in Roadways: Laboratory Examination of Self-Cementing Characteristics," ASCE Journal of Materials in Civil Engineering Vol. 27, Issue 10. [https://doi.org/10.1061/\(ASCE\)MT.1943-5533.0001245](https://doi.org/10.1061/(ASCE)MT.1943-5533.0001245)
- 37) Johnson, E., Clyne, T (2012). "Recycled Asphalt Pavement: MnROAD Study of Fractionated RAP". Minnesota Local Research Board (LRRB) Investigation 864 and, MPR Project No. 6-(022).
- 38) Kang, D. H., Gupta, S. C., Ranaivoson, A. Z., Siekmeier, J., & Roberson, R. (2011). Recycled materials as substitutes for virgin aggregates in road construction: I. Hydraulic and mechanical characteristics. Soil Science Society of America Journal, 75(4), 1265-1275. <https://doi.org/10.2136/sssaj2010.0295>
- 39) Kim, W., and Labuz, J. (2007). "Resilient Modulus and Strength of Base Course with Recycled Bituminous Material". Research Report # 2007-5, Minnesota Department of Transportation, 270 p.
- 40) Kuo, Shiou-San, Hesham Mahgoub, and Abdenour Nazef, (2002). "Investigation of Recycled Concrete Made with Limestone Aggregate for a Base Course in Flexible

- Pavement,” *Transportation Research Record: Journal of the Transportation Research Board* 1787, pp 99-108.
- 41) Li, C., Ashlock, J., White, D., and Vennapusa, P. (2017). “Permeability and Stiffness Assessment of Paved and Unpaved Roads with Geocomposite Drainage Layers,” *Applied Sciences*, 7(7), 718, <https://doi.org/10.3390/app7070718>.
 - 42) Lukanen, E.O., and C.G. Kruse. (2000) “Optimization of Recycled Asphalt Concrete and Base Materials for Bases of New Asphalt Concrete Pavements,” Report No. SD97-03, South Dakota Department of Transportation, Pierre, SD.
 - 43) Merritt, D. K., G. K. Chang, and J. L. Rutledge, (2015). “Best Practices for Achieving and Measuring Pavement Smoothness, A Synthesis of State-of Practice,” FHWA/LA.14/550. Louisiana Transportation Research Center, Baton Rouge, LA.
 - 44) Nokkaew, K., Tinjum, J., Benson, C. (2012). “Hydraulic Properties of Recycled Asphalt Pavement and Recycled Concrete Aggregate” ASCE GeoCongress 2012: State of the Art and Practice in Geotechnical Engineering, <https://doi.org/10.1061/9780784412121.152> pp. 1476-1485.
 - 45) Poon, Chi Sun, and Dixon Chan, (2006). “Feasible use of Recycled Concrete Aggregates and Crushed Clay Brick as Unbound Road Sub-base,” *Construction and Building Materials* 20.8, pp 578-585.
 - 46) Poon, Chi-Sun, X. C. Qiao, and Dixon Chan, (2006). “The Cause and Influence of Self-Cementing Properties of Fine Recycled Concrete Aggregates on the Properties of Unbound Sub-base,” *Waste management* 26, no. 10, pp. 1166-1172.
 - 47) Powell, W.D., Potter, J.F., Mayhew, H.C., and Nunn, M.E. (1984). “The Structural Design of Bituminous Roads,” TRRL Report LR 1132, 62p.
 - 48) Saeed, A., Hall, J., and Barker, W. (2001). “Performance-Related Test of Aggregates for Use in Unbound Pavement Layers,” National Cooperative Highway Research Program (NCHRP) Report 453, Transportation Research Board, National Research Council, Washington, D.C.
 - 49) Saeed, A. (2008). “Performance-Related Tests of Recycled Aggregates for Use in Unbound Pavement Layers,” National Cooperative Highway Research Program (NCHRP) Report 598, Transportation Research Board, National Research Council, Washington, D.C.
 - 50) Sangiorgi, C., Tataranni, P., Simone, A., Vignali, V., Lantieri, C., Dondi, G. (2017). “A Laboratory and Field Evaluation of Cold Recycled Mixture for Base Layer Entirely Made with Reclaimed Asphalt Pavement,” *Construction and Building Materials*, 138, <http://dx.doi.org/10.1016/j.conbuildmat.2017.02.004>, pp. 232–239.
 - 51) Seferoglu, A., Seferoglu, M., Akpınar. (2018). “Investigation of the Effect of Recycled Asphalt Pavement Material on Permeability and Bearing Capacity in the Base Layer,” *Advances in Civil Engineering*, Volume 2018, Article ID 2860213, 6 pages, <https://doi.org/10.1155/2018/2860213>
 - 52) Song, Y. and Ooi, P. (2010). “Resilient Modulus Characteristics of Varying Percent of Reclaimed Asphalt Pavement,” ASCE GeoShanghai International Conference 2010, [https://doi.org/10.1061/41104\(377\)6](https://doi.org/10.1061/41104(377)6), *Paving Materials and Pavement Analysis*, pp 43-50.

- 53) Stolle, D., Guo, P., Emery, J. (2014). "Mechanical Properties of Reclaimed Asphalt Pavement - Natural Aggregate Blends for Granular Base," Canadian Journal of Civil Engineering 41(6), DOI: 10.1139/cjce-2013-0009.
- 54) Tabatabai, H., Titi, H.H., Lee, C.W., Qamhia, I., and Puerta Fella, G. (2013) "Investigation of Testing Methods to Determine Long-Term Durability of Wisconsin Aggregates," Research Report, Wisconsin Department of Transportation SPR # 0092-10-08, Wisconsin Highway Research Program, Madison, WI, 104 p.
- 55) Tabatabai, H., Titi, H. H., Lee, C. W. (2018). "Assessment of Tests to Determine Long-Term Durability of Wisconsin Aggregates," Journal of Materials in Civil Engineering, American Society of Civil Engineers. [https://doi.org/10.1061/\(ASCE\)MT.1943-5533.0002463](https://doi.org/10.1061/(ASCE)MT.1943-5533.0002463)
- 56) Thakur, S.C., Han, J., Chong, W.K., and Parsons, R.L. (2010). "Laboratory evaluation of physical and mechanical properties of recycled asphalt pavement as a base course material." Proceedings of the GeoShanghai International Conference 2010, June 3 to 5, Shanghai, China
- 57) Titi, H. H., Tabatabai, H., Faheem, A., and Dakwar, M. (2018). "Evaluation of the Long-Term Degradation and Strength Characteristics of In-situ Wisconsin Virgin Base Aggregates under HMA Pavements," Research Report, Wisconsin Department of Transportation SPR # 0092-15-06, Wisconsin Highway Research Program, Madison, WI.
- 58) Titi, H. H., Dakwar, M., Sooman, M., and Tabatabai, H. (2018). "Long Term Performance of Gravel Base Course Layers in Asphalt Pavements," Journal of Case Studies in Construction Materials, Elsevier, <https://doi.org/10.1016/j.cscm.2018.e00208>
- 59) Tutumluer, E., Moaveni, M., and Qamhia, I. Aggregate quality requirements for pavements. National Cooperative Highway Research Program (NCHRP) No. Project 20-05, Topic 48-10. Transportation Research Board, 2018.
- 60) Tutumluer, E., (2012). "Practice for Unbound Aggregate Pavement Layers," National Cooperative Highway Research Program (NCHRP) Synthesis Topic 43-03, Transportation Research Board, National Research Council, Washington, D.C.
- 61) Webster, S.L., Grau, R.H., and Williams, T.P. (1992). "Description and Application of Dual Mass Dynamic Cone Penetrometer." Instruction Rep. GL-92-3, U.S. Army Engineer Research and Development Center, Waterways Experiment Station, Vicksburg, MS, 50 p.
- 62) Webster, S.L., Brown, R.W., and Porter, J.R. (1994). "Force Projection Site Evaluation Using the Electronic Cone Penetrometer (ECP) and the Dynamic Cone Penetrometer (DCP)," Technical Report GL-94-17, U.S. Army Engineer Research and Development Center, Waterways Experiment Station, Vicksburg, MS, 172 p.
- 63) Weyers, R.E., Williamson, G.S., Mokarem, D.W., Lane, D.S., and Cady, P.D., (2005). "Testing Methods to Determine Long Term Durability of Wisconsin Aggregate Resources," Wisconsin Highway Research Program SPR# 0092-02-03, WHRP 06-07, 91 p.

- 64) White, D.J., Ceylan, H., Jahren, C., Phan, T.H., Kim, S.H., Gopalakrisnan, K., Suleiman, M. (2008). Performance Evaluation of Concrete Pavement Granular Subbase and Pavement Surface Condition Evaluation. IHRB Project TR-554, CTRE Project 06-250, July 2008, Ames, Iowa.
- 65) Wisconsin Department of Transportation (WisDOT) (2018), Standard Specifications for Highway and Structure Construction, 2018 edition, Madison.

Appendix A

Survey of State DOTs on:

Performance of Recycled Concrete Aggregate (RCA) and Reclaimed Asphalt Pavement (RAP) as Base Layers in HMA Pavements



Performance of Recycled Concrete Aggregate (RCA) and Reclaimed Asphalt Pavement (RAP) as Base Layers in HMA Pavements

Introduction

Dear Survey Participant,

This survey is part of a research project funded by the Wisconsin Department of Transportation (WisDOT). The research is focused on the performance of HMA pavements with Recycled Concrete Aggregate (RCA) and Reclaimed Asphalt Pavement (RAP) base layers compared with the most commonly used crushed stone aggregate base.

Your input is valuable to our research effort and is highly appreciated.

Thank you in advance.

Hani H. Titi, Ph.D., P.E., M.ASCE

Associate Professor

Associate Director for Pavements at the Center for By-products Utilization (CBU)

Department of Civil and Environmental Engineering

University of Wisconsin-Milwaukee

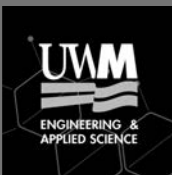
EMS 1139

3200 N. Cramer St.

Milwaukee, WI 53211

Phone : (414) 229-6893

Fax : (414) 229-6958



Performance of Recycled Concrete Aggregate (RCA) and Reclaimed Asphalt Pavement (RAP) as Base Layers in HMA Pavements

Problem Statement

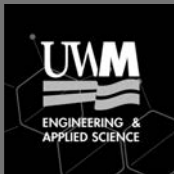
There has been great interest in recent years in using Recycled Asphalt Pavement (RAP) and

Recycled Concrete Aggregate (RCA) as base course in Wisconsin and elsewhere for the economic and environmental benefits offered by such practice. Recent examples include the I-94 corridor reconstruction in Kenosha, Racine and Milwaukee Counties, and the Beltline reconstruction in Dane County.

Laboratory studies showed that RAP and RCA have resilient modulus values equal to or higher than typical natural aggregates and also generally higher durability, in particular to freeze-thaw cycles. However, it is also recognized that RAP exhibits temperature sensitivity and larger permanent deformations than natural aggregates and RCA exhibits tufa formation and potentially lower drainability than natural aggregates.

How these characteristics manifest themselves in the field, especially in northern climates, can only be assessed by long-term observation of field performance. For this purpose, Minnesota Department of Transportation (MnDOT) constructed and monitored test sections at the MnROAD facility through a pooled fund, in which Wisconsin Department of Transportation (WisDOT) was a member. These test sections showed comparable performance to the control section of natural aggregate 2009-2013. However, there are reports now that rutting and cracking are being observed.

Wisconsin Department of Transportation (WisDOT) has been using RAP and RCA as base course for over thirty years. The qualitative assessment of WisDOT roads constructed with RAP and RCA is that they are performing adequately. This anecdotal impression needs to be verified quantitatively if the use of RAP and RCA in base aggregates is to continue. A quantitative review of WisDOT experience through collection and comparison of pavement distress surveys of roadways using RAP and RCA as base course compared with those using natural mineral aggregates is needed.



Performance of Recycled Concrete Aggregate (RCA) and Reclaimed Asphalt Pavement (RAP) as Base Layers in HMA Pavements

Information

1. Survey Participant Information

Full Name:

Agency:

Position:

Area of Expertise:

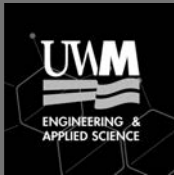
Email:

Phone Number:

2. What is the most commonly used material in base course layers for HMA pavement?

- Crushed stone aggregate
- Gravel/crushed gravel
- Soil-cement

Other (or comment)



Performance of Recycled Concrete Aggregate (RCA) and Reclaimed Asphalt Pavement (RAP) as Base Layers in HMA Pavements

RCA & RAP Basics

3. Does your department allow the use of **Recycled Concrete Aggregate (RCA)** materials in HMA pavement as:

	Yes	No	N/A
Regular base course layers in HMA pavements	<input type="checkbox"/>	<input type="checkbox"/>	<input type="checkbox"/>
Drainable base course layers in HMA pavements	<input type="checkbox"/>	<input type="checkbox"/>	<input type="checkbox"/>
Subbase course layers in HMA pavements	<input type="checkbox"/>	<input type="checkbox"/>	<input type="checkbox"/>

Comment

4. Does your department allow the use of **Reclaimed Asphalt Pavement (RAP)** materials in HMA pavement as:

	Yes	No	N/A
Regular base course layers in HMA pavements	<input type="checkbox"/>	<input type="checkbox"/>	<input type="checkbox"/>
Drainable base course layers in HMA pavements	<input type="checkbox"/>	<input type="checkbox"/>	<input type="checkbox"/>
Subbase course layers in HMA pavements	<input type="checkbox"/>	<input type="checkbox"/>	<input type="checkbox"/>

Comment

5. Compared with the most commonly used material as base course, what is the approximate percentage of RCA use?

6. Compared with the most commonly used material as base course, what is the approximate percentage of RAP use?

7. What are your agency's current goals regarding the use of RCA and RAP?

8. Does your department have any of the following specifications for **Recycled Concrete Aggregate (RCA)** use as base layer materials :

	Yes	No
Particle size distribution	<input type="checkbox"/>	<input type="checkbox"/>
Percent fines (less than #200 sieve)	<input type="checkbox"/>	<input type="checkbox"/>
Plasticity	<input type="checkbox"/>	<input type="checkbox"/>
Absorption	<input type="checkbox"/>	<input type="checkbox"/>
Abrasion - Micro-Deval	<input type="checkbox"/>	<input type="checkbox"/>
Sodium sulfate soundness	<input type="checkbox"/>	<input type="checkbox"/>
LA Abrasion	<input type="checkbox"/>	<input type="checkbox"/>
Freeze-thaw	<input type="checkbox"/>	<input type="checkbox"/>

Comment

9. Does your department have any of the following specifications for **Reclaimed Asphalt Pavement (RAP)** use as base layer materials :

	Yes	No
Particle size distribution	<input type="checkbox"/>	<input type="checkbox"/>
Percent fines (less than #200 sieve)	<input type="checkbox"/>	<input type="checkbox"/>
Plasticity	<input type="checkbox"/>	<input type="checkbox"/>
Absorption	<input type="checkbox"/>	<input type="checkbox"/>
Abrasion - Micro-Deval	<input type="checkbox"/>	<input type="checkbox"/>
Sodium sulfate soundness	<input type="checkbox"/>	<input type="checkbox"/>
LA Abrasion	<input type="checkbox"/>	<input type="checkbox"/>
Freeze-thaw	<input type="checkbox"/>	<input type="checkbox"/>

Comment



Material Performance

10. Do you have issues/problems related to RCA performance as base layers?

Drainage	<input type="text"/>
Freeze/Thaw	<input type="text"/>
Self-cementation or Secondary Rehydration	<input type="text"/>
Degradation	<input type="text"/>
Other Problems (please mention)	<input type="text"/>

11. Do you have issues/problems related to RAP performance as base layers?

Drainage	<input type="text"/>
Freeze/Thaw	<input type="text"/>
Degradation	<input type="text"/>
Other Problems (please mention)	<input type="text"/>

12. Do you have a case history or example on performance issues of:

Good performing pavements on RCA bases? Publications?	<input type="text"/>
Good performing pavements on RAP bases? Publications?	<input type="text"/>
Bad performing pavements on RCA bases? (What went wrong? What was the problem?)	<input type="text"/>
Bad performing pavements on RAP bases? (What went wrong? What was the problem?)	<input type="text"/>

13. Do you have any of the following HMA pavement performance issues when using RCA base layer?

	Yes	No
Fatigue Cracking	<input type="radio"/>	<input type="radio"/>
Rutting	<input type="radio"/>	<input type="radio"/>
Ride Quality	<input type="radio"/>	<input type="radio"/>
Heave	<input type="radio"/>	<input type="radio"/>
Transverse Cracking	<input type="radio"/>	<input type="radio"/>
Pumping	<input type="radio"/>	<input type="radio"/>

Other (please specify)

14. Do you have any of the following HMA pavement performance issues when using RAP base layer?

	Yes	No
Fatigue Cracking	<input type="radio"/>	<input type="radio"/>
Rutting	<input type="radio"/>	<input type="radio"/>
Ride Quality	<input type="radio"/>	<input type="radio"/>
Heave	<input type="radio"/>	<input type="radio"/>
Transverse Cracking	<input type="radio"/>	<input type="radio"/>
Pumping	<input type="radio"/>	<input type="radio"/>

Other (please specify)



Performance of Recycled Concrete Aggregate (RCA) and Reclaimed Asphalt Pavement (RAP) as Base Layers in HMA Pavements

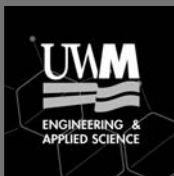
Construction Methods

* 15. What construction control method do you use for RCA and RAP bases?

Compaction	<input type="text"/>
LWD	<input type="text"/>
Stiffness Gauge	<input type="text"/>
DCP	<input type="text"/>
Other	<input type="text"/>

* 16. Do you allow the sole use of RCA or RAP? Or do you blend/mix with other materials (such as RAP+RCA mixture or RCA+Virgin Aggregate mixture)?

	Yes	No
RAP-RCA Blend	<input type="radio"/>	<input type="radio"/>
Comment	<input type="text"/>	
RAP-Crushed Aggregate (or Gravel) Blend	<input type="radio"/>	<input type="radio"/>
Comment	<input type="text"/>	
RCA-Crushed Aggregate (or Gravel) Blend	<input type="radio"/>	<input type="radio"/>
Comment	<input type="text"/>	
RCA-RAP-Crushed Aggregate (or Gravel) Blend	<input type="radio"/>	<input type="radio"/>
Comment	<input type="text"/>	



Performance of Recycled Concrete Aggregate (RCA) and Reclaimed Asphalt Pavement (RAP) as Base Layers in HMA Pavements

Issues & Concerns

17. Rate the importance (or magnitude) of the following the potential barriers within your agency to using **RCA** in pavement foundations on a scale of 0-5:

	0	1	2	3	4	5
Concerns regarding durability of source concrete	<input type="radio"/>					
Concerns regarding RCA gradation (fines)	<input type="radio"/>					
Concerns regarding RCA foundation strength and/or stability	<input type="radio"/>					
Concerns regarding environmental impacts (alkaline runoff, leachate, etc.)	<input type="radio"/>					
Economics (cost of producing RCA, crushing, screening, hauling, etc.)	<input type="radio"/>					

Other (please specify)

18. Rate the importance (or magnitude) of the following the potential barriers within your agency to using **RAP** in pavement foundations on a scale of 0-5:

	0	1	2	3	4	5
Concerns regarding durability of source concrete	<input type="radio"/>					
Concerns regarding RAP gradation (fines)	<input type="radio"/>					
Concerns regarding RAP foundation strength and/or stability	<input type="radio"/>					
Concerns regarding environmental impacts	<input type="radio"/>					
Economics (cost of producing RAP, milling, screening, hauling, etc.)	<input type="radio"/>					

Other (please specify)

* 19. Do you have any structural capacity issues with HMA pavements on RCA bases? RAP bases?

20. How do you compare HMA pavement performance with RCA or RAP base versus the most common base (e.g., versus similar pavements with virgin aggregate base layers)?

	Yes	No	NA
HMA pavements with RCA base exhibited good performance	<input type="radio"/>	<input type="radio"/>	<input type="radio"/>
Comment	<input type="text"/>		
HMA pavements with virgin aggregate base exhibited good performance	<input type="radio"/>	<input type="radio"/>	<input type="radio"/>
Comment	<input type="text"/>		
HMA pavements with blend of RCA-RAP-Aggregate exhibited good performance	<input type="radio"/>	<input type="radio"/>	<input type="radio"/>
Comment	<input type="text"/>		
HMA pavements with blend of RCA-RAP exhibited good performance	<input type="radio"/>	<input type="radio"/>	<input type="radio"/>
Comment	<input type="text"/>		

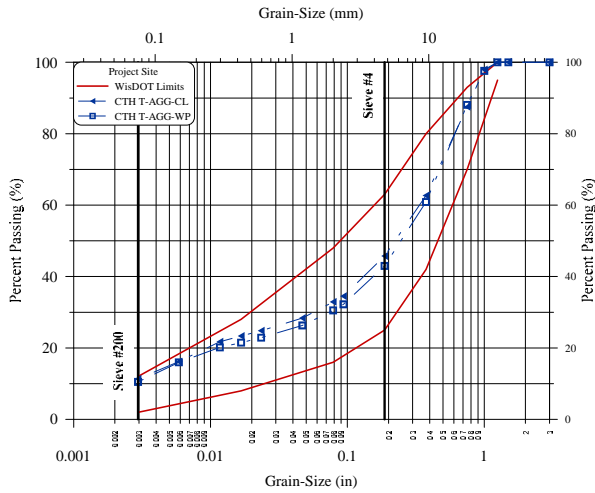
21. When RCA is used as base layers do you have any issues with HMA performance compared with similar pavements with virgin aggregate base layers?

22. When RAP is used as base layers do you have any issues with HMA performance compared with similar pavements with virgin aggregate base layers?

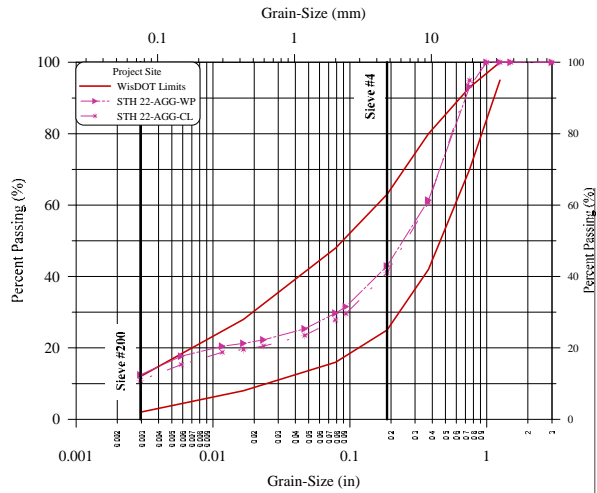
23. Do you have any comment on RCA and or RAP that you believe is important to this issue? Please specify

Appendix B

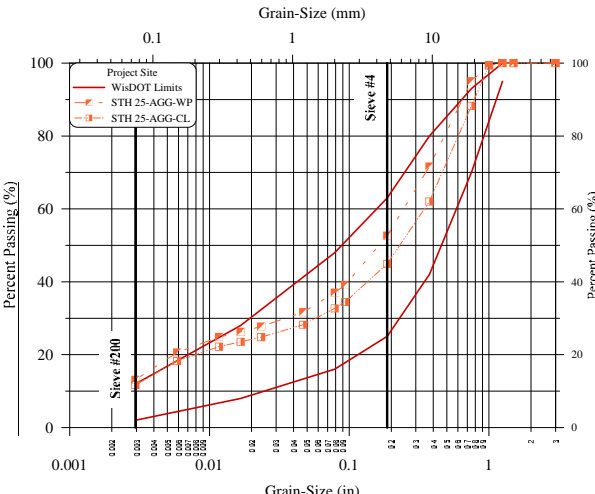
Particle Size Distribution of the Investigated Base Aggregates



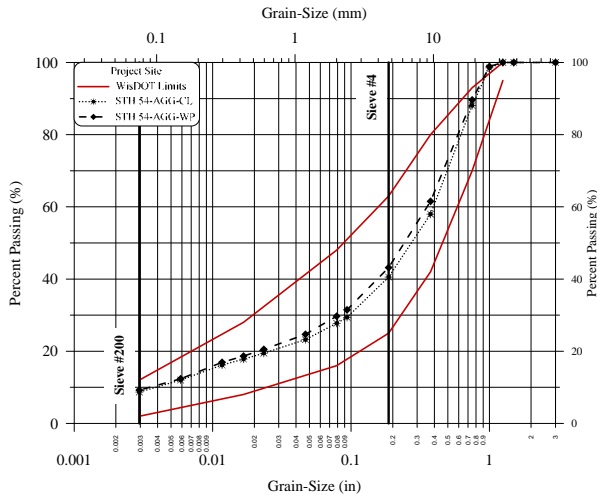
(a): CTH T WP and CL



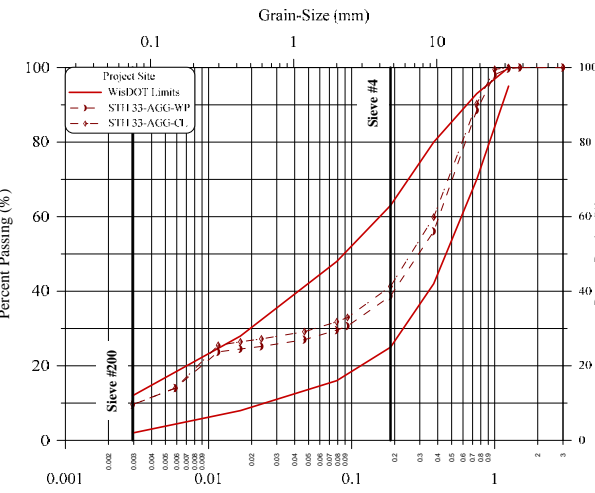
(b): STH 22 WP and CL



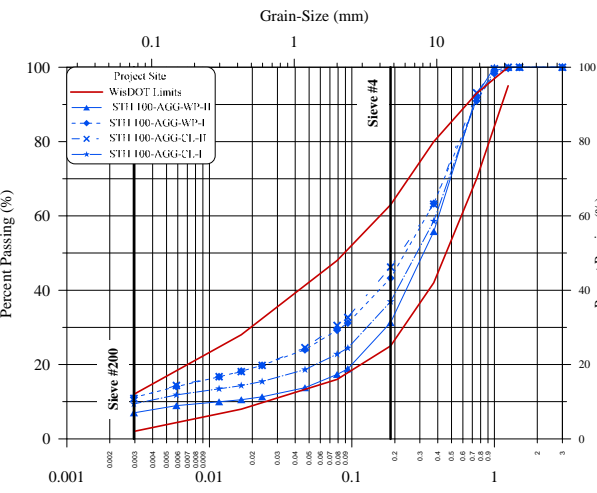
(c): STH 25 WP and CL



(d): STH 54 WP and CL

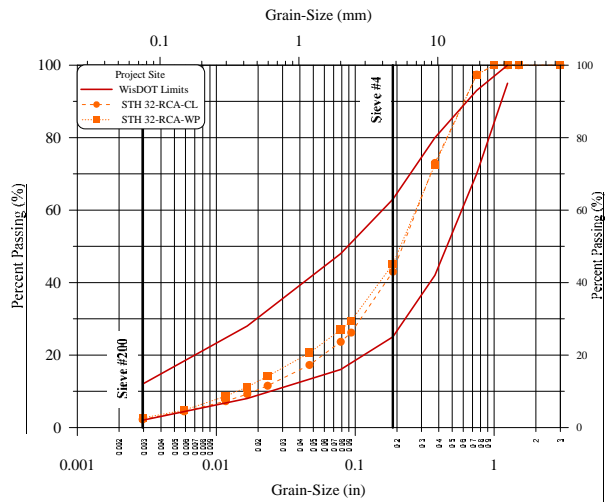


(e): STH 33 WP and CL

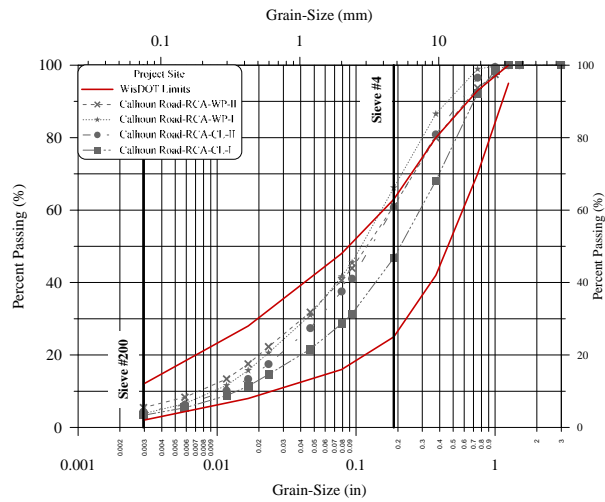


(f): STH 100 WP-I, II and CL-I, II

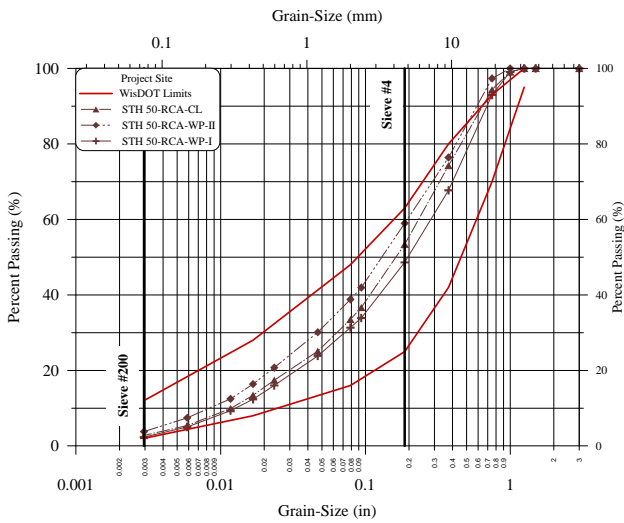
Figure B1: Particle size distribution of the investigated crushed aggregate base course and the current WisDOT gradation specification limits for the 1¼" dense graded base course materials.



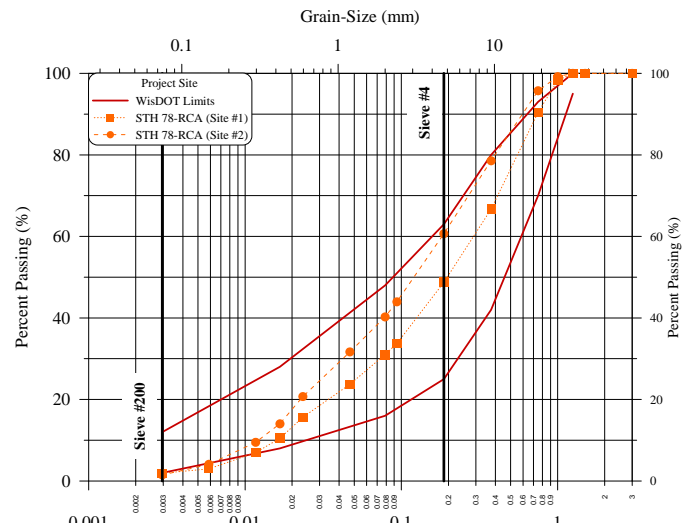
(a): STH 32 WP and CL



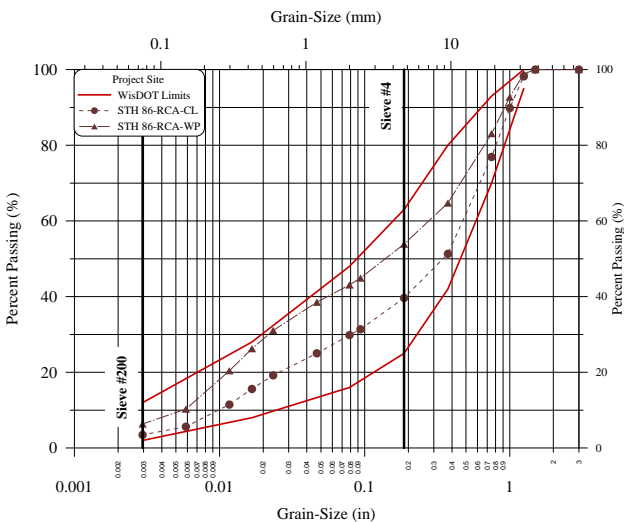
(b): Calhoun WP-I, II and CL-I, II



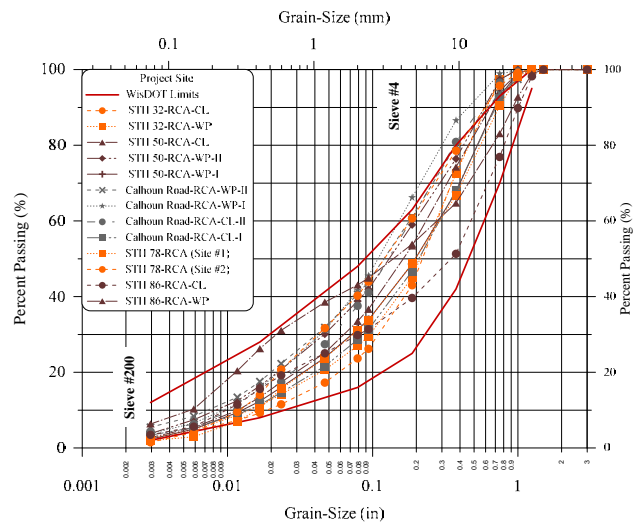
(c): STH 50 WP-I, II and CL



(d): STH 78 (site#1), (site#2)



(e): STH 86 WP and CL



(f): All RCA Project

Figure B2: Particle size distribution of the investigated RCA base course and the current WisDOT gradation specification limits for the 1¼" dense graded base course materials.

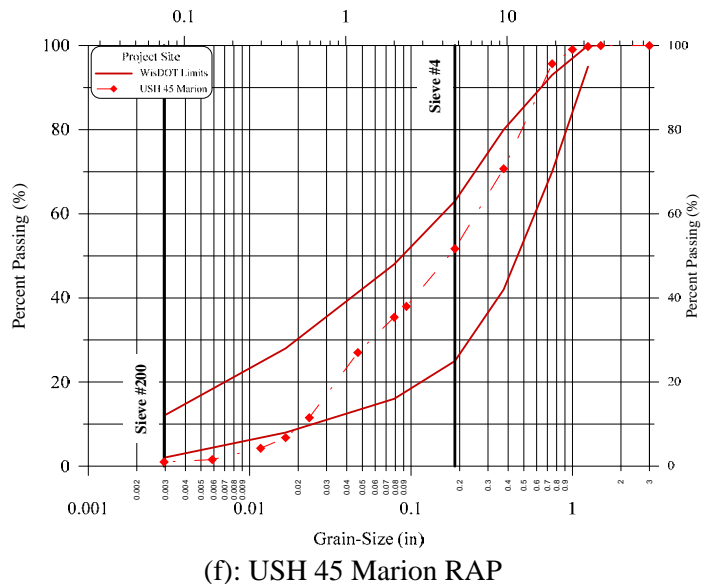
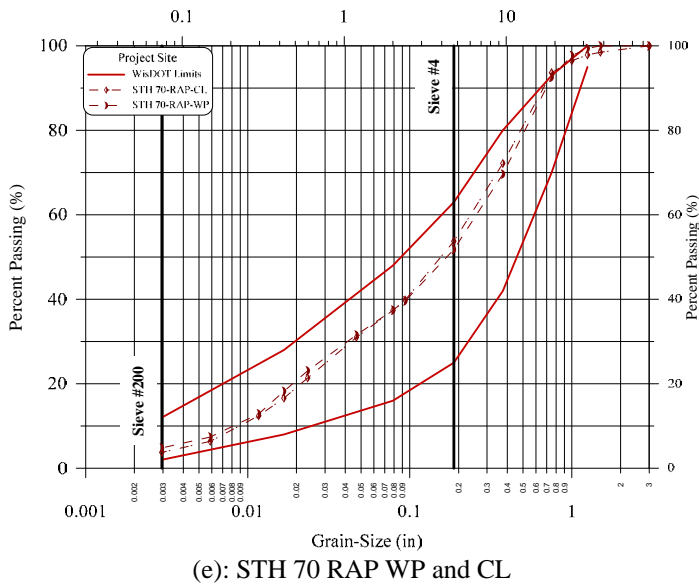
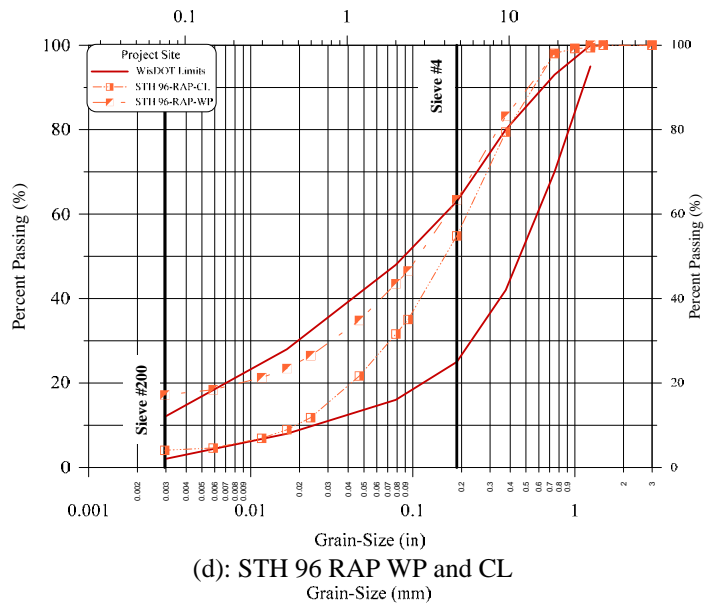
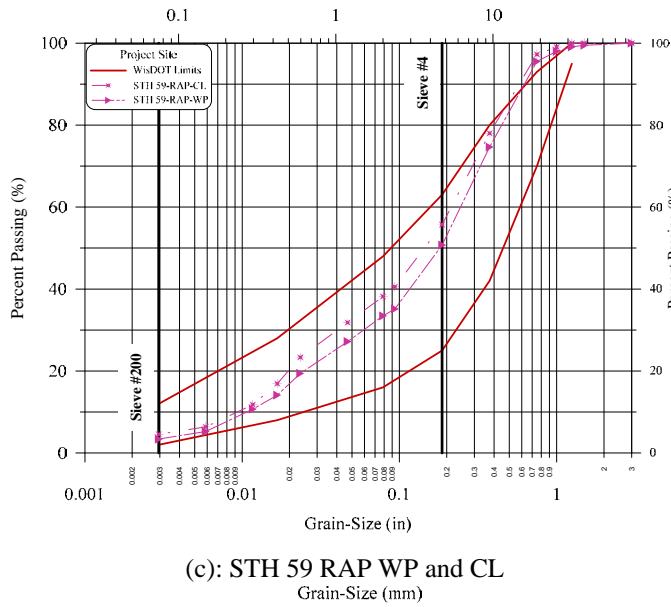
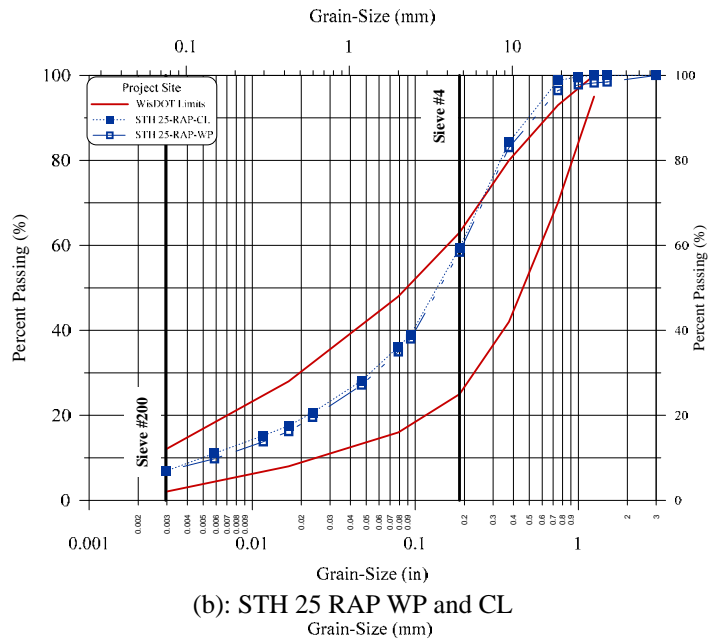
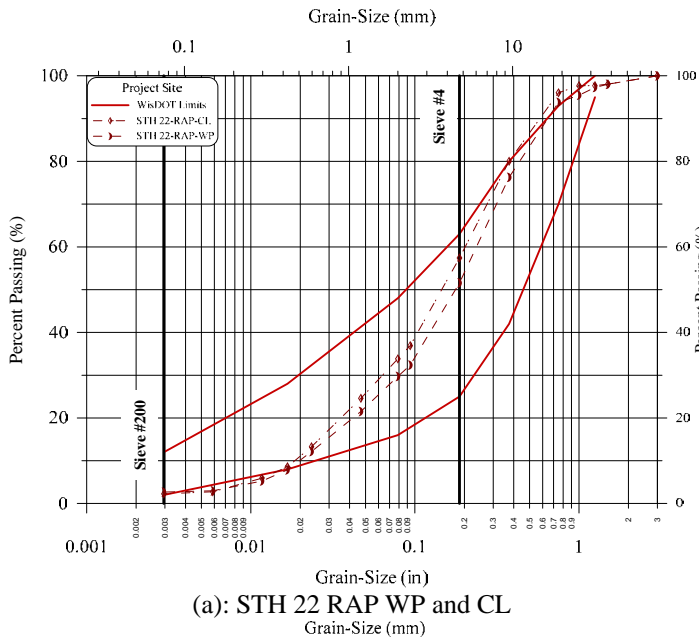
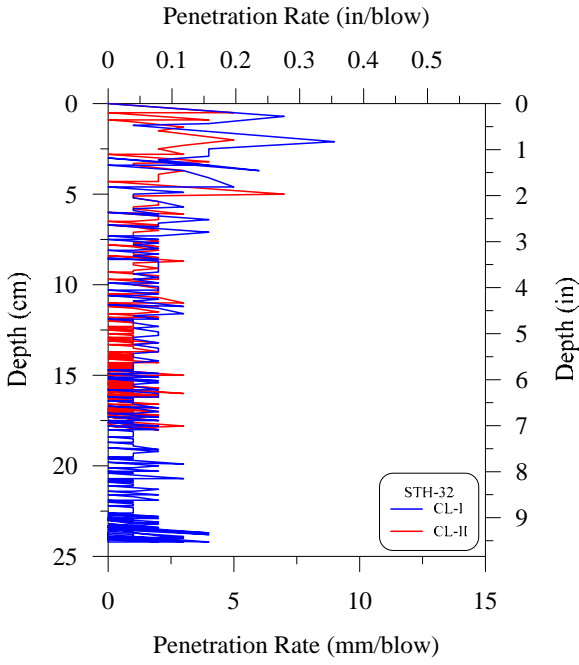


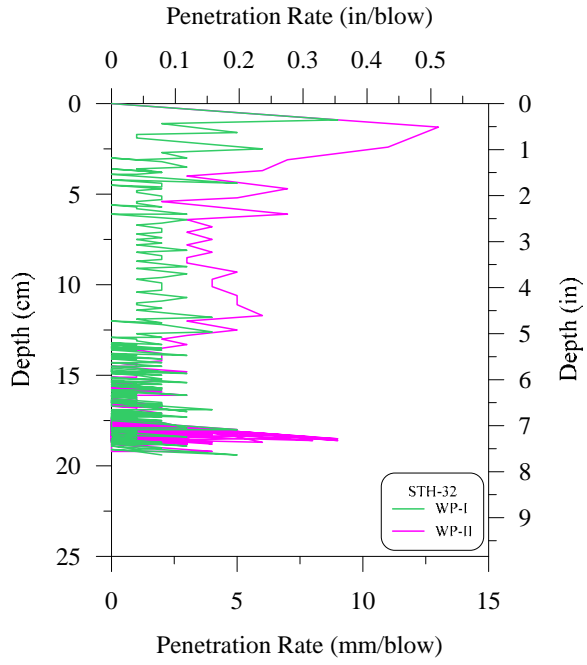
Figure B3: Particle size distribution of the investigated RAP base course and the current WisDOT gradation specification limits for the 1¼" dense graded base course materials.

Appendix C

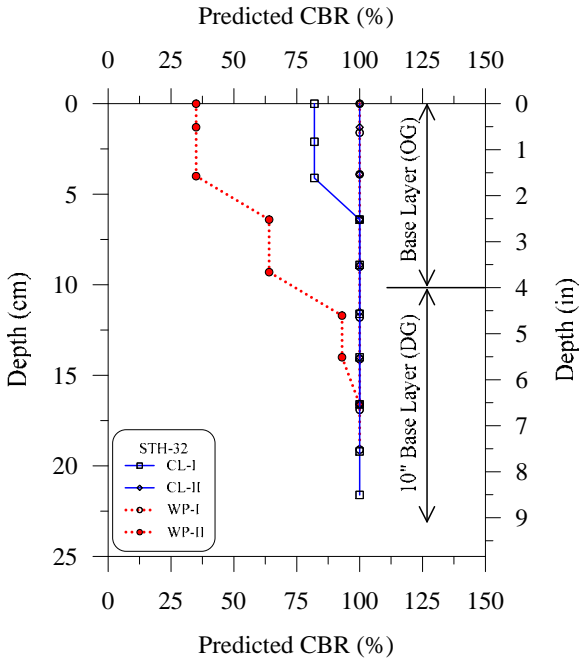
Dynamic Cone Penetrometer Test Results



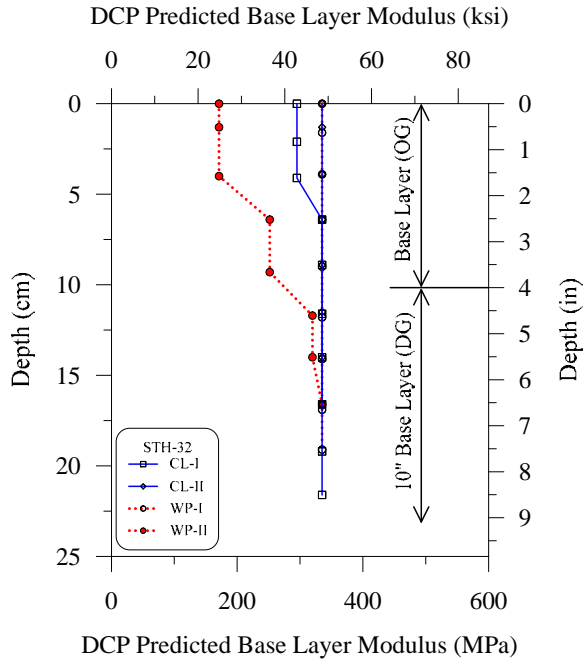
(a) DCP tests STH 32, CL-I, CL-II



(b) DCP tests STH 32, WP-I, WP-II

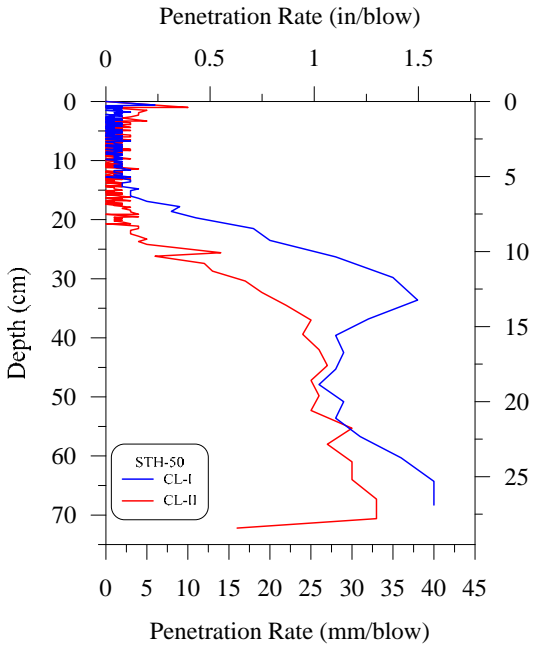


(c) Predicted CBR (%) STH 32

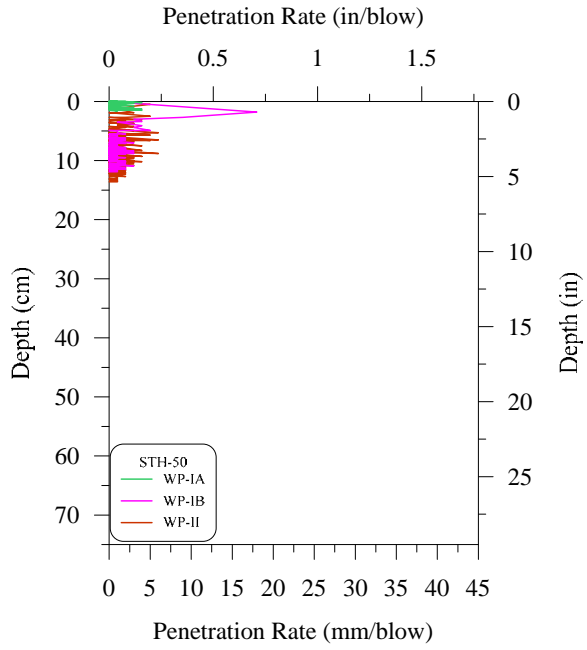


(d) Base layer modulus by DCP test STH 32

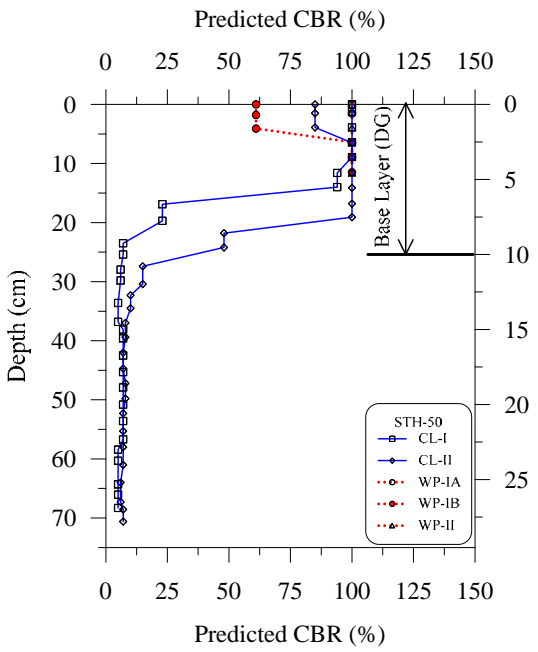
Figure C1: Penetration resistance with depth from DCP and distribution with depth of estimated CBR and base layer modulus from DCP test (RCA Base Coarse STH 32).



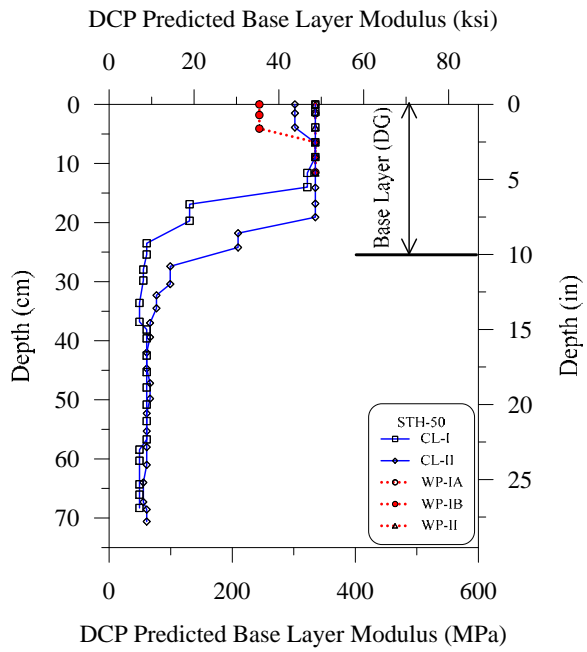
(a) DCP tests STH 50, CL-I, CL-II



(b) DCP tests STH 50, WP-IA, WP-IB, WP-II

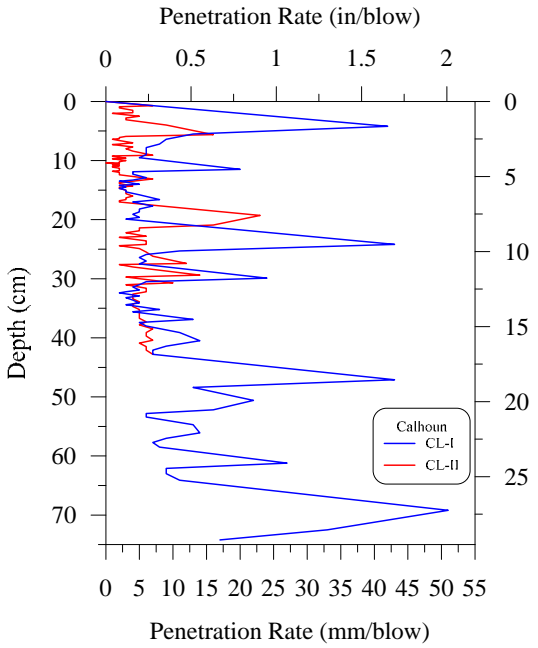


(c) Predicted CBR (%) STH 50

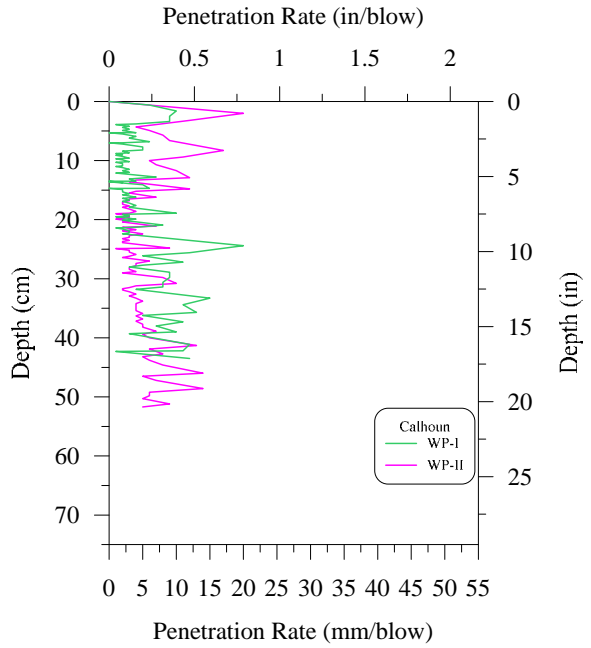


(d) Base layer modulus by DCP test STH 50

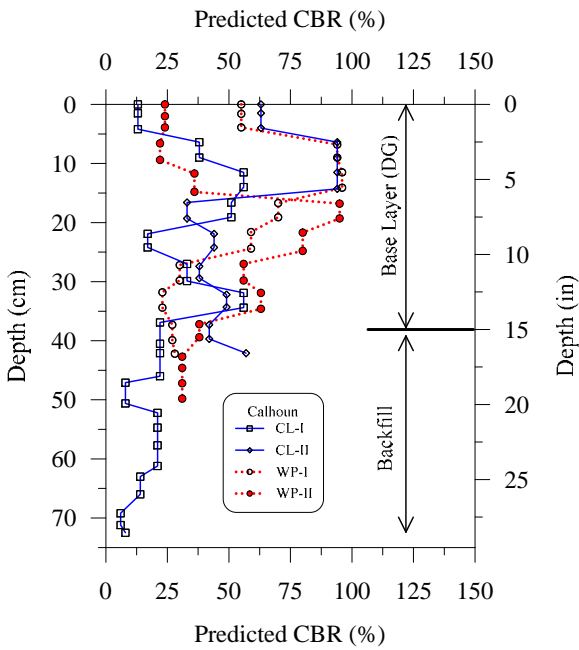
Figure C2: Penetration resistance with depth from DCP and distribution with depth of estimated CBR and base layer modulus from DCP test (RCA Base Coarse STH 50).



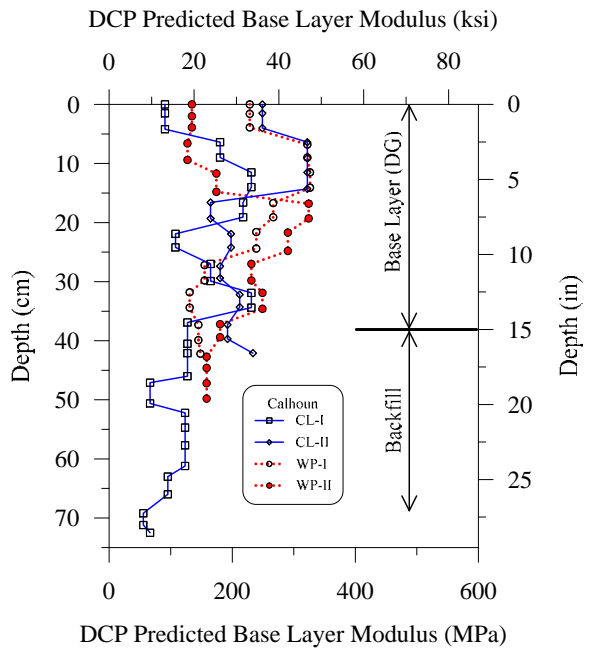
(a) DCP tests Calhoun, CL-I, CL-II



(b) DCP tests Calhoun, WP-I, WP-II

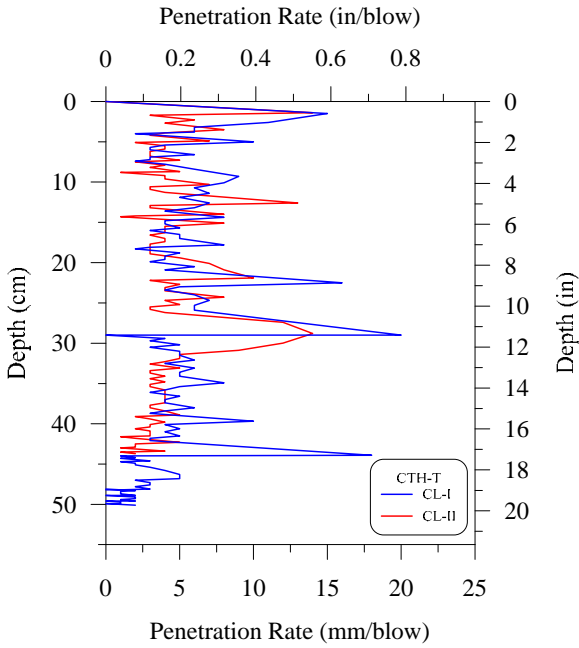


(c) Predicted CBR (%) Calhoun

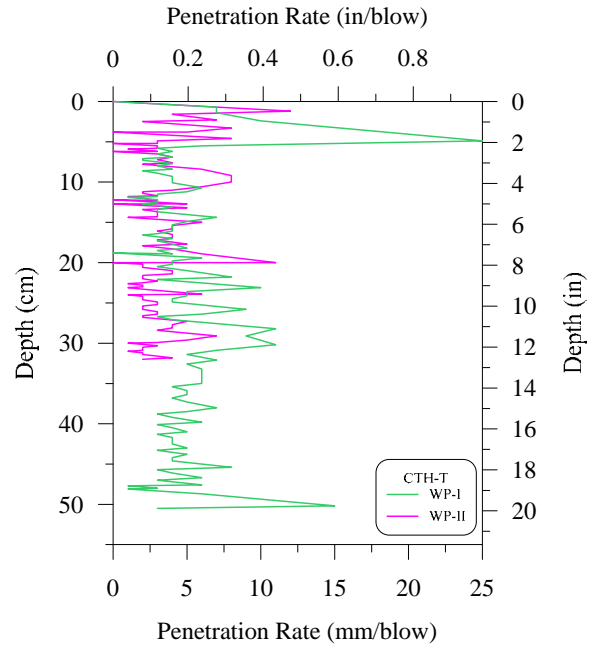


(d) Base layer modulus by DCP test Calhoun

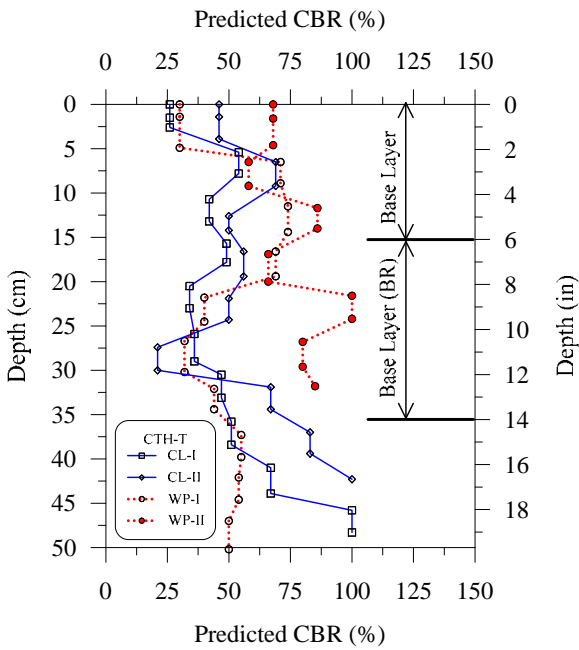
Figure C3: Penetration resistance with depth from DCP and distribution with depth of estimated CBR and base layer modulus from DCP test (RCA Base Coarse Calhoun).



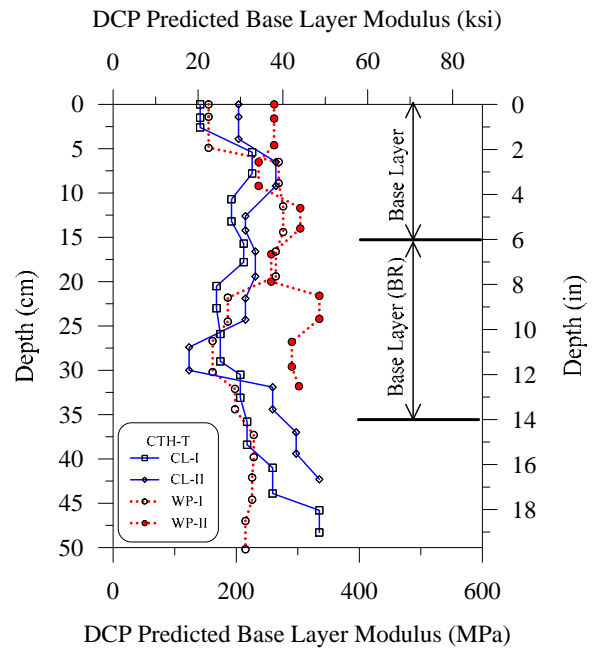
(a) DCP tests CTH T, CL-I, CL-II



(b) DCP tests CTH T, WP-I, WP-II

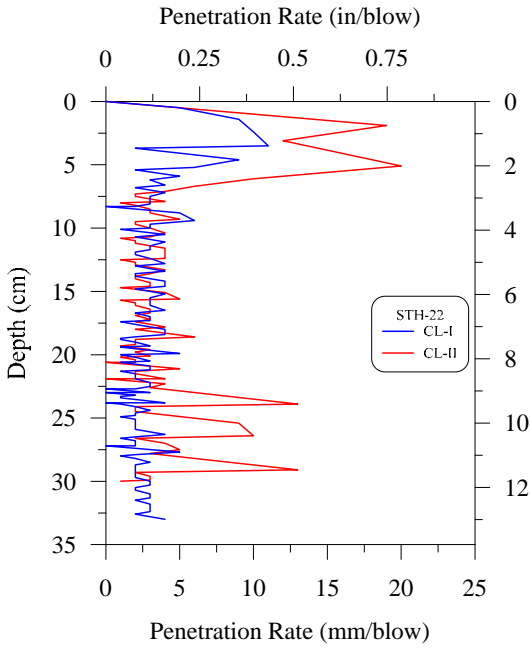


(c) Predicted CBR (%) CTH T

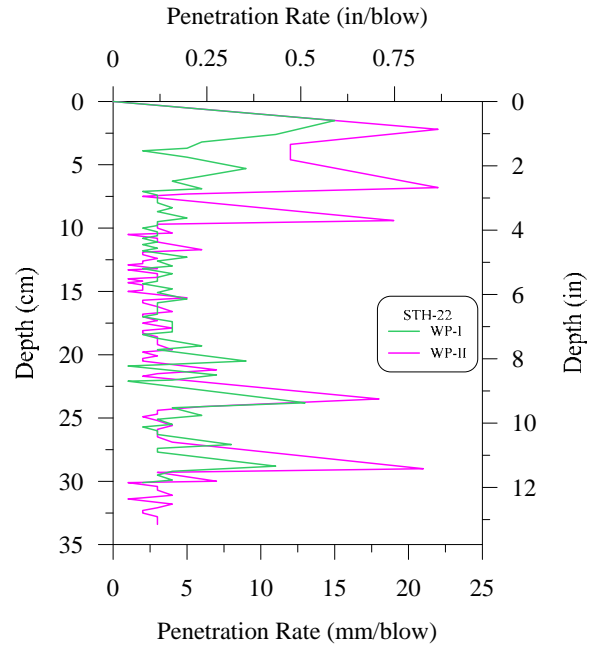


(d) Base layer modulus by DCP test CTH T

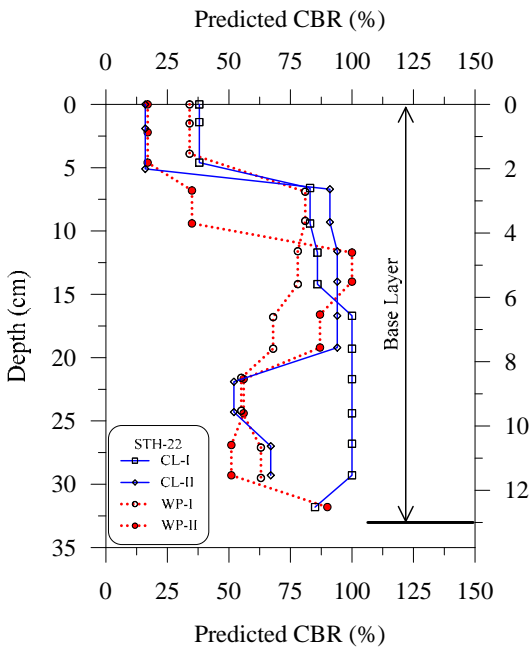
Figure C4: Penetration resistance with depth from DCP and distribution with depth of estimated CBR and base layer modulus from DCP test (CA CTH T).



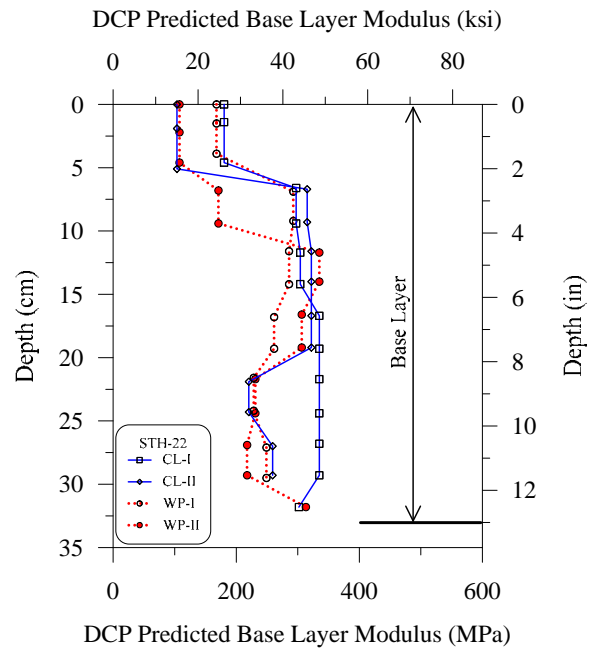
(a) DCP tests STH 22, CL-I, CL-II



(b) DCP tests STH 22, WP-I, WP-II

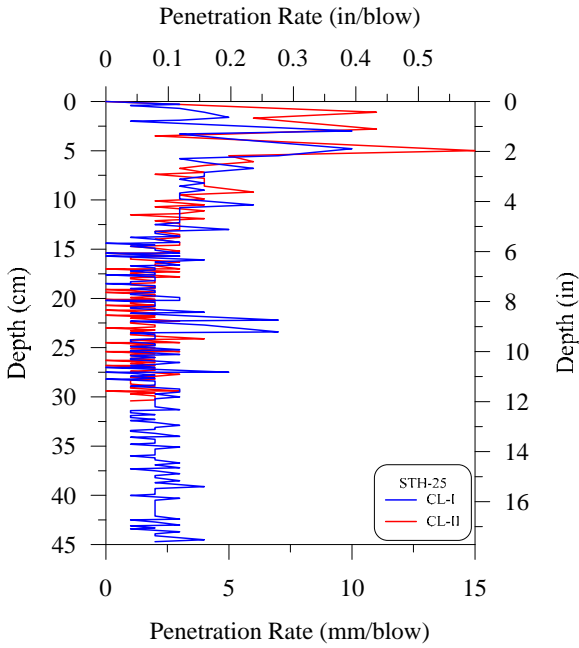


(c) Predicted CBR (%) STH 22

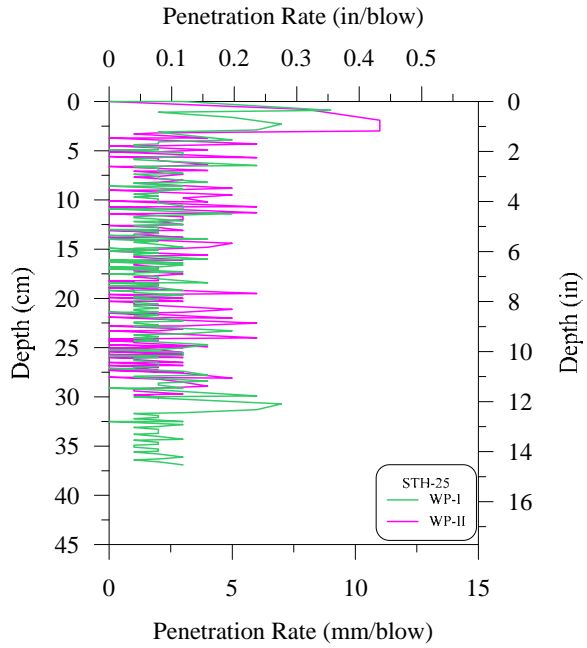


(d) Base layer modulus by DCP test STH 22

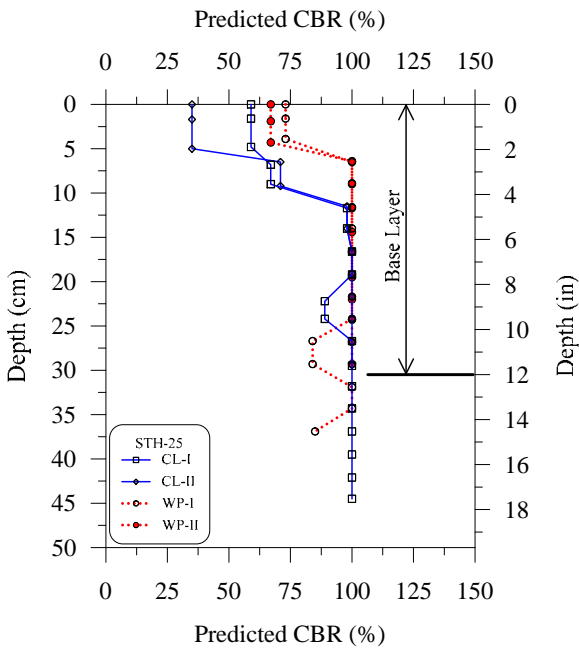
Figure C5: Penetration resistance with depth from DCP and distribution with depth of estimated CBR and base layer modulus from DCP test (CA STH 22).



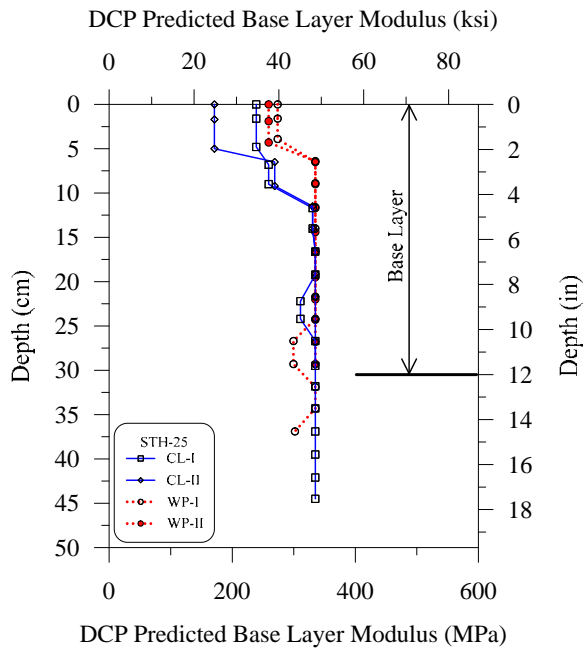
(a) DCP tests STH 25, CL-I, CL-II



(b) DCP tests STH 25, WP-I, WP-II

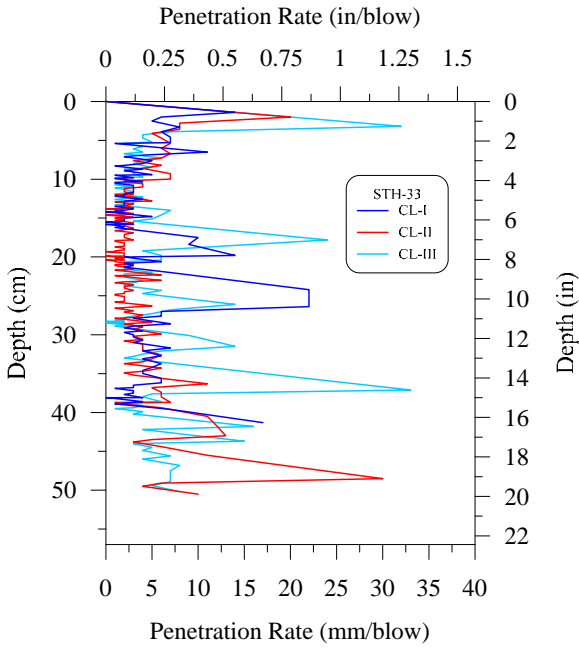


(c) Predicted CBR (%) STH 25

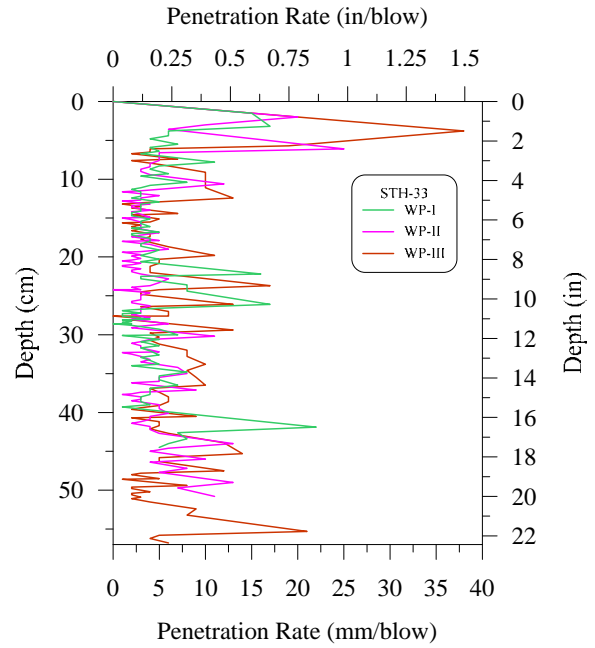


(d) Base layer modulus by DCP test STH 25

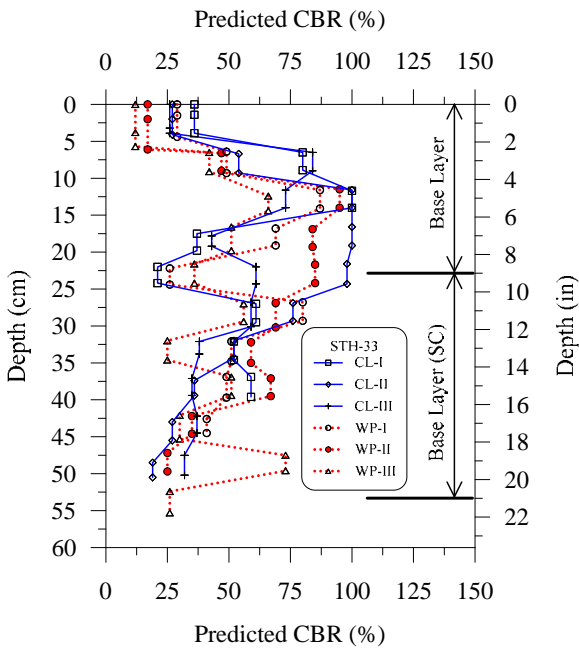
Figure C6: Penetration resistance with depth from DCP and distribution with depth of estimated CBR and base layer modulus from DCP test (CA STH 25).



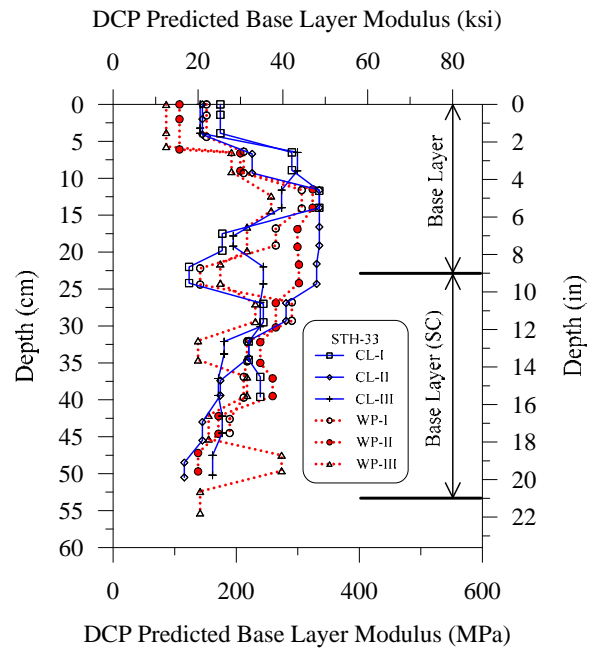
(a) DCP tests STH 33, CL-I, CL-II, CL-III



(b) DCP tests STH 33, WP-I, WP-II, WP-III

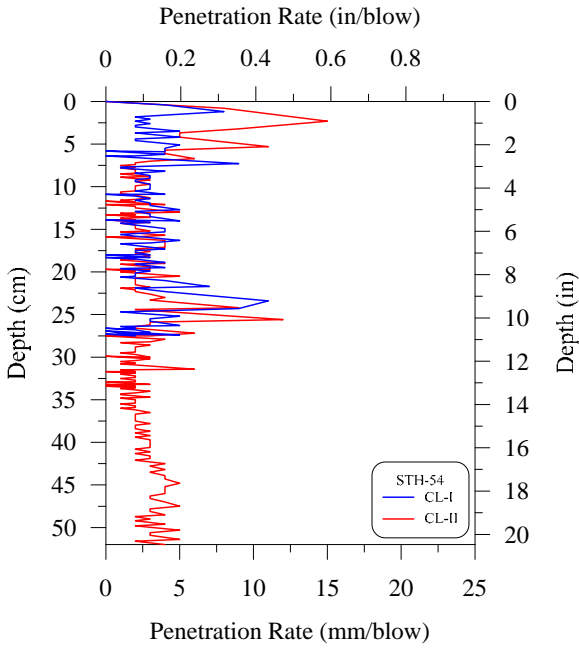


(c) Predicted CBR (%) STH 33

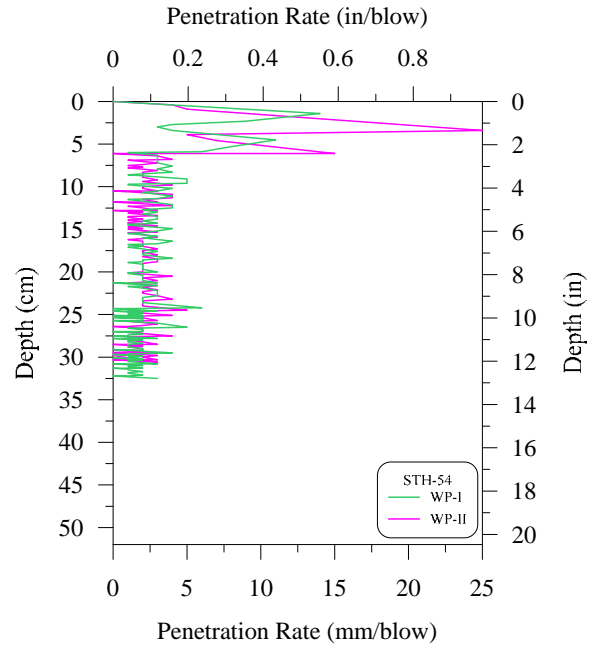


(d) Base layer modulus by DCP test STH 33

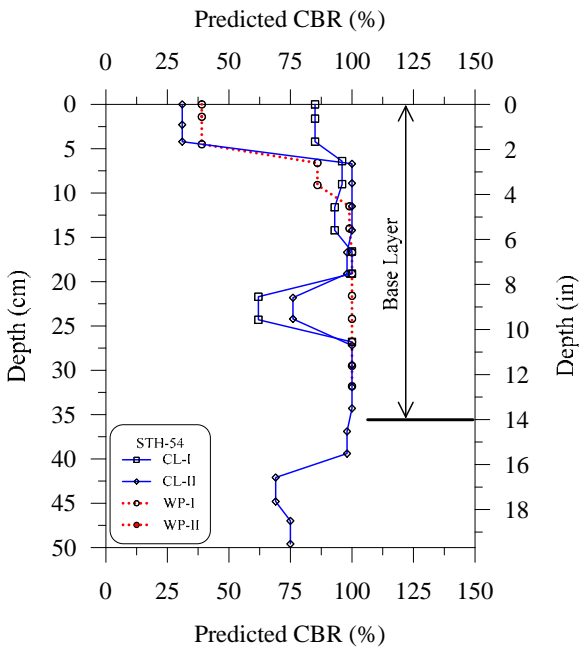
Figure C7: Penetration resistance with depth from DCP and distribution with depth of estimated CBR and base layer modulus from DCP test (CA STH 33).



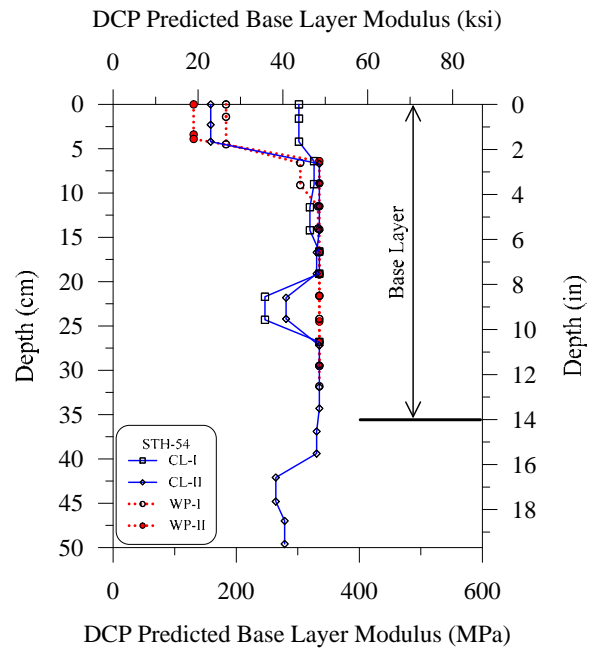
(a) DCP tests STH 54, CL-I, CL-II



(b) DCP tests STH 54, WP-I, WP-II

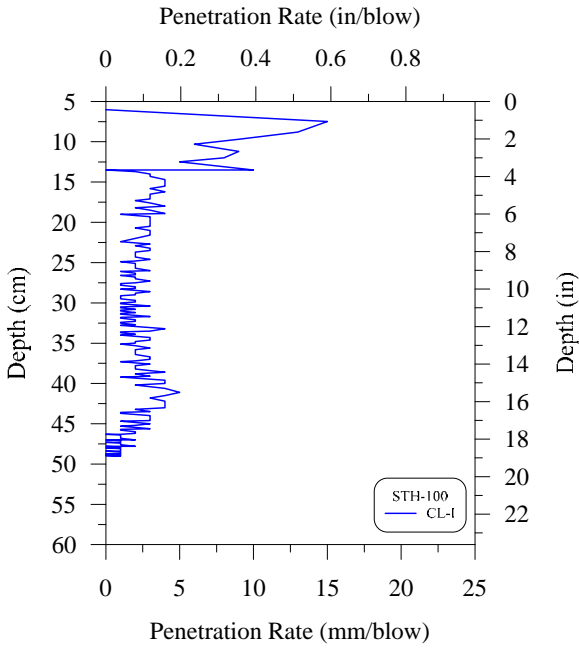


(c) Predicted CBR (%) STH 54

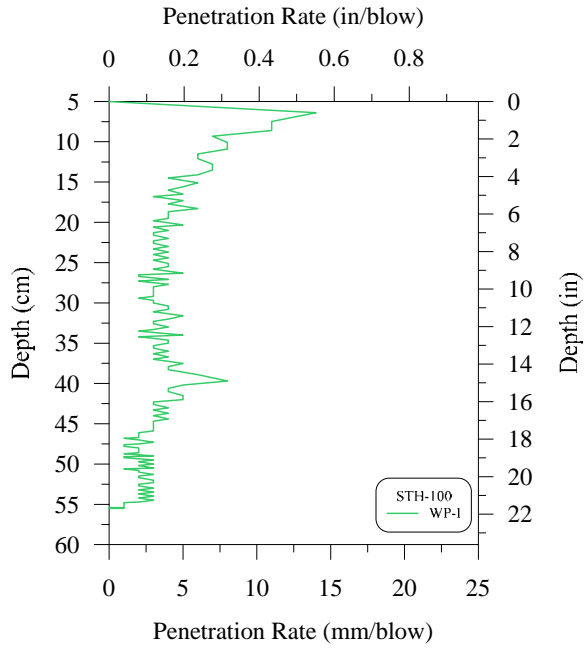


(d) Base layer modulus by DCP test STH 54

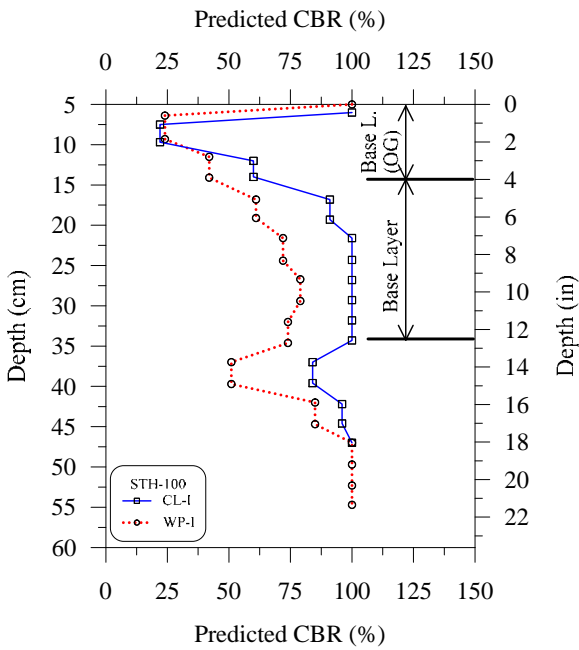
Figure C8: Penetration resistance with depth from DCP and distribution with depth of estimated CBR and base layer modulus from DCP test (CA STH 54).



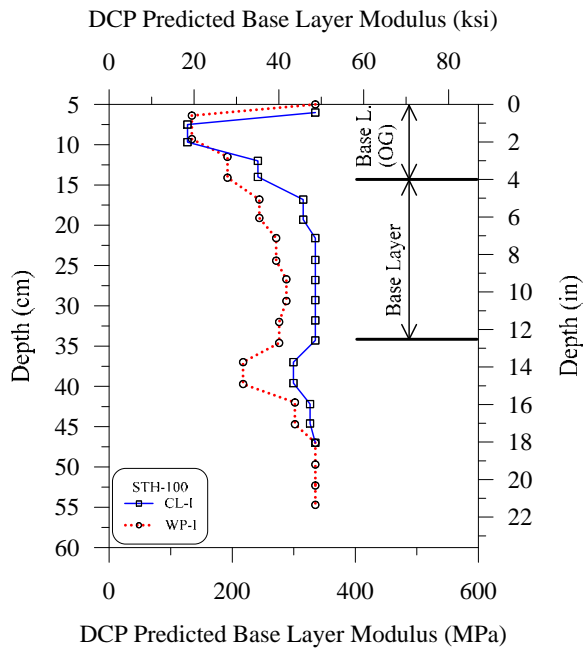
(a) DCP tests STH 100, CL-I



(b) DCP tests STH 100, WP-I

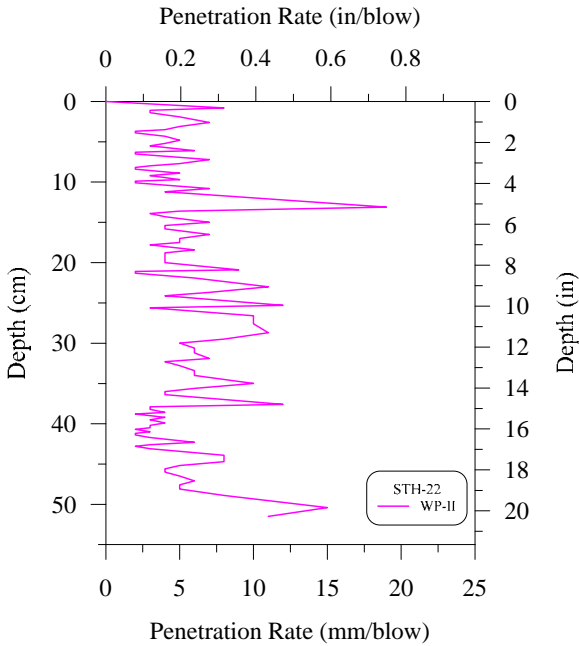


(c) Predicted CBR (%) STH 100

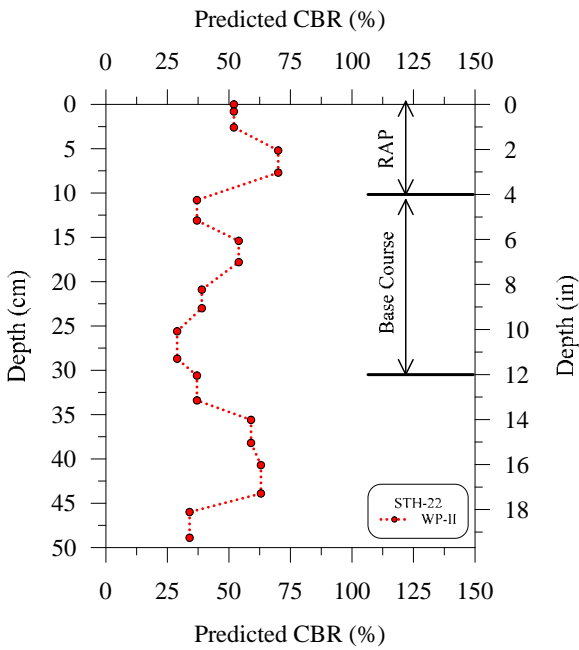


(d) Base layer modulus by DCP test STH 100

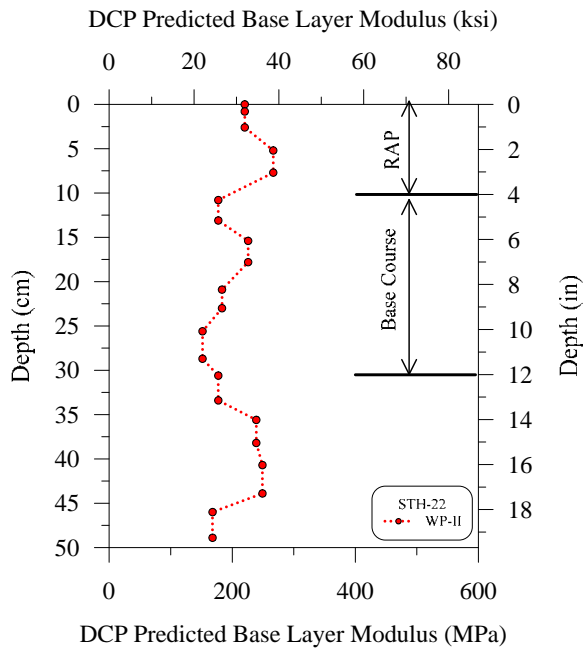
Figure C9: Penetration resistance with depth from DCP and distribution with depth of estimated CBR and base layer modulus from DCP test (RCA STH 100).



(a) DCP tests STH 22, WP-II

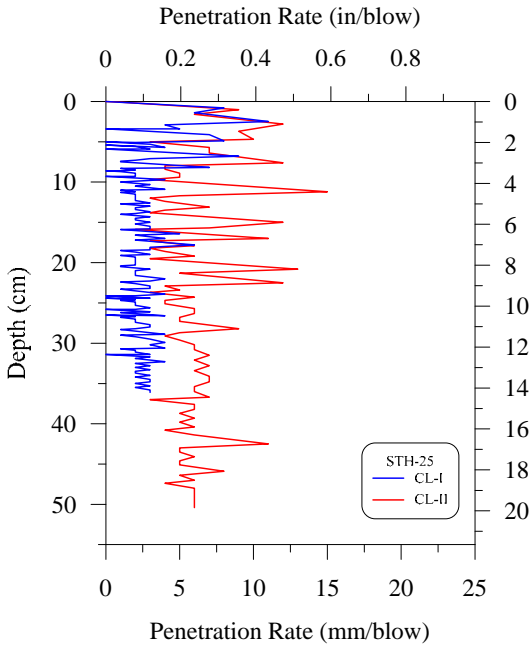


(b) Predicted CBR (%) STH 22

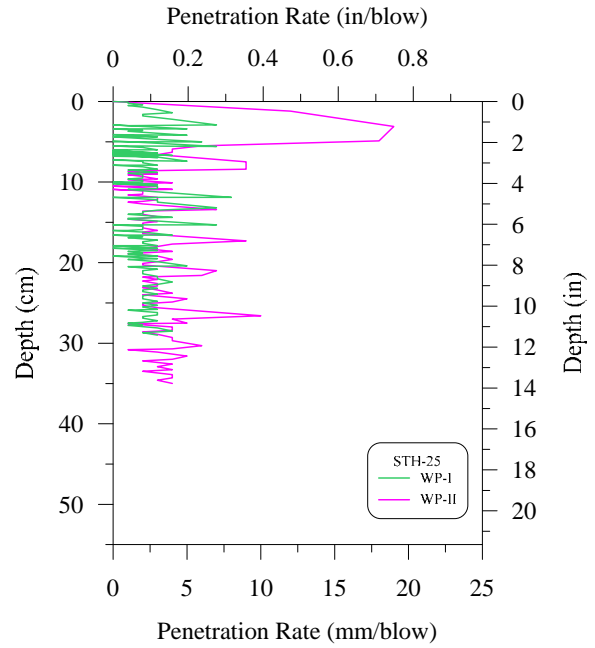


(c) Base layer modulus by DCP test STH 22

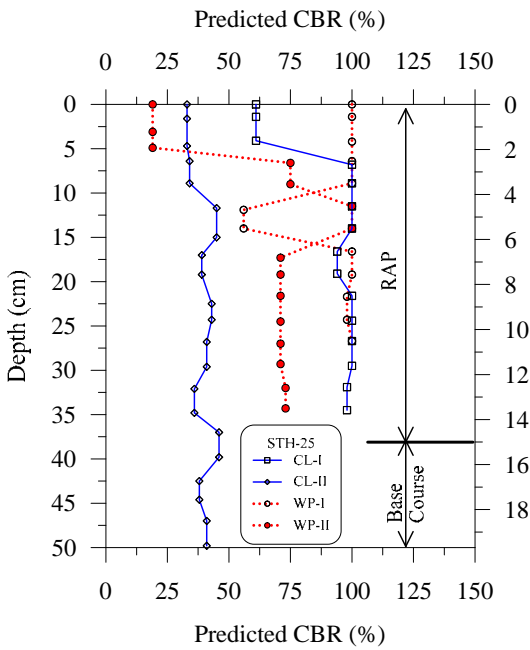
Figure C10: Penetration resistance with depth from DCP and distribution with depth of estimated CBR and base layer modulus from DCP test (RAP STH 22).



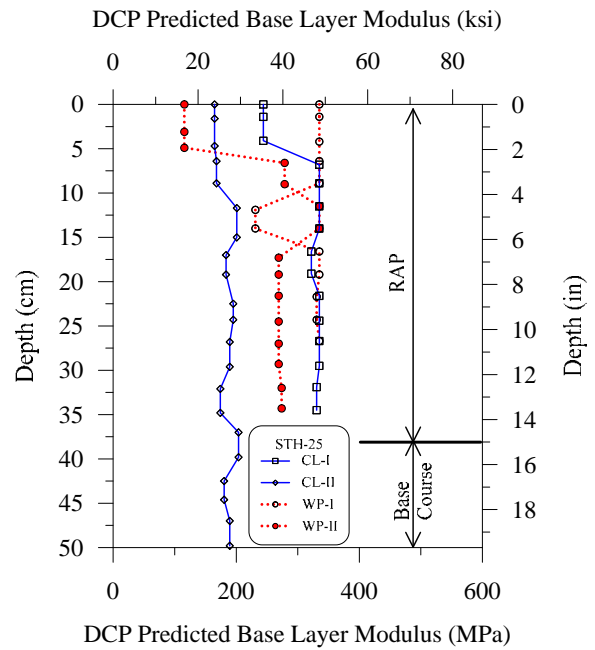
(a) DCP tests STH 25, CL-I, CL-II



(b) DCP tests STH 25, WP-I, WP-II

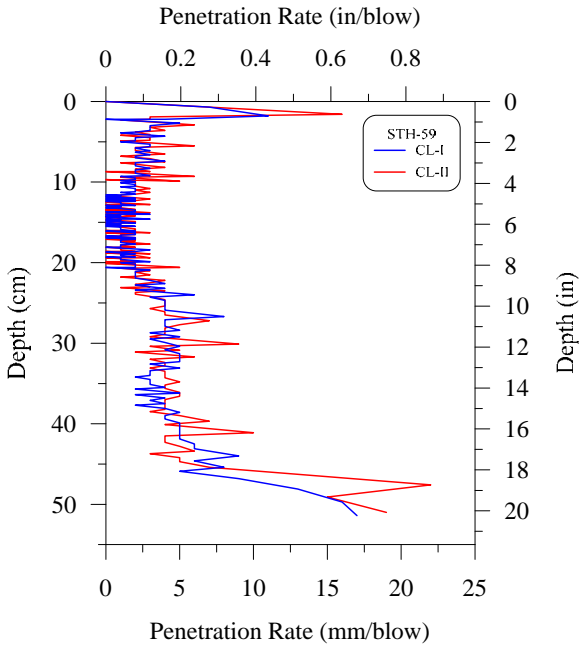


(c) Predicted CBR (%) STH 25

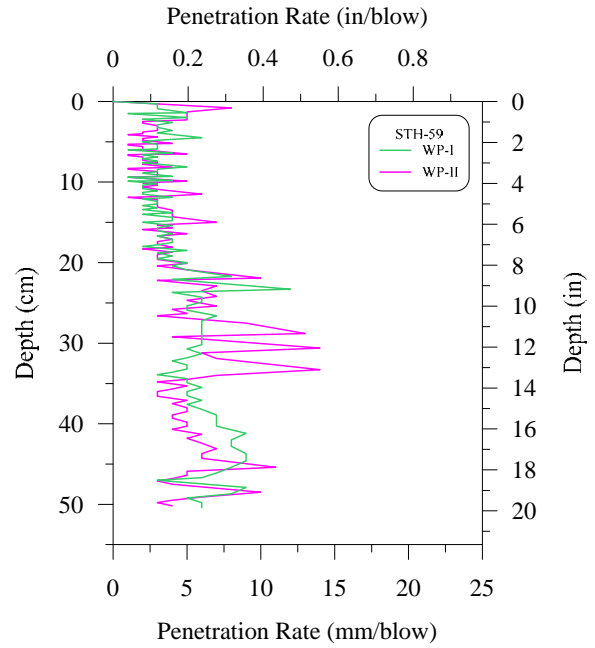


(d) Base layer modulus by DCP test STH 25

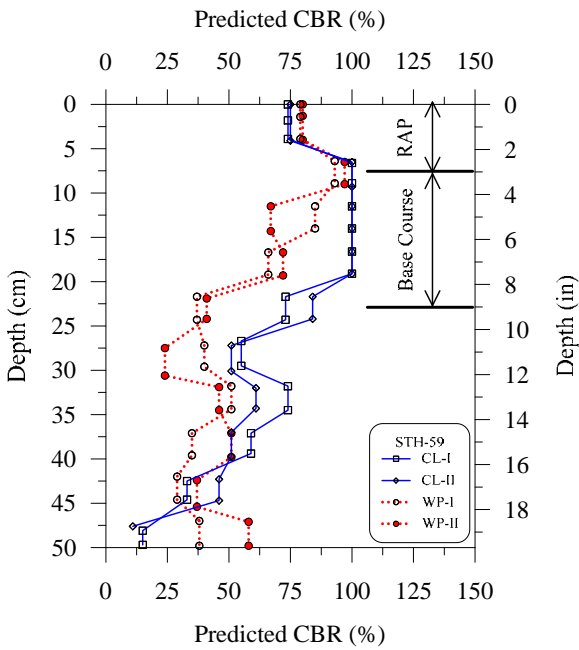
Figure C11: Penetration resistance with depth from DCP and distribution with depth of estimated CBR and base layer modulus from DCP test (RAP STH 25).



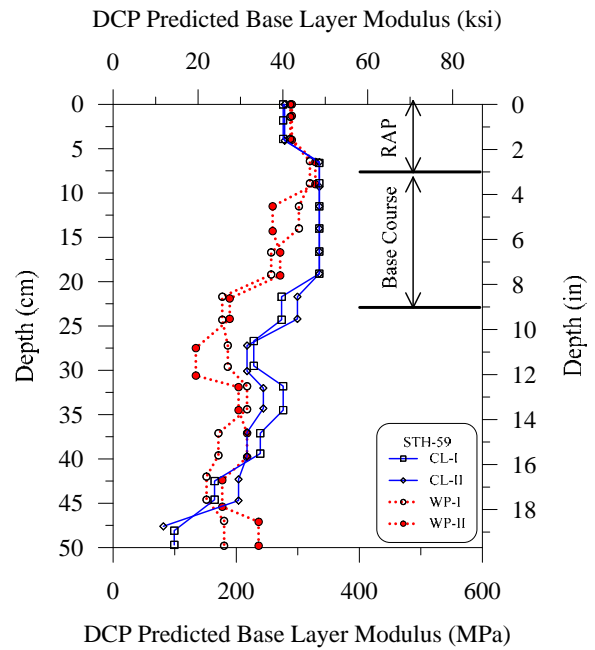
(a) DCP tests STH 59, CL-I, CL-II



(b) DCP tests STH 59, WP-I, WP-II

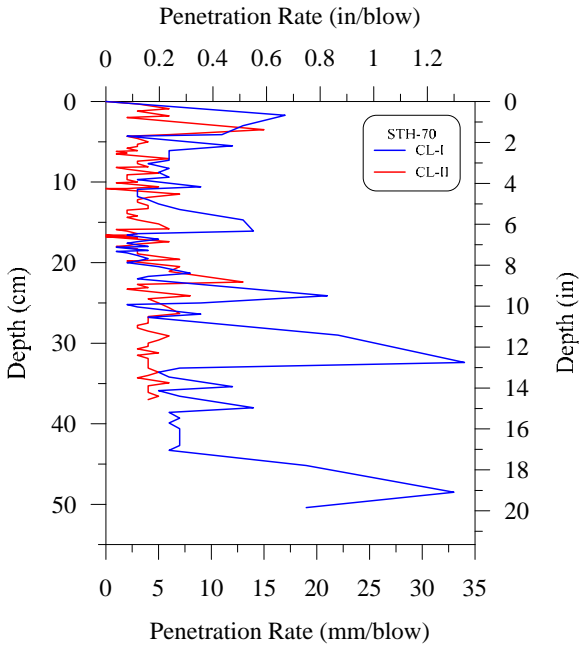


(c) Predicted CBR (%) STH 59

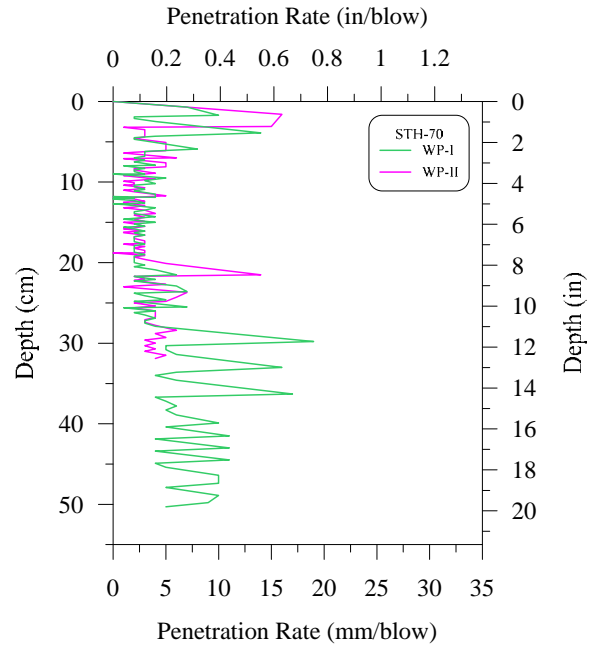


(d) Base layer modulus by DCP test STH 59

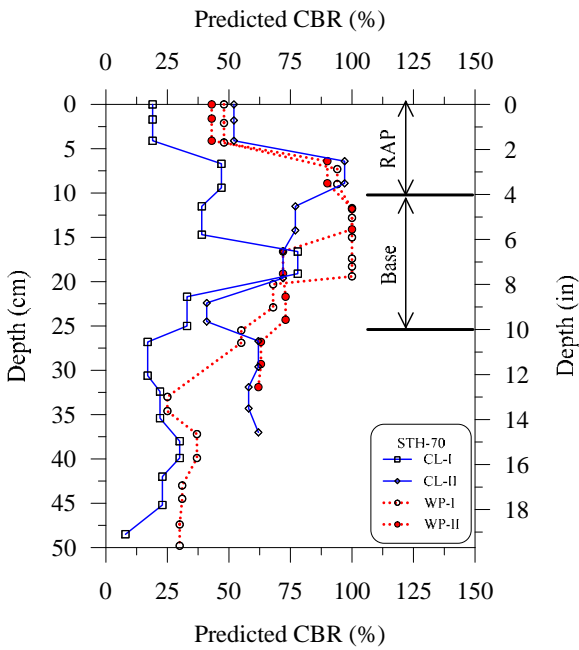
Figure C12: Penetration resistance with depth from DCP and distribution with depth of estimated CBR and base layer modulus from DCP test (RAP STH 59).



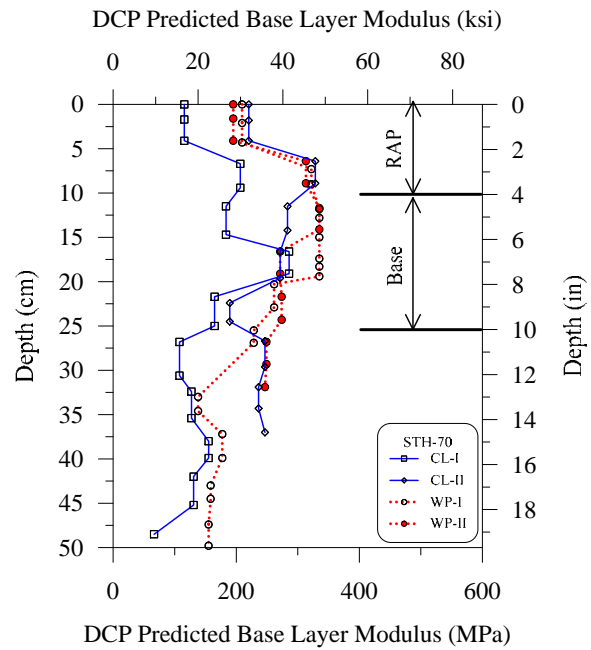
(a) DCP tests STH 70, CL-I, CL-II



(b) DCP tests STH 70, WP-I, WP-II

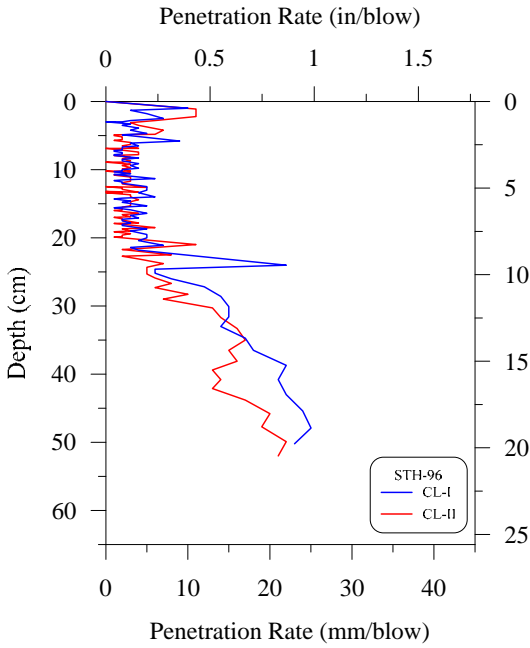


(c) Predicted CBR (%) STH 70

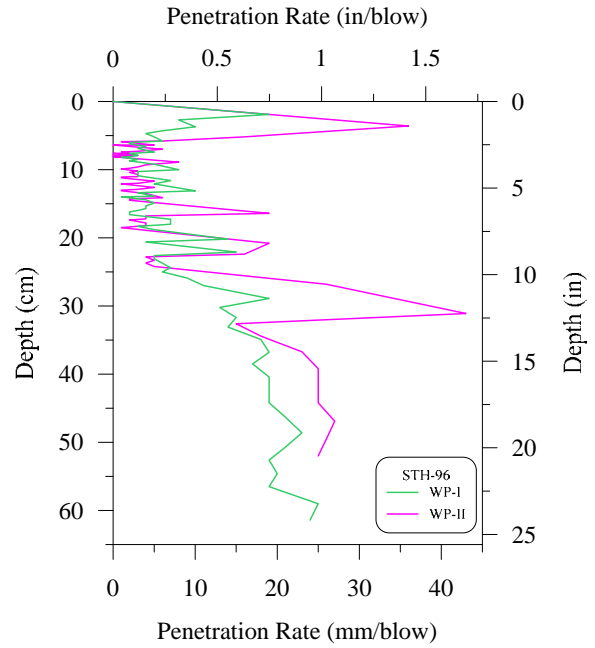


(d) Base layer modulus by DCP test STH 70

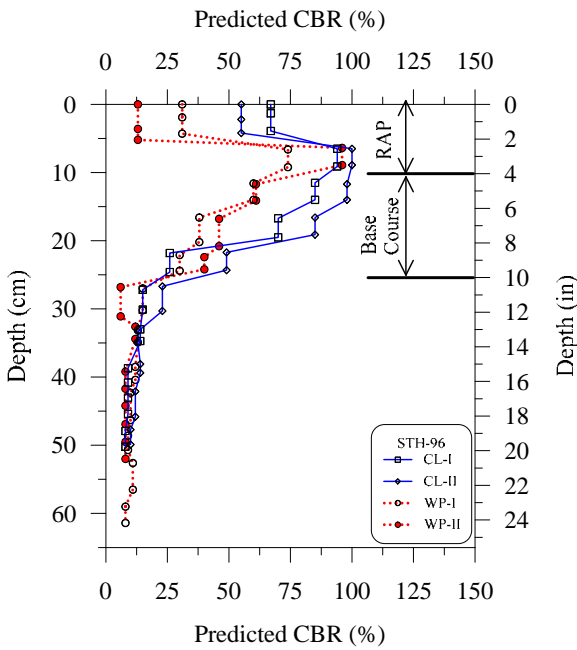
Figure C13: Penetration resistance with depth from DCP and distribution with depth of estimated CBR and base layer modulus from DCP test (RAP STH 70).



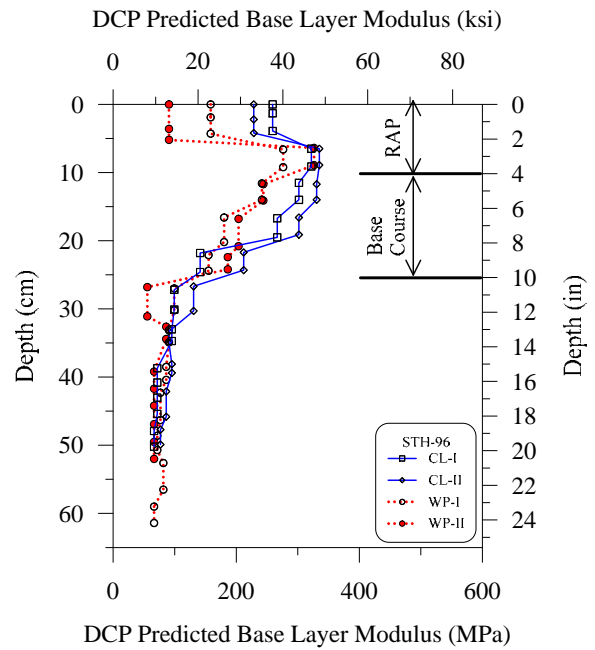
(a) DCP tests STH 96, CL-I, CL-II



(b) DCP tests STH 96, WP-I, WP-II



(c) Predicted CBR (%) STH 96



(d) Base layer modulus by DCP test STH 96

Figure C14: Penetration resistance with depth from DCP and distribution with depth of estimated CBR and base layer modulus from DCP test (RAP STH 96).

Appendix D

Typical Sections of the Investigate HMA Pavements and Measured Dimensions and Unit Weight of HMA Cores

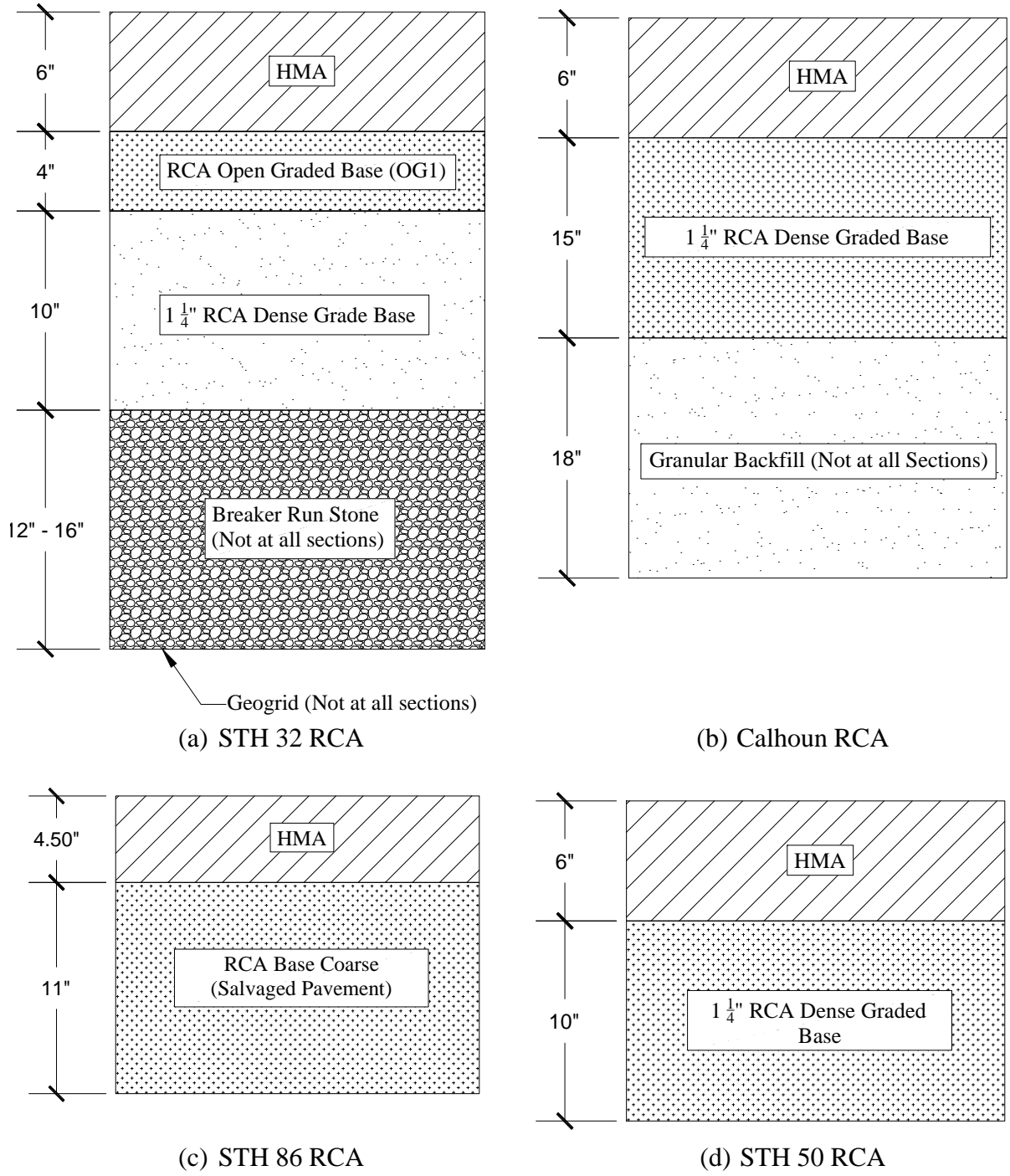
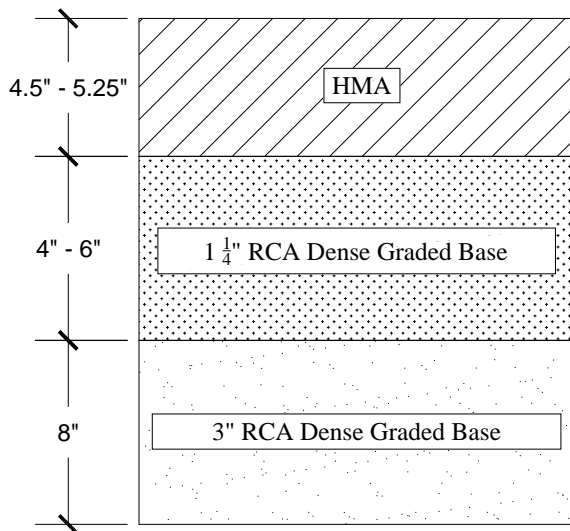
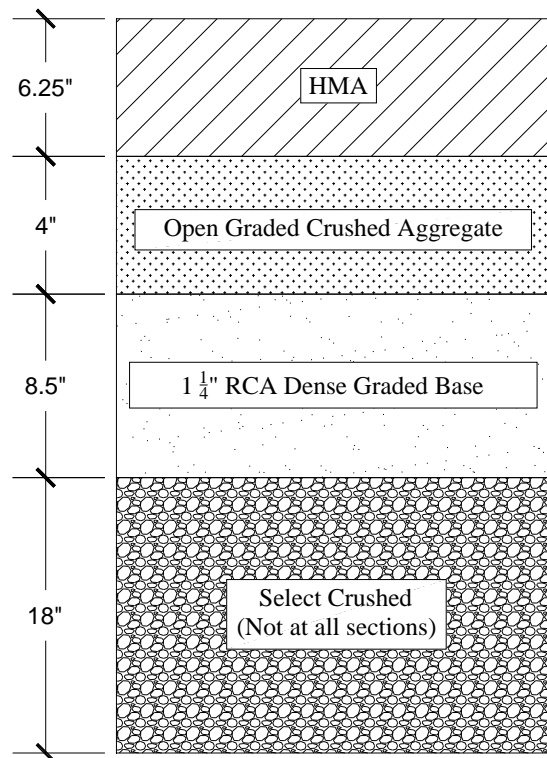


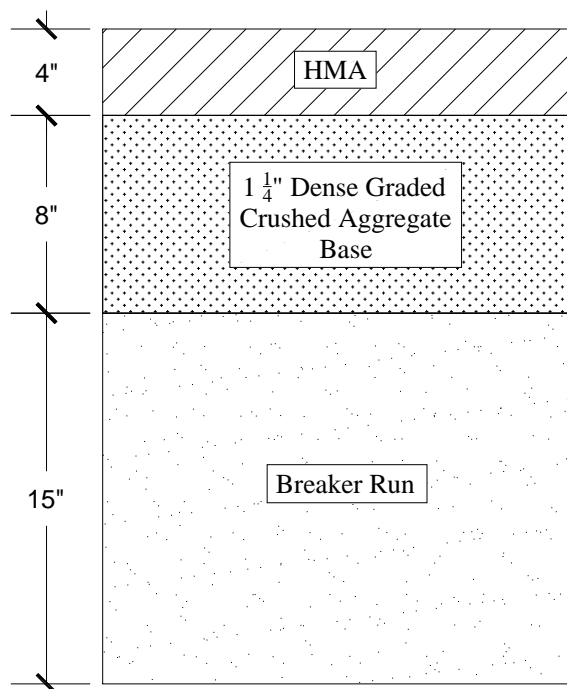
Figure D1: Typical sections of the investigate HMA pavements.



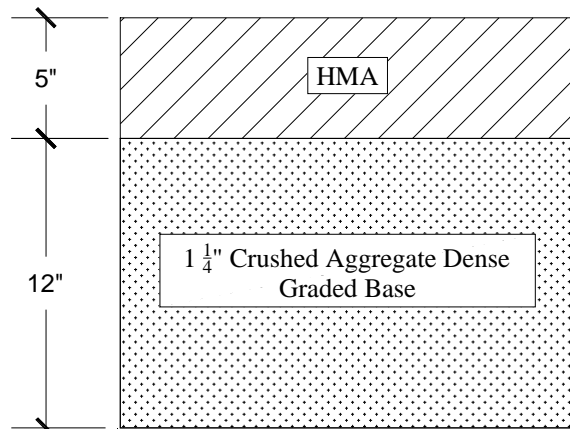
(a) STH 78 RCA



(b) STH 100 RCA

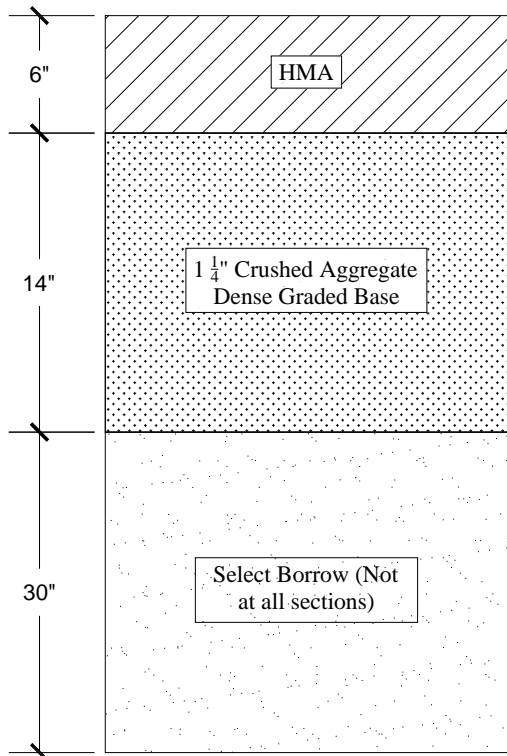


(c) STH 59 CA

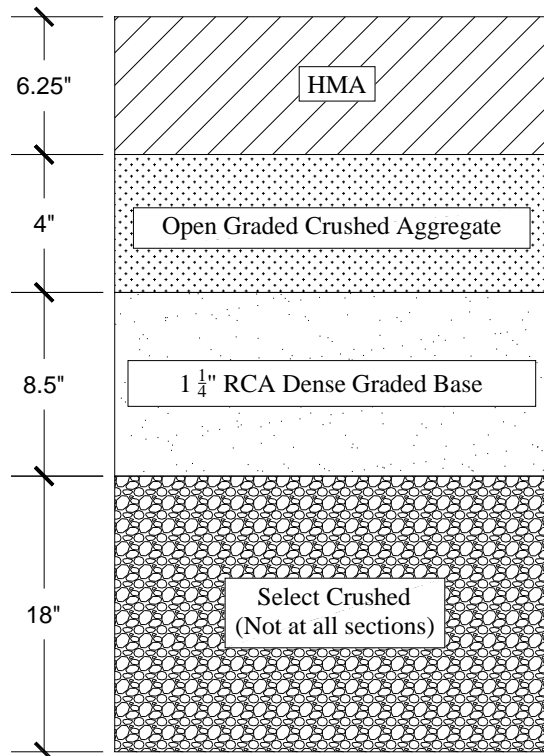


(d) STH 25 CA

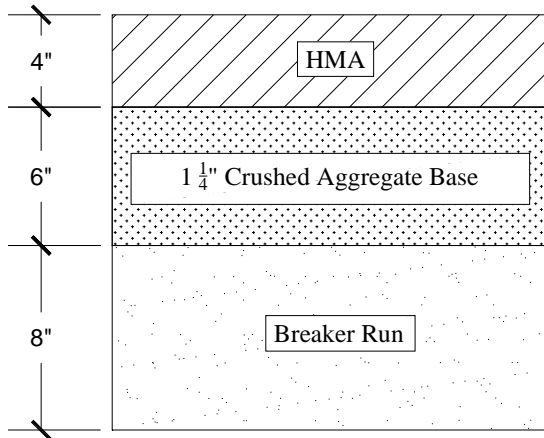
Figure D2: Typical sections of the investigate HMA pavements.



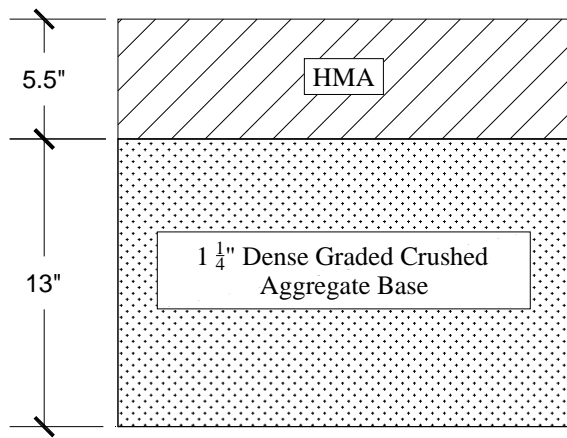
(a) STH 54-22 Waupaca CA



(b) STH 100 CA

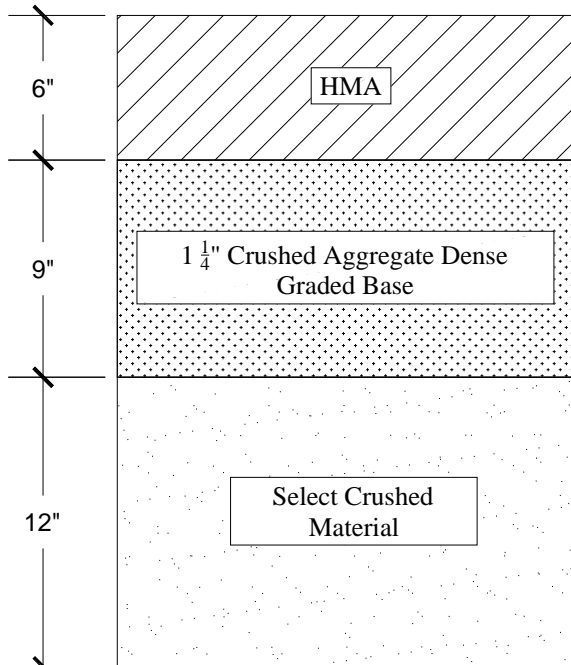


(c) CTH T CA

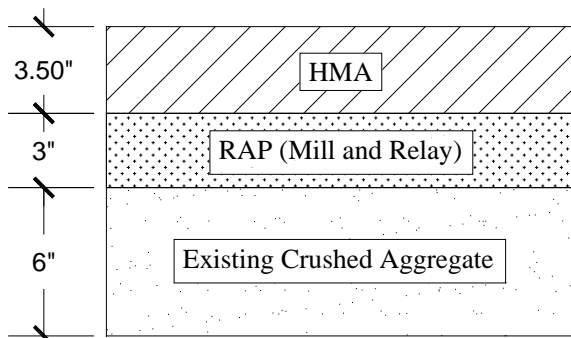


(d) STH 22 CA

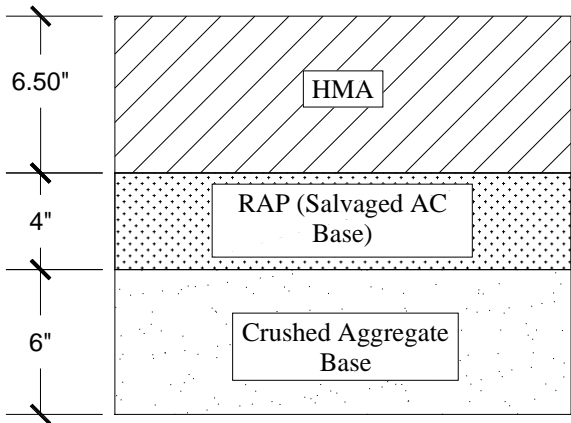
Figure D3: Typical sections of the investigate HMA pavements.



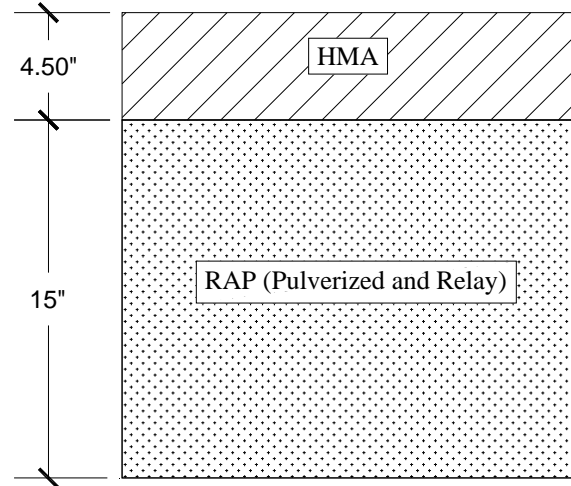
(a) STH 33 CA



(b) STH 59 RAP

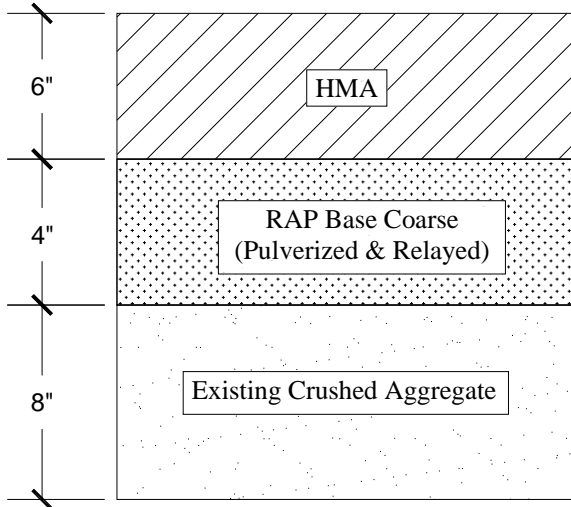


(c) STH 96 RAP

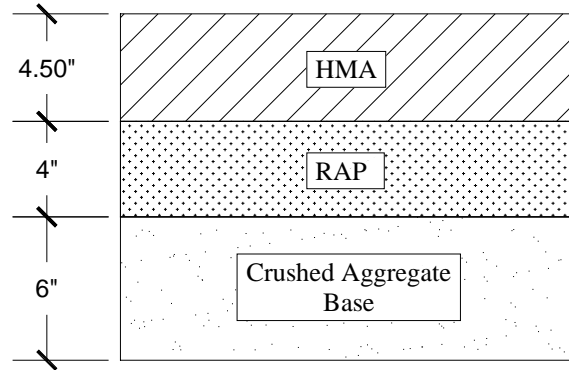


(d) STH 25 RAP

Figure D4: Typical sections of the investigate HMA pavements.



(a) STH 22 RAP



(b) STH 70 RAP

Figure D5: Typical sections of the investigate HMA pavements.

Table D1: Measured dimensions and unit weight of the HMA cores from pavement sections with CA base layers.

Project Site	Thickness (in)				Diameter (in)				Unit Weight (pcf)
	H ₁	H ₂	H ₃	H _{avg} *	D ₁	D ₂	D ₃	D _{avg} *	
STH 22/54 CL I	5.50	5.47	5.53	5.50	7.59	7.63	7.63	7.61	147.4
STH 22/54 CL II	5.67	5.41	5.47	5.52	7.68	7.67	7.66	7.67	143.7
STH 22/54 WP I	5.72	5.66	5.79	5.72	7.67	7.66	7.68	7.67	142.3
STH 22/54 WP II	5.70	5.59	5.57	5.62	7.66	7.66	7.66	7.66	141.7
STH 22 CL I	5.21	5.33	5.33	5.29	7.66	7.67	7.67	7.67	131.2
STH 22 CL II	5.58	5.57	5.44	5.53	7.68	7.67	7.68	7.68	145.0
STH 22 WP I	5.28	5.41	5.53	5.41	7.71	7.69	7.67	7.69	146.1
STH 22 WP II	5.44	5.50	5.45	5.46	7.65	7.67	7.66	7.66	147.5
STH 33 CL I	5.94	5.84	5.83	5.87	7.70	7.69	7.70	7.70	145.5
STH 33 CL II	5.87	5.90	5.80	5.86	7.69	7.69	7.69	7.69	145.9
STH 33 CL III	5.89	5.87	5.85	5.87	7.69	7.69	7.69	7.69	144.6
STH 33 WP I	6.03	5.89	6.22	6.05	7.97	7.76	7.75	7.82	137.4
STH 33 WP II	6.07	6.83	6.31	6.40	7.69	7.71	7.70	7.70	137.2
STH 33 WP III	5.97	6.07	5.94	5.99	7.68	7.70	7.68	7.69	145.5
CTH T CL I	5.16	5.17	5.10	5.14	7.67	7.66	7.69	7.67	125.0
CTH T CL II	4.98	4.96	5.04	4.99	7.72	7.72	7.71	7.72	137.7
CTH T WP II	4.86	4.83	4.91	4.87	7.68	7.73	7.70	7.70	143.5
CTH T WP I	4.76	4.79	4.82	4.79	7.70	7.71	7.71	7.70	141.7
STH 25 CL I	4.26	4.42	4.29	4.32	7.70	7.68	7.67	7.68	142.1
STH 25 CL II	4.47	4.43	4.23	4.38	7.68	7.68	7.69	7.68	143.1
STH 25 WP I	3.47	3.56	3.55	3.53	7.69	7.68	7.69	7.68	138.6
STH 25 WP II	3.58	3.63	3.78	3.66	7.65	7.72	7.70	7.69	137.4
STH 59 WP I	4.02	4.04	4.07	4.04	7.88	7.87	7.80	7.85	132.7
STH 59 WP II	3.99	4.00	3.87	3.95	7.76	7.80	7.80	7.78	135.2
STH 59 WP III	3.99	4.00	3.87	3.95	7.82	7.86	7.80	7.83	122.4
STH 59 WP IV	3.80	3.80	3.76	3.78	7.74	7.79	7.87	7.80	127.8

Note: * Average of three measurement were taken for each core and averaged them to represent the average height and diameter.

** Core is split

Table D2: Measured dimensions and unit weight of the HMA cores from pavement sections with RCA base layers.

Project Site	Thickness (in)				Diameter (in)				Unit Weight (pcf)
	H ₁	H ₂	H ₃	H _{avg} *	D ₁	D ₂	D ₃	D _{avg} *	
STH 100 CL I	2.13	2.10	2.10	5.74	7.60	7.62	7.65	7.62	149.1
	3.64	3.57	3.66						
STH 100 CL II	5.70	5.82	5.85	5.79	7.67	7.66	7.66	7.66	146.4
STH 100 WP I	5.72	5.74	5.74	5.73	7.66	7.65	7.66	7.66	142.4
STH 100 WP II	5.84	5.82	5.84	5.83	7.66	7.65	7.64	7.65	146.2
STH 50 CL I (S1)	6.74	6.73	6.68	6.72	7.62	7.64	7.63	7.63	148.9
STH 50 CL II (S1)	6.75	6.74	6.87	6.79	7.64	7.68	7.64	7.65	148.1
STH 50 WP I (S1)	7.03	7.02	7.05	7.03	7.65	7.65	7.65	7.65	146.8
STH 50 WP II (S1)	7.00	7.08	7.11	7.06	7.64	7.60	7.63	7.62	145.6
STH 50 WP III (S1)	6.79	6.75	6.79	6.77	7.64	7.63	7.64	7.63	148.1
STH 50 CL I (S2)	6.45	6.42	6.46	6.44	5.93	5.95	5.91	5.93	143.0
STH 50 CL II (S2)	6.53	6.62	6.41	6.52	5.92	5.93	5.96	5.94	143.4
STH 50 WP I (S2)	5.98	6.02	6.10	6.03	5.92	5.97	5.93	5.94	141.7
STH 50 WP II (S2)	6.24	6.48	6.33	6.35	5.96	5.91	5.93	5.93	142.0
STH 32 CL I (S1)	7.03	6.95	7.11	7.03	7.63	7.64	7.64	7.64	148.3
STH 32 CL II (S1)	6.96	7.17	7.15	7.09	7.64	7.64	7.64	7.64	147.8
STH 32 WP I (S1)	6.94	6.91	6.86	6.90	7.63	7.65	7.64	7.64	148.8
STH 32 WP II (S1)	7.12	7.10	7.15	7.12	7.60	7.61	7.65	7.62	148.9
STH 32 CL I (S2)	5.71	5.66	5.63	5.67	5.92	5.93	5.94	5.93	146.4
STH 32 CL II (S2)	5.67	5.72	5.71	5.70	6.04	5.94	5.93	5.97	144.5
STH 32 WP I (S2)	6.01	6.16	6.12	6.10	5.92	5.93	5.94	5.93	148.0
STH 32 WP II (S2)	6.27	6.10	6.31	6.23	6.05	5.92	5.94	5.97	146.8
Calhoun Rd. CL I	6.00	6.32	6.27	6.20	7.62	7.64	7.59	7.61	143.0
Calhoun Rd. CL II	5.75	5.84	5.88	5.82	7.66	7.63	7.63	7.64	150.9
Calhoun Rd. WP I	6.29	6.34	6.15	6.26	7.72	7.64	7.65	7.67	140.1
Calhoun Rd. WP II	5.61	5.77	5.66	5.68	7.66	7.65	7.65	7.65	147.6
STH 86 WP I**	2.80	2.67	2.77	5.88	7.61	7.61	7.65	7.62	141.6
	3.11	3.17	3.12						
STH 86 WP II**	2.55	2.61	2.48	5.06	7.65	7.63	7.61	7.63	148.9
	2.47	2.48	2.58						

Table D3: Measured dimensions and unit weight of the HMA cores from pavement sections with RAP base layers.

Project Site	Thickness (in)				Diameter (in)				Unit Weight (pcf)
	H ₁	H ₂	H ₃	H _{avg} *	D ₁	D ₂	D ₃	D _{avg} *	
STH 96 CL I	2.71	2.78	2.76	7.10	7.64	7.65	7.66	7.65	146.5
	4.37	4.35	4.32						
STH 96 CL II	6.93	6.93	6.91	6.92	7.65	7.64	7.67	7.65	148.0
STH 96 WP I	2.48	2.38	2.482	6.91	7.65	7.70	7.67	7.67	142.7
	4.46	4.47	4.454						
STH 96 WP II**	2.53	2.54	2.54	6.69	7.66	7.66	7.70	7.67	144.9
	4.09	4.20	4.17						
STH 70 CL I	4.97	4.94	5.01	4.97	7.65	7.66	7.65	7.65	145.9
STH 70 CL II	5.04	5.01	5.03	5.03	7.66	7.69	7.67	7.67	144.3
STH 70 CL III	4.91	4.82	4.91	4.88	7.67	7.67	7.68	7.67	146.1
STH 70 WP I	4.95	5.02	4.97	4.98	7.66	7.68	7.67	7.67	148.2
STH 70 WP II	4.95	5.00	4.98	4.98	7.64	7.63	7.67	7.65	149.0
STH 70 WP III	5.00	4.92	4.95	4.96	7.66	7.69	7.67	7.67	149.6
STH 22 CL I	5.53	5.50	4.84	5.29	7.69	7.66	7.64	7.66	133.5
STH 22 CL II	3.57	3.46	3.42	3.48	7.64	7.62	7.61	7.62	144.7
STH 22 WP I	*Unreadable Broken to bits								
STH 22 WP II	4.43	4.45	4.52	4.46	7.67	7.65	7.67	7.66	151.7
STH 59 CL I	3.42	3.58	3.50	3.50	7.68	7.69	7.68	7.68	145.8
STH 59 CL II	3.68	3.75	3.98	3.80	7.67	7.69	7.66	7.67	138.7
STH 59 WP I	3.25	3.31	3.22	3.26	7.68	7.70	7.73	7.70	139.6
STH 59 WP II	3.34	3.41	3.37	3.37	7.87	7.88	8.00	7.92	128.7
STH 25 CL I	4.66	4.80	4.80	4.75	7.68	7.71	7.63	7.67	136.4
STH 25 CL II	4.88	4.85	4.88	4.87	7.70	7.72	7.66	7.70	138.8
STH 25 CL III	4.71	4.75	4.73	4.73	7.80	7.69	7.69	7.73	138.2
STH 25 WP I	5.05	5.12	5.21	5.12	7.82	7.79	7.72	7.77	138.1
STH 25 WP II	5.30	5.38	5.32	5.33	7.75	7.71	7.75	7.73	132.9
STH 25 WP III	5.00	5.11	5.30	5.14	7.67	7.68	7.67	7.67	144.6

Note: * Average of three measurement were taken for each core and averaged them to represent the average height and diameter.

** Core is split

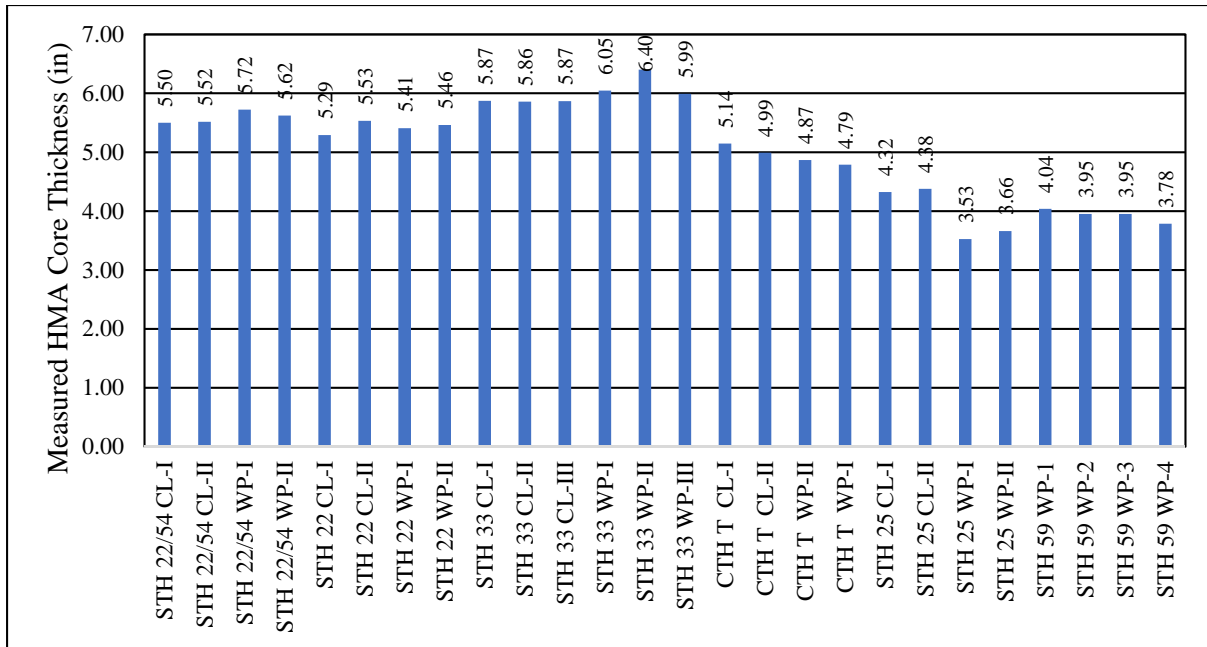


Figure D6: Thickness of HMA cores from pavement sections with CA base layers.

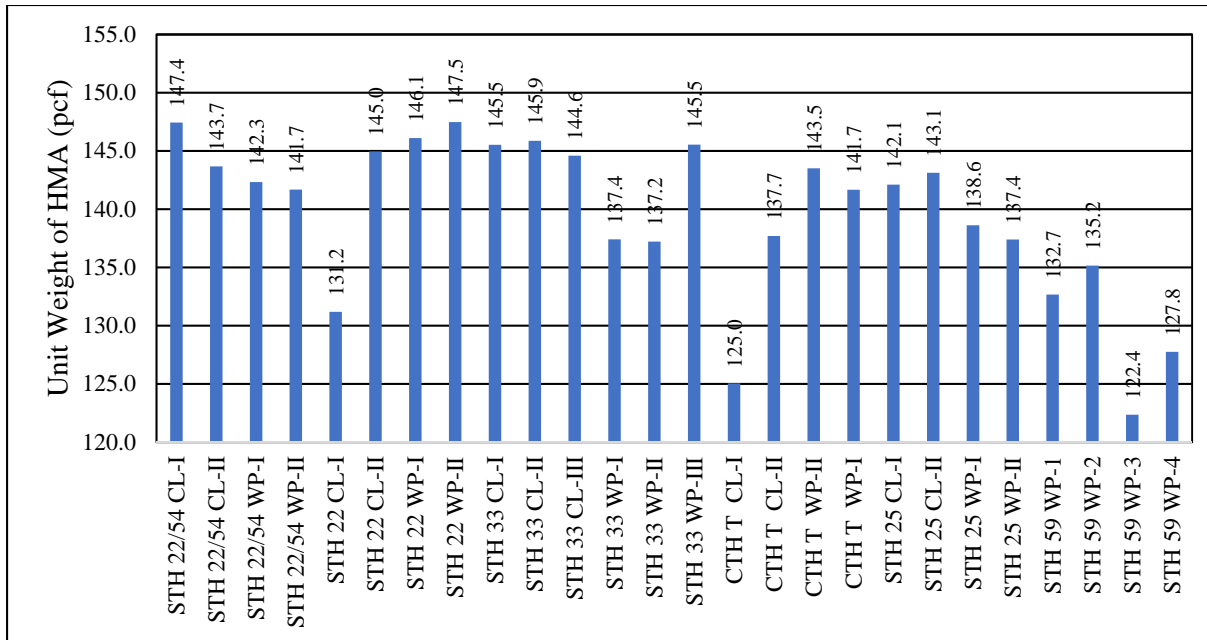


Figure D7: Unit weight of HMA cores from pavement sections with CA base layers

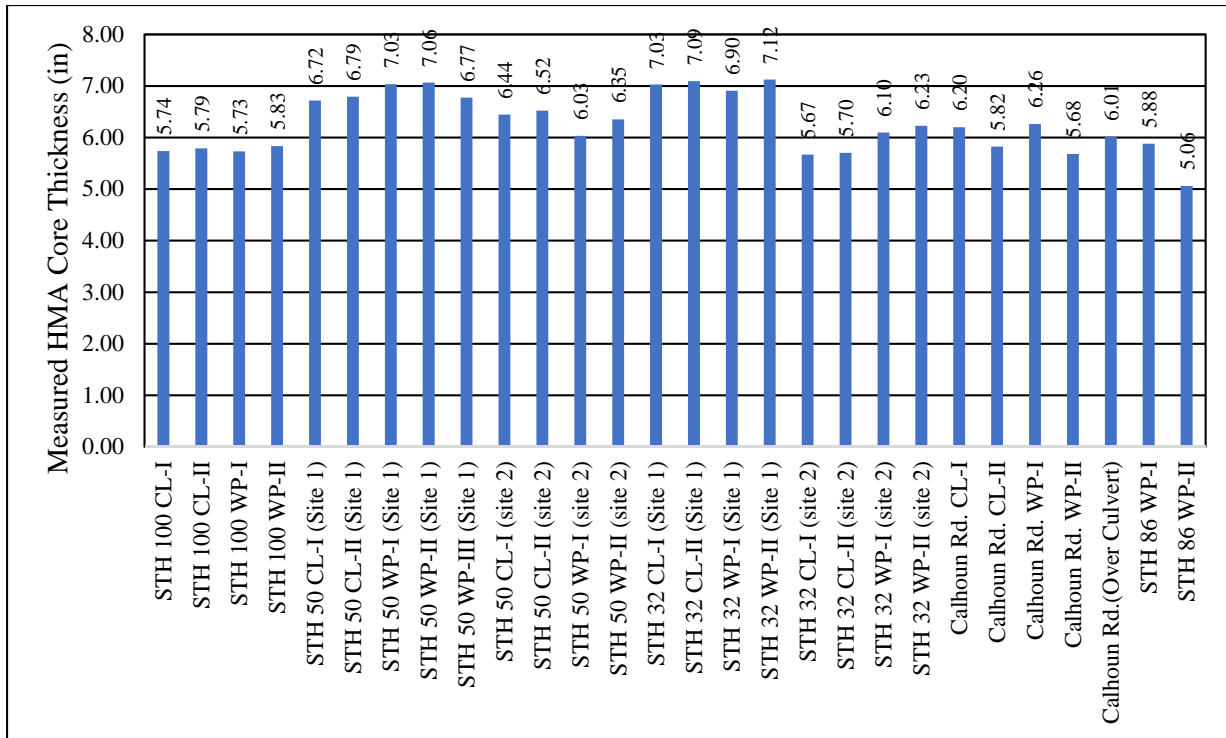


Figure D8: Thickness of HMA cores from pavement sections with RCA base layers

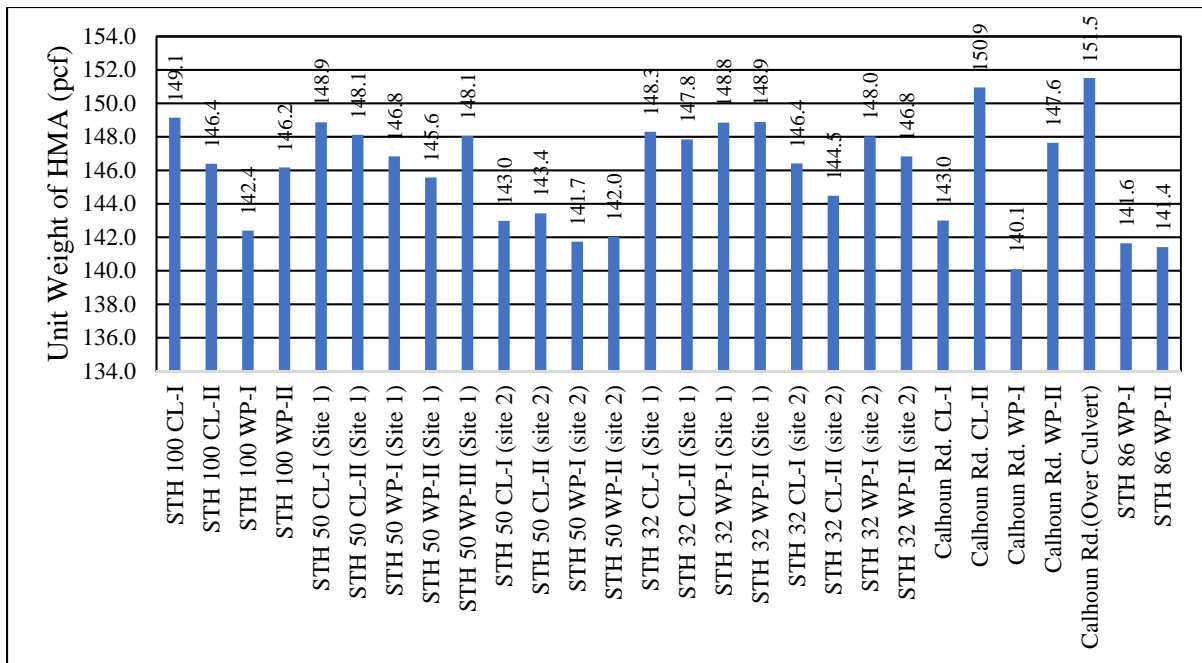


Figure D9: Unit weight of HMA cores from pavement sections with RCA base layers

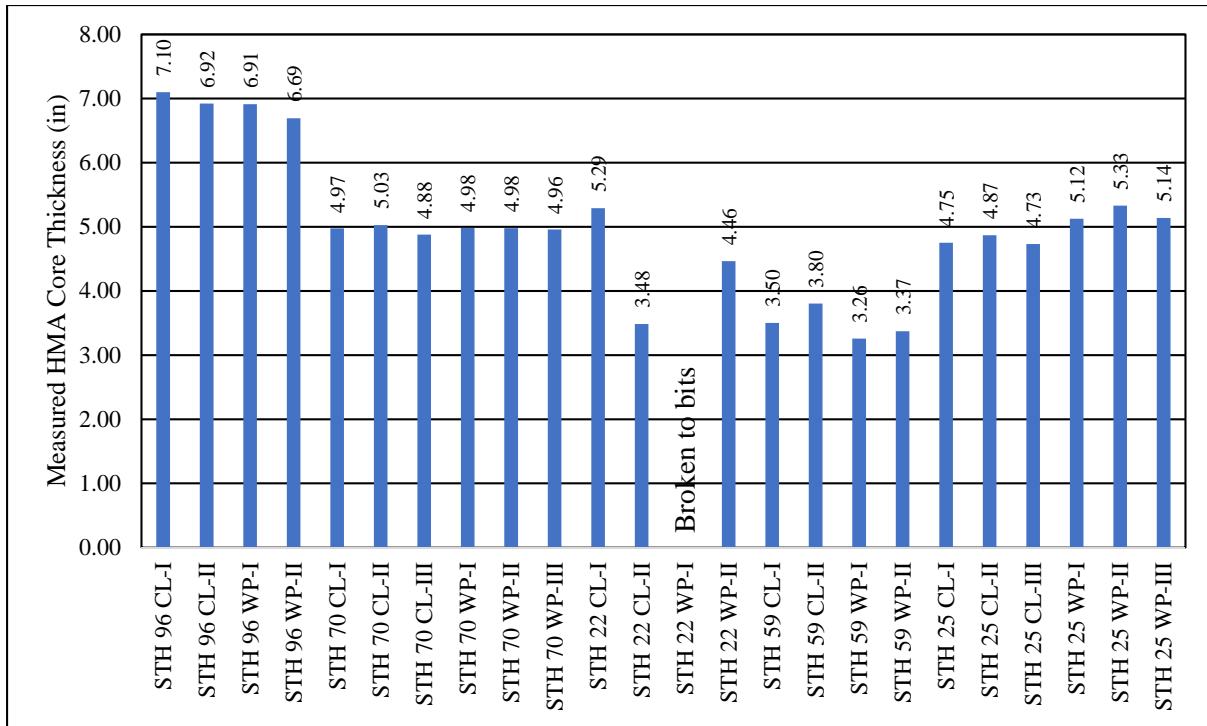


Figure D10: Thickness of HMA cores from pavement sections with RAP base layers

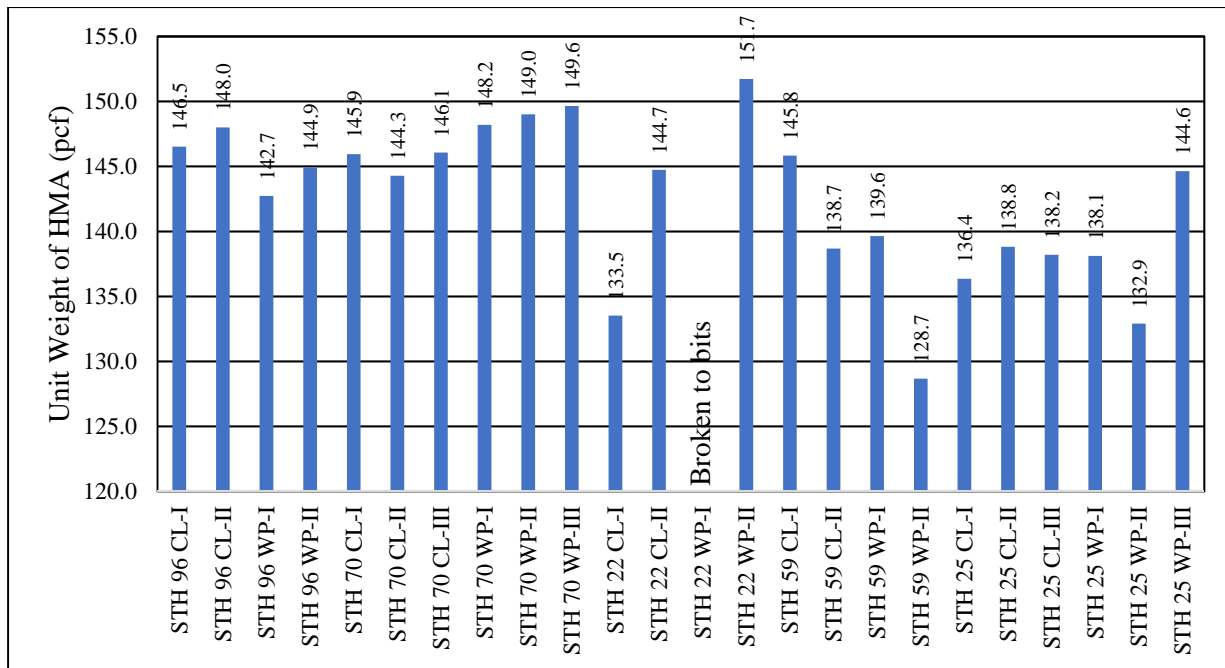
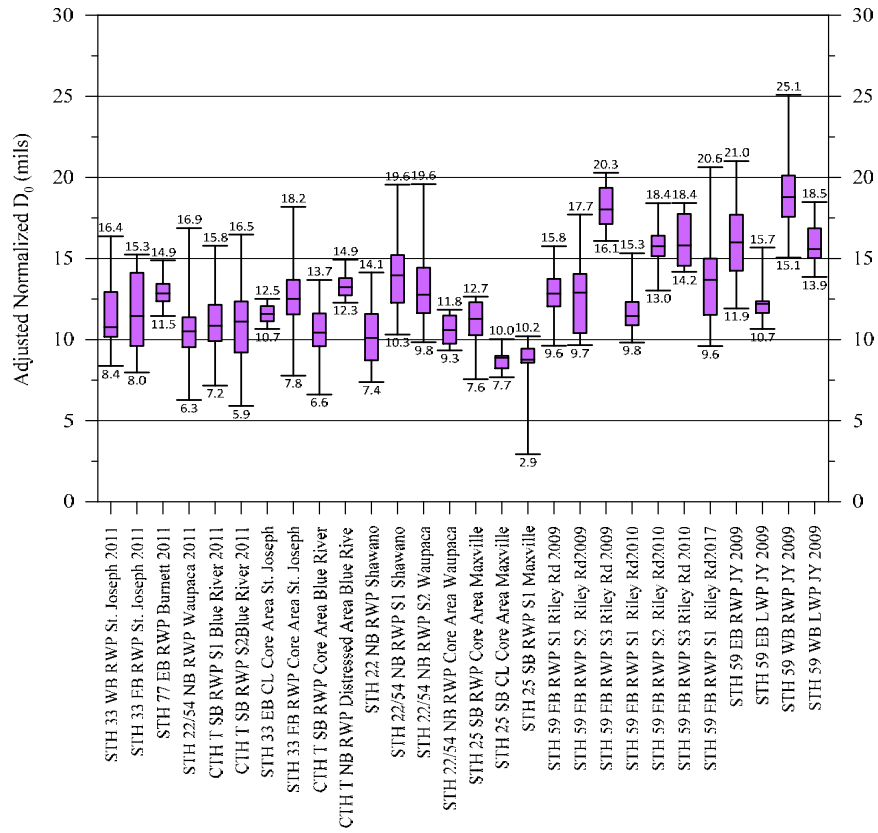
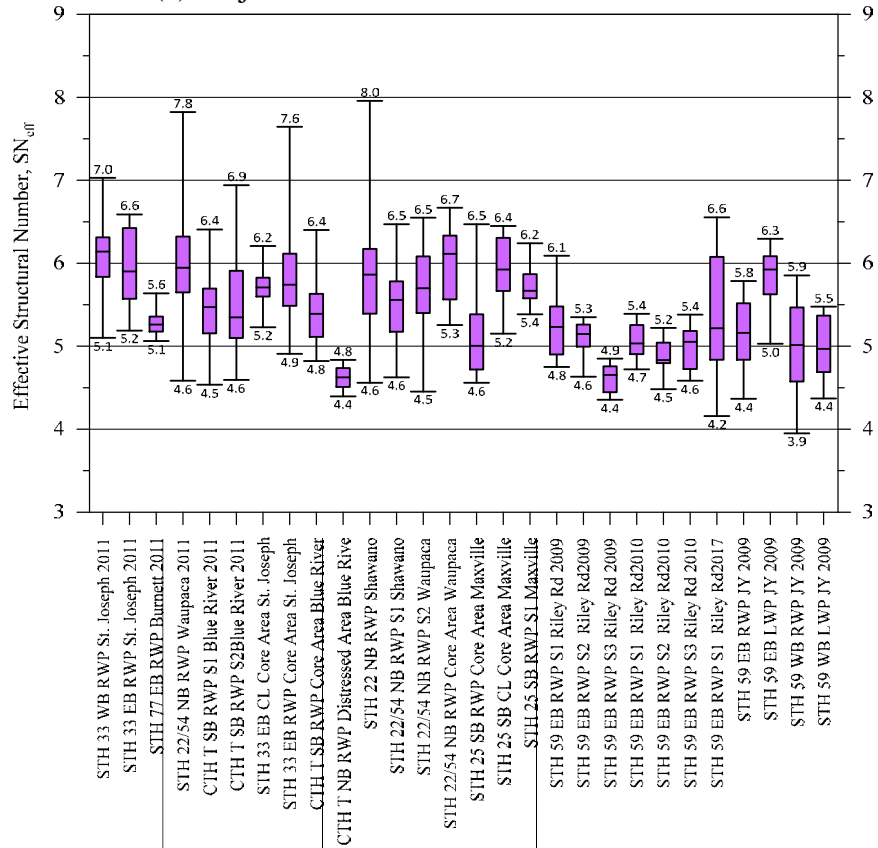


Figure D11: Unit weight of HMA cores from pavement sections with CA base layers

Appendix E
Results of the FWD Tests

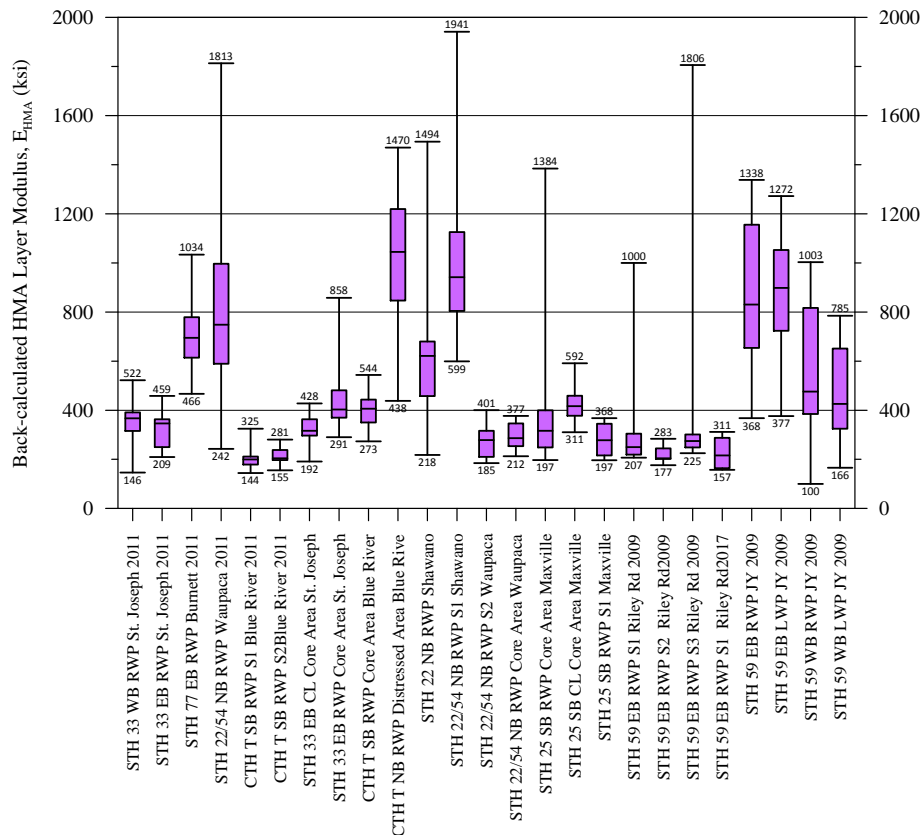


(a) Adjusted normalized measured deflection D_0

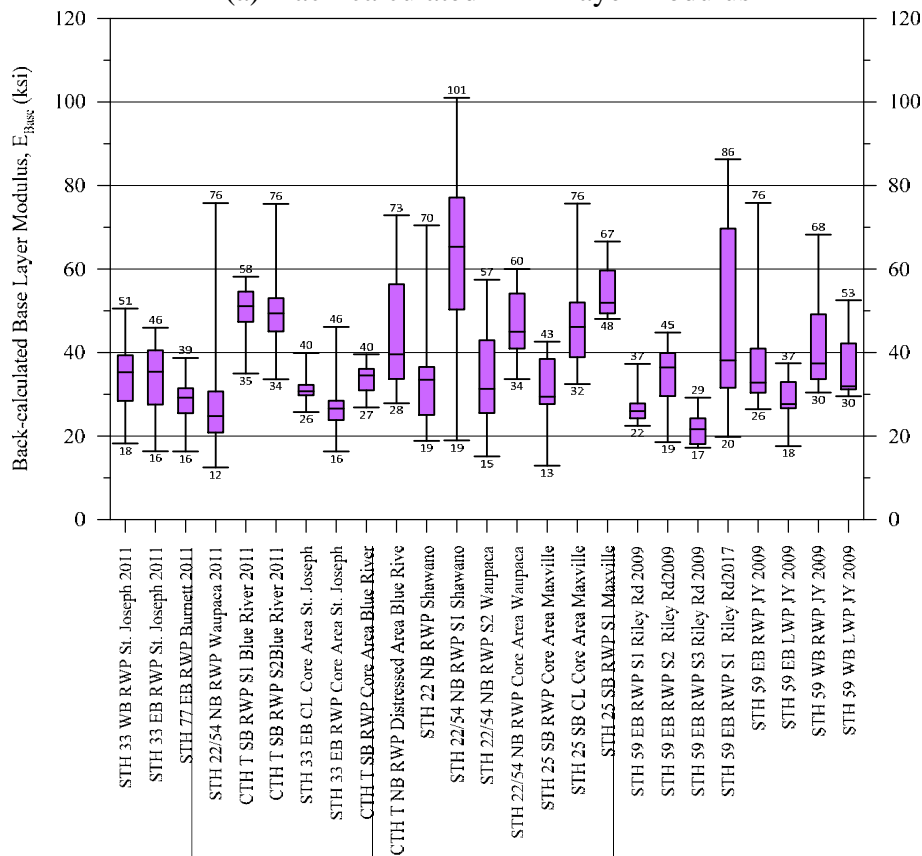


(b) Structural capacity

Figure E1: Box-Whisker plot depicting the minimum, the first quartile, the median, the third quartile, and the maximum of FWD test results and analysis D_0 and SN_{eff} for pavement section with CA base layers.

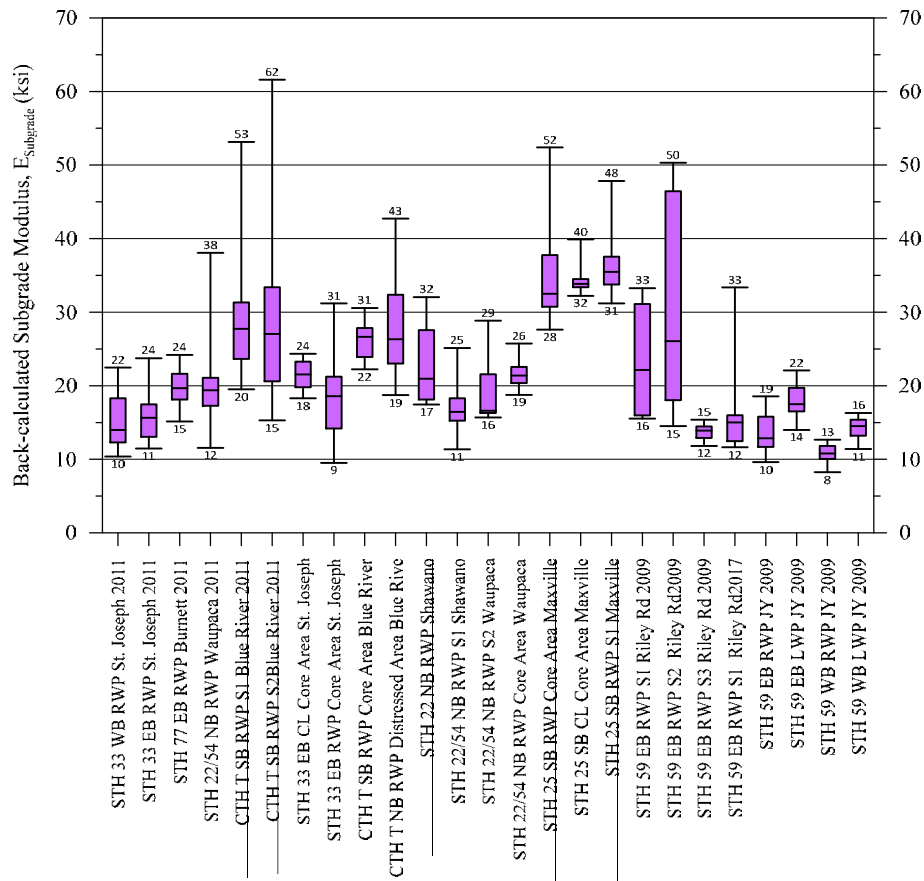


(a) Back-calculated HMA layer modulus



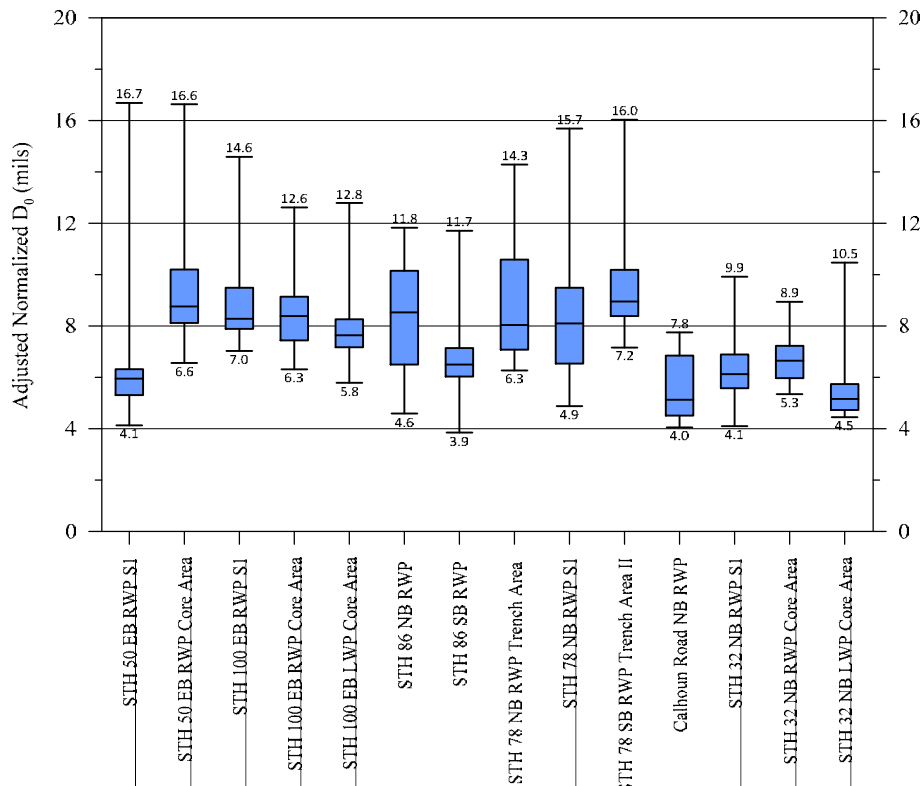
(b) Back-calculated CA base layer modulus

Figure E2: Box-Whisker plot depicting the minimum, the first quartile, the median, the third quartile, and the maximum of FWD test results for pavement section with CA base layers.

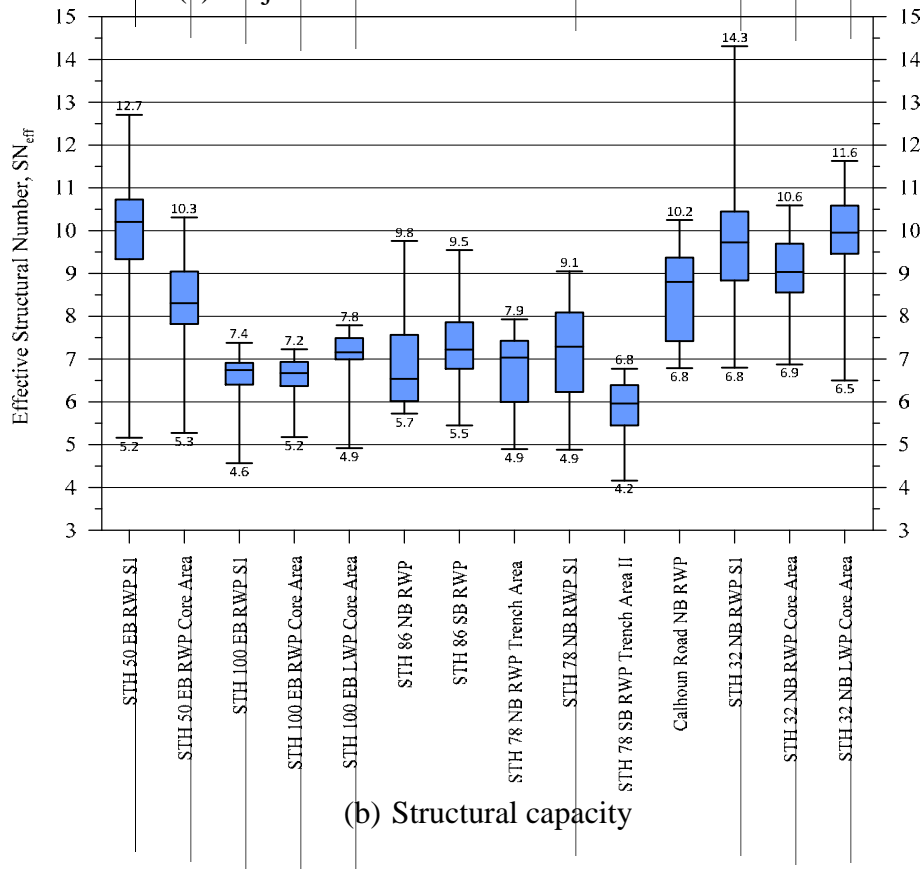


(c) Back-calculated subgrade modulus

Figure E2(Cont.): Box-Whisker plot depicting the minimum, the first quartile, the median, the third quartile, and the maximum of FWD test results for pavement section with CA base layers.

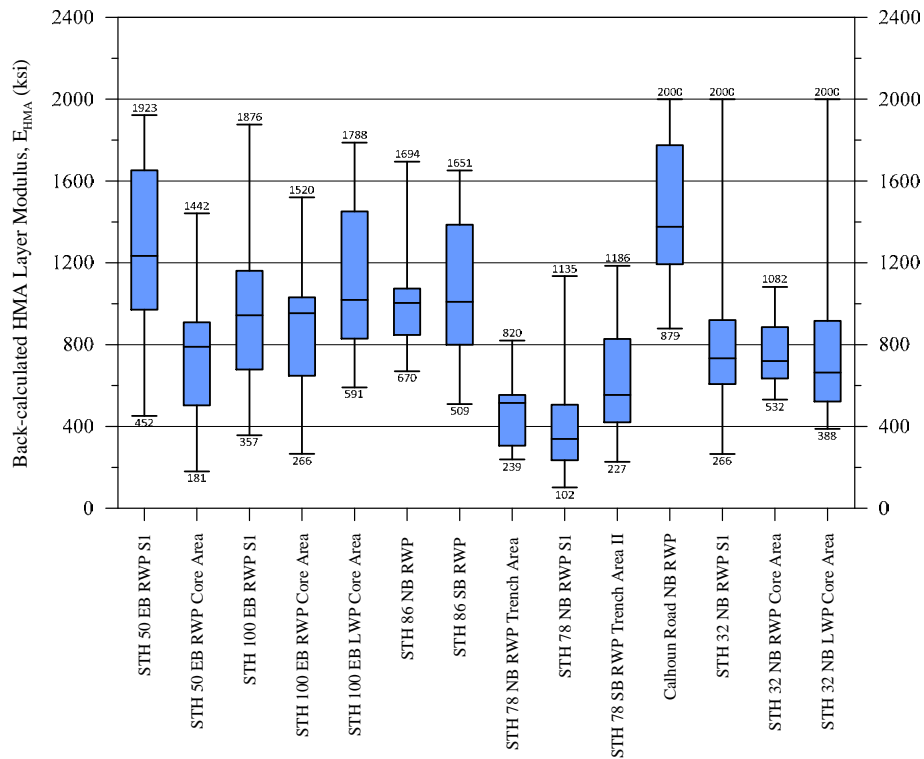


(a) Adjusted normalized measured deflection D_0

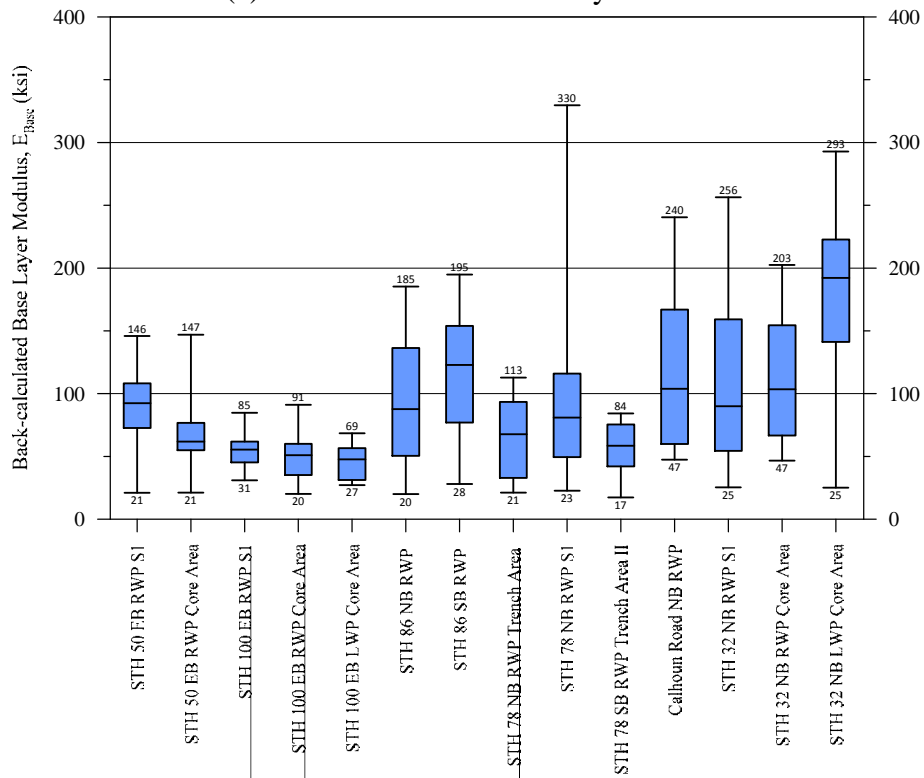


(b) Structural capacity

Figure E3: Box-Whisker plot depicting the minimum, the first quartile, the median, the third quartile, and the maximum of FWD test results and analysis D_0 and SN_{eff} for pavement section with RCA base layers.

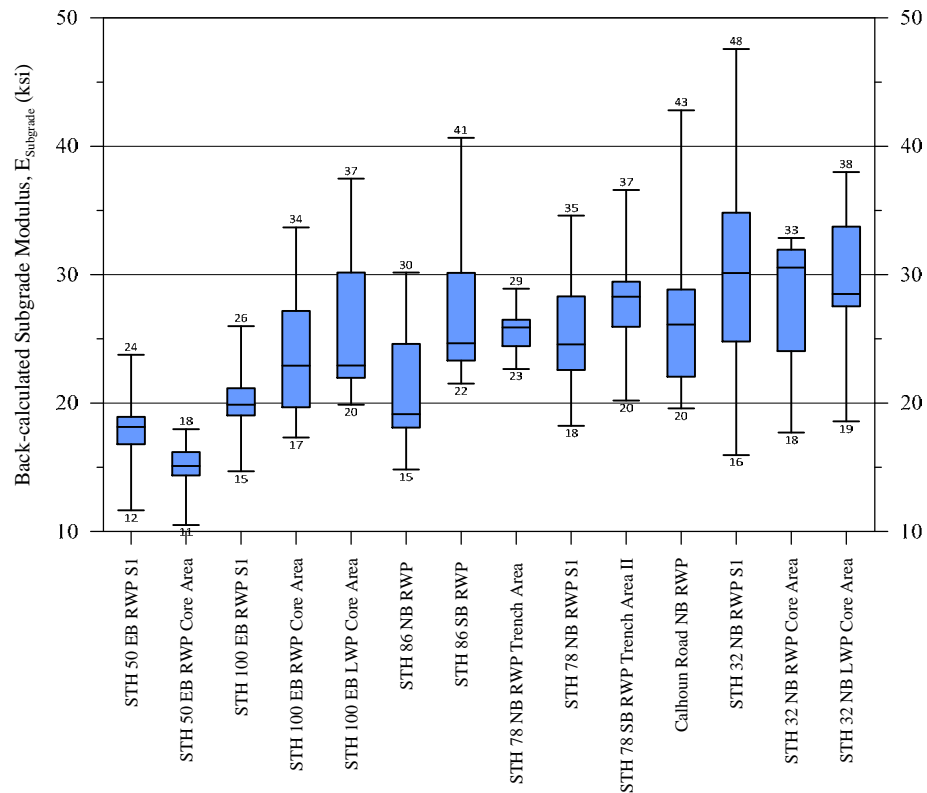


(a) Back-calculated HMA layer modulus



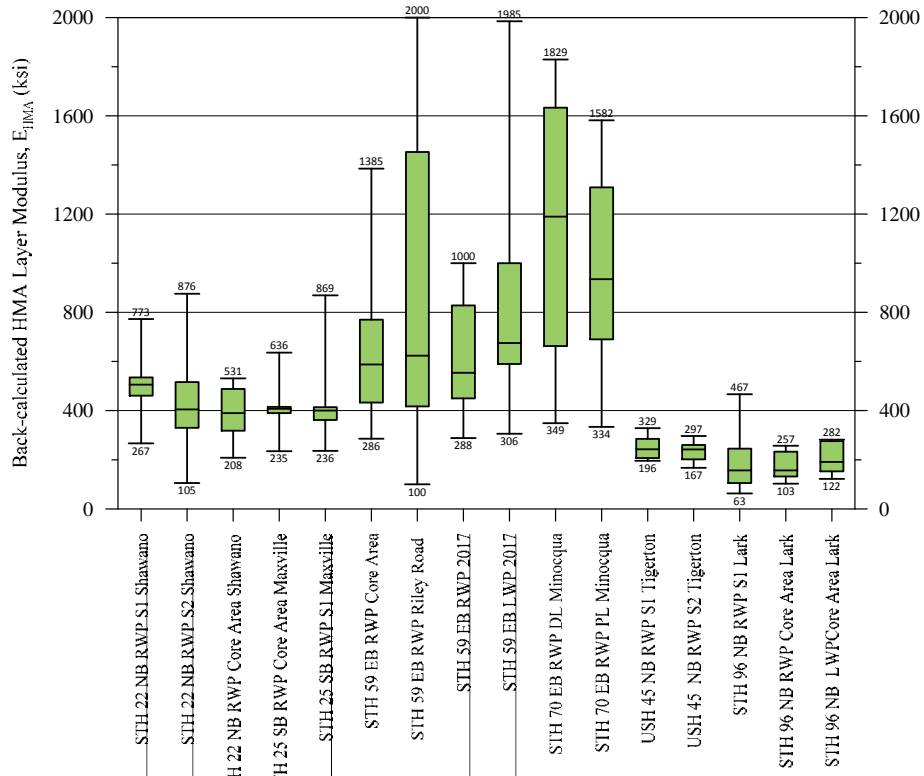
(b) Back-calculated RCA base layer modulus

Figure E4: Box-Whisker plot depicting the minimum, the first quartile, the median, the third quartile, and the maximum of FWD test results for pavement section with RCA base layers.

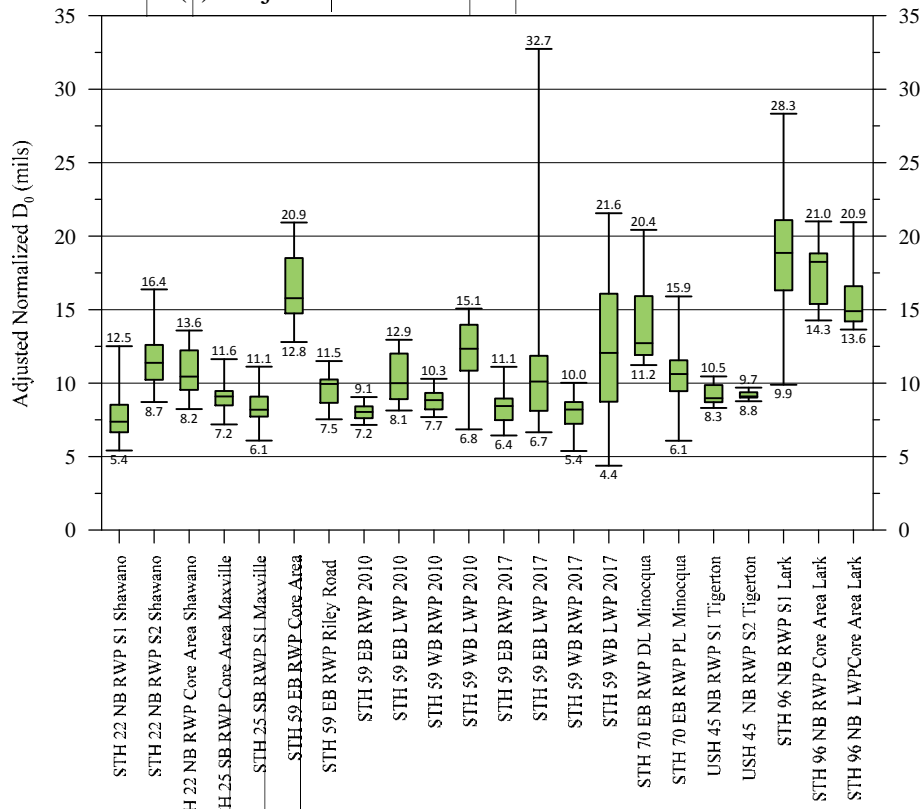


(c) Back-calculated subgrade modulus

Figure E4(Cont.): Box-Whisker plot depicting the minimum, the first quartile, the median, the third quartile, and the maximum of FWD test results for pavement section with RCA base layers.

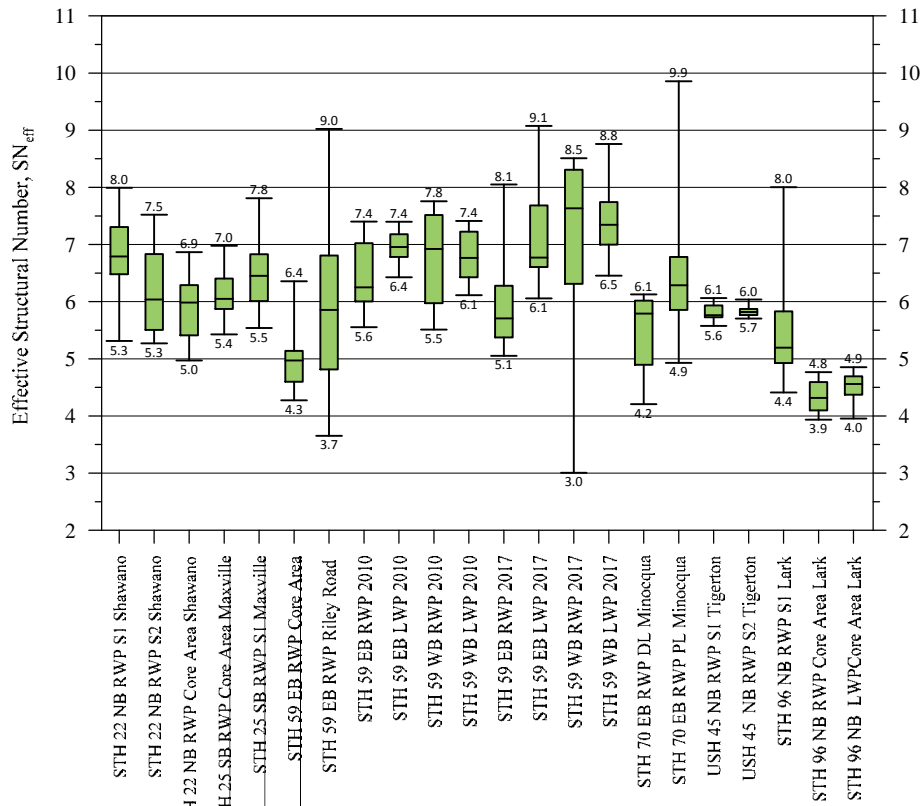


(a) Adjusted normalized measured deflection D_0

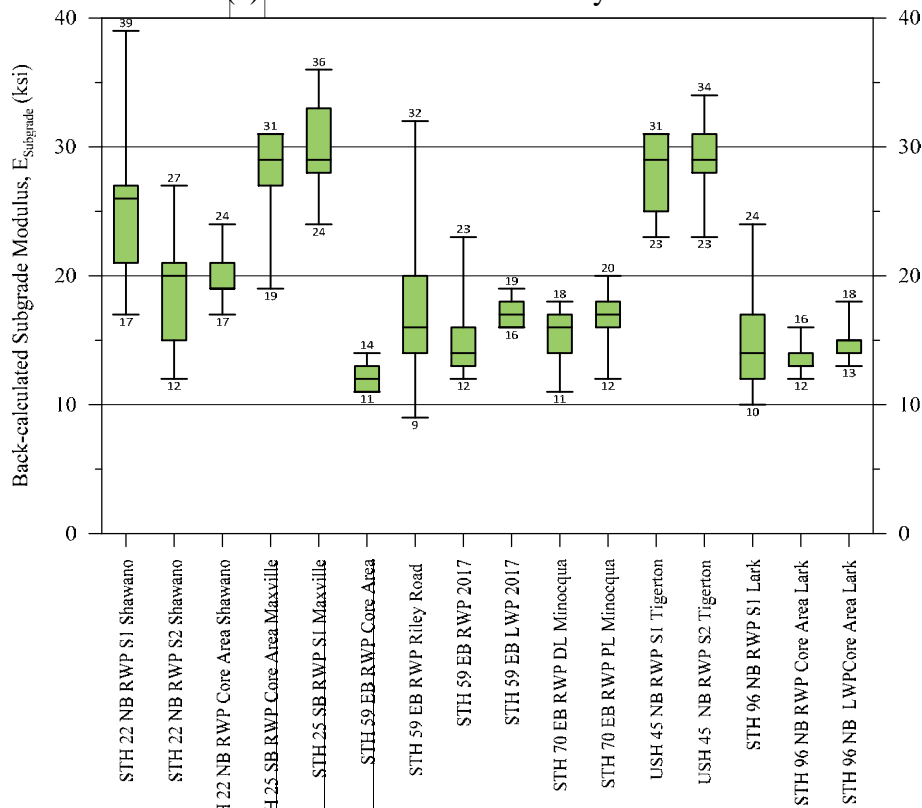


(b) Structural capacity

Figure E5: Box-Whisker plot depicting the minimum, the first quartile, the median, the third quartile, and the maximum of FWD test results and analysis D_0 and SN_{eff} for pavement section with RAP base layers.



(a) Back-calculated HMA layer modulus



(b) Back-calculated RCA base layer modulus

Figure E6: Box-Whisker plot depicting the minimum, the first quartile, the median, the third quartile, and the maximum of FWD test results for pavement section with RCA base layers.

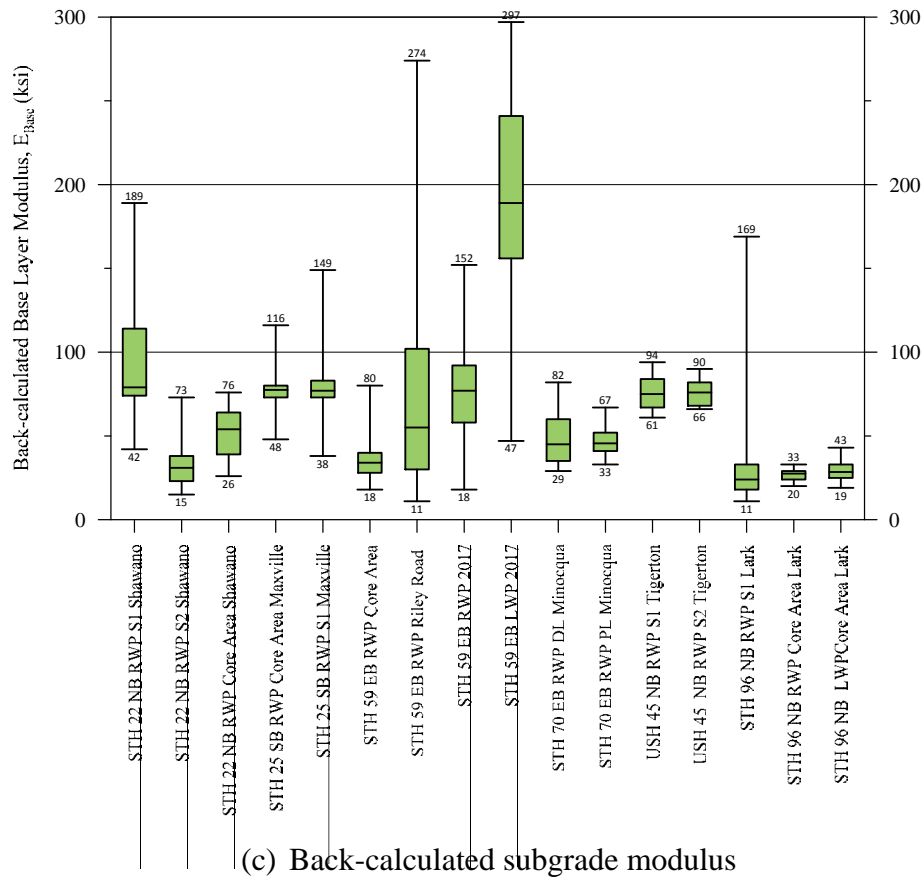
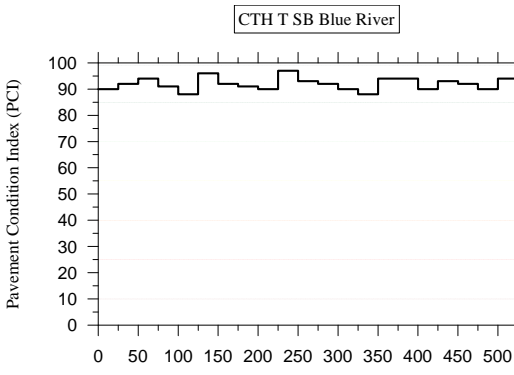


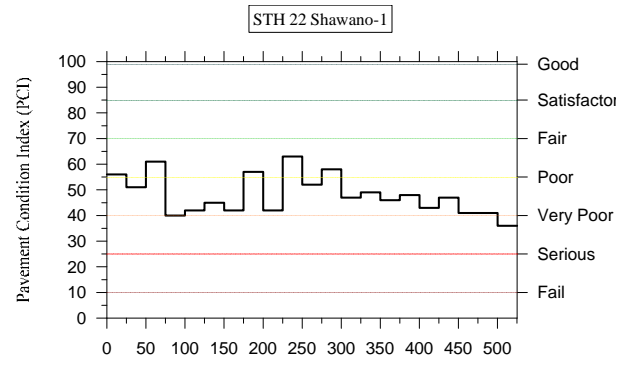
Figure E6(Cont.): Box-Whisker plot depicting the minimum, the first quartile, the median, the third quartile, and the maximum of FWD test results for pavement section with RAP base layers.

Appendix F

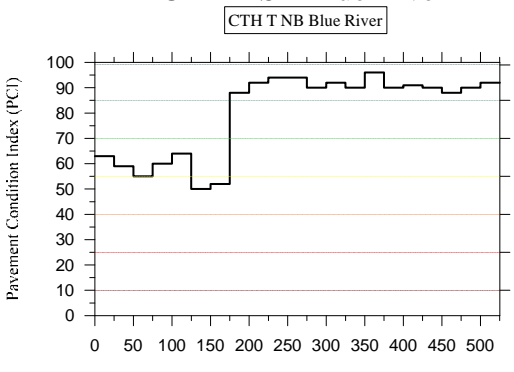
Pavement Condition Index for all Pavement Test Sections



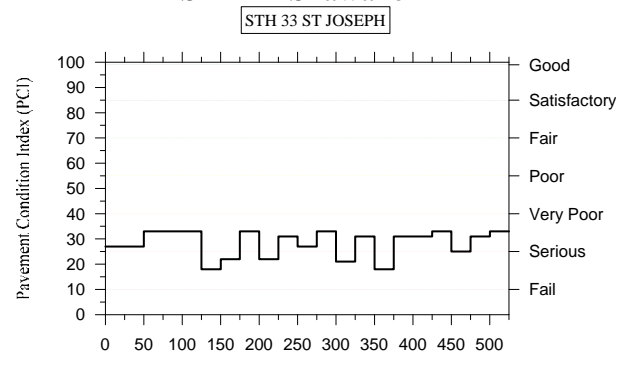
Distance from the Start of Pavement Section (ft)
CTH T SB Blue River



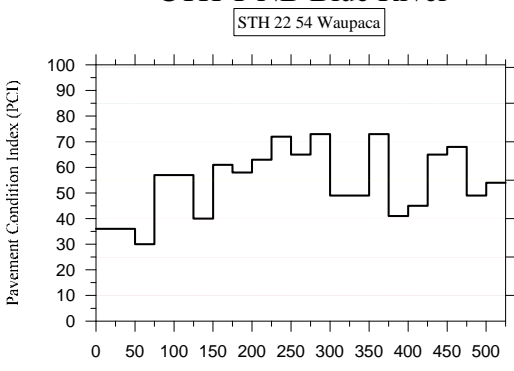
Distance from the Start of Pavement Section (ft)
STH 22 Shawano-1



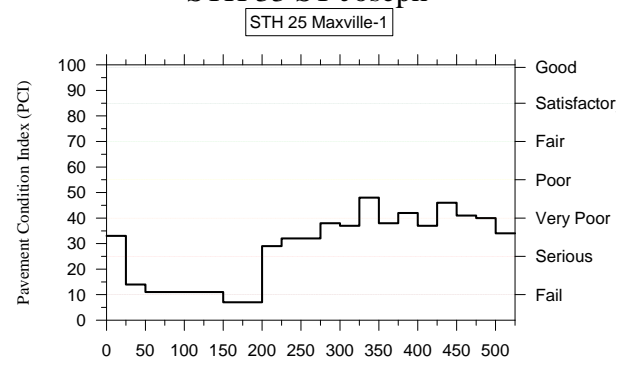
Distance from the Start of Pavement Section (ft)
CTH T NB Blue River



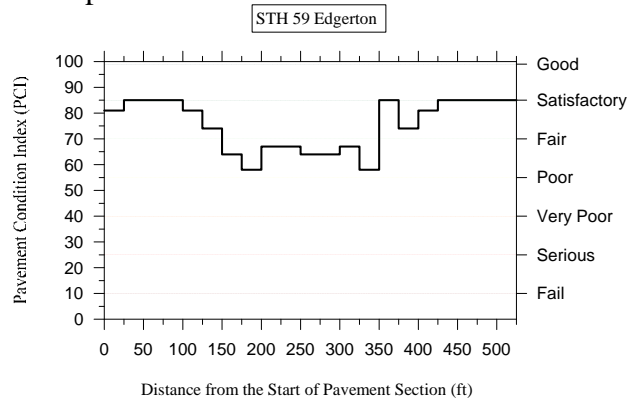
Distance from the Start of Pavement Section (ft)
STH 33 ST Joseph



Distance from the Start of Pavement Section (ft)
STH 22 54 Waupaca

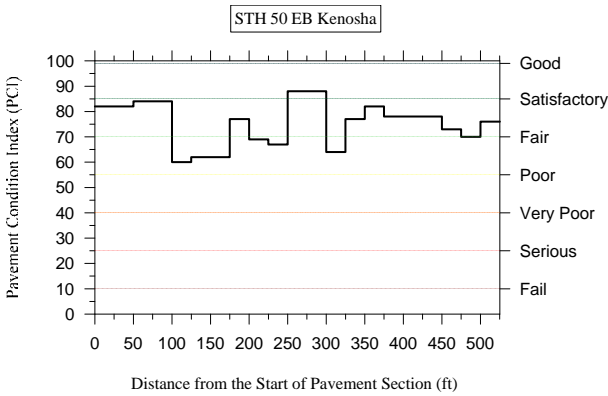


Distance from the Start of Pavement Section (ft)
STH 25 Maxville-1

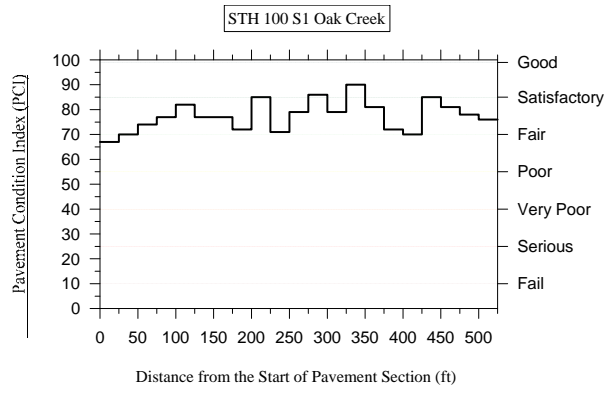


Distance from the Start of Pavement Section (ft)
STH 59 Edgerton

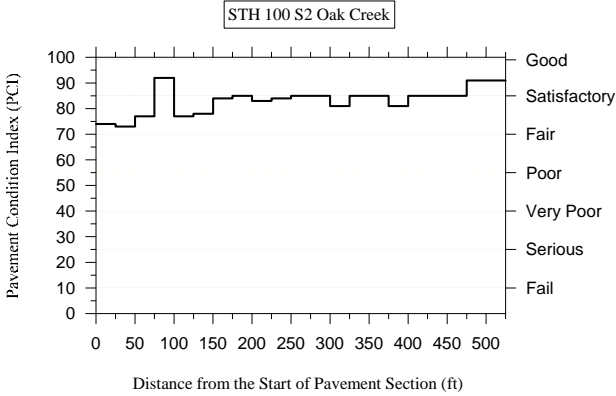
Figure F1: Pavement condition index (PCI) for pavement test sections with CA base layer.



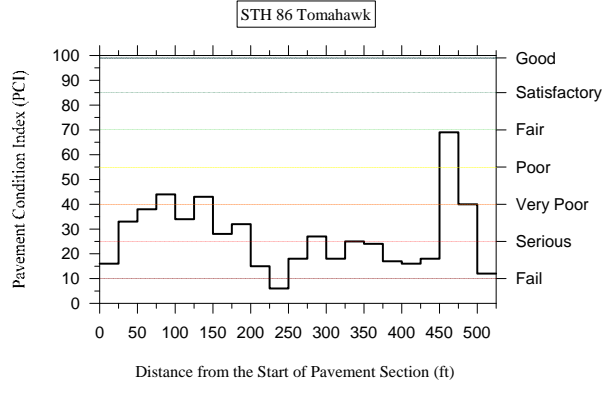
STH 50 EB Kenosha



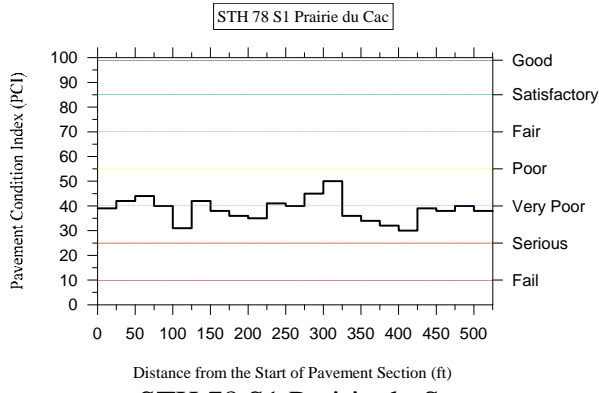
STH 100 S1 Oak Creek



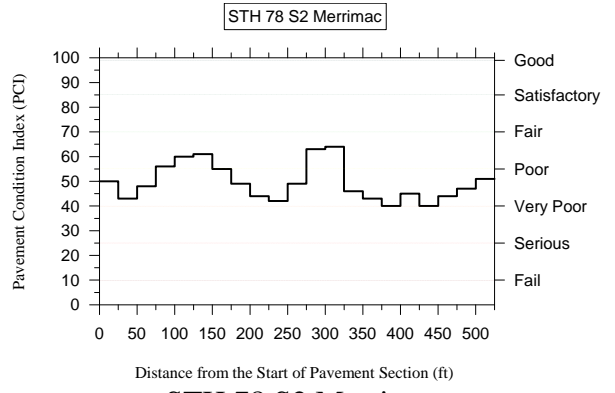
STH 100 S2 Oak Creek



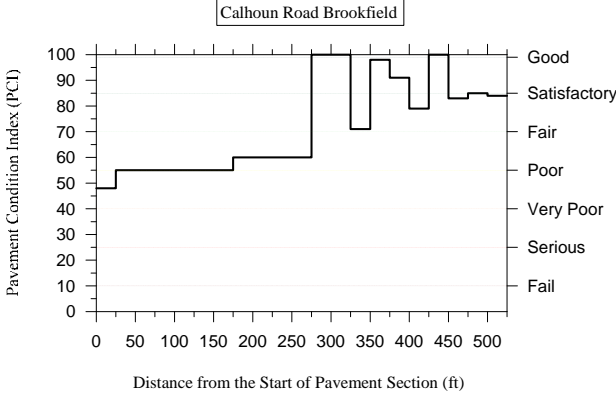
STH 86 Tomahawk



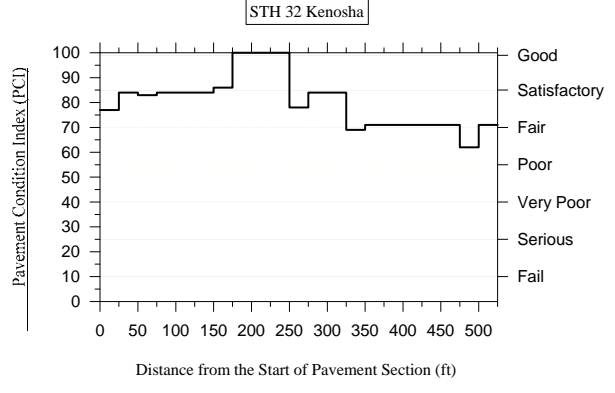
STH 78 S1 Prairie du Sac



STH 78 S2 Merrimac



Calhoun Road Brookfield



STH 32 Kenosha

Figure F2: Pavement condition index (PCI) for pavement test sections with RCA base layer.

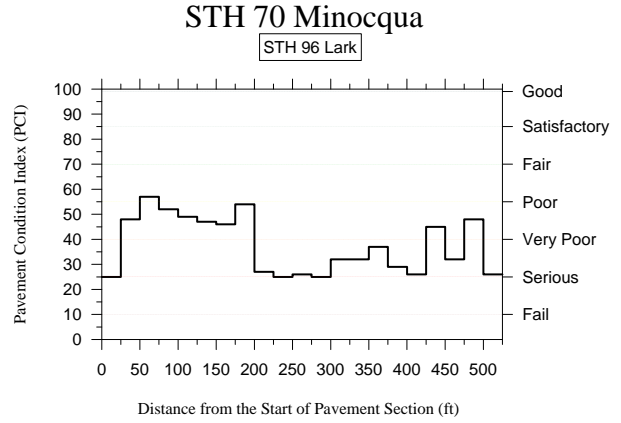
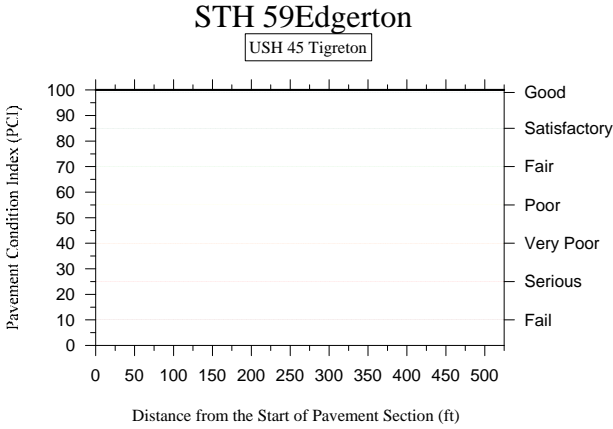
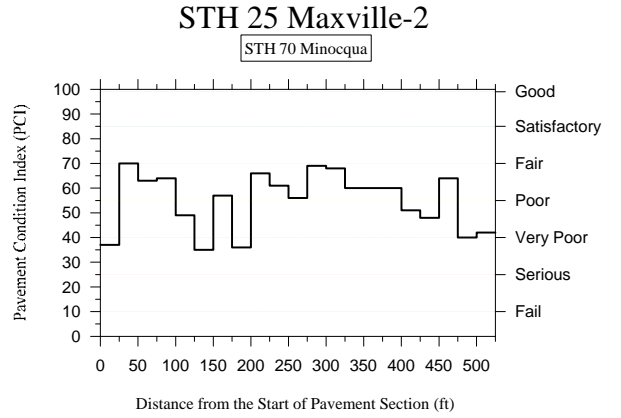
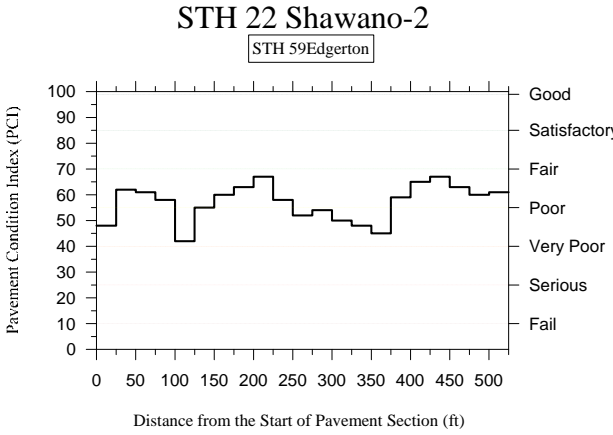
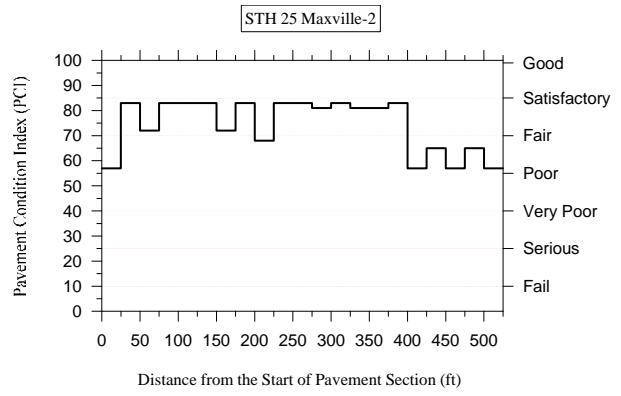
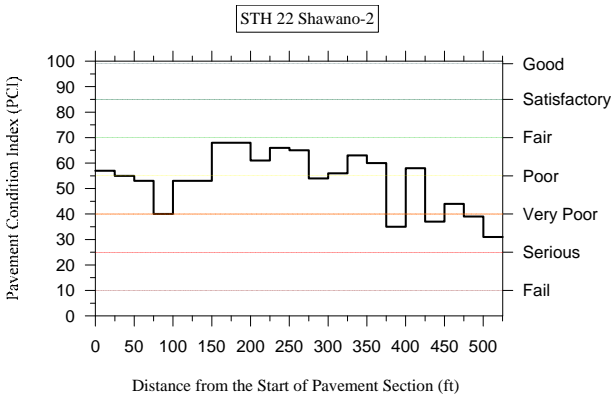


Figure F3: Pavement condition index (PCI) for pavement test sections with RAP base layer.

Appendix G

IRI Results from Pavement Surface Profiles Measurements

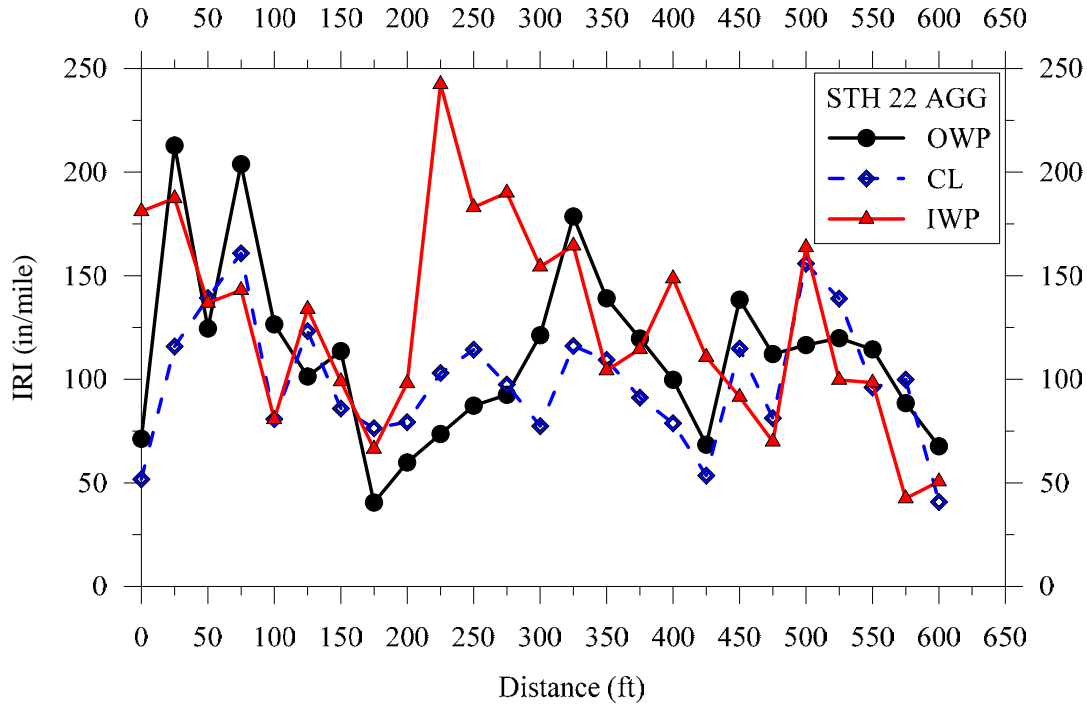


Figure G1: Ride quality measurement (international roughness index) for pavement test section with CA base layer at STH 22.

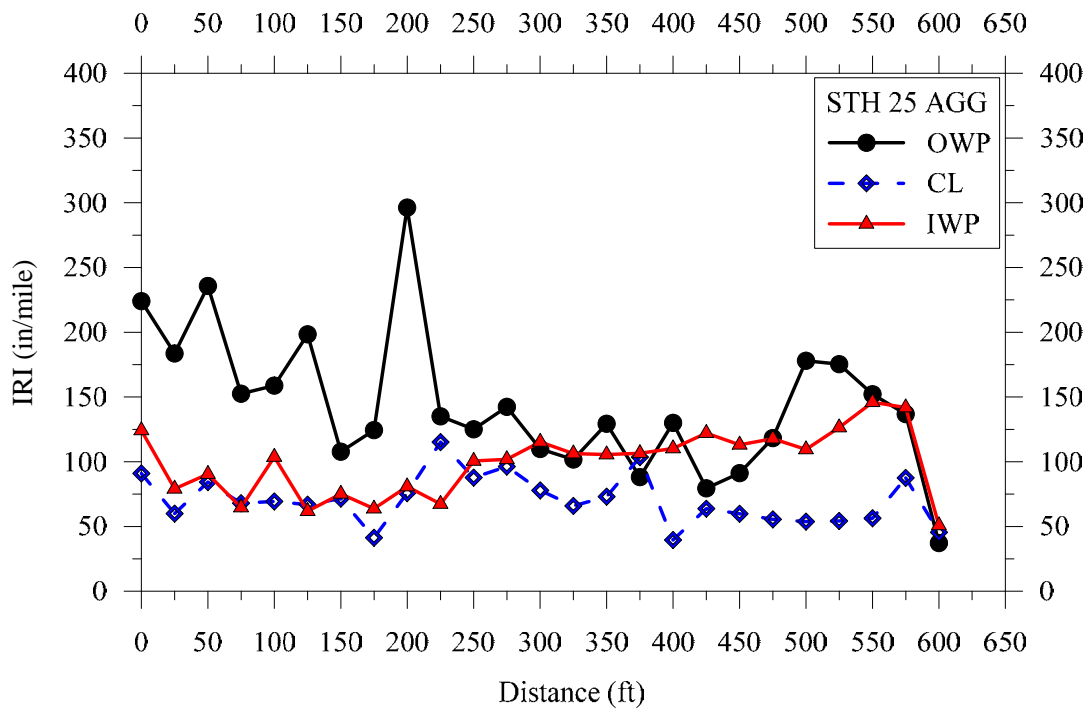


Figure G2: Ride quality measurement (international roughness index) for pavement test section with CA base layer at STH 25.

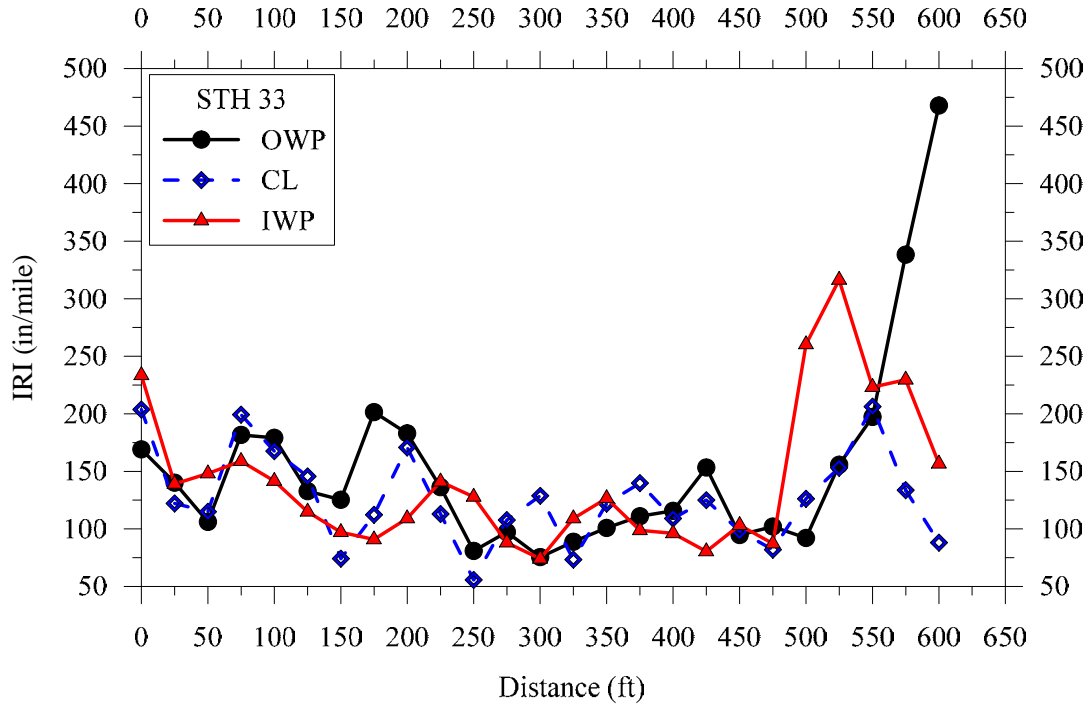


Figure G3: Ride quality measurement (international roughness index) for pavement test section with CA base layer at STH 33.

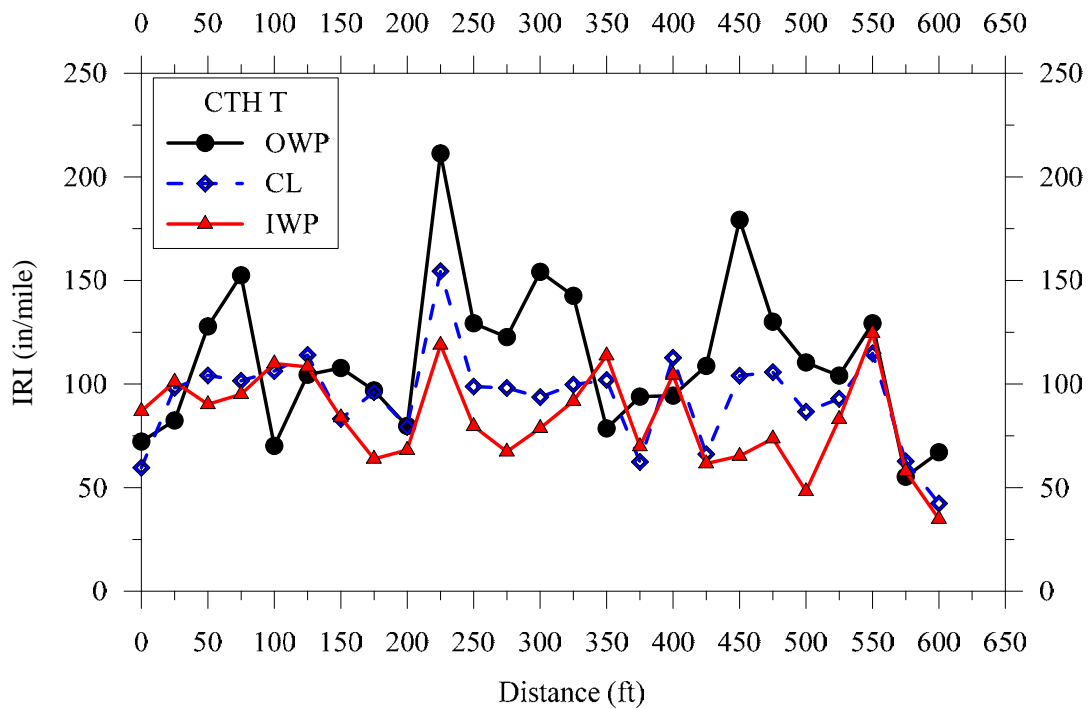


Figure G4: Ride quality measurement (international roughness index) for pavement test section with CA base layer at CTH T.

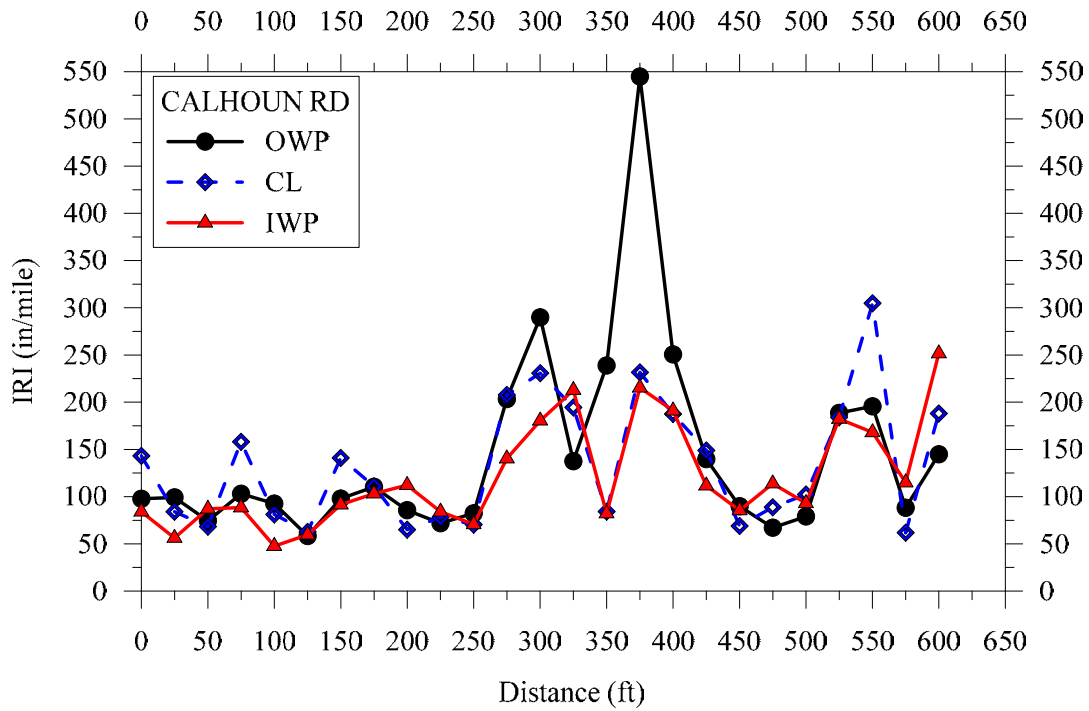


Figure G5: Ride quality measurement (international roughness index) for pavement test section with RCA base layer at Calhoun Road.

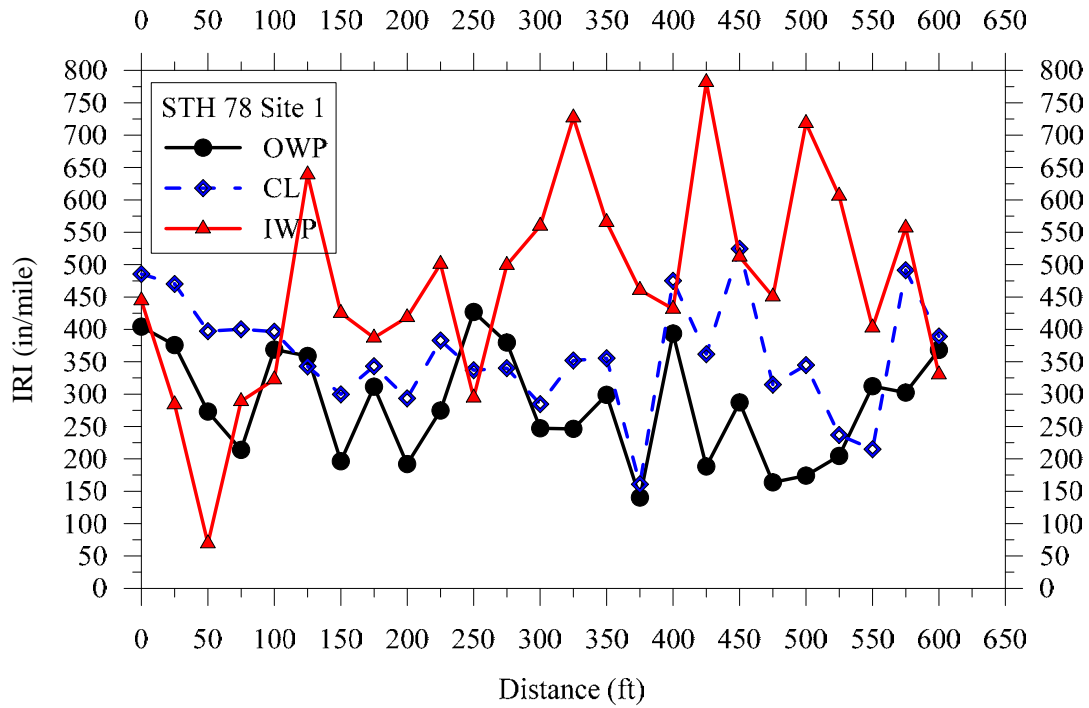


Figure G6: Ride quality measurement (international roughness index) for pavement test section with RCA base layer at STH 78 (S1).

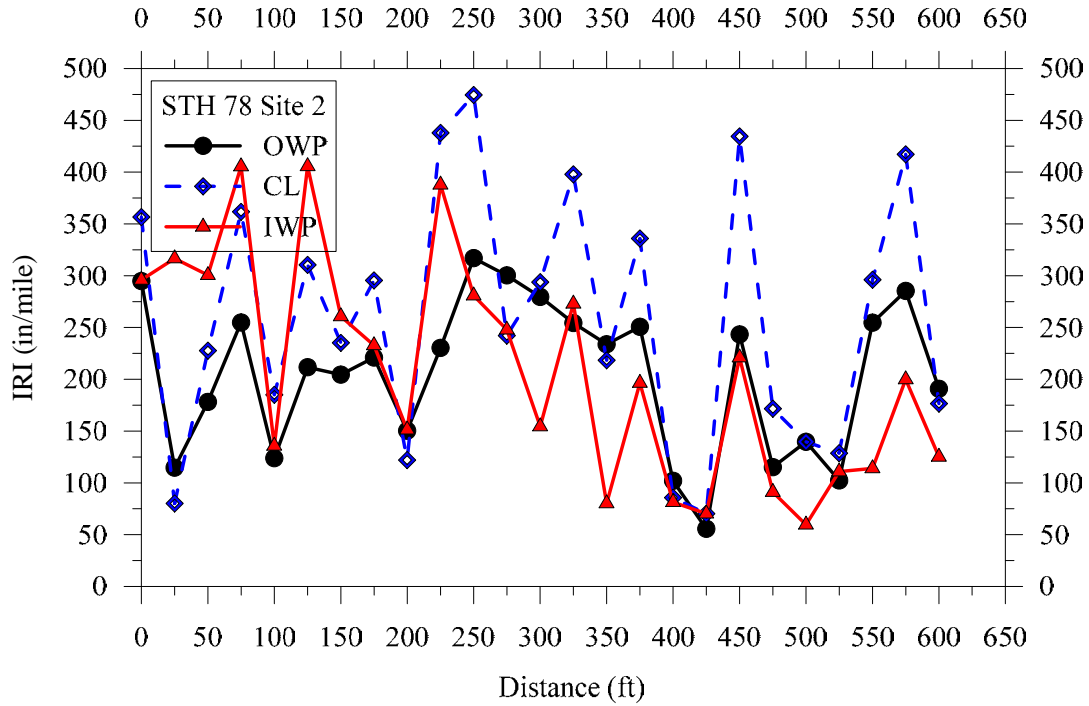


Figure G7: Ride quality measurement (international roughness index) for pavement test section with RCA base layer at STH 78 (S2).

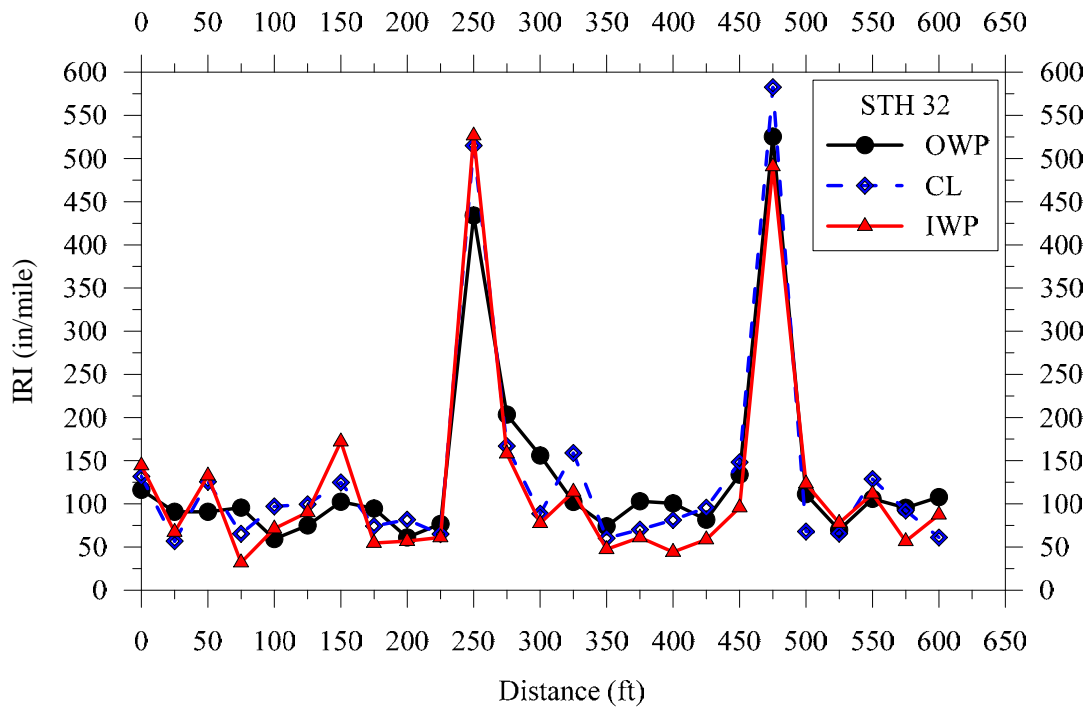


Figure G8: Ride quality measurement (international roughness index) for pavement test section with RCA base layer at STH 32.

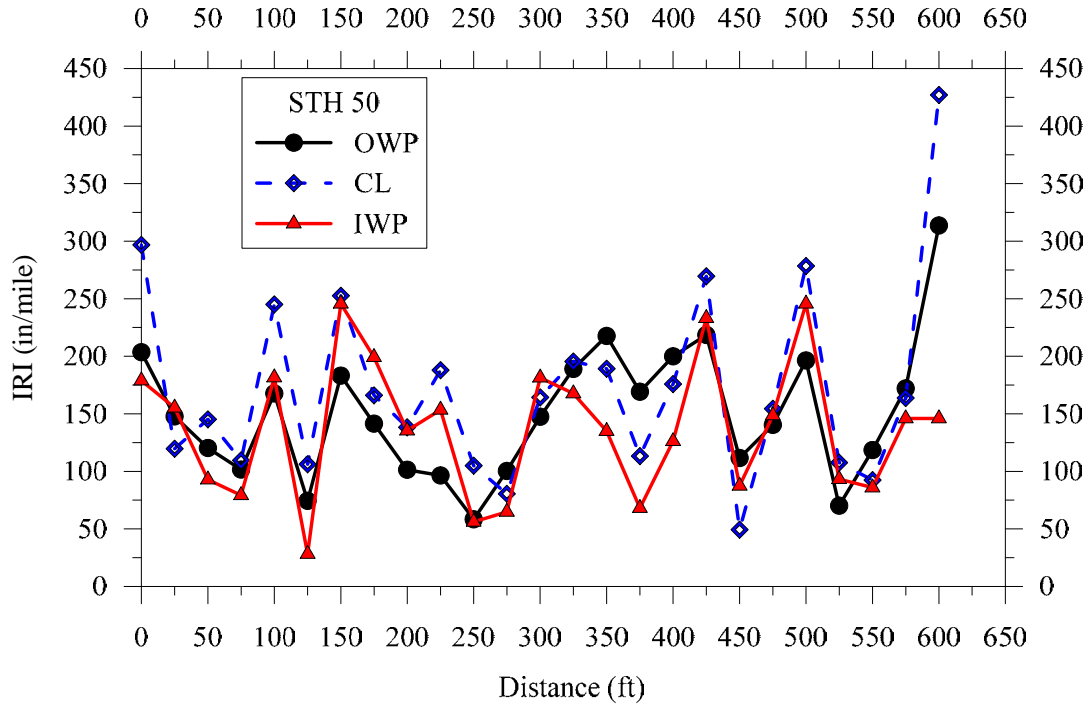


Figure G9: Ride quality measurement (international roughness index) for pavement test section with RCA base layer at STH 50.

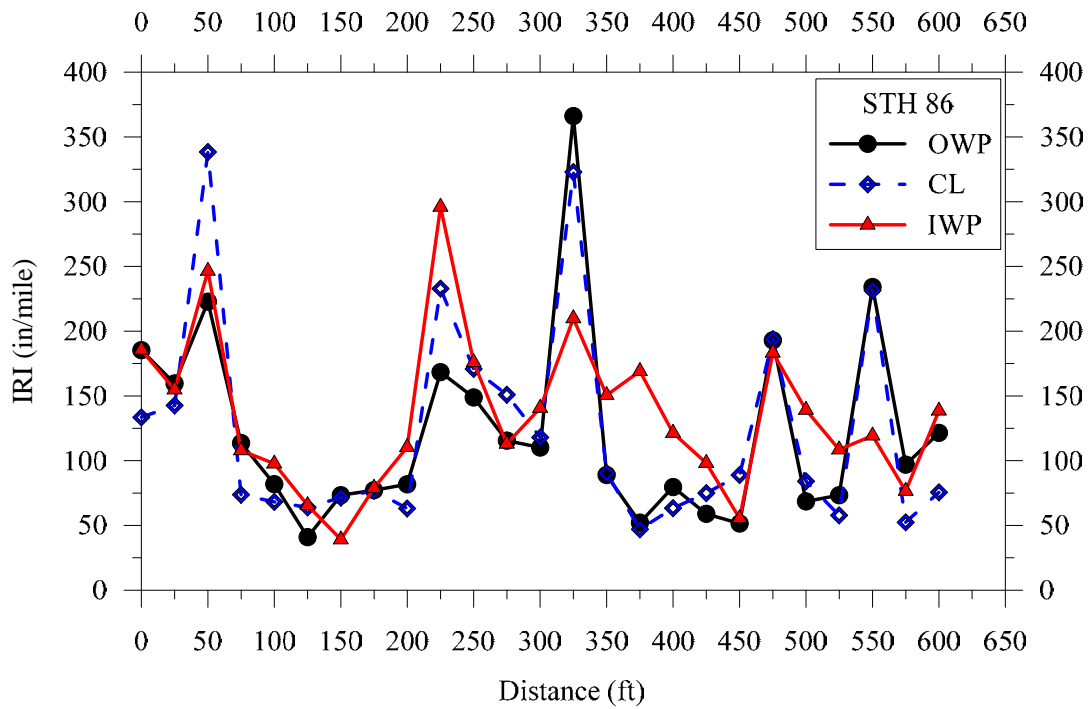


Figure G10: Ride quality measurement (international roughness index) for pavement test section with RCA base layer at STH 86.

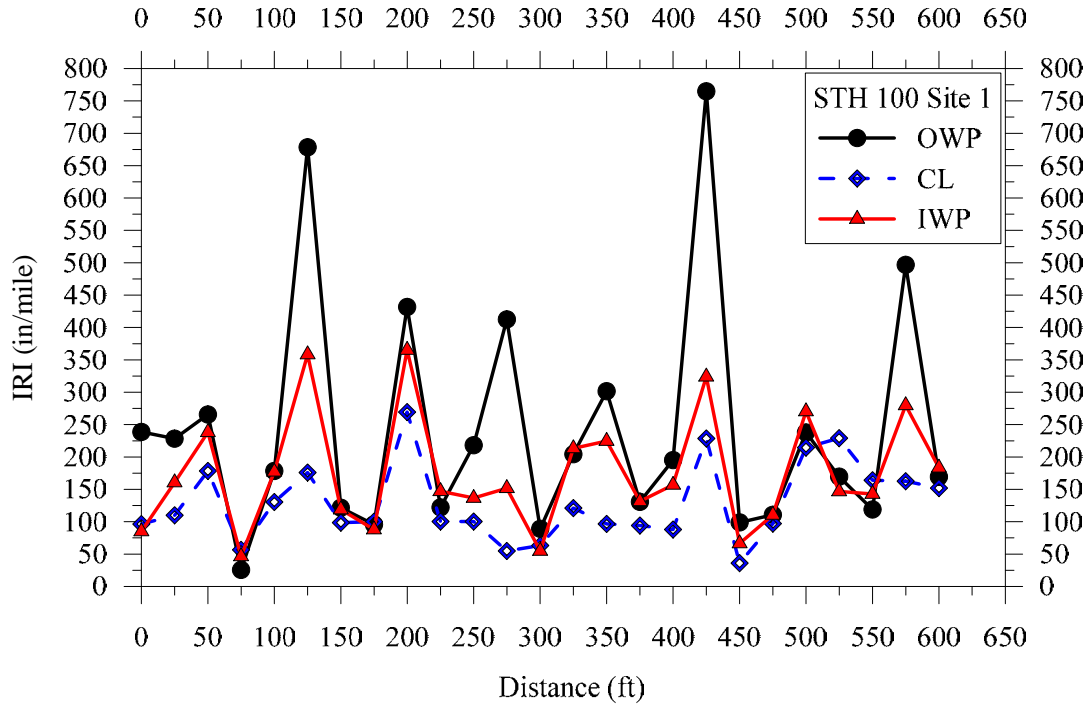


Figure G11: Ride quality measurement (international roughness index) for pavement test section with RCA base layer at STH 100 (S1).

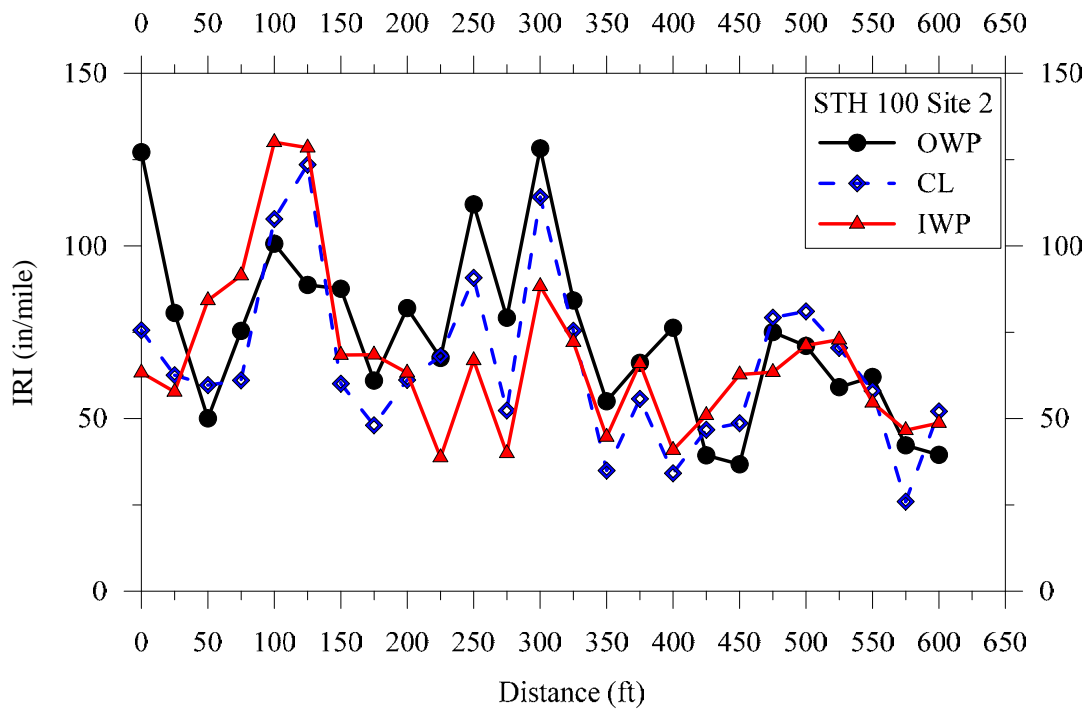


Figure G12: Ride quality measurement (international roughness index) for pavement test section with RCA base layer at STH 100 (S2).

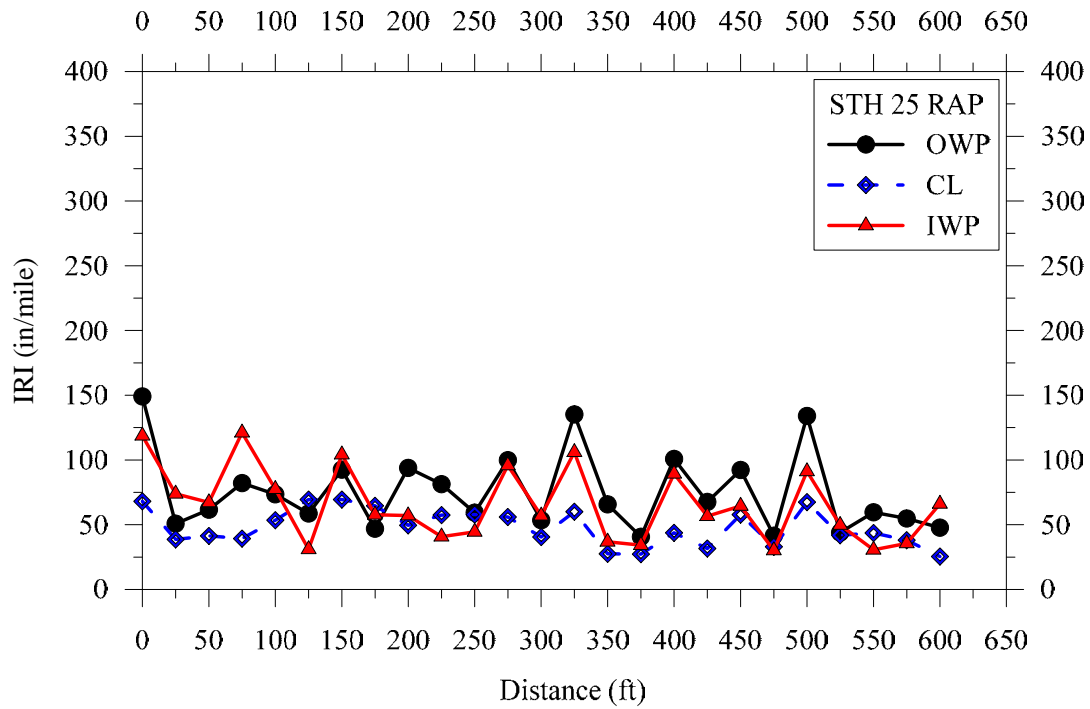


Figure G13: Ride quality measurement (international roughness index) for pavement test section with RAP base layer at STH 25.

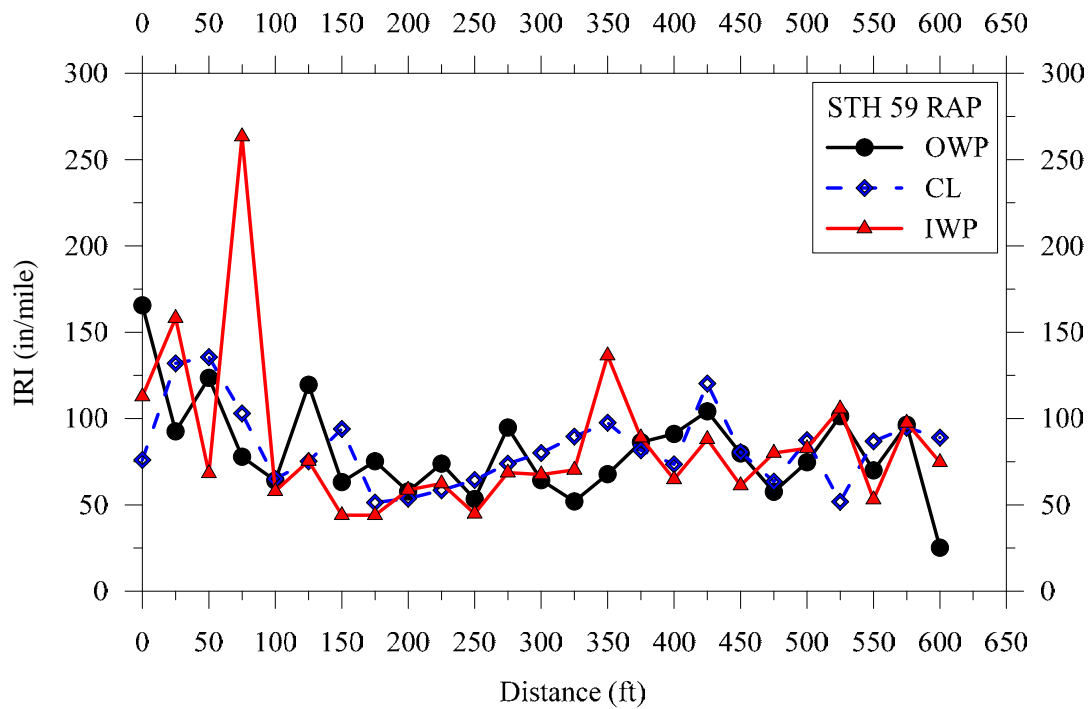


Figure G14: Ride quality measurement (international roughness index) for pavement test section with RAP base layer at STH 59.

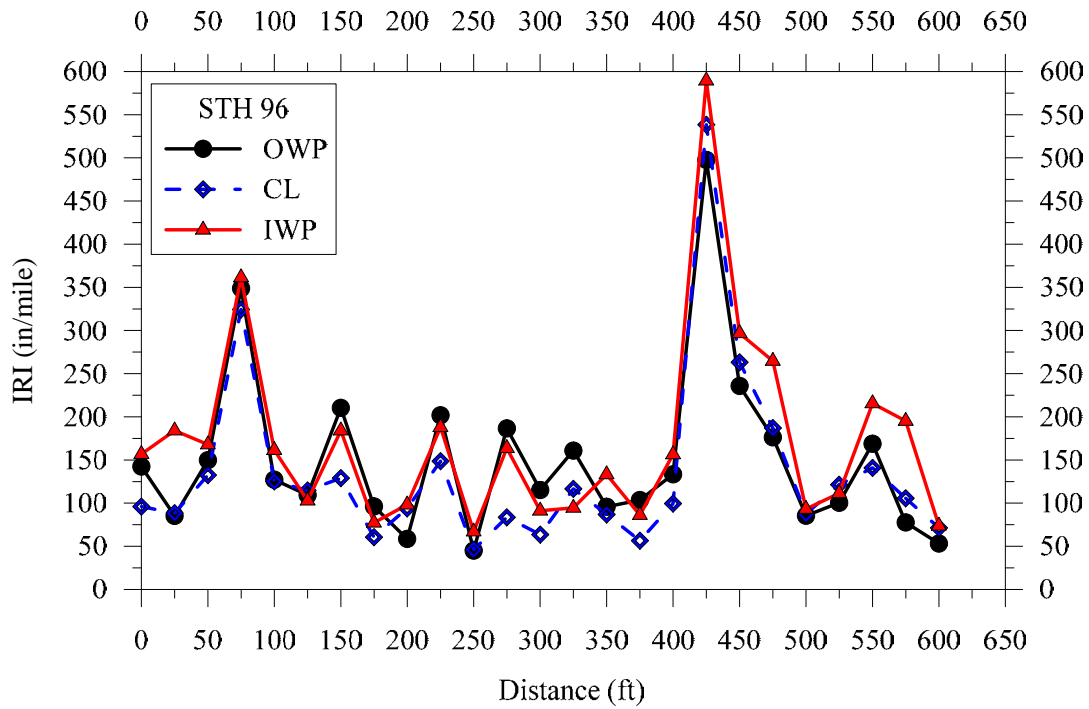


Figure G15: Ride quality measurement (international roughness index) for pavement test section with RAP base layer at STH 96.

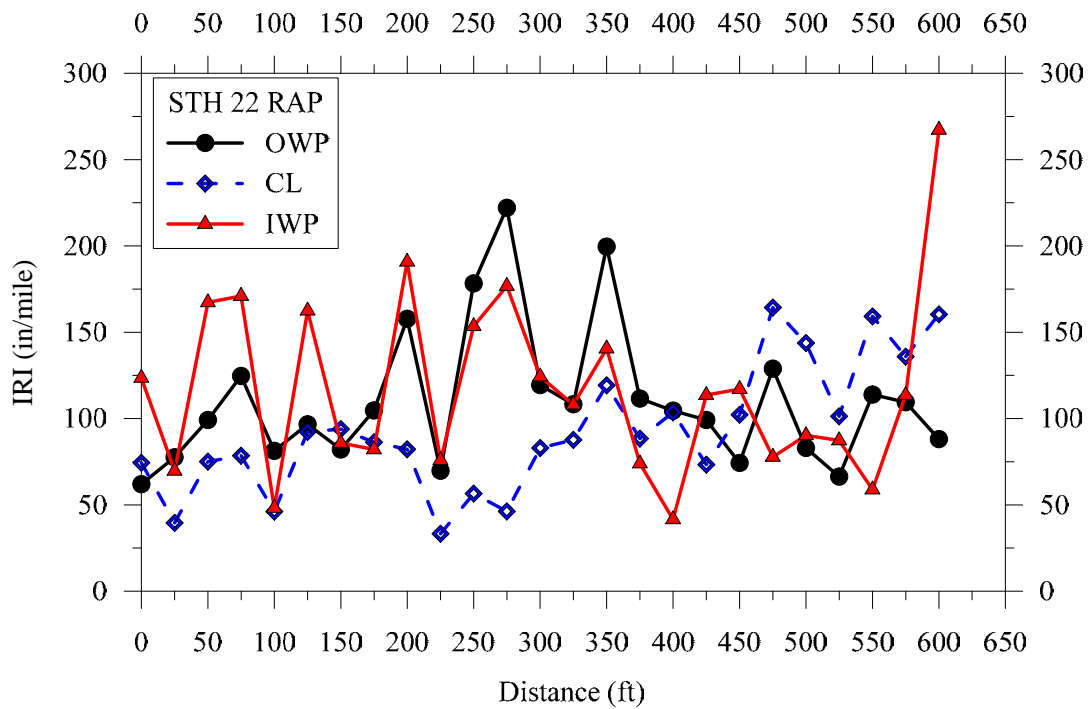


Figure G16: Ride quality measurement (international roughness index) for pavement test section with RAP base layer at STH 22.

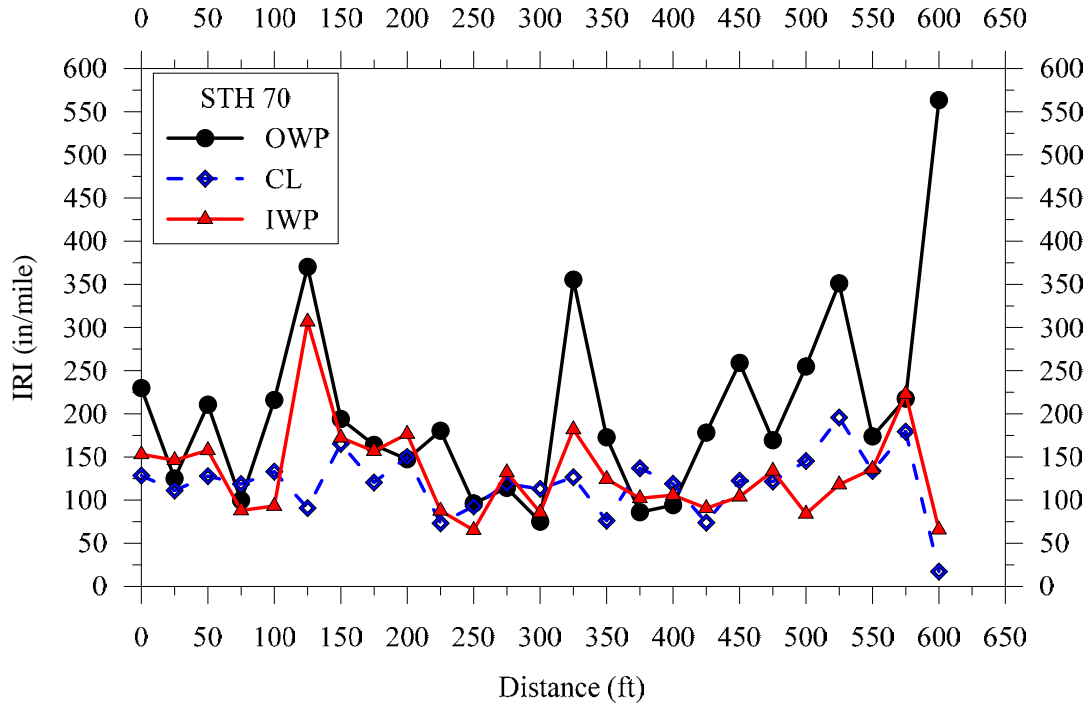


Figure G17: Ride quality measurement (international roughness index) for pavement test section with RAP base layer at STH 70.

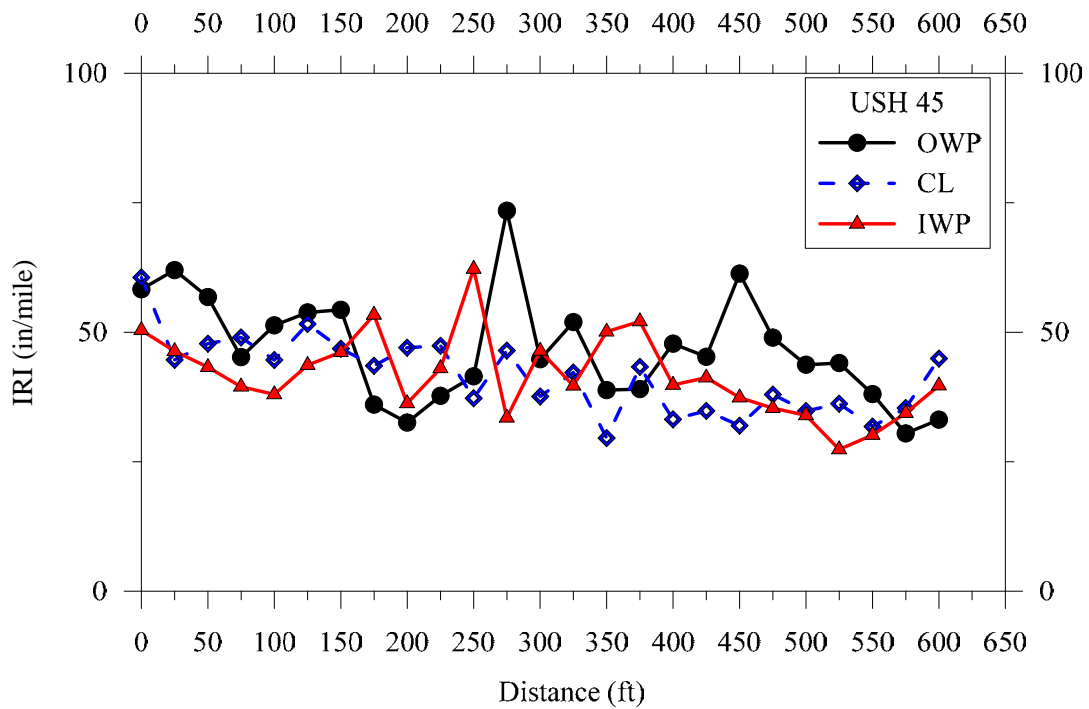


Figure G18: Ride quality measurement (international roughness index) for pavement test section with RAP base layer at USH 45.